GEOPHYSICS

Vol. XXVI, No. 5 October, 1961

Proposed Standards for Seismic Amplifiers . . . and What They Mean to Field Records . . . . . *L. B. McManis* 543
The Use of Photo-Resistive Cells as Losser Elements in a Transistorized Seismic Amplifier . . . . . *F. W. Hafer* 550
A Crustal Structure Refraction Survey in South Texas . . . . . *Ira H. Cram, Jr.* 560
Minimum Statistical Uncertainty of the Seismic Refraction Profile . . . . . *J. S. Steinhart and R. P. Meyer* 574
Refraction and Reflection of Sonic Energy in Velocity Logging. . . . . *Vladimir S. Tuman* 588
Experimental and Field Data for the Dual-Frequency Phase-Shift Method of Airborne Electromagnetic Prospecting . . . . . *N. R. Paterson* 601
Radioactivity of Volcanic Sediments in Brazos County, Texas. *Wm. L. Russell and R. O. Steinhoff* 618
The Directivity Problem for a Buried Line Source . . . *Freeman Gilbert and Leon Knopoff* 626
Radiation Resistance of a Vertical Magnetic Dipole Over an Inhomogeneous Earth *J. C. Negi* 635

DEPARTMENTS

Discussions and Communications
Faults and Earth Tides . . . . . *Danilo A. Rigassi* 643
Excerpts from an Address Given Before the Annual Conference of the Division of Earth Sciences, National Research Council . . . . . *Charles C. Bates* 644
Rapid Computation of Gravity Anomalies for Irregularly Shaped Three-Dimensional Bodies . . . . . *Amalendu Roy* 645
Vela Uniform Research Program in Seismology 647
Correction 648
Reviews 649
Publications Received 653
Patents 654
Contributors 662
Membership Applications Received 665
Announcements 666
Abstracts
Bulletin (Izvestiya) 668
Personal Items 670

Published by the
Society of Exploration Geophysicists

apperception*

. . . is the *PLUS* quality which distinguishes a NATIONAL seismic exploration program. Let National Geophysical Company aid you in *your search for oil.*

*clear discernment by intelligent interpretation of existing findings in light of past experience.

NATIONAL GEOPHYSICAL COMPANY, INC. . . Dallas . . Houston

2345 W. Mockingbird Lane, Dallas 35 Texas, FLeetwood 2-2671

NATIONAL GEOPHYSICAL COMPANY OF CANADA, LTD . . . Calgary, Alberta, Canada

FOREIGN AFFILIATE: namco INTERNATIONAL INCORPORATED • P. O. BOX 35666, Dallas

Please mention GEOPHYSICS when answering advertisers

GEOPHYSICS

Published by the Society of Exploration Geophysicists

EDITORIAL STAFF 1959-1961

NELSON C. STEENLAND, Editor
GEOPHYSICAL ASSOCIATES INTERNATIONAL, BOX 22007, HOUSTON 27, TEXAS

L. L. NETTLETON, Assistant Editor
GEOPHYSICAL ASSOCIATES INTERNATIONAL, BOX 22007, HOUSTON 27, TEXAS

ASSOCIATE EDITORS

G. E. ARCHIE, Well Logging
SHELL DEVELOPMENT CO., BOX 481, HOUSTON 1, TEXAS

ROBERT J. BEAN, Gravity
SHELL OIL CO., SHELL BLDG., 1008 W. 6TH ST., LOS ANGELES 54, CALIF.

ARTHUR A. BRANT, Mining Geophysics
NEWMONT EXPLORATION LTD., BRIAR RIDGE ROAD, R.F.D. 1, DANBURY, CONN.

ROBERT JASTROW, Space Physics
CHIEF, THEORETICAL DIVISION AND DIRECTOR, INSTITUTE FOR SPACE STUDIES, GODDARD SPACE FLIGHT CENTER, 475 RIVERSIDE DRIVE, NEW YORK 27, N.Y.

NORMAN R. PATERSON, Magnetics
HUNTING SURVEY CORPORATION, LTD., 1450 O'CONNOR DRIVE, TORONTO 16, ONTARIO, CANADA

O. F. RITZMANN, Patents
THE GULF COMPANIES, GULF BLDG., PITTSBURGH 30, PENNSYLVANIA

EDGAR J. STULKEN, Seismic Field Techniques and Operations
GEOPHYSICAL SERVICE INC., BOX 35084, AIR LAWN STATION, DALLAS 35, TEXAS

F. A. VAN MELLE, Seismic Theory and Experimental Seismology
SHELL DEVELOPMENT CO., BOX 481, HOUSTON 1, TEXAS

JOHN H. HYDEN, Publication Manager
SHELL BLDG., TULSA 19, OKLAHOMA

Manuscripts of technical papers submitted for publication in GEOPHYSICS should be sent directly to the Editor.

Reviews of geophysical literature published outside of this journal should be sent to the Chairman of the Reviews Committee.

Announcements, news items, and personal items should be sent to the Business Manager.

Form of Manuscripts and instructions for its preparation may be found in GEOPHYSICS, v. 19, p. 141-153. Reprints of this style guide may be obtained from the Business Manager upon request.

Responsibility for all statements and opinions made in GEOPHYSICS must be assumed by the respective authors.

Discussions and Letters to the Editor are welcomed by the Editor.

Subscriptions are given to all members of the Society in good standing as part payment for their dues. For non-members and organizations the subscription rate is $10.00 per year in the United States and its possessions and $10.50 per year in all other countries.

Change of Address Notice should be sent to the Business Manager (see next page). Claims for non-receipt must be sent within 3 months of date of publication.

Single Copy price is $2.50 to members and $3.00 to non-members. For foreign shipment add 20¢ per copy. Order subscriptions and single copies from the Business Manager.

Microcard copies of all back issues of GEOPHYSICS are available through the business office—prices upon request.

Advertising rates will be furnished by the Business Manager upon request. No advertisements will be accepted for prospecting methods based on hypotheses which conflict with the accepted principles of physics.

Permission to Copy text material from GEOPHYSICS is limited to one page and is granted on the express condition that reference be made to the source of the material. Larger text excerpts and illustrations from GEOPHYSICS may not be reproduced without written permission of the Editor.

Indexed regularly by Engineering Index, Inc. and by The Applied Science and Technology Index.

Published by George Banta Company, Inc., Menasha, Wisconsin. Issued six times a year in February, April, June, August, October and December. Second-class postage paid at the Post Office at MENASHA, WISCONSIN, under the Act of March 3, 1879. Acceptance for mailing at the special rate of postage provided for in the Act of February 28, 1925, embodied in paragraph 4, Section 538, P. L. & R., authorized March 19, 1941. Copyright 1961 by the Society of Exploration Geophysicists.

Society of Exploration Geophysicists

The *Society of Exploration Geophysicists* had its beginning in 1930 when it was organized in Houston, Texas as the *Society of Petroleum Geophysicists*, the name being changed to its present form in 1936. The Society is dedicated to the advancement of the science of geophysics and the art of geophysical prospecting. Through its journal GEOPHYSICS it supplies a medium for the dissemination of new knowledge in these fields.

Headquarters, Shell Bldg., Tulsa 19, Oklahoma

COLIN CAMPBELL, *Business Manager*
WILLIAM F. LATTING, JR., *Assistant Business Manager*

COUNCIL (1960–1961)

J. P. WOODS — *President*
Atlantic Refining Co., Box 2819, Dallas, Texas

JOHN C. HOLLISTER — *First Vice-President*
Colorado School of Mines, Golden, Colorado

ROBERT C. KENDALL — *Vice-President*
Shell Oil Co., 1700 Broadway, Denver, Colorado

FRANCIS A. HALE — *Secretary-Treasurer*
California Standard Co., 1021-38th Ave., S.W., Calgary, Alta., Canada

NELSON C. STEENLAND — *Editor*
Geophysical Associates International, Box 22007, Houston 27, Texas

T. O. HALL — *Past-President*
General Geophysical Co., 750 Houston Club Bldg., Houston, Texas

DISTRICT REPRESENTATIVES

Ark-La-Tex Geophysical Society
Bill C. Tucker (1961)

Canadian Society of Exploration Geophysicists
Norman J. Christie (1961)
R. A. Boulware (1961)
E. L. Erickson (1962)

Casper Geophysical Society
A. C. Austin (1961)

Coastal Bend Geophysical Society
C. C. Mason (1961)

Cochabamba Geophysical Society
J. Roger Heggblom (1961)

Dallas Geophysical Society
J. Frank Rollins (1961)
Wm. C. Woolley (1961)
Edgar J. Stulken (1962)

Denver Geophysical Society
C. A. Swartz (1961)

Geophysical Society of Edmonton
G. D. Garland (1961)

Fort Worth Geophysical Society
Paul H. Ledyard (1961)

Four Corners Geophysical Society
W. J. Osterhoudt (1962)

Geophysical Society of Houston
S. B. Stewart (1961)
James M. Wilson (1961)
Robert B. Briggs (1962)

Jackson Geophysical Society
W. W. Ogden (1962)

Montana Geophysical Society
Clyde W. Kerns (1961)

New Mexico Geophysical Society
Robert L. Tucker (1961)

Oklahoma City Geophysical Society
A. J. Oden (1961)

Pacific Coast Section
F. F. Lambrecht (1961)
O. K. Fuller, Jr. (1962)
Klaas van der Weg (1962)

Permian Basin Geophysical Society
B. F. Owings, Jr. (1961)
Richard A. Baile (1962)

Regina Geophysical Society
A. C. Armstrong (1961)

Geophysical Society of South Texas
W. Harry Mayne (1961)

Southeastern Geophysical Society
Aart deJong (1961)
Clark E. Allen (1962)

Southwest Louisiana Geophysical Society
Jack D. Wallner (1961)

Geophysical Society of Tulsa
Wm. M. Erdahl (1961)
James F. Johnson (1961)
Craig Ferris (1963)

Utah Geophysical Society
L. D. Oster (1961)

Asociacion Venezuela de Geofisica
Dennis C. Meyer (1961)

COMPETENCE—*firmly based on twenty-nine years of experience*

Seismic Explorations Incorporated

Tomorrow's needs for better methods of acquiring and interpreting seismic data . . . in terms of geologic structure . . . are being used today at SEI.

SEISMIC EXPLORATIONS, INCORPORATED

P. O. BOX 13057 HOUSTON, TEXAS

Midland Shreveport Denver

Except for Imagination

YESTERDAY'S TOOLS ARE OBSOLETE. ■ EXCEPT FOR IMAGINATION IN CONCEIVING BETTER TOOLS — AND FOR PERSEVERANCE IN MAKING THEM WORK — THERE WOULD BE NO PROGRESS. ■ SCHLUMBERGER WORKS FOR THE PROGRESS OF THE OIL INDUSTRY THROUGH THE DEVELOPMENT OF MORE EFFICIENT SERVICES. ■ SERVICES INTRODUCED BY SCHLUMBERGER DURING THE PAST SIX YEARS ACCOUNT FOR MORE THAN HALF THE LOGGING OPERATIONS RUN TODAY.

SCHLUMBERGER

LEADS IN DEVELOPING NEW SERVICES

Artifacts of the American Paleolithic Age.

SUSTAINING MEMBERS

For information on Sustaining Membership write to
The Business Manager
Shell Bldg., Tulsa 19, Oklahoma

EMPIRE GEOPHYSICAL, INC., 6000 Camp Bowie Blvd., Fort Worth, Texas
VARIAN ASSOCIATES, 611 Hansen Way, Palo Alto, California

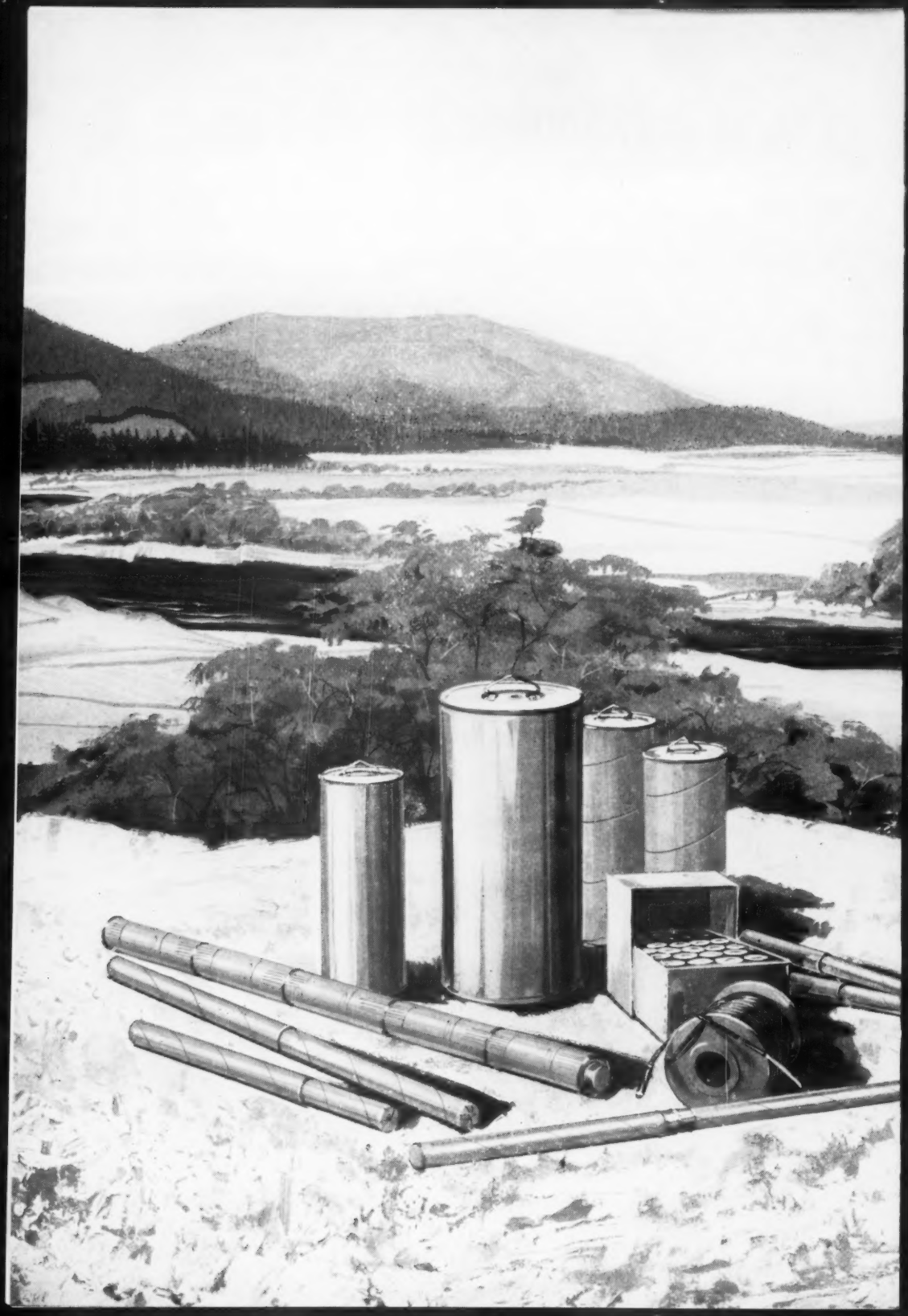

What have we done for you lately?

Nature is no more willing to yield her treasures to you today than she was last year or the year before. But oil prospecting *is* getting more efficient and more fruitful, on land and on sea, because you have better tools to work with.

Here are some of those tools. Some are new within the past year, some are old. If there are any you haven't tried, may we suggest that a call to your Du Pont Explosives representative or distributor might bring new levels of accuracy and economy to your work?

1. New Telescoping "Elcord" Delay Units now permit you to match velocities more accurately, more easily, and at lower cost than ever in sequential shooting.

You can extend the unit to any length, 5′ to 9′, to get the precise velocity you need. Three delay intervals (1.8, 1.4 and 1.0 milliseconds) cover velocities of, respectively, 3,000 to 6,000 ft./sec.; 5,000 to 7,500; 5,500 to 9,500. Advantages include savings of 10% to 35% in cost of delays; velocities accurate within 2%; stability to heat or cold, even when stored for long periods; no field calculations needed to match velocities.

2. New "Nitramite" WW lowers the cost of offshore seismic shooting. It is a high-quality nitro-carbo-nitrate in a special waterproof fiberboard drum with metal ends, costing less than "Nitramon" WW.

3. "Nitramon" WW—The time-tested offshore nitro-carbo-nitrate in a rugged, all metal can. Outstanding from the standpoints of seismic energy production, safety, convenience, and resistance to adverse storage conditions. Especially recommended for foreign work. Available in 5, 10, 16⅔, 20, 25, 40 and 50-pound units.

4. "Nitramon" S, for land work, is a nitro-carbo-nitrate packed in threaded, all metal cans which may be screwed together easily to form a very rigid column. Must be shot with "Nitramon" S Primer. Equal to 60% dynamite in the production of seismic energy. Highly recommended for deep-hole work and sleeper charges. Immune to heat or cold and highly resistant to corrosion. Neither "Nitramon" WW nor "Nitramon" S can be detonated by flame, shock, rifle bullets, or a commercial blasting cap.

5. Seismograph 60% "Hi-Velocity" Gelatin. This type of gelatin dynamite inherently has both high water resistance and excellent storage properties. In the Du Pont product, they are outstandingly good, due to the use of a special ingredient. Seismograph 60% "Hi-Velocity" is strongly recommended for deep hole work and sleeper charges on the basis of its exceptional ability to withstand the desensitizing effects of high water pressure and long periods of immersion. It is also highly recommended for foreign work, which almost always involves poor storage conditions and long periods of time between manufacture and use.

6. "Seismogel". This grade is a straight gelatin similar to Seismograph 60% "Hi-Velocity", but with a lower nitroglycerin content. It is, therefore, not as water resistant and is not recommended for depths over 300 feet or for sleeper charges except under favorable conditions.

7. "Seismex". A non-gelatinous ammonia dynamite with additives that give enough water resistance for work in many areas. "Seismex" should not be used if the water depth exceeds 200 feet, or for sleeper charges regardless of depth.

8. "Seismex" PW. Similar to "Seismex" but lower in cost. "Seismex" PW was designed especially for shallow-hole and surface pattern shooting. It has sufficient water resistance for shallow holes which will be loaded and shot on the same work day.

9. "SSS" Electric Blasting Caps are accurate, dependable, static-resistant. They outsell the nearest competitor two to one. Packed to suit your convenience—duplex or single wires, spool-wound or figure-8 fold, lengths up to 400′.

10. Water-Work Boosters are specially waterproofed charges for priming "Nitramon" and "Nitramite" WW. Also used with gelatin dynamite for additional assurance of detonation under exceptionally severe water conditions.

For details, call your Du Pont Explosives representative or distributor. Or write Du Pont, 2446 Nemours Building, Wilmington 98, Delaware.

SEISMIC AIDS

Better Things For Better Living . . . *Through Chemistry* DU PONT REG U.S. PAT OFF

Now—a complete reflection-refraction seismograph in a 30-pound package.

The FS2 Portable Seismograph is an instrument breakthrough which is expected to extend the use of seismic surveys to many new and different applications. Developed by Hunting engineers over a period of 3 years, this instrument is now being used on engineering, mining and research projects across North America in answer to the need for an all-purpose seismograph for shallow engineering and mining work. Normally operated with a sledge-hammer source and a two-man crew, the instrument's use is extended by caps and dynamite to cover all seismic problems where portability, versatility and speed are important.

Salient features:

- ► Based on the use of dry electro-sensitive (facsimile) paper, the FS-2 registers seismic arrivals directly, permanently and without processing on an accurate base.
- ► Because all events are permanently recorded, the FS-2 can be used for refraction or reflection while insuring the utmost in interpretability.
- ► Recommended particularly as a refraction instrument in the 50-150 ft. depth range, the FS-2 can be used to depths in excess of 500 ft. (with the hammer source) in the reflection mode.
- ► Rapid and economical operation are brought about by portability, method of recording and low initial cost.
- ► Two complete input channels (geophones, amplifiers, filters, pulse-shapers) and built-in coincidence circuitry make instrument directional, suppress surface noise.

For further details, contact our New York office

HUNTING GEOPHYSICAL SERVICES, INC.
(Contractors and Consultants)
10 Rockefeller Plaza, New York 20, N.Y.

A Member of the World-wide Hunting Group.

EXPLORER*

completely field proved around the world!

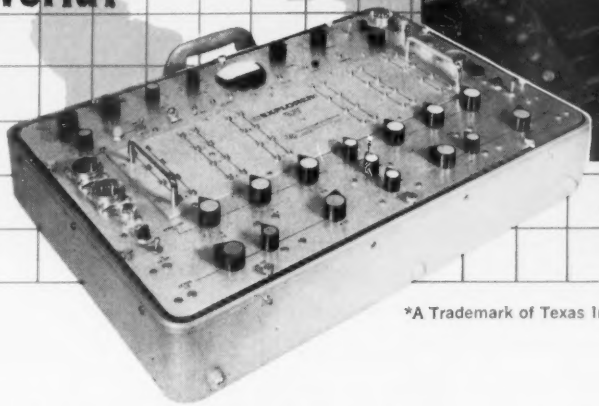

All-Transistorized TI Seismic System on location in South America.

*A Trademark of Texas Instruments

Texas Instruments Model 8000 All-Transistorized Seismograph, the EXPLORER, is building customer satisfaction with superior performance in difficult environmental conditions, vehicle-mounted or back-packed.

On every continent—in deserts, in swamps, in the toughest kind of terrain —the EXPLORER's portability, operating speed and proved reliability are resulting in trustworthy data gathering with significant economies. It has an unmatched performance/pound ratio!

With its fewer packages and fewer connections, the EXPLORER is faster, easier to set up, and can go anywhere two men can go. Power requirement is 80% below typical vacuum-tube systems, warm-up time eliminated.

The 8000 System's 5-200 cps range covers all practical frequencies from refraction through high resolution reflection. It is readily adaptable to all types of direct or FM recorders. A wide choice of AGC rates, fixed gains and TVG options is provided.

Tens of thousands of field hours have proved the dependable full-range performance and unequalled savings in field operating costs of EXPLORER —the industry's *first* all-transistorized seismograph.

Write for complete information . . .

APPARATUS DIVISION
PLANTS IN HOUSTON
AND DALLAS, TEXAS

TEXAS INSTRUMENTS
INCORPORATED
3609 BUFFALO SPEEDWAY
P. O. BOX 66027 HOUSTON 6, TEXAS

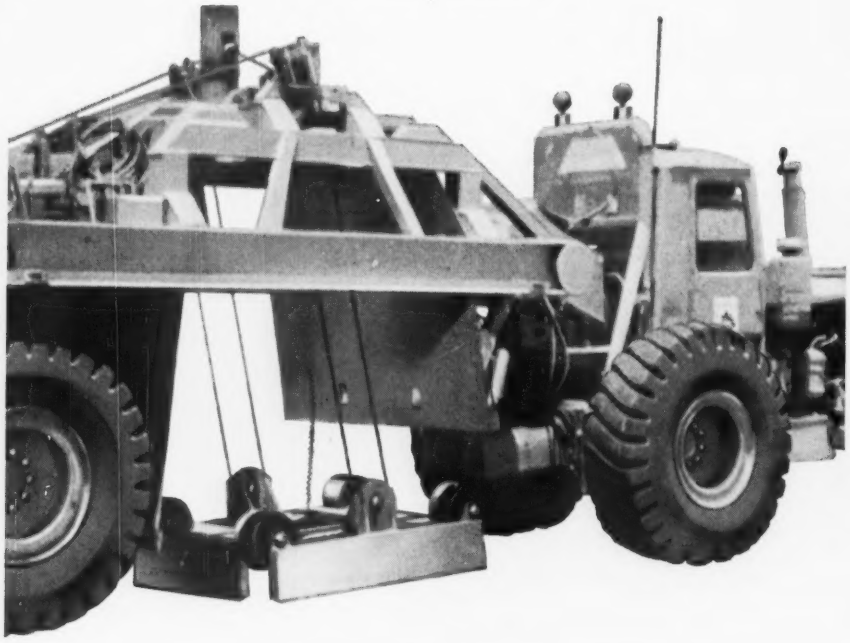

THE STOMPER
GIVES DEPENDABLE DATA–AT A NEW LOW COST

The great new Stomper obtains seismic records with substantial savings. Labor costs are cut; there are no bit costs and dynamite and cap costs; permit costs are usually reduced.

The self-propelled Stomper vehicle drops weights of 3 to 5½ tons from a height of eight or nine feet. Location can be changed and the weight dropped about five times a minute. This rapidity of action provides dependable data faster than other techniques. There are some areas where the Stomper technique provides usable data that could not be obtained by conventional seismic methods.

Call IX, JA 9-9168, Houston, Texas, and let us tell you how we can supply you with the top value in the type of geophysical survey work you need.

INDEPENDENT EXPLORATION CO.

Geophysical Surveys

Houston — Midland — Denver — New Orleans — Lafayette
Tripoli — Las Palmas — London — Paris — Algiers

GEOPHYSICAL INSTRUMENTS DESIGNED AND MANUFACTURED BY FORTUNE ELECTRONICS

Fortune

Fortune Electronics' compact, lightweight magnetic recording equipment is exactingly engineered and constructed to give accurate, dependable service in any climate. Yet, they cost less initially, cost less to maintain.

Give Better Performance, Longer.

Cost you less!

SR-5

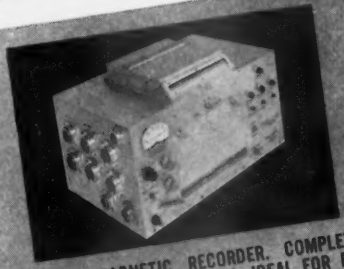

"BUFFERLESS" MAGNETIC RECORDER. COMPLETE TAPE SYSTEM CONTAINED IN ONE UNIT. IDEAL FOR PORTABLE OPERATION. WEIGHT: 60 LBS. SIZE: 11"x18¼"x11⅛".

SR-3

SR-3 DIRECT RECORDER SWITCHING-AMPLIFIER

DIRECT RECORDING SYSTEM — ADAPTABLE TO ANY EXISTING SYSTEM. GIVES THE FINEST TRANSIENT AND STEADY STATE RESPONSE. CONTAINED IN TWO 50-LB. UNITS.

DC-1

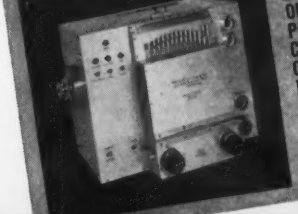

DIRECT RECORD-PLAY-BACK SYSTEM FOR OFFICE OR FIELD USE. PRODUCES A STATICALLY AND DYNAMICALLY CORRECTED PLAYBACK OF 24 OR MORE CHANNELS SIMULTANEOUSLY. WEIGHT: 82 LBS. SIZE: 15"x18"x14".

For complete details or for an office demonstration, write or call:

Fortune Electronics, Inc.

H. H. HAPPEL—H. H. HAPPEL, JR.

2505 SOUTH BOULEVARD, HOUSTON, TEXAS

Represented in Dallas, Texas and Tulsa, Oklahoma by Indel Supply Company

REPUTATION: *Leadership in geophysical instrumentation*

REASON: *General Geophysical develops and produces its own custom-built instruments*

The ruggedness and reliability of the instruments and equipment used in General Geophysical's work mean better, faster service with less chance of error or of costly delay. Example—the General-built GEOPAC system that is famed for geophysical plotting and computing. Now, as shown above, General crews have portable GEOPAC units which provide fully corrected seismic records in the field.

General's extensive laboratory facilities offer you an important flexibility—equipment and instruments can be quickly custom designed and manufactured to fit the special needs of a job, to fit a special area and to fit your special requirements.

Find out for yourself the reasons behind General's reputation for leadership in geophysical instrumentation. Call General today . . .

General
GEOPHYSICAL COMPANY
Houston Club Building • Houston, Texas

Paris, France
Edmonton, Alberta
Nassau, Bahamas
Tripoli, Libya

When your contract is with General, the percentage for successful exploration is in your favor!

UNITED
GEOPHYSICAL
CORPORATION

MORE
THAN A
QUARTER
CENTURY OF
SUCCESSFUL
GEOPHYSICAL
SERVICES
THROUGHOUT
THE WORLD

UNITED
GEOPHYSICAL

UNITED GEOPHYSICAL CORPORATION

SEISMOGRAPH • GRAVIMETER • MAGNETOMETER

P. O. Box M, 2650 E. Foothill Blvd., Pasadena, California
Suite 203, 2920 Weslayan, Houston 27, Texas
422 North Main Street, Tulsa, Oklahoma
3074 S. Winona Court, Denver, Colorado
1221 Pinewood Drive, Pittsburgh 16, Pennsylvania
531 Eighth Avenue S. W., Calgary, Alberta, Canada
P. O. Box 1861, Anchorage, Alaska
194 rue de Rivoli, Paris 1er, France
Av. Pres. Vargas, 435, 19° andar, Rio de Janeiro, Brazil
Casilla 1155, Cochabamba, Bolivia
Casilla 26-D, Punta Arenas, Magallanes, Chile
P. O. Box 268, Tripoli, Libya
Calle Triana No. 140, Las Palmas, Gran Canaria, Isles Canarias
P. M. B. 2119, Lagos, Nigeria
P. O. Box 1032, Tehran, Iran
¼ New South Head Road, Vaucluse, New South Wales, Australia

GEOPHYSICS ADVERTISERS

Aero Service Corp. 49
Alden Equipment Co. 23
American Cyanamid 26
Askania-Werke 53
Atlas Powder Company 15

Bible Geophysical Co. 37
Century Geophysical Co. 39
Compagnie Generale de Geophysique ..36–37
Continental Geophysical Co. 64

Decca Navigator Co. Ltd. 42
Bert F. Duesing, Inc. 14
Du Pont—Explosives 6–7
Du Pont—Photo Products 48

Eastman Kodak Co. 38
Economic Geology 37
Electrodynamic Instrument Corp. .....
.....65, 67, 69, 71, 72–73
Electro-Technical Labs 31–34

Fairchild 60
Fortune Electronics 11

General Geophysical Co. 12
Geophysical Associates Int'l. 16
Geophysical Service Inc. .....4th cover
Griffin Tank & Welding Service 66

Hall-Sears, Inc. 74
Herb J. Hawthorne 41
Hunting Geophysical Services 8

Marine Geophysical Services 70
Mayhew Supply Co., Inc. 30
E. V. McCollum & Co. .....facing 17
Minnesota Mining & Mfg. Co. 63

National Geophysical Co. .....2nd cover

Petty Geophysical Engineering Company 52

Robert H. Ray Co. 47
Rogers Geophysical Companies 22

Schlumberger Well Surveying Corp. 4, 40
Seismic Engineering Co. 68
Seismic Explorations, Inc. 3
Seismograph Service Corp. .....3rd cover
Seismos GmbH 62
Sharpe, E. J. Ltd. 24–25
Southwestern Industrial Electronics ..54–59

Techno Instruments 29
Texas Instruments 50–51
Tidelands Exploration Co. 28

United ElectroDynamics 27
United Geophysical Corp. 13

Vector Mfg. Co. 43–46

Wallace & Tiernan, Inc. 35
Western Geophysical Co. 61

Professional Directory .....Begins 17

BERT F. DUESING, INC.

"Selling Atlas Explosives"

AND

Manufacturers of Blasting Agents

Magazines and Plant
BIG LAKE, TEXAS

phone
Big Lake 500

Magazines
HASKELL, TEXAS

phone
UNion 4-2456

with blasting caps . . .

it's what's inside that counts

For seismic prospecting, there's no electric blasting cap that beats **STATICMASTER®**.

• IMPROVED STATIC RESISTANCE is demonstrated by exhaustive tests under actual field conditions and by six years service with leading exploration crews. Over 3,000,000 Staticmaster Caps have been sold, with no report of accidental detonation attributed to static!

• DEPENDABILITY tops the field due to exclusive built-in, pretested Atlas electric match. UNIFORMITY in pattern shooting is enhanced because electric match allows bridge wire to be double checked for resistance before and after final cap assembly.

• SAFETY is increased by use of low sensitivity Atlas HNM (hexanitromannite) in primer charge.

• WATER RESISTANCE all the way from cap to top of hole is assured by tough enamel coating on wires, beneath the vinyl insulation...and by genuine rubber plug in cap, hex-crimped to provide 100% watertight seal.

Tell your supplier you want **STATICMASTER** Electric Blasting Caps and Atlas explosives and blasting agents on every trip.

ATLAS
CHEMICAL INDUSTRIES, INC.
EXPLOSIVES DIVISION
WILMINGTON 99, DELAWARE

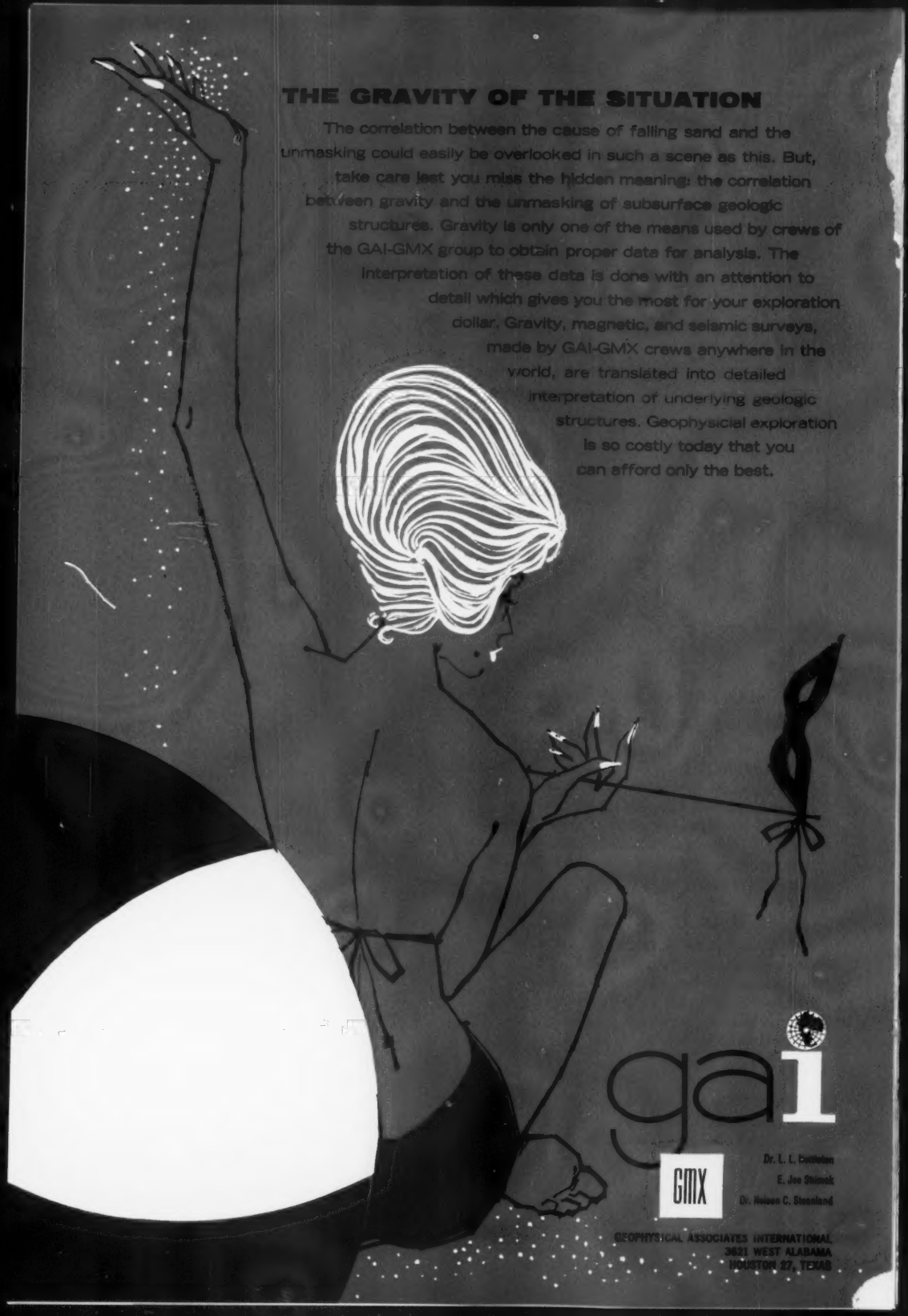
THE GRAVITY OF THE SITUATION
The correlation between the cause of falling sand and the unmasking could easily be overlooked in such a scene as this. But, take care lest you miss the hidden meaning: the correlation between gravity and the unmasking of subsurface geologic structures. Gravity is only one of the means used by crews of the GAI-GMX group to obtain proper data for analysis. The interpretation of these data is done with an attention to detail which gives you the most for your exploration dollar. Gravity, magnetic, and seismic surveys, made by GAI-GMX crews anywhere in the world, are translated into detailed interpretation of underlying geologic structures. Geophysicial exploration is so costly today that you can afford only the best.
gai
GMX
Dr. L. L. Contoin
E. Joe Stimek
Dr. Nelson C. Steenland
GEOPHYSICAL ASSOCIATES INTERNATIONAL
3621 WEST ALABAMA
HOUSTON 27, TEXAS

Volume XXVI OCTOBER, 1961 Number 5

GEOPHYSICS

PROPOSED STANDARDS FOR SEISMIC AMPLIFIERS . . . AND WHAT THEY MEAN TO FIELD RECORDS*

LOUIS B. McMANIS†

Abstract: Seismic amplifier performance may be categorized broadly into AGC action, filtering, and distortion (including noise). Eight specifications can define the characteristics of each as follows:

AGC— 1. Steady-state AGC including "burst-out"
2. AGC control vs frequency
3. Dynamic AGC action
4. AGC distortion effects

Filtering— 5. Amplitude response
6. Phase response

Noise and 7. Pre-filter distortion

Distortion—8. Internal amplifier noise

These eight specifications allow a user to predict, and consequently allow for, amplifier action—both desirable and deleterious—in obtaining field records.

The author proposes that these specifications, coupled with the usual "external" specifications, be considered as a starting point for establishing a standardized method of specifying seismic amplifier characteristics similar to the SEG "Standard Methods of Specifying Performance" for magnetic recording.

To define a seismic amplifier's action completely, it is necessary to measure all its characteristics under all conditions which can exist in field use. Some of the effects, such as AGC control and filtering, are desirable or necessary. Some, such as distortion and noise, are undesirable and result from design limitations imposed by size, weight, and cost. They must all be known, however, in order to evaluate an amplifier or understand its effects on field records.

The three basic areas to be considered—AGC, filtering, and noise and distortion—are divided into the eight specifications of Figure 1. Many of these specifications are not normally published or even measured.

It is proposed that these specifications be considered for at least a starting point in establishing

DYNAMIC AMPLITUDE RESPONSE
- Steady-State AGC Including Distortion under "Burst-Out Conditions"
- Steady-State AGC Action vs Frequency
- AGC Speed
- AGC Distortion vs Frequency

FILTERING
- Frequency Response
- Phase Response

NOISE AND DISTORTION
- Pre-Filter Distortion
- Internal Amplifier Noise

EXTERNAL SPECIFICATIONS
Number of Units—Dimensions and Weights
Total Weight and Volume
Power Consumption, Standby and Operate

FIG. 1.

* Presented at the 30th Annual SEG Meeting, Galveston, Texas, November 9, 1960. Manuscript received by the Editor January 24, 1961.

† SIE Division of Dresser Electronics, Houston, Texas

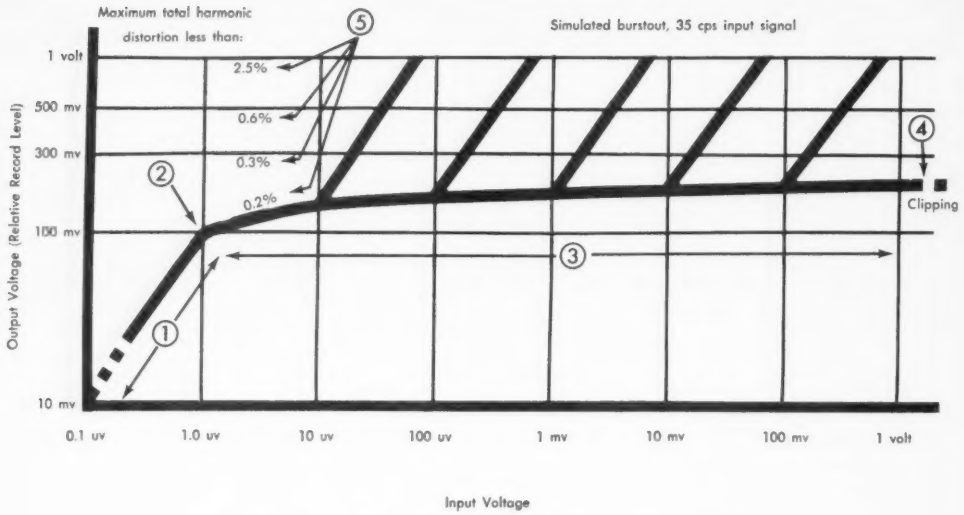

FIG. 2. AGC characteristics including distortion under burst-out conditions.

a standardized method of specifying amplifier characteristics similar to those standards which have been established for magnetic recording.

To determine data for all following specifications, it is necessary that the amplifier be fed from and work into proper impedances. All other accepted engineering procedures should be followed as is usual in performing laboratory tests.

DYNAMIC AMPLITUDE RESPONSE (AGC)

Specification 1—Steady State AGC Action Including Distortion at "Burst-out"

In order to conserve space and yet present an easily read graph of data obtained, the form of presentation shown in Figure 2 has been selected. This graph of output voltage versus imput voltage shows (1) linear gain region, or that portion of amplifier action where the input signal is of insufficient amplitude to actuate the AGC circuit; (2) AGC threshold, or the point where AGC action first begins to affect amplifier gain; (3) total AGC range, the slope of which is variously termed "flatness, stiffness, or dynamics"; (4) maximum signal-handling capability, usually denoted by initiation of severe distortion and/or loss of AGC action with rapidly increasing output; and (5) values of distortion for signal "burst-out," "burst-out" being defined as the condition where input signal increases occur so rapidly that the AGC action does not begin to change the amplifier gain significantly. These "burst-out" conditions correspond to outstanding reflections on field records.

This graph is obtained in two parts. The usual AGC curve is secured by injecting a 25–40 cps input voltage. Amplitude is set to various levels from the linear gain region before threshold up to the overload point. Resulting output voltage across a load impedance simulating the galvanometer is plotted.

"Burst-out" characteristics are obtained by locking the AGC loop gain at several input levels, such as 10 and 100 microvolts and 1, 10, and 100 millivolts. Then the input voltage is increased until desired increase in output voltage results. Existing harmonic distortion is measured for each desired point.

The form of presentation shown states "burst-out distortion" present at selected output voltage rather than for constant steps of input voltage increase. In this manner it can be more easily interpreted as specific oscillograph record levels.

Action of amplifier characteristics described in this specification is easily noted on final record appearance. (1) The flatter the total curve can be made, the more uniform will be high- and low-level energy amplitude on the seismogram. (2) Excessive burst-out distortion will cause high-

amplitude reflection peaks to distort and consequently be apparently misplaced timewise. This distortion is especially important when using very slow AGC speeds. Here sudden bursts of high reflection energy will not be reduced in amplitude rapidly, yet they should be reproduced with as little distortion as possible. (3) A linear gain region extending too far before AGC action starts usually implies lack of amplifier sensitivity. "Loss" of low-level reflection results.

Specification 2—Steady State AGC Action Versus Frequency

The graph representing this specification is shown in Figure 3. It is obtained by injecting an input signal of approximately 1 millivolt to the amplifier and plotting amplifier output versus frequency. A rise in output at low frequencies indicates that the amplifier will produce records having low-frequency signals larger in amplitude than equivalent higher-frequency signals. This is particularly noticeable if the AGC does not properly control ground-roll signals when they are present in a record.

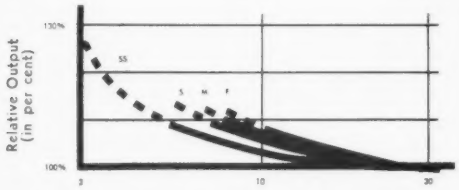

FIG. 3. AGC control for low frequency input signal.

Specification 3—AGC Speeds

Perhaps no facet of amplifier design has received more comment in recent years than the "optimum AGC speed." It is not the purpose of this paper to comment on what constitutes the "best" control but only to present a means of defining these speeds which will allow comparison between different amplifiers or speeds within the same amplifier. Both attack and release times must be determined in order to evaluate properly AGC speeds.

Following conventional electrical engineering nomenclature, these time constants are defined as shown in Figure 4. Normally, signal increases and decreases of 10 and 20 db are sufficient to define the curves. Data thus obtained are then plotted as shown in Figure 5 for attack or "step-up" time and in Figure 6 for release or "step-down" times.

It should be noted that either the attack or release speed alone does not sufficiently define AGC action, e.g., a very fast clamp and slow release will cause the "masking" of weak reflections which closely follow strong reflections.

Experience is the best teacher in evaluating performance from these curves. If a consistent measurement method is used, the interpreter can more easily estimate the effects between different AGC speeds or between amplifiers of different designs.

Specification 4—AGC Distortion Versus Frequency (For Various AGC Speeds)

There is always a maximum usable AGC speed. If the frequency of input signal is so low that the AGC action has time to start reducing amplifier gain during a half-cycle of signal, there must necessarily result some signal distortion. This is a normal and unavoidable effect in any seismic amplifier. In practical amplifiers the AGC should not seriously modify individual half-cycles of normal medium-frequency seismic signals. However, if the AGC elements introduce any additional distortion, the resulting deterioration of signal waveshape becomes much more severe and sets in much more rapidly. Nonlinear response of AGC losser elements and unstable AGC circuitry are the most common causes of this additional distortion.

The sample plot of Specification 4 is shown in Figure 7. Examination of these data will reveal at what lower-frequency limits various AGC speed settings should be used.

FILTERING

Specification 5—Frequency Response (For All Filter Settings)

Although frequency response curves are almost always published, it is suggested that a standard format be used. This particular format, shown in Figure 8, is logarithmically spaced to satisfy engineers but labeled in percent for those who abhor decibels.

In order to check the stability of filter elements with varying signal levels, the responses should also be plotted for more than one input level, if significant.

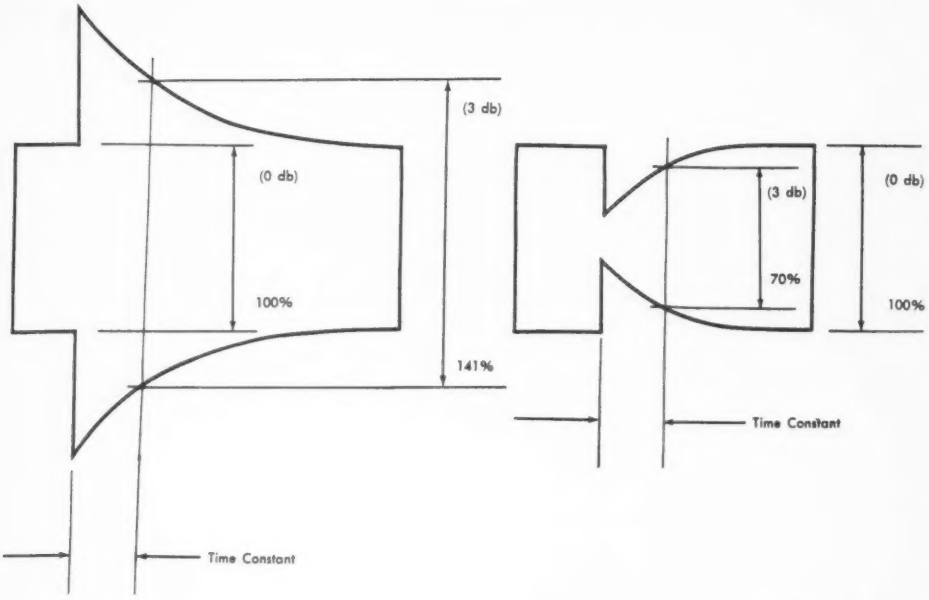

FIG. 4. (left) AGC time constants for increasing signal. (right) AGC time constants for decreasing signal.

Most filter curves are labeled with numbers indicative of the cut-off frequencies and slope of cut-off. When more than one section of filtering is available, it should be displayed separately as in Figure 9.

Specification 6—Phase Response

It would be desirable from the users' point of view if amplifiers produced no phase shift. If this phenomenon could be produced, no "filter-lag" corrections on records would be required. Since this is not possible (without magnetic recording or similar techniques), phase shift data should be presented so that the effects on a record can be easily evaluated. Proper filter design—linear phase shift within the useful spectrum, zero-frequency intercept of integral 180 degree multiples, etc.—will produce the most consistent phase corrections. A proposed method for displaying phase response is illustrated in Figure 10. As is shown here, the Filter "Out" response should be displayed, as well as having phase curves of all usable filters available. As is true for amplitude response, phase response should be determined for various input levels, if significant.

NOISE AND DISTORTION

Specification 7—Pre-Filter Distortion

This is the distortion produced by any amplifier elements preceding the low-cut filter. The low-

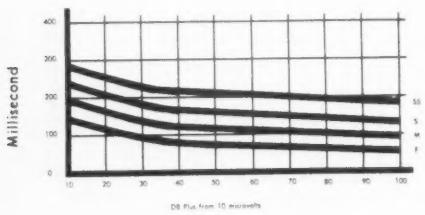

FIG. 5. AGC time constants. Step-up.

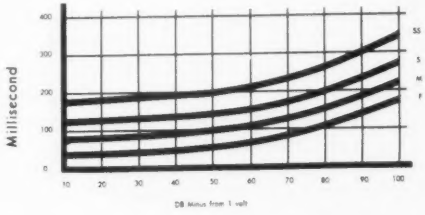

FIG. 6. AGC time constants step-down.

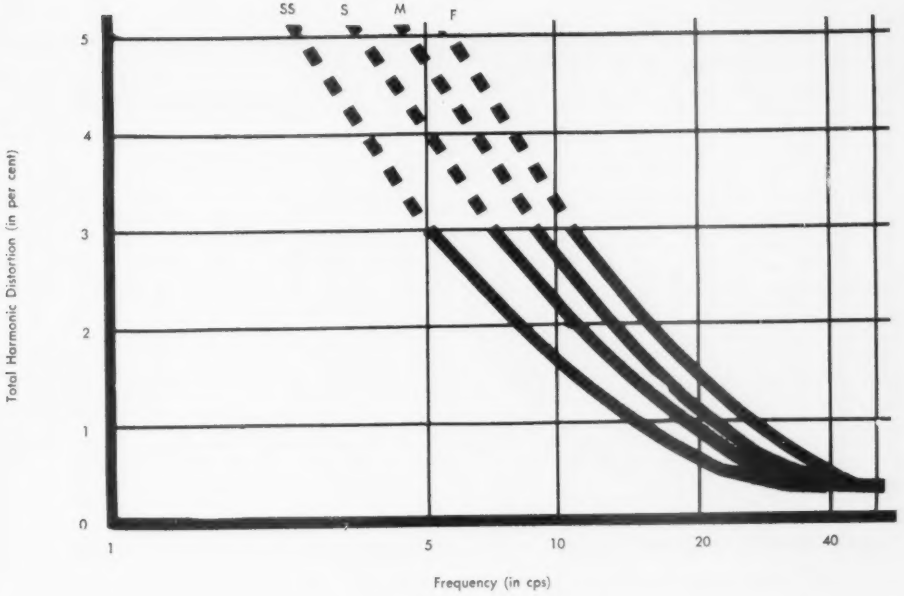

FIG. 7. AGC distortion versus frequency.

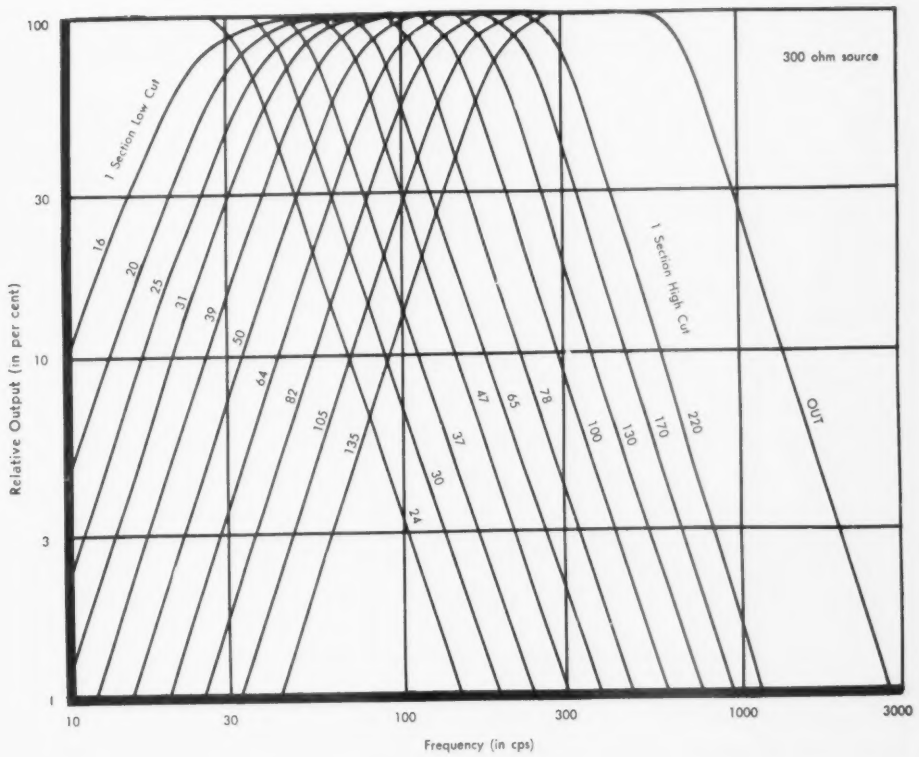

FIG. 8. Frequency response.

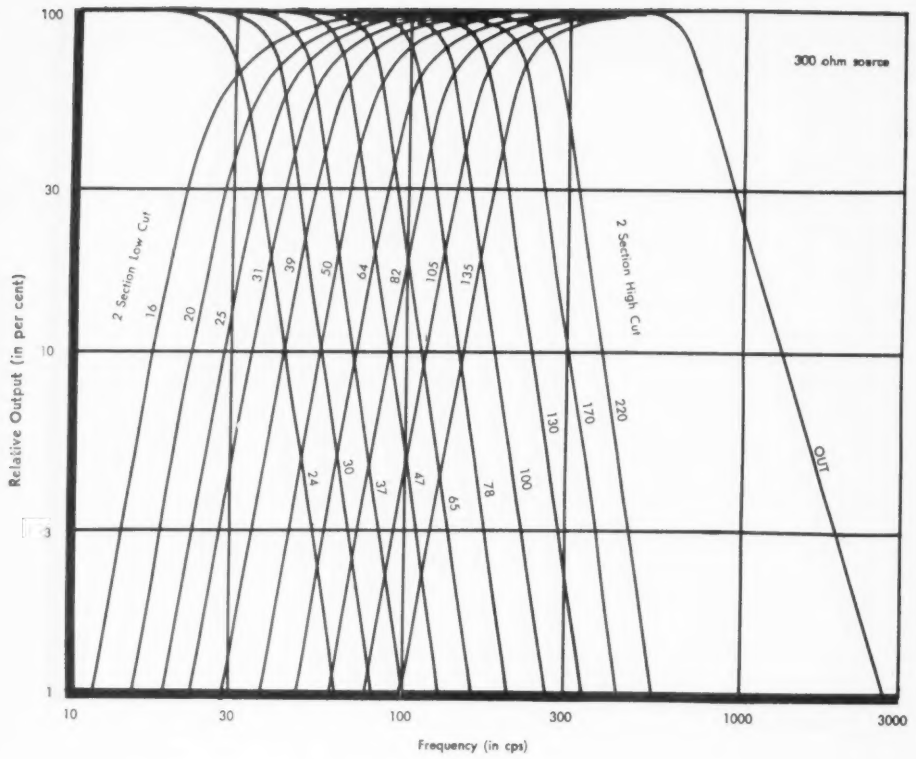

FIG. 9. Frequency response.

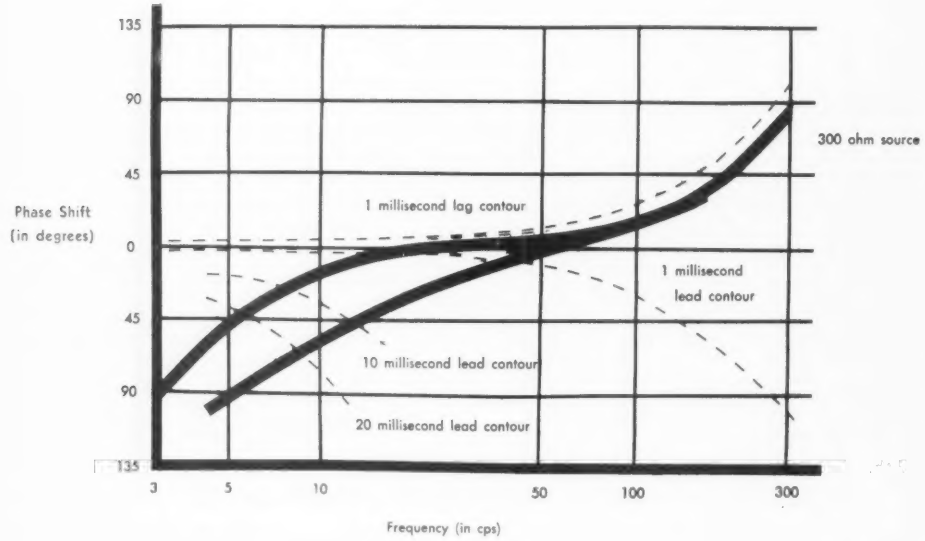

FIG. 10. Phase shift.

cut filter, by its rising response characteristic, emphasizes this type of distortion. Such distortion is, therefore, particularly undesirable and results in harmonics of ground-roll, or other unwanted low-frequency signals, interfering with the higher-frequency reflections. An example will quickly illustrate. Suppose that you are using a low-cut filter which nominally starts cutting at 25 cps and is down to approximately 1/60 at 12 cps. Furthermore, assume that ground-roll of 12 cps is being fed into the amplifier. The 2nd and 3rd harmonics —24 cps and 36 cps respectively—generated by distorting components preceding the low-cut filter will be emphasized by 36 db. This is a multiplying factor of 60. If the ground roll signal is 60 times larger than the desired reflection signal, ground roll harmonics and reflection signals will have equal amplitude on the record. This type of distortion measurement is shown in Figure 11 and should be shown as a function of frequency at various input signal levels. Note that any distortion created in the low-cut filter should be included in the measurement.

Specification 8—Internal Amplifier Noise

This noise, generated within the amplifier, should be determined by taking a record with the nominal input impedance across amplifier input terminals. The resulting record may then be summarized by stating peak-to-peak (maximum) noise as compared to a one-microvolt, calibrating input signal. The peak-to-peak deviation should be selected from a half-second section of the record. A longer interval is not required since normally only the final section of a field seismogram will be affected by amplifier noise. An essential part of amplifier noise data is the statement of amplifier bandwidth (including galvanometers) while determining noise. The amplifier should be checked with filters "out" and with several representative filters in the signal path.

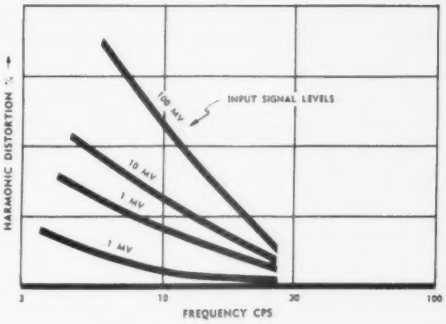

FIG. 11. Pre-filter distortion.

Although not part of this set of specifications, it is obviously important to consider other noise-generating sources external to the amplifier, such as camera hash, vibrators in power supplies, etc.

These noises are quite common and generally easily recognized by their consistent appearance on all traces. It should be noted that neither geophone spread noise nor 60-cycle pickup is considered in this specification.

External Specifications

In addition to the preceding eight specifications, it is also important to state the following amplifier characteristics: number of units, dimensions and weight of each; total weight and volume; power consumption—standby and operate, relays actuated, etc.

The preceding specifications plus the external data are sufficient and necessary to describe the performance of a seismic amplifier accurately. If this type of data is consistently used, it will create a better understanding of the weaknesses and strong points of seismic amplifiers. Application of the data will result in better field records and a better understanding of those records obtained.

GEOPHYSICS, VOL. XXVI, NO. 5 (OCTOBER, 1961), PP. 550–559, 17 FIGS.

THE USE OF PHOTO-RESISTIVE CELLS AS LOSSER ELEMENTS IN A TRANSISTORIZED SEISMIC AMPLIFIER*

FRED W. HEFER†

Abstract: The usual advantages of transistorized amplifiers—lowered power consumption, lighter weight, improved compactness, and increased reliability—are often cited. A fifth consideration is improved performance.

One of the elements previously limiting amplifier performance is the AGC losser device. A photo-resistive device can approach five idealized requirements quite closely. The amplifier described uses four cells of photo-resistive material mounted in a common configuration. The four cells are illuminated from a common miniature lamp. Voltage for the lamp is derived from AGC control circuits. Resistance of the cells, and hence loss across them, depends on the level of illumination.

Temperature compensation is achieved for the entire amplifier by use of a "fifth" stage with current derived from it being fed back to the other four primary amplifying stages.

Amplifier performance and stability are illustrated by graphs of pertinent data.

INTRODUCTION

The use of semiconductors in the design and construction of geophysical field equipment yields several advantages compared to vacuum tube designs. Four of these are often mentioned and well known.

1. Lower Power Consumption
2. Less Weight
3. Improved Compactness
4. Increased Reliability

A fifth advantage to be considered is the possibility of improved circuit performance. This paper describes a transistorized amplifier design in which photo-resistive cells are used for losser elements. Performance obtained is illustrated by a series of graphs.

THE IDEAL AGC LOSSER

Figure 1 shows the basic element of a typical seismic amplifier. Control of input signals is accomplished by the feedback action of the AGC circuit with signal loss across each losser element in the amplifier signal path.

Figure 2 shows a typical AGC losser circuit. Most widely used in this circuit is a diode bridge arrangement similar to the one shown. If the elements of this bridge are "Perfect" and remain in such idealized condition, this type of circuit has relatively few disadvantages. However, in actual practice the ideal is only approached. Furthermore, deviation from desired conditions usually becomes wider as the amplifier is used in the field.

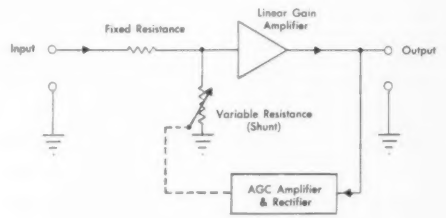

FIG. 1. Simplified block diagram of typical seismic amplifier.

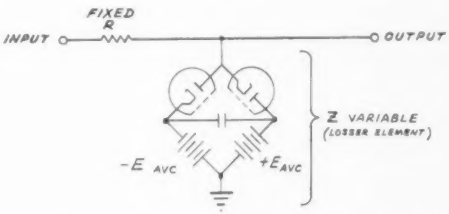

FIG. 2. Typical diode bridge AGC losser circuit.

* Presented at the 30th Annual Meeting, SEG, November 9, 1960. Manuscript received by the Editor January 24, 1961.

† SIE Division of Dresser Electronics, Houston, Texas.

CHARACTERISTICS OF AN IDEAL LOSSER ELEMENT

The Ideal Losser Element should:

1. be pure resistance,
2. cause no interaction in signal path when control voltage is applied,
3. have a large control range,
4. have a short time constant,
5. be a low noise element,
6. cause no distortion when the seismic signal is impressed across it, and
7. be stable with respect to time and temperature.

FIG. 3. Characteristics of an ideal losser element.

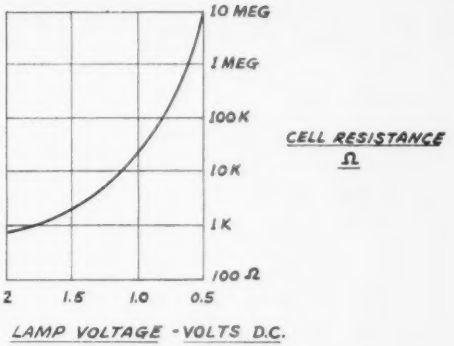

FIG. 4. Resistance of photo-resistive cell versus voltage applied to lamp.

Various other schemes of AGC control have been tried with varying degrees of success. To summarize this familiar subject, it can be said that an ideal losser element for use in seismic amplifiers should have the characteristics shown in Figure 3.

A photo-resistive element such as a cadmium sulfide or cadmium selenide cell possesses these characteristics to a marked degree. An AGC loop employing cadmium sulfide cells has proven to be better in almost all respects than conventional circuits.

Pure Resistance

A photo-resistive cell changes resistance as the illumination to which it is exposed changes. The cell acts as a variable resistor and therefore fulfills the first requirement of an ideal AGC element. The relationship between resistance and illumination level is a linear one in the resistance region of interest for operation of an AGC loop. However, it is well known that proper AGC operation requires nonlinear response within the loop. This necessary nonlinearity results from the exponential relationship between light output and voltage applied to an incandescent filament lamp. Figure 4 displays this property of the AGC element and illumination source being discussed.

No Interaction

Figure 5 shows a cluster of four such cells grouped around the AGC control element, the light source, and the placement of these elements in a seismic amplifier. Note that there is no direct electrical connection from the control element to the amplifier signal path. Undesirable interaction within the signal path is thereby eliminated. Coupling is accomplished *only* through the light path of the lamp. Thus, we fulfill the second requirement of having an element causing no interaction in the signal path.

Large Control Range and Short Time Constant

Our third requirement calls for a large control range; that is, a large resistance change within a practical change of illumination level. Resistance changes of 1,000-to-1 ranging from 1K ohm resistance to over 1 megohm can be achieved in this element. The practical limitations are the time constants of the cells. This is the ability to change resistance in a time shorter than the shortest AGC time constant, requirement four on the list. With this limitation, the practical control range can still include about 80-to-1 change in resistivity, a control range of about 38 db per cell. Since a number of cells can be placed in the circuit controlled by one loop, control ranges of 120 to 140 db are within practical limits.

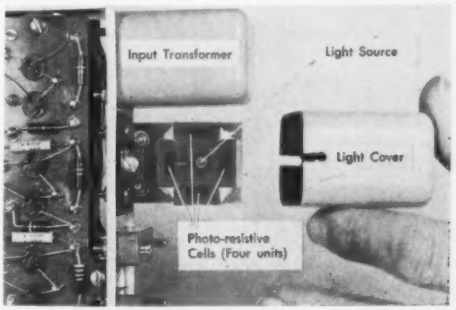

FIG. 5. Four AGC losser cells mounted around common light source.

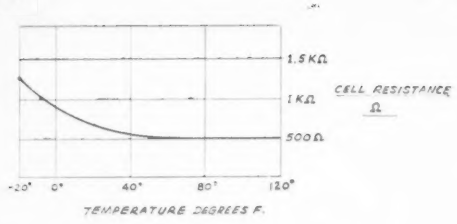

FIG. 6. Cell resistance versus temperature.

Low Noise

In respect to requirement number five, tests have shown that the noise level of the cell lies considerably under the noise level expected in a good seismic amplifier, making it possible to place a losser element in front of the first gain stage. This point will be discussed further.

No Distortion

It is well known that a diode losser bridge will produce distortion of the signal voltage across the bridge. The photo-conductive element does not produce distortion. Voltages as high as 100 VDC or AC can be handled, limited only by the maximum power dissipation of approximately $\frac{1}{4}$ to 1 watt per cell with cells of practical sizes. This fulfills requirement six.

Stability

The element is made stable versus time by embedding in clear epoxy or placement in a vacuum bottle. At low temperatures the cell changes resistance as shown in Figure 6. This change will affect the sensitivity of the amplifier but not the slope of the AGC curve. Other circuit means can be devised to minimize this effect. For practical application, the cells can be matched to ± 25 percent at any point of their resistance curves.

Losser Location

Vacuum tube amplifiers work at high impedance levels looking into the input of the amplifier stage. Because of this, the variable impedance used, the AGC losser, is placed as a shunt element in parallel with the input impedance (Figure 7). When the input signal is small, the variable impedance is a high value and minimum loss occurs. At the same time, the vacuum tube requirement of high input impedance for maximum signal-to-noise ratio at low signal levels is fulfilled. On the other hand, transistors are basically current amplification devices with low input impedance at the amplifier input terminals. Transistors, at the same time, demand low input impedance for optimum signal-to-noise ratio. Values of one to two K ohms yield the best results. To devise a shunt element with a practical ratio of minimum to maximum resistance, minimum fixed loss and optimum input impedance for low noise stages become a problem in transistor circuits. The logical solution here is the placement of the losser as a *series* element. Since photoresistive cells are circuit-wise "floating variable resistors" not requiring any electrical ground termination, they are ideally suited for this circuit arrangement. Figure 8 shows the AGC losser arranged as a series element.

Noise of Transistors versus Vacuum Tubes

The discussion of circuit noise in seismic amplifiers will be limited to a viewpoint of practical application. Basically, it can be said that modern transistors *can* outperform vacuum tubes in respect to signal-to-noise ratio in the *band pass* and at the *impedance levels* in which a seismic amplifier has to work. Transistors have the obvious advantage of freedom from hum and microphony. Their noise figures show more consistency versus life than vacuum tubes. Their low impedance levels guarantee more freedom from pickup of

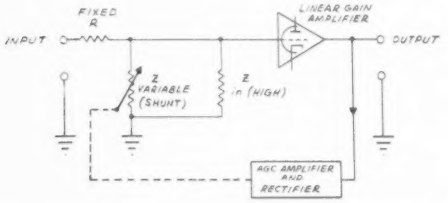

FIG. 7. Typical vacuum-tube amplifier with variable AGC element in parallel with high input impedance.

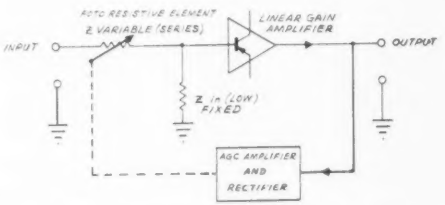

FIG. 8. Transistor amplifier with AGC losser as series element.

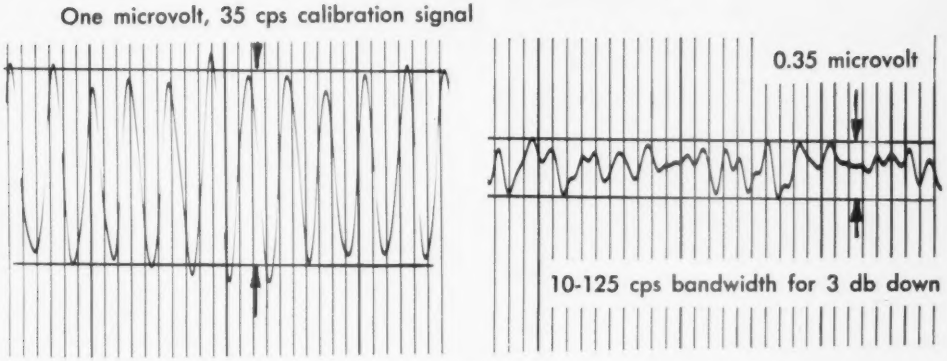

FIG. 9. Oscillographic record showing noise from transistorized seismic amplifier.

numerous sources often so troublesome to cure in multichannel seismic amplifier systems of vacuum tube design. A low noise transistor amplifier stage demands *specific* input resistance, collector current, and voltage. The oscillographic record of Figure 9 shows the circuit noise of a standard transistor amplifier. The noise figure includes an insertion loss of approximately 6 db in the first losser element and no step-up in the input transformer. The first stage works at an impedance level of approximately 2,500 ohms, 0.3 milliamps collector current, and 2 volts collector voltage. The noise of 0.335 microvolt is measured on a peak-to-peak basis over a time interval of 0.3 seconds. The calibration signal is a one microvolt rms signal at 35 cps displayed on a peak-to-peak basis. The pass band is 3 db down at 10 cps and 125 cps. The next oscillographic record in Figure 10 shows the low-frequency electronic noise of a transistor refraction amplifier. The pass band is 3 db at 1 cps and 20 cps. The source impedance is 6,000 ohms.

PERFORMANCE DATA

Steady-State Control and Burst-out Distortion

Figure 11 shows the steady-state and "overshoot" or burst-out characteristics of the amplifier, including distortion figures under AGC control. The maximum gain of this amplifier is limited through a DC clipper arrangement on a lamp driver stage. This clipper will limit the lamp voltage, and hence the maximum brilliance of the lamp, to a value where the series resistance of the losser elements in the amplifier signal path will limit the

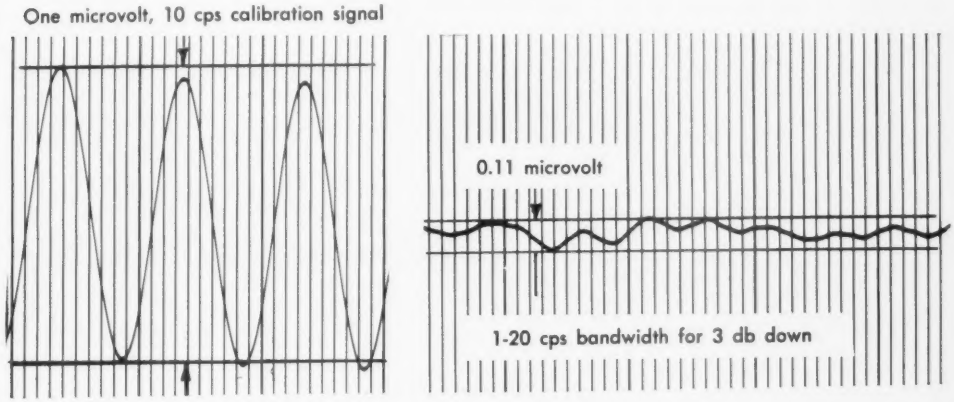

FIG. 10. Low-frequency noise in transistorized seismic amplifier.

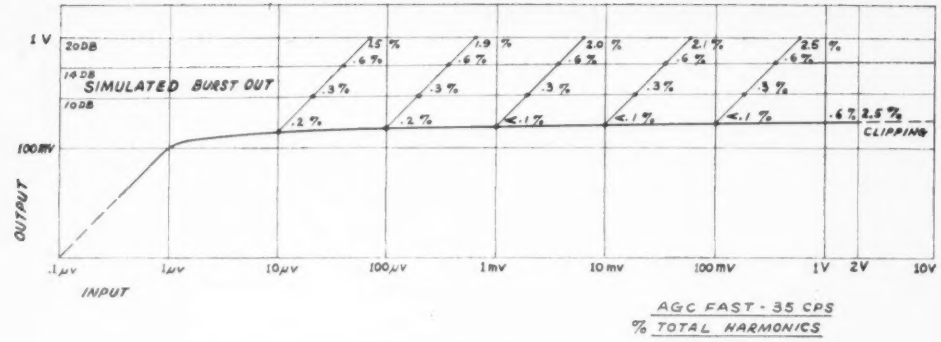

FIG. 11. Steady-state AGC action including burst-out distortion for seismic amplifier embodying design principles described.

maximum linear gain to 100 db.

The following nonlinear portion of the AGC curve rises 6 db over the range of 120 db of input signal. The "stiffness" is determined by the gain in the overall AGC loop. This stiffness can be adjusted from a minimum of approximately 3 db rise of ouptut signal to a linear gain condition through a control on the input of the AGC amplifier. Consequently, the burst-out condition of the amplifier can be simulated by increasing the input signal and decreasing the gain in the AGC amplifier which will cause a rise of signal level through the amplifier and at the output terminals. The distortion values are total harmonics measured on a typical amplifier.

The distortion figures shown in Figure 11 constitute an improvement over conventional vacuum tube design.

AGC Control at Low Frequencies

The graph of Figure 12 demonstrates the ability of this amplifier to control the amplitude of a sig-

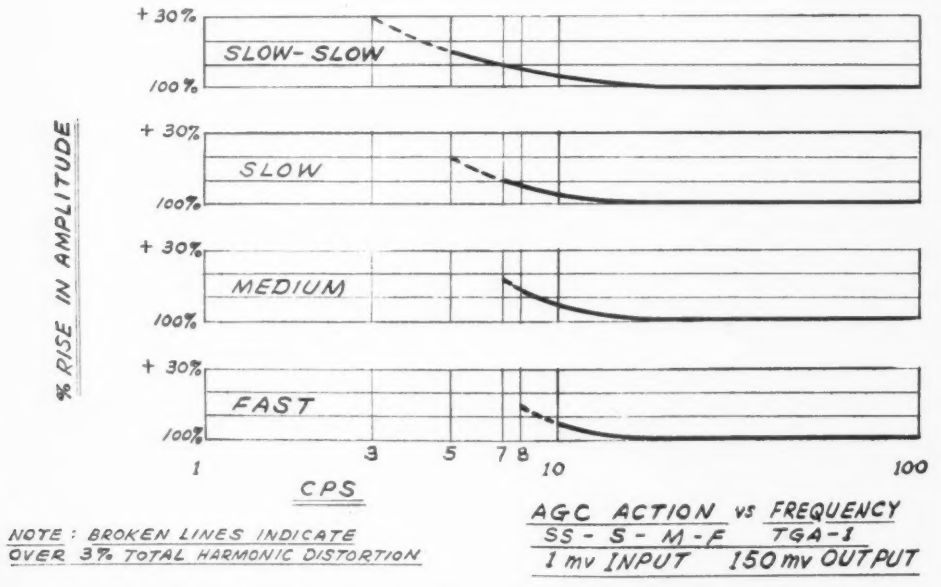

FIG. 12. AGC control throughout amplifier pass-band including low-frequency action.

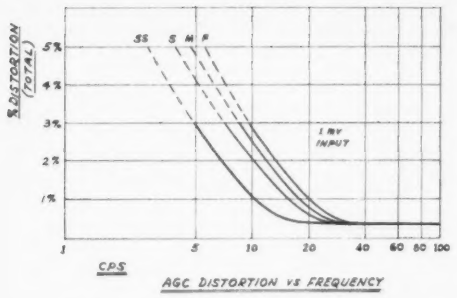

FIG. 13. AGC distortion at low frequencies.

nal throughout the amplifier pass band. Control of the signal amplitude can be properly achieved only if the AGC acts on the envelope of a signal, not on the instantaneous signal amplitude values. As the signal reaches a lower frequency region, control during the duration of a cycle occurs, causing rise in amplitude and distortion. An AGC loop with photo-resistive elements shows considerably better control characteristics and lower distortion than is found in loops with diode bridges. In the latter, control action during a cycle simulates a DC unbalancing condition causing the loop to lose control at considerably higher frequencies. The "slow-slow" position of the new transistorized amplifier will allow control of frequencies as low as five cycles with approximately 3 percent distortion at this frequency. The amplitude rises approximately 15 percent over mid-spectrum values. This position makes possible low frequency refraction recording under AGC control for the recovery of secondary or deeper arrivals.

The rise of distortion as input voltage frequency is lowered, and the recovery-attack times of the AGC are of interest in evaluation of a seismic amplifier. Figure 13 shows the total harmonic distortion at four different time constants. Between "fast" and "slow-slow," frequencies from 10 to 5 cps respectively are under AGC control if a distortion of 3 percent is acceptable. It is interesting to mention that the loop is under full control at all input levels up to 1 volt

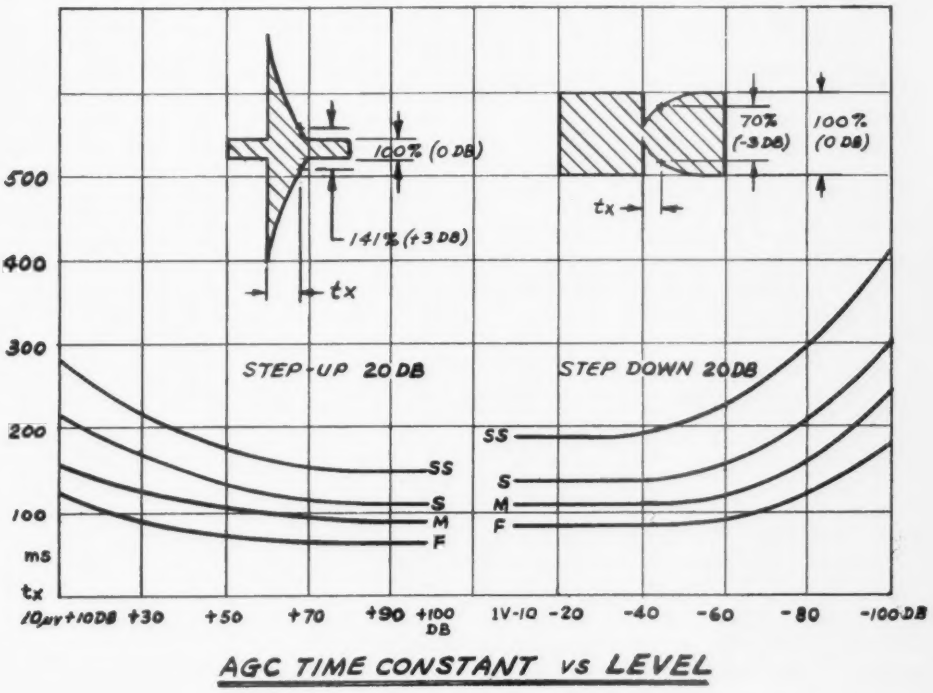

FIG. 14. AGC time constants for various input signal levels.

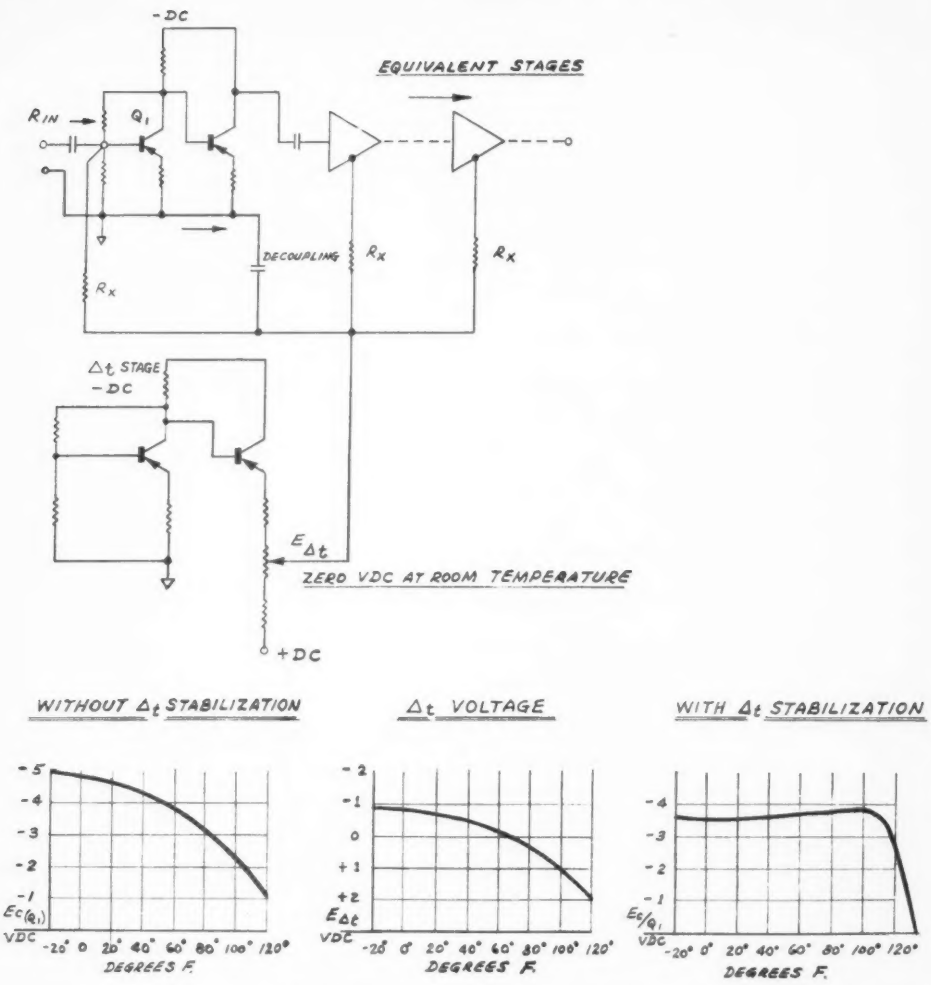

FIG. 15. Temperature stabilization technique.

within its normal dynamic burst-out range of approximately 20 db.

Attack and Release Time Constants

The attack and release time constants are shown in Figure 14 for 20 db step-up or step-down in signals. T_x in milliseconds (recovery or release time) is indicated as the time it takes the signal to recover within 3 db of the final amplitude. The time constants shown provide good, rapid, front-end control after first arrivals. Equalization of the attack and release time has been indicated through field tests to be better in controlling the incoming energy throughout the body of the records. Other common specifications such as frequency, phase response, filter curves, etc., do not vary greatly from conventional vacuum tube systems and are, therefore, of no interest in the frame of this discussion.

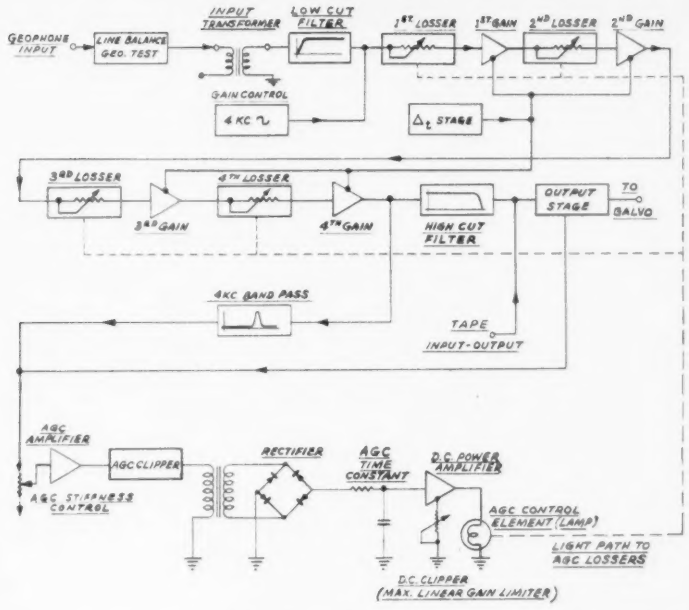

FIG. 16. Block diagram of complete channel of transistorized seismic amplifier described in paper.

Temperature Stabilization (Figure 15)

Commonly used methods of environmental temperature stabilization by means of DC feedback through emitter resistors, feedback from the collector to the base, or stabilization through thermistors have some drawbacks in consideration of the requirements on a seismic amplifier with respect to extreme low-frequency response, high gain, and constant input impedance. An amplifier stage can be devised optimizing on impedance, gain, and signal-to-noise ratio through moderate amounts of DC and AC feedback. This amplifier stage usually will not be stable with temperature changes. Its I_{co} will change considerably with changes in temperature. Having one or more equivalent amplifier stages to be controlled, this can be achieved by duplicating the thermal characteristic of these stages through adding an equivalent stage and feeding its change of collector voltage versus temperature through proper attenuation, decoupling, and DC cancelling at room temperature to the base of each of the other amplifier stages. The effectiveness of the arrangement is somewhat dependent on the similarity of the I_{co} and h_{fe} parameter which can be selected. This means of temperature stabilization is effective in the temperature range from $-20°$ to $+120°$ F if adequate control voltage through initial self-biasing is provided. The necessary resistive network can be calculated as

$$R_x = \frac{h_{fe} \times R_{in}}{2} - R_{in}$$

where

$R_x = \Delta t$ correction-voltage feed resistor,
h_{fe} = d-c forward current transfer ratio (for common emitter circuit), and
R_{in} = input resistance.

AMPLIFIER BLOCK DIAGRAM

Figure 16 shows the block diagram for one channel of the complete transistorized seismic amplifier. The line balance and geophone test circuitry is followed by the input transformer. This transformer has a step-up ratio of 1:2. The low-cut filter is placed on the secondary of the input

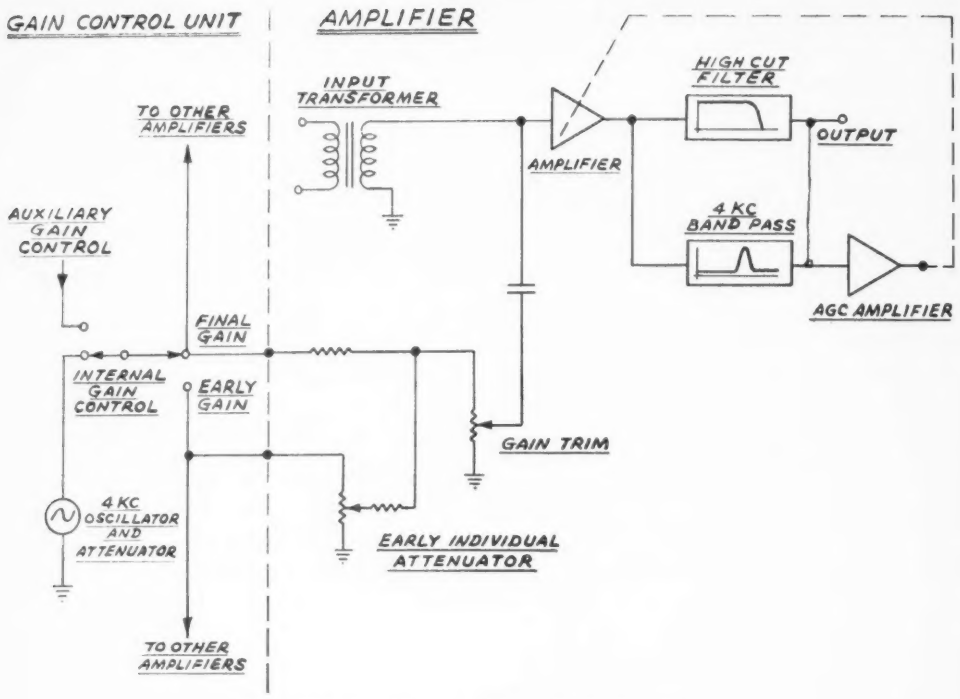

FIG. 17. Gain control circuits of transistorized amplifier.

transformer outside the AGC loop. A magnetic latching type relay, needing only a short pulse for switching and no holding current, controls the "in" and "out" positions for this filter. The filter is of constant K design with 18 and 36 db per octave slopes, fixed termination, variable L and C's. The cutoff frequencies are logarithmically spaced from 16 to 135 cps in ten positions. The first losser element is placed ahead of the first gain stage assuring optimum dynamic condition for this first stage. The following three stages of gain and three series losser elements provide optimum balance of gain and attenuation throughout the input signal range of 120 db. Each gain stage exhibits approximately 32 db of gain. Each losser is capable of 36 db attenuation. The fixed insertion loss of each losser at maximum gain amounts to approximately 6 db per losser. The high-cut filter with choice of 18 or 36 db per octave slopes has also fixed termination, variable L, and variable C's. Ten positions of cutoff frequencies from 23 to 235 cps are provided. Remote filter switching is done by a magnetic latching type relay. The output to the galvos is RC coupled, eliminating the need of an output transformer. An AGC amplifier stage provides additional gain before clipping of the AGC signal for equalization of release and attack time constants. A full-wave rectifier circuit converts the AC signal to the DC control voltage. After application of the desired time constant, this DC signal is fed to a DC power amplifier which drives the illumination source for the AGC elements.

GAIN CONTROL

Gain control in the amplifier is achieved through insertion of a 4-KC rider signal on the input of the amplifier as shown in Figure 17. The rider bypasses the high-cut filter and will react on the AGC DC control voltage with the same effect as a signal in the pass band. Consequently,

a linear change in rider voltage will provide a nearly linear change in gain of the amplifier. The nonlinearity amounts to 6 db, the slope of the AGC curve, throughout the control range of 120 db. Only one signal source is needed for control of all amplifiers in one system, allowing the use of a single master gain control for all amplifiers. Early gain and final gain signals are independent from each other. The early gain signal has provision for attenuation on each individual amplifier for tapering of first arrivals.

Programmed gain control is possible through insertion of an *auxiliary* 4-KC signal. The 4-KC signal amplitude can be programmed to vary the gain of all amplifiers in lieu of the regular AGC with a very short time constant. This method of gain control is very well suited for conducting amplitude studies of seismic energy.

CONCLUSION

All the normally-used attributes of transistor design can be coupled with a photo-resistive cell as the losser element to produce a seismic amplifier with desirable performance characteristics.

GEOPHYSICS, VOL. XXVI, NO. 5 (OCTOBER, 1961), PP. 560-573, 10 FIGS.

A CRUSTAL STRUCTURE REFRACTION SURVEY IN SOUTH TEXAS*

IRA H. CRAM, JR.†

Abstract: On August 11, 1960, sixty oil exploration and research seismograph crews attempted to record two shots detonated in the Texas Gulf Coastal Plain. Shotpoint *A* was located 16 miles northwest of Cleveland, Texas. Shotpoint *B* was located 27 miles northwest of Victoria, Texas. The shotpoint line is approximately parallel to the strike of the Cenozoic sediments and the distance between shotpoints is 260.2. km. More than 3,000 lb of explosives were placed in five holes at each shotpoint. The top of the charge was at a depth of 95 ft and the bottom at 250 ft at each shotpoint. The regional Bouguer anomaly is −25 mgal. The shot instant was keyed to a 140 cps reference signal transmitted by radio station KTRH, Houston, Texas. First and later refracted arrivals were used to determine the velocity structure which was supported by events identified as reflections from the refractors. The results indicate the following thickness-velocity relationships: 2.0 km of 2.3 km/sec material, 5.3 km of 3.94 km/sec material, 12.5 km of 5.38 km/sec material, and 13.2 km of 6.92 km/sec material. The Mohorovicic discontinuity is represented by a velocity of 8.18 km/sec, and the total crustal thickness is 33.0 km.

Possible geologic identities of the refractors are as follows: the 2.3 km/sec and 3.9 km/sec layers represent the Cenozoic and Mesozoic sediments, the 5.4 km/sec layer represents Paleozoic and Precambrian rocks, the 6.9 km/sec layer is the high-velocity crustal layer, and the 8.18 km/sec zone represents upper mantle material.

The South Texas velocity section appears to correlate well with adjacent measurements in the Gulf of Mexico and in northeastern Arkansas.

INTRODUCTION

The Texas Coastal Plain is probably the most geologically and geophysically investigated area in the world. These investigations have, of course, been restricted to the upper part of the sedimentary section in the search for petroleum. Prior to 1960 no long offset seismic refraction profile had been shot to determine the crustal structure beneath the Texas Coastal Plain. Richards and Walker (1959), with the cooperation of the oil industry, demonstrated in the Alberta Plains of Western Canada that standard exploration seismograph equipment could be used to delineate deep crustal structure.

The Texas Coastal Plain is a natural area for a cooperative venture of this type because of the tremendous amount of seismic work being conducted continuously. Late in the spring of 1960 a number of oil and geophysical companies were contacted to ascertain the feasibility of conducting a cooperative project to determine the depth of the Mohorovicic discontinuity and the sedimentary thickness beneath the Texas Coastal Plain. The companies were receptive to the idea, so arrangements were made for obtaining explosives, permitting shotpoints, drilling shot holes, and providing a suitable time synchronization system. On the shot date, August 11, 1960, sixty exploration and research seismic field, parties located in southwestern Louisiana, east and south Texas attempted to record two shots which were detonated at 15:35 and 14:08 CST.

LOCATION, INSTRUMENTATION, AND RECORDING

Location of Shotpoints and Recording Stations

Both shotpoints were located by short plane table surveys run from existing control points. The geographic coordinates of the recording stations were supplied by the individual field parties. These coordinates were determined to the nearest second from the base maps in use on the individual field parties, and the accuracy of the coordinates is assumed to be ±1 second. The base maps used were produced by many different organizations, and it has been assumed that no error has been introduced into the coordinates because of map differences.

The Profile

Shotpoint *A* is located approximately 16 miles northwest of Cleveland, Texas. Shotpoint *B* is located approximately 27 miles northwest of

* This paper is a portion of a thesis submitted to the faculty of Rice University in partial fulfillment of the requirements for the degree of Doctor of Philosophy.

† Pure Oil Co. Research Center, Crystal Lake, Illinois.

Victoria, Texas (Figure 1). The distance between the shotpoints is 260.2 km. The bearing of the shotpoint line is N 39 E which is approximately parallel to the strike of the Cenozoic sediments (N 44 E) in the area. Figure 1 shows the areal distribution of the shotpoints and recording stations which did record refracted energy. It can be seen that the recording stations do not lie on a straight line. The reason for this is that the field parties recorded the shots at production locations on their own prospects. Individual spread lengths varied from 0.27 km to 1.51 km and were more or less randomly oriented with respect to the shot aximuth. The area covered by the survey is approximately 20,000 sq mi, excluding the two stations to the west and the one to the northeast. Arrival times from these three stations were not used in determining the velocity structure.

Shotpoints

Shotpoint *A* was a five-hole pattern. The pattern was T shaped with 50-ft hole spacing. The holes were drilled to a depth of 250 ft using a 5¼-inch bit and were loaded from 95 to 250 ft in depth. The holes were plugged with gravel. The total charge at shotpoint *A* was 3,300 lb of 60 percent dynamite. The cap leads were connected in series for shooting.

Shotpoint *B* was a five-hole pattern. The shape of the pattern was pentagonal with 50-ft hole spacing. The hole diameters and charge distribution were not uniform, but over-all the holes were loaded from 93 to 250 ft in depth. The holes were plugged with gravel. The total charge at shotpoint *B* was 3,080 lb of 60 percent dynamite. The cap leads were connected in parallel for shooting.

Time Synchronization System

The selection of a suitable time synchronization system was of the greatest importance to the success of the project. In order to obtain maximum participation, the system had to be simple. It had to require no major modification of standard equipment, and it had to be able to be recorded throughout the intended survey area. Several methods were considered. Keying the project to station WWV, Bureau of Standards Time Signal, or transmitting a time signal and/or time break by short-wave radio were rejected for two reasons. First, these methods would have required that all recording stations have short-wave radio receivers, and it was felt that this additional requirement would have reduced the total number of participants. Second, short-wave reception is generally unreliable during daylight hours, and the shots were going to be detonated during normal working hours. The possibility of using the telephone system to send a time break over wire was also investigated. This method was rejected because it would have been necessary to designate the actual locations of the recording stations several weeks in advance of the shot date. Since the locations of the recording stations would become known only after the shots were detonated, this was impossible. Finally, the standard broadcast band was considered. Radio station KTRH (740 kc) in Houston, Texas, agreed to transmit a time synchronization signal. The signal consisted of two parts. The first part was a voice alert. The second part was an interrupted 140 cps tone of approximately 10.6 seconds total duration. This signal was transmitted three times on the shot date at predesignated times. The third signal was a precaution against a misfire at one of the shotpoints. Figure 2 exhibits the 140 cps reference tone, the time break, and the refracted arrivals at shotpoint *B*. By referring the time break to the reference signal, the time break can be transferred to all recordings obtained from shotpoint *B*. This timing system proved to be excellent.

Geophones, Amplifiers, and Recording

It should be pointed out that the instrumentation of this project was not optimum. This was unavoidable because seismograph equipment operating on the Texas Coastal Plain is reflection equipment. According to work done by Veitsman (1957) in the U.S.S.R., the frequency of the refracted arrivals from the deep crustal layers was expected to be in the range 9–14 cps. The response of the reflection equipment at these low frequencies was expected to be poor. The situation could be improved by using low-frequency geophones (2, 4.5, 7.0 cps), and all participating field parties were urged to obtain low-frequency geophones if possible.

The participants were requested to record the shots in the lowest possible filter settings with the maximum permissible gain and no automatic gain control. Each participant was asked to record one 150-ft roll of recording paper for each shot (about 2 minutes at normal camera speeds) and to send the undeveloped recordings to Rice University for developing.

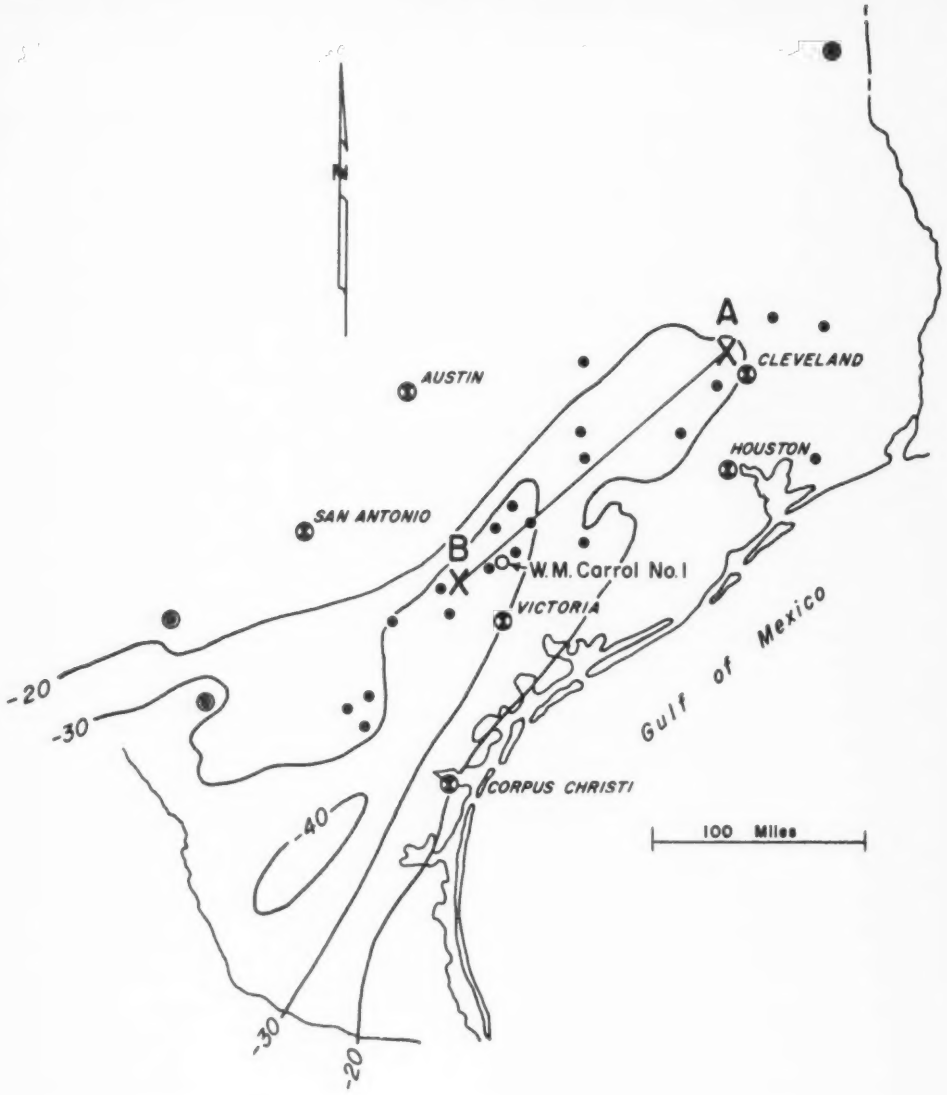

FIG. 1. Approximate Location of Shotpoints and Recording Stations.

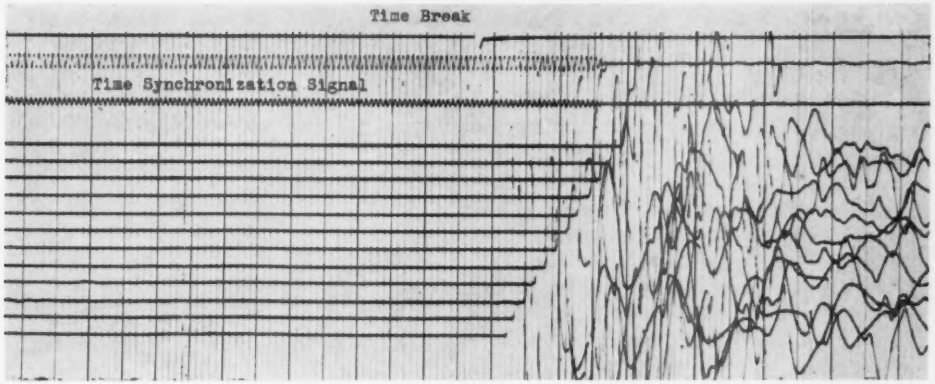

Charge: 3080 lbs
Offset: 0.10-0.43 km N 45 E

FIG. 2. Time Break at Shotpoint *B*.

Recording Statistics

Sixty field parties attempted to record the shots. Twenty-six parties did record identifiable refracted energy from one or both shotpoints. It should be stated clearly that there were a number of valid reasons for not recording identifiable refracted energy. On the shot date there was a stationary rain front over most of the survey area which was accompanied by scattered thunder showers. Due to this weather front, the desired maximum gains generally could not be used. The equipment in use was primarily reflection equipment, and the response in the lower frequency ranges was poor, especially at great distances. Locally there were other background disturbances which could not be controlled, such as airplanes, railroad trains, highway traffic, etc.

The maximum distance at which recording was attempted was 535 km. The maximum distance at which refracted energy was identified was 269.2 km. Table 1 summarizes the range-response statistics of the survey. The average distance of the stations that recorded identifiable refracted energy was 114 km from the source. The average range of the stations which did not record refracted energy but were within the maximum recorded range was 214 km. The remainder of the stations were at an average range of 401 km from the source.

In an attempt to remove the effect of the weather, that is, to predict what would have happened had the weather conditions been optimum, it has been *assumed* that the amplitude of the refracted arrival is inversely proportional to the square of the distance from the source. Then, choosing a reference amplitude (A_1) at a range of one kilometer, a number N can be defined as follows:

$$N = 10 \log \frac{A_x}{A_1} = -20 \log R_x$$

where A_x and R_x are the amplitude and range at distance x from the shotpoint. This number N is assumed to be comparable to dbv (decibel-volts). Figure 3 is a plot of N against R. Table I shows that the average range of crews which did record energy is 114 km. Figure 3 indicates that at a range of 114 km $N = -41$. If it is assumed that

Table I. Range-Response Statistics for Crews Attempting to Record Shots*

Group	Avg. Rn. (km)	Avg. Geophone Frequency	Down db @ 10 cps
Did Record†	114	11.1	3.7
Did not Record (Less than 269.2 km)	214	15.0	4.0
Did not Record (More than 269.2 km)	401	13.2	1.9

* Data exclude crews reporting outside disturbances such as highway traffic, airplanes, etc.
† Maximum distance recorded was 269.2 km.

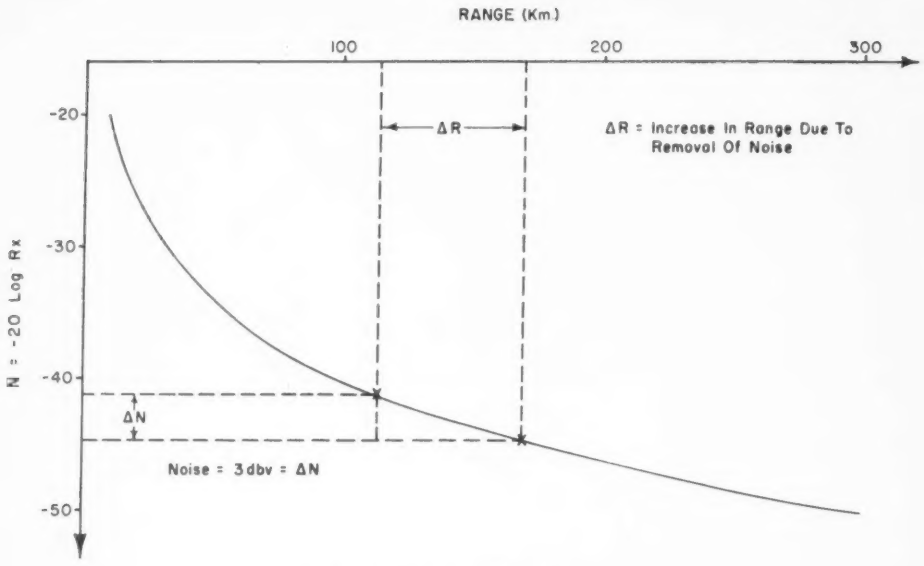

FIG. 3. Amplitude Attenuation Curve.

the background noise increased 3 dbv because of the weather, it can be seen that by removing the background noise it would have been possible to record $N = -44$. This corresponds to increasing the range to 160 km.

The same logic can be applied to the geophones. If it is accepted that a five-cycle geophone is optimum (or at least the most satisfactory of the less expensive commercially available geophones), then the gain loss due to the high frequency geophones is approximately 6 dbv. This indicates that with the five-cycle geophones it would have been possible to record $N = -47$, which corresponds to an average range of 220 km.

These figures are approximate and subject to the *assumptions* made. They do indicate, however, that with optimum weather conditions and low-frequency geophones, the effective average range would have been more than doubled.

Organization and Operating Time Used

The organization of this project took approximately two months. The actual time required to record all three time synchronization signals was 1.25 hours. As reported by the individual field parties, the actual recording time used was 2.95 hrs./crew, the field preparation time was 3.12 hrs./crew, and the office preparation time was 3.25 hrs./crew. Seven full days, plus one day travel time, were needed to drill the two shotpoint patterns.

COMPUTATION PROCEDURES

Distance Computations

The distances between shotpoints and recording stations were calculated by a method presented by Richter (1943). Using this method, distances up to 555 km can be calculated, with an error not exceeding 0.1 km, from the following expression:

$$R = \Delta x \sec \theta = \Delta y \csc \theta$$

where

$$\theta = \arctan (\Delta y / \Delta x),$$
$$\Delta x = A \Delta \lambda,$$
$$\Delta y = B \Delta \phi.$$

In these formulae R is the required distance between the two points, $\Delta\lambda$ and $\Delta\phi$ are the differences in minutes of longitude and latitude of the two points, A and B are the lengths in kilometers of one minute of latitude and longitude at the mean latitude of the two points, and θ is the angle between the latitude and R. Richter (1958) has

tabulated A and B at intervals of one degree from 0° to 70°. He has also tabulated (1943, 1958) A and B at intervals of one minute from 30° to 40°. For this project, Richter's tables were extended from 27° 45′ to 29° 59′.

Refraction and Reflection Computation

The computational procedure used to determine the layering has been a standard method for a number of years (Nettleton, 1940; Jakosky, 1950; Officer, 1958; Dobrin, 1960). The fundamental assumptions are as follows:

1. Each layer is bounded on top and bottom by planes.
2. Each layer transmits seismic waves with a constant velocity.
3. At the interface between two layers the seismic ray is bent according to Snell's Law.
4. The travel time will be unchanged by an interchange of shotpoint and recording station (Reciprocity Principle).
5. The layers are horizontal.

If the above assumptions are correct, then a time-distance plot of the refracted arrivals from one refractor will lie on a straight line which has an equation of the form

$$T = x/V + T_i \qquad (1)$$

where T is the travel time, x is the distance, V is the velocity in the high velocity layer (refractor), and T_i is the intercept time at $x=0$. The general equation for the (m-1) layered case can be conveniently written in the following form:

$$T_m = \frac{x}{V_m} + 2\sum_{n=1}^{(m-1)} \frac{h_n\sqrt{V_m^2 - V_n^2}}{V_m V_n} \qquad (2)$$

where h_n is the layer thickness.

Using the same assumptions, the time-distance curves for the reflected arrivals are given in parametric form for the (m-1) layered case by the following equations:

$$X = 2\sum_{n=1}^{(m-1)} \frac{h_n V_n P}{\sqrt{1 - P^2V_n^2}}$$
$$t = 2\sum_{n=1}^{(m-1)} \frac{h_n}{V_n\sqrt{1 - P^2V_n^2}} \qquad (3)$$

where h_n is the thickness of a particular layer with velocity v_n, t is the two-way travel time, x is the distance from the source, and P is the ray constant.

TRAVEL TIME CURVES AND THICKNESSES

The original intent had been to reverse the profile. However, after the initial examination of the records and tentative time-distance plots of the first arrivals had been made, it was concluded that the data were insufficient to consider the profile reversed. It was decided to plot all of the first arrivals on one time-distance plot regardless of source or azimuth. From this combined time-distance plot a tentative velocity structure was computed. Since the profile is not reversed, this procedure necessarily assumes that the various refractors are horizontal. This is believed to be a reasonable assumption since the majority of recording stations are more or less on strike (Figure 1). The records were then re-examined for second and later arrivals which would either prove or disprove the velocity structure obtained from the first arrivals. It was found that the later arrivals which were present appeared to substantiate the initial time-distance plot of the first arrivals. In most cases where the local spread directions were within 30° of the shotpoint azimuth, the apparent velocities across these spreads were useful in determining the velocity layer from which the event was refracted.

The velocities and intercept time were determined by the method of least squares. In Figure 4 the lines computed from equation (1) are shown along with the first and later arrivals used in the least square computations. Using equation (2), the thicknesses of the layers were computed from the intercept times and the following values for velocity and thickness were obtained:

Velocity (km/sec)	*Thickness (km)*
2.3	2.0
3.94±0.03	5.3
5.38±0.06	12.5
6.92±0.03	13.2
8.18±0.05	

where the velocity 2.3 km/sec is slightly less than the average velocity computed from, 6,000 +0.6z, ft/sec and the ranges indicated for the other velocities are the probable errors. The depth of the Mohorovicic discontinuity (8.18 km/sec refractor) is 33.0 km.

Having obtained the velocity-thickness relationships shown above, it was decided to re-

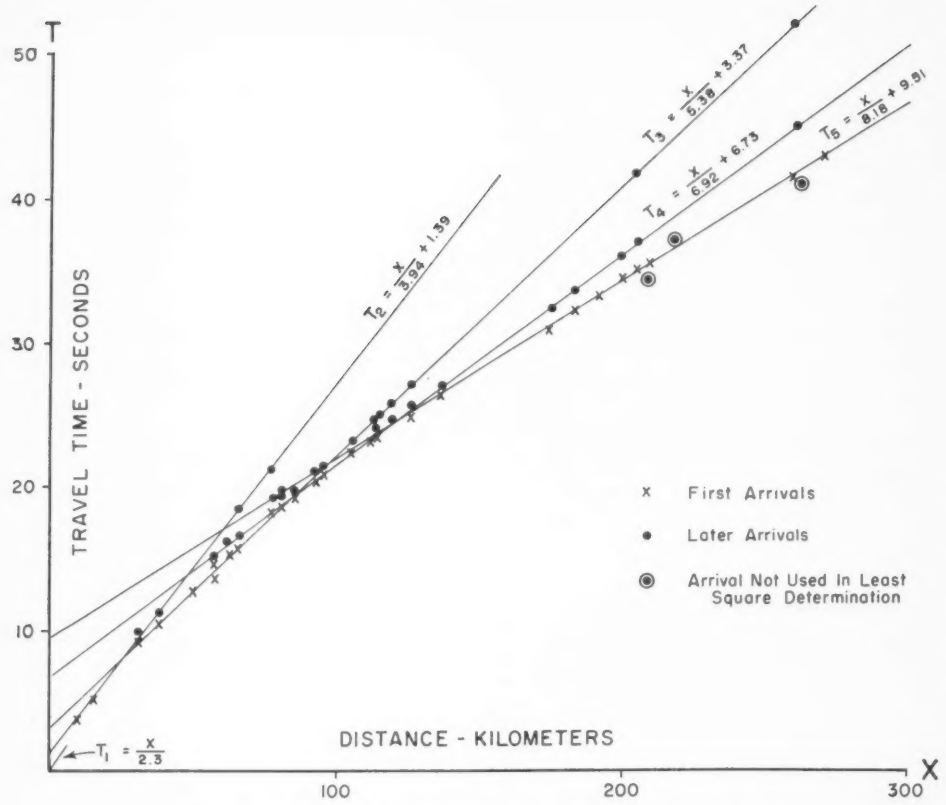

FIG. 4. Time-Distance Curves of Refracted Arrivals.

examine the records in an attempt to identify reflections from the refractors. Using the velocity-thickness data obtained from the refraction results and equation (3), the four reflection time-distance curves shown in Figure 5 were computed. Also shown in Figure 5 are events which have been interpreted as reflections. The short line segments represent events which have been interpreted as reflections from the refractors. The slope of these line segments is the approximate observed moveout reduced to a 2-km spread length and corrected for azimuth.

The interpretive procedure outlined above is extremely useful for sorting out events seen on long offset recordings. Figure 6 is presented as evidence of the utility of this interpretive technique. The events marked on the record have been identified as follows:

1. The first event (T_3) is interpreted as the refracted arrival from the second refractor.
2. The second event (T_4) is interpreted as the refracted arrival from the third refractor.
3. The third event (t_3) is interpreted as the reflected arrival from the third refractor.
4. The fourth event (t_2) is interpreted as the reflected event from the second refractor.
5. The fifth event (t_4) is interpreted as the reflected event from the fourth refractor.

The approximate ray paths are illustrated in Figure 7.

Two more records are shown in Figure 8. The various events which can be seen on these records are identified in Figure 8. The quality of the records presented in Figures 6 and 8 is better than the average for the survey.

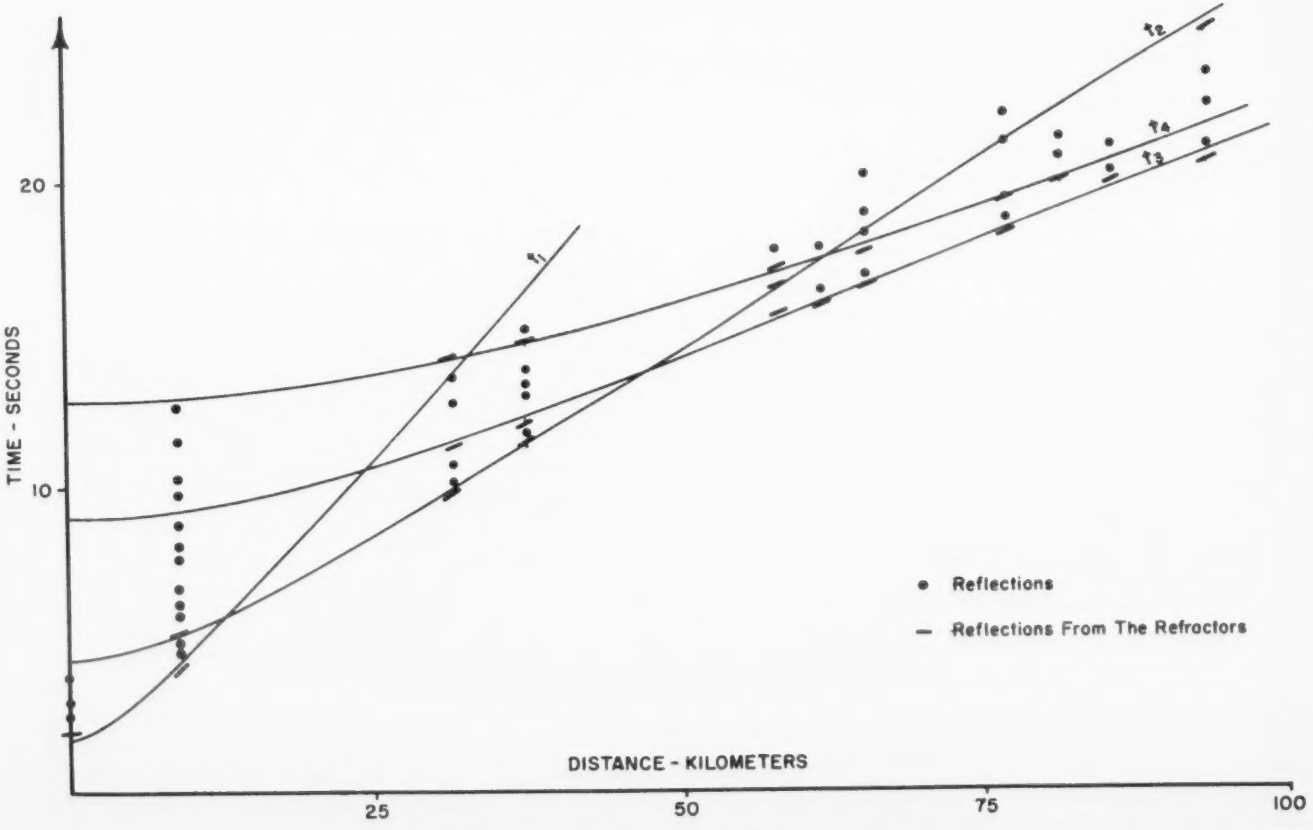

FIG. 5. Time-Distance Curves of Reflected Arrivals.

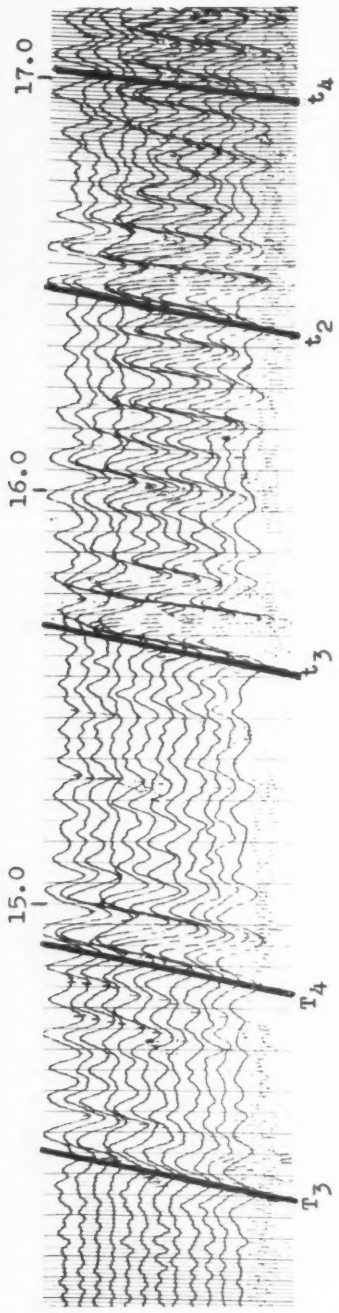

Source: Shotpoint *B*
Offset: 58.3 km N 74 E

Fig. 6. Specimen Record (See Figure 7 for Ray Paths).

The critical distances and cross-over distances were computed and are tabulated below

	Critical Distance (km)	*Cross-over Distance (km)*
1st Refractor	3	8
2nd Refractor	13	29
3rd Refractor	39	81
4th Refractor	71	125

The above information indicates, for example, that the refracted arrival for the third refractor cannot exist at ranges less than 39 km and that it is the first arrival in the range 81 km to 125 km.

It was mentioned earlier that the arrival times from the most northerly and the two most westerly recording stations (Figure 1) were not used in the least squares calculations. These stations are isolated from the main body of recording stations by distances of 100 km to 215 km. In Figure 4 the arrival times from these stations have been plotted. It can be seen that these arrival times fall close to the 8.18 km/sec line suggesting that the crustal thickness may be more or less constant under the entire Texas Coastal Plain region.

GRAVITY & MAGNETIC DATA

Woollard (1959) has studied the relationship between the magnitude of the Bouguer anomaly and the depth of the Mohorovicic discontinuity. He indicates that the relationship is exponential and that the slope of the curve at the seacoast is approximately 14.5 mgal/km. Seismic and gravity data indicate that the depth of the Mohorovicic discontinuity for the seacoast section is −32.0 km (Woollard, 1959). If the above assumptions are correct, it is possible to estimate the depth of the Mohorovicic discontinuity if the regional Bouguer anomaly is known. Figure 1 shows the Bouguer isogals (Logue, 1954) for the Texas Coastal Plain region, and the regional Bouguer anomaly is estimated to be approximately −25 mgal. Applying this concept to the survey area, the estimated depth to the Mohorovicic discontinuity is 33.4 km, which is in good agreement with the 33.0 km obtained from the refraction data.

Magnetic data presented by Nettleton (1952) suggest that in the vicinity of the South Texas profile the depth to the basement is about 10.7 km.

GEOLOGIC INTERPRETATION OF THE REFRACTORS

Possible geologic identities of the refractors are as follows:

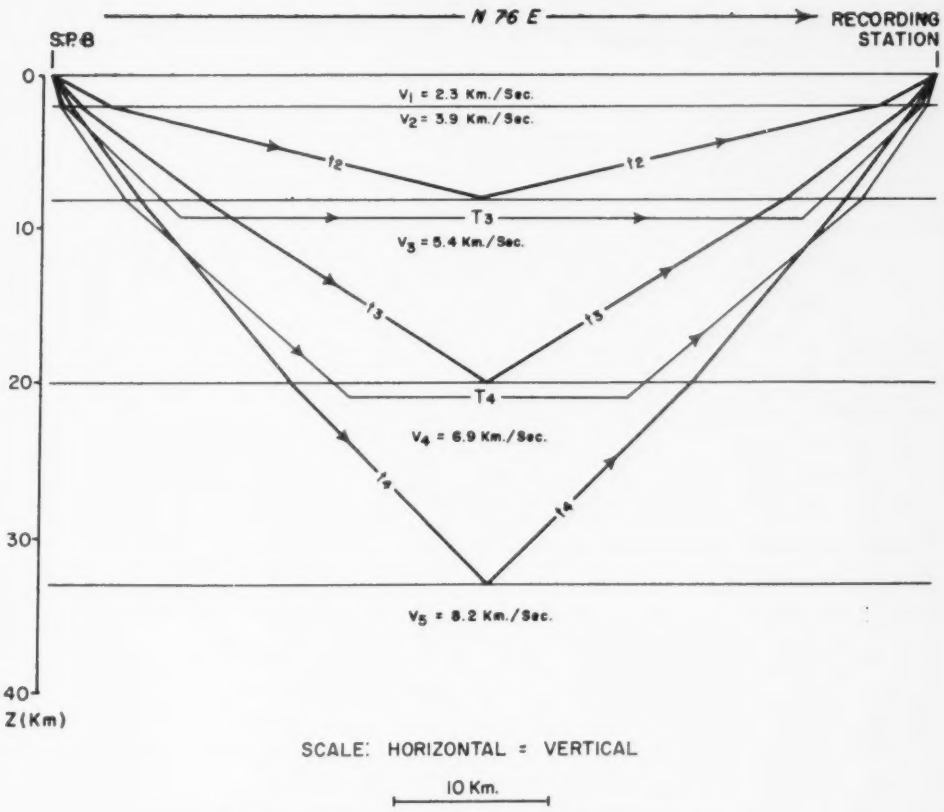

FIG. 7. Approximate Ray Paths for Specimen Record (Figure 6).

1. The 2.3 km/sec and 3.9 km/sec layers represent the Cenozoic and Mesozoic sediments.

2. The 5.4 km/sec layer represents Paleozoic and Precambrian metasediments and acidic igneous rocks. Utilizing the magnetic data (Nettleton, 1952) the depth to the magnetic basement is approximately 10.7 km. If the magnetic basement is taken to be the Precambrian basement, then the thickness of the Paleozoic metasediments is approximately 3.4 km.

3. The 6.9 km/sec layer represents material similar in velocity characteristics to the essentially oceanic crusts of the Gulf of Mexico (Ewing, 1960) and the Caribbean Sea (Officer, 1959).

4. The 8.2 km/sec layer represents upper mantle material by definition.

CORRELATION WITH ADJACENT MEASUREMENTS

Figure 9 indicates the approximate locations of profiles *V*-1-22, 24, 25, and 28 obtained by the Lamont Geological Observatory (Ewing, M., 1955; Ewing, J., 1960). Also shown are the Texas Coastal Plain profile (*AB*) and the Little Rock, Arkansas profile obtained by the University of Wisconsin group (Woollard, personal communication, 1961). Profile *V*-1-22 is located in the Sigsbee Deep. Profile *V*-1-25 is located at the base of the Sigsbee escarpment, and profile *V*-1-28 is located on the continental slope.

The velocity correlations shown in Figure 10 are accepted as having structural significance, and it is assumed that the materials within each layer are related. Since all of these sections are located within one broad geologic province, this assumption should be reasonable.

It can be seen from Figure 10 that the total crustal thickness decreases from 33.0 km at profile *AB* to 17.0 km at profile *V*-1-22. Also, the

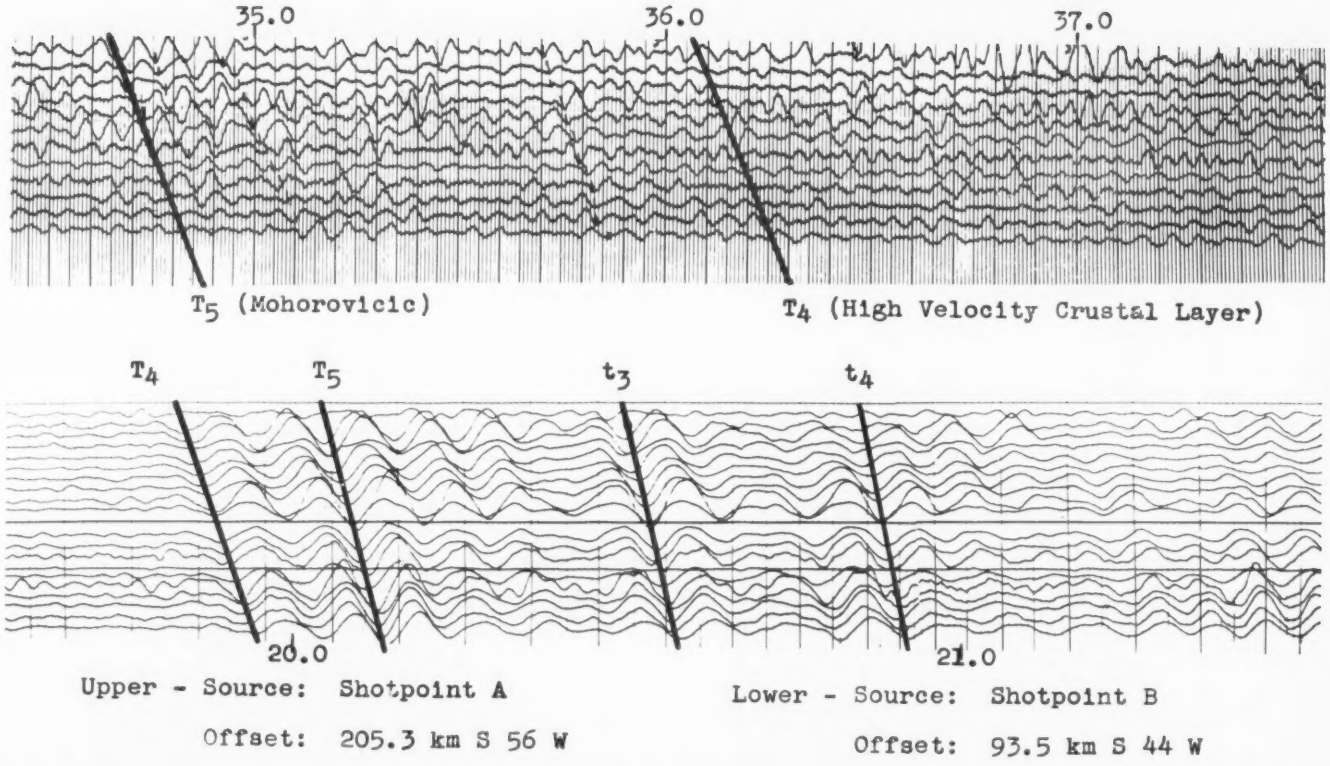

FIG. 8. Sample Records.

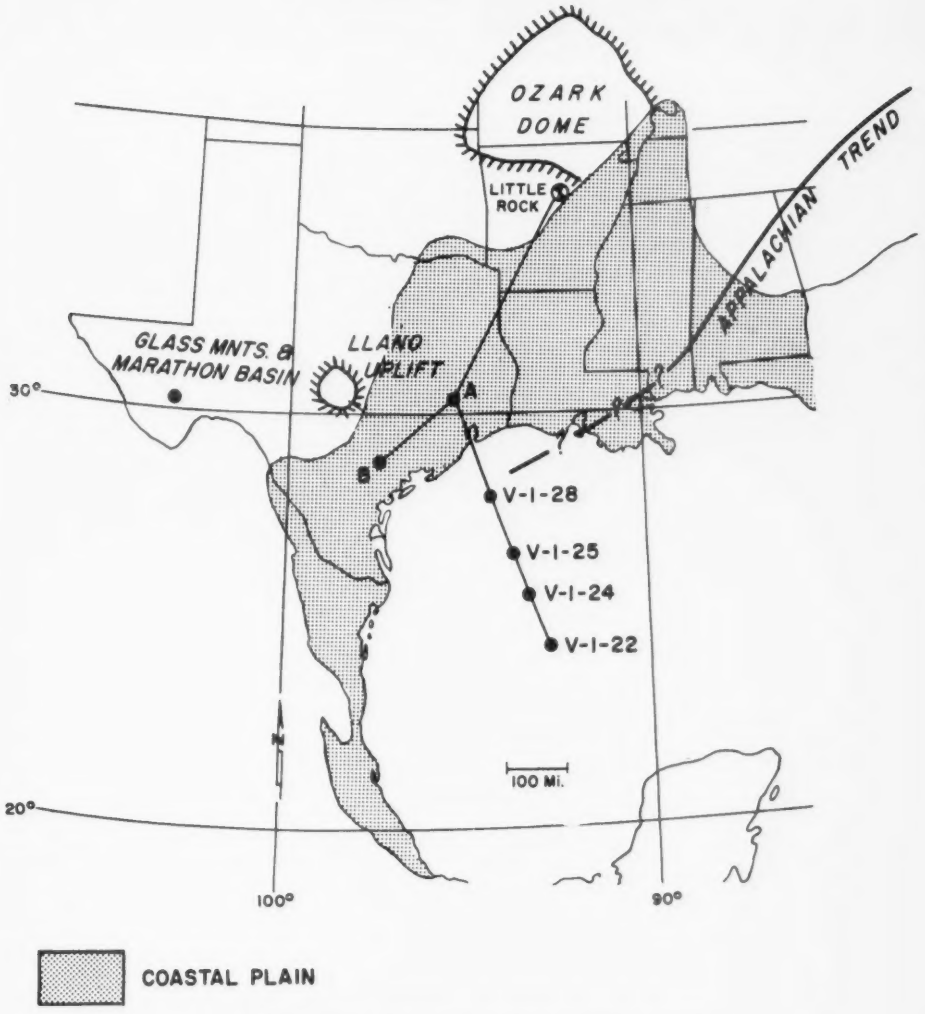

FIG. 9. Approximate Locations of Measured Velocity Sections.

thickness of the continental material (material with velocity less than 6.6 km/sec) decreases from 19.8 km at profile *AB* to 7.0 km at profile *V*-1-22, excluding water thickness (1.5 km/sec material). The high-velocity crustal layer thickens from 6.0 km at profile *V*-1-22 to 13.2 km at profile *AB*. Figure 10 indicates that the 5.3 km/sec refractor rises to a depth of 6.0 km at profile *V*-1-28. Ewing (1960) suggests that this rise may represent a continuation of the Appalachian system (Figure 9).

Figure 10 also shows the velocity section for northeastern Arkansas. This profile is not reversed. A correlation of the 5.2 km/sec Arkansas refractor with the 5.4 km/sec refractor at profile *AB* appears reasonable. However, Woollard (personal communication, 1961) states that "the change at 2.0 km from a velocity of 4.6 km/sec to 5.2 km/sec is undoubtedly related to a change in compressibility with depth and increasing pressure." Since the 5.4 km/sec refractor beneath profile *AB* is almost certainly not due to a change in

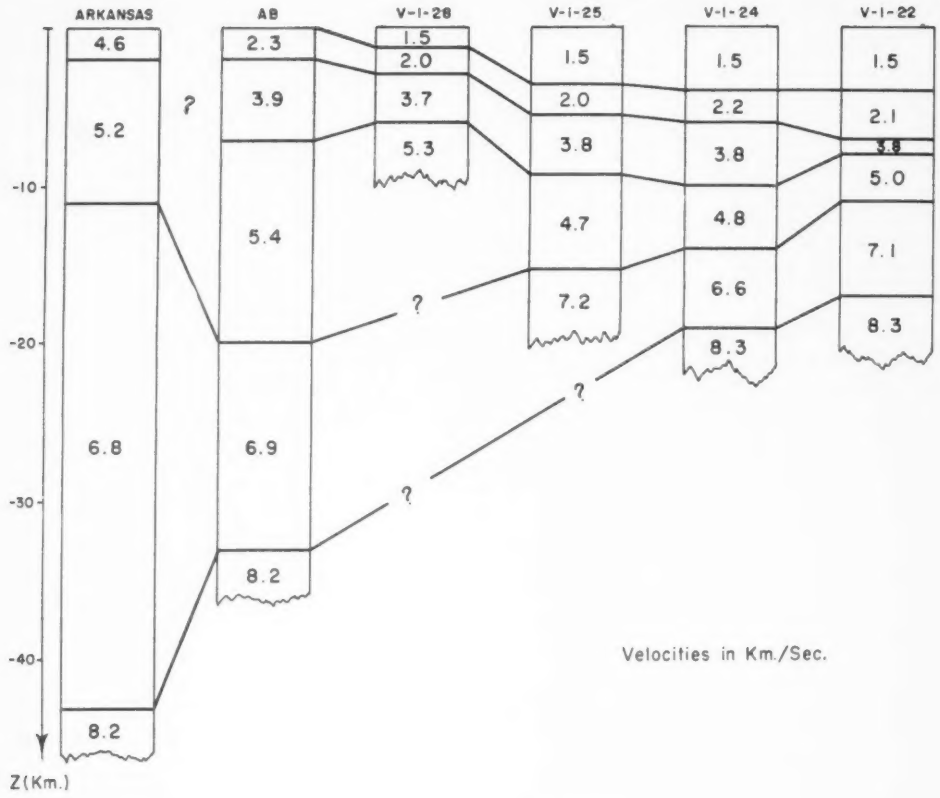

FIG. 10. Correlation of Velocity Sections.

compressibility with depth and increasing pressure, this correlation with the Arkansas section represents only a velocity similarity and probably has neither structural nor lithologic significance. The correlations of the 6.8 km/sec and 8.2 km/sec. refractors in Arkansas with the 6.9 km/sec and 8.2 km/sec refractors at profile *AB* are assumed to be valid. These correlations indicate that the total crustal thickness increases to 43.3 km and that the high-velocity crustal layer thickens to 32.0 km in northeastern Arkansas.

CONCLUSIONS

The following conclusions can be drawn from the data presented.

1. A radio time-synchronization signal transmitted by a commercial radio station is adequate for long-distance refraction shooting and during daylight hours it is preferable to short-wave transmission.

2. A joint venture of the type described requires no more than three hours recording time per crew plus about six hours of office and laboratory time per crew.

3. Using standard reflection equipment with low-frequency geophones and optimum weather conditions, the effective average recording range would probably have been at least 220 km.

4. Woollard's seacoast gradient of 14.5 mgal/km adequately predicts the depth of the Mohorovicic discontinuity beneath the Texas Coastal Plain in the vicinity of the profile *AB*.

5. The thickness of Cenozoic and Mesozoic sediments beneath the profile *AB* is 7.3 km.

6. The total thickness of continental material beneath the profile *AB* is 19.8 km.

7. The depth to the Mohorovicic discontinuity beneath the profile AB is 33.0 km.

8. The velocity section AB appears to correlate well with adjacent measured velocity sections in the Gulf of Mexico and northeastern Arkansas.

ACKNOWLEDGMENTS

The writer wishes gratefully to acknowledge the following organizations and individuals for their active participation in this project.

E. I. duPont de Nemours & Company, Hercules Powder Company, and Southwestern Pipe, Inc., Explosive Division, for providing explosives; John Richards, Cuero, Texas, and the U. S. Department of Agriculture for granting shotpoint permits; Robert H. Ray Geophysical Company for drilling the shot holes; Economy Mud Products Company for supplying drilling mud; Radio Station KTRH in Houston, Texas, for supplying the time-synchronization signal; Arkansas Fuel Oil Company, Atlantic Refining Company, Chevron Oil Company, Continental Oil Company, Cyprus Oil Company, General Geophysical Company, Geophysical Associates International, Geophysical Services, Inc., Gulf Oil Corporation, Humble Oil & Refining Company, Independent Exploration Company, Index Geophysical Surveys Corporation, Keystone Exploration Company, Lion Oil Company, M. L. Randall Explorations, McCollum Laboratories, Mobil Oil Company, National Geophysical Company, Pan American Petroleum Corporation, Petty Geophysical Engineering Company, Phillips Petroleum Company, Precision Exploration Company, Rayflex Exploration Company, Research Explorations, Inc., Robert H. Ray Geophysical Company, Reynolds-Southwestern Corporation, Seismic Explorations, Inc., Shell Oil Company, Skelly Oil Company, Standard Oil Company of Texas, States Exploration Company, Sun Oil Company, Sunray Midcontinent Oil Company, Tennessee Gas & Oil Company, Texaco, Inc., The California Company, The Superior Oil Company, Tidelands Exploration Company, Tidewater Oil Company, Union Producing Company, Union Texas Natural Gas Corporation, United Geophysical Corporation, and Western Geophysical Company for allowing their field seismograph parties time to record the shots; The Houston Geological and Geophysical Societies, the National Science Foundation, and the Rice University Seismological Station fund for financial and moral support for the writer; Electro-Technical Laboratories, and Hall-Sears Company for supplying low-frequency geophones.

The writer is indebted to Mr. David E. Park, Jr. (Geology Department, Rice University) who was very active during the initial phases of this project and occupied shotpoint A on the shot date. Dr. Gerald C. Phillips (Physics Department, Rice University) and Dr. John J. W. Rogers (Geology Department, Rice University) critically read the manuscript and offered helpful suggestions. Dr. Jean-Claude De Bremaecker (Geology Department, Rice University) followed the project from conception to completion and his many helpful suggestions and criticisms are gratefully acknowledged.

REFERENCES

Dobrin, M. B., 1960, Introduction to geophysical prospecting: New York, McGraw-Hill Book Co., Inc., 446 p.

Ewing, J., Antoine, J., and Ewing, M., 1960, Geophysical measurements in the western Caribbean Sea and in the Gulf of Mexico: J. Geophys. Research, v. 65, p. 4087–4126.

Ewing, M., Worzel, J. L., Ericson, D. B., and Heezen, B. C., 1955, Geophysical and geological investigations in the Gulf of Mexico, Part 1: Geophysics, v. 20, p. 1–18.

Jakosky, J. J., 1950, Exploration Geophysics: Los Angeles, Trija Publishing Co., 1196 p.

Logue, L., 1954, Gravity anomalies of Texas, Oklahoma, and United States: The Oil and Gas Journal, v. 52, no. 50 (supplement).

Nettleton, L. L., 1940, Geophysical prospecting for oil: New York, McGraw-Hill Book Co., Inc., 444 p.

——— 1952, Sedimentary volumes in Gulf Coastal Plain of the United States and Mexico. part VI: Geophysical aspects: Bull. G.S.A., v. 63, p. 1221–1228.

Officer, C. B., 1958, Introduction to the theory of sound transmission: New York, McGraw-Hill Book Co., Inc., 284 p.

——— Ewing, J., Hennion, D., Harkrider, D., and Miller, D., 1959, Geophysical investigations in the eastern Caribbean: Summary of 1955 and 1956 cruises: Physics and Chemistry of the Crust, v. 3, p. 17–109.

Richards, T. C., and Walker, D. J., 1959, Measurement of the thickness of the earth's crust in the Alberta Plains of western Canada: Geophysics, v. 24, p. 262–284.

Richter, C. F., 1943, Calculation of small distances: Bull. S.S.A., v. 33, p. 243–250.

——— 1958, Elementary seismology: San Francisco, W. H. Freeman and Co., 768 p.

Veitsman, P. S., 1957, The correlation of seismic waves in seismic depth sounding in the earth's crust: Bull. of the Academy of Sciences of the U.S.S.R. Geophysical Series, n. 12, p. 9–28 (in English).

Woollard, G. P., 1959, Crustal structure from gravity measurements: J. Geophys. Research, v. 64, p. 1521–1544.

GEOPHYSICS, VOL. XXVI, NO. 5 (OCTOBER, 1961), pp. 574–587, 5 FIGS.

MINIMUM STATISTICAL UNCERTAINTY OF THE SEISMIC REFRACTION PROFILE*

JOHN S. STEINHART† AND ROBERT P. MEYER‡

Abstract: Interpretation of refraction results resolves in finding a model that fits the data as closely as possible. In many cases several plausible models may be postulated. Criteria are then required to evaluate the uncertainty of these models especially to determine if the data are sufficiently good to distinguish among the models. By expanding the depth function in a Taylor series, a straightforward evaluation of statistical uncertainty may be made. The problems of obtaining estimates of uncertainty for the parameters are discussed, and the method is outlined for estimating uncertainty of the depths. This estimate of the statistical uncertainty is shown to be a minimum in the sense that it may be said that the uncertainty is at least as large as the estimate. Finally, the applicability of least squares procedures to refraction work is discussed, and it is shown that the method of least squares is preferred for the purpose of the minimum estimate.

INTRODUCTION

Kinsman (1957) in his admirable polemic on geophysical applications of statistics, concludes that "the job of the scientist is to invent a story which accounts for a set of observations, and then decide how likely that story is." The "how likely" problem for the results of long-range seismic refraction measurements has plagued investigators for a long time. More recently Gutenberg (1959, p. 6) has discussed the abuses in the name of "expected accuracy." The sources of error in refraction work are not very well defined; and, since subjective procedures necessarily enter into the results, one should be suspicious of possible statistical bias. These difficulties put a complete statistical treatment out of reach. If, however, the travel time graph is viewed as a problem in statistical model fitting, it is clear that the scatter of the observations around the fitted lines implies some uncertainty in the values of any results derived from the graph. This uncertainty *can* be estimated, and the uncertainty thus obtained will be a *minimum* estimate of the uncertainty in the sense that it may be said "for the given model, the uncertainty is at least this large." The treatment here was developed to deal with crustal studies, from which the numerical examples are drawn; but the treatment applies equally to exploration refraction.

The uncertainty obtained is immediately useful in at least two ways. (1) It is possible to decide, for example, when further complication of the model no longer yields significantly different depths for a given set of observations, and (2) it is possible to compare the "goodness of fit" of the models imposed on several different sets of data since the estimate of the uncertainty is objective.

In the following sections some brief background is given, and the common sources of errors in seismic refraction are discussed. The methods of obtaining the parameters and their confidence limits for a model are then given for the cases of both single-ended and reversed profiles. For single-ended profiles the estimate of uncertainty depends upon the method of computation. Thus, both of the common methods are discussed. Two methods of obtaining uncertainties in the depths are then given, a conventional propagation of variance method and a method utilizing the linear terms of a Taylor expansion of the depth function. The Taylor expansion method is shown to be preferable. Finally, the validity of the method of least squares is discussed.

BACKGROUND

Previous investigations into the accuracy of seismic refraction have taken the direction of assessing the errors arising from particular sources;

* Manuscript received by the Editor November 25, 1960.

† Nat'l. Science Foundation Fellow at Dept. of Terrestrial Magnetism, Carnegie Institution of Washington.

‡ Geophysics Research Center, Department of Geology, University of Wisconsin.

the effects of omitting surface layers have been discussed by Zirbel (1954), the consequences of omitting intermediate layers by Shima (1957) and Hales and Sacks (1958). Khalevin (1956) discusses accuracy of calculated depths and dips as a function of velocity ratios and the accuracy of velocity determinations. Epinat'eva, in a series of papers (1948, 1955a, 1955b), discusses a number of topics affecting accuracy of results when the model has layers with small velocity contrasts. There is also a substantial literature on the effects of low-velocity layers (for example Gutenberg, 1954; Bath, 1956). A number of these papers provide useful methods for calculation of the magnitude of the error from particular sources. None treat the problem of estimating statistically the uncertainty implied by the fact that no chosen model is a perfect fit to the observed points.

The method of least squares has been widely employed to find a "best fitting" velocity line and at times, to set limits on the velocities thus obtained. However, the value of least squares, or any other "best fit" procedure, lies not only in providing an unbiased estimate of the parameters of the model but also in providing an estimate of the uncertainty in the results. This matter has been emphasized by Dix (1952, p. 275) and Bullard, et al (1940, p. 46). These estimates of uncertainty are rarely made for intercepts, crossover distances, or, the quantity usually of most interest, depth. When error estimates are given, the procedure by which they were determined is seldom. Hence the statement of uncertainty is of little value for comparison with other results.

THE MODEL AND SOURCES OF ERROR

In general a model is sought to fit the observations. Here it is assumed that this model has the following properties: (1) The sub-surface consists of layers with planar interfaces. (2) Within the layers the velocity is uniform and isotropic. (3) These velocities increase with depth, thus $V_n > V_{n-1}$, where the nth layer lies below the $(n-1)$st layer.

Having chosen this model as a starting point, some of the departures from the model commonly found in the real earth are

(1) deviations of the interfaces from planes,
(2) surface irregularities (elevation differences),
(3) horizontal velocity variations (esp. common for upper layers),
(4) continuous velocity increases with depth (within layers), and
(5) velocity reversals.

Very little will be said about item five. Velocity reversals require more information than the usual travel-time profile provides for their identification. This does not mean that these errors are small, only that they require different treatment. Even when undetected velocity reversals are present, a minimum estimate of the uncertainty is still obtained.

Items 1 through 3 will appear as residuals on the travel-time graph of the model and will thus be included in the estimate of uncertainty in the answer, provided only that the dimensions of the irregularities are small with respect to the total dimensions of the profile.

For continuous velocity increase within a layer, the matter is not so clear. If a straight line is fitted where a curve is actually required, some of the error due to the curvature will show up in the larger estimate of uncertainty of the result since the points will not fit a straight line. As a larger number of line segments are used to approximate the curve, the approximation becomes increasingly good. Ewing and Leet (1932) have worked out several numerical examples of such straight line approximations.

FITTING THE MODEL

The result of a set of refraction observations is a set of number pairs in distance and time. An attempt is then made to fit line segments, straight lines in this model, to the points with each line representing a velocity discontinuity at the base of a layer. Estimates of the parameters of these lines, confidence limits for these parameters, and confidence limits for the depths of the interfaces are to be obtained.

The classical least squares model will be adopted; that is, one variable without error, in this case the distance. All the error is assumed to be in the times observed. This assumption physically requires that the errors in distance be small in comparison to the time errors. This condition does obtain since distances in long-range work are usually measured to 1 part in 1,000 or better, while the observed deviations of time amount to 1 part in 100 or more.

LEAST SQUARES AND CONFIDENCE REGIONS FOR HORIZONTAL LAYERS

Least square method of fitting the line segments

For a line $T=t_0+\lambda X$ from N points (t_i, x_i), the least squares estimates of parameters λ and t_0 are given by

$$\lambda = \frac{\sum x_i t_i - \frac{\sum x_i \sum t_i}{N}}{\sum x_i^2 - \frac{(\sum x_i)^2}{N}}, \equiv \frac{\text{Covariance } (x_i, t_i)}{s_{xx}}, \quad (1)$$

where equation (1) also serves to define the quantity, s_{xx}, and

$$t_0 = \frac{\sum x_i \sum x_i t_i - \sum t_i \sum x_i^2}{(\sum x_i)^2 - N(\sum x_i^2)}. \quad (2)$$

$$h_n = \frac{X_{n,n+1}}{2}\left(\frac{V_{n+1}-V_n}{V_{n+1}+V_n}\right)^{1/2} + \sum_{k=1}^{n-1} h_k \frac{\left(\frac{1}{V_k^2}-\frac{1}{V_n^2}\right)^{1/2} - \left(\frac{1}{V_k^2}-\frac{1}{V_{n+1}^2}\right)^{1/2}}{\left(\frac{1}{V_n^2}-\frac{1}{V_{n+1}^2}\right)^{1/2}}, \quad (5)$$

These forms are chosen from the several equivalent ones because they are directly useful for computing the results. (See, for example, Hoel, 1954.)

The uncertainty in the values of the parameters may now be estimated. The parameters for which estimates are desired depend on the method of computation used in calculating the depths. Two computational methods are commonly used:

(a) The time-intercept method in which the thickness of layer n is given by

$$h_n = \frac{t_{0,n+1}V_n}{2\cos i_{n,n+1}} - \frac{V_n}{\cos i_{n,n+1}} \sum_{k=1}^{n-1} \frac{h_k \cos i_{k,n+1}}{V_k} \quad (3)$$

where

h_k = thickness of kth layer,
t_{0k} = zero distance time intercept for kth line on the travel time graph,
V_k = velocity in kth layer, and
$\cos i_{k,n+1}$ = cosine of the angle defined by $\sin i_{k,n+1} = V_k/V_{n+1}$.

It is more convenient for the statistical analysis to rewrite equation (3) in terms of slopes of the lines (the reciprocal of velocities), whence

$$h_n = \frac{t_{0,n+1}}{2(\lambda_n^2 - \lambda_{n+1}^2)^{1/2}} - \frac{1}{(\lambda_n^2 - \lambda_{n+1}^2)^{1/2}} \cdot \sum_{k=1}^{n-1} h_k(\lambda_k^2 - \lambda_{n+1}^2)^{1/2} \quad (4)$$

where the parameters are λ_k and t_{0k}.

(b) The critical-distance method in which the thickness of the layer n is given by

which, again rewritten in terms of the slopes of the lines, is

$$h_n = \frac{X_{n,n+1}}{2}\left(\frac{\lambda_n - \lambda_{n+1}}{\lambda_n + \lambda_{n+1}}\right)^{1/2} + \sum_{k=1}^{n-1} h_k \frac{(\lambda_k^2 - \lambda_n^2)^{1/2} - (\lambda_k^2 - \lambda_{n+1}^2)^{1/2}}{(\lambda_n^2 - \lambda_{n+1}^2)^{1/2}} \quad (6)$$

where $X_{k,k+1}$ is the crossover distance for the k and $k+1$ layers, and the parameters are λ_k, and $X_{k,k+1}$.

Estimate of the uncertainty of the slope

It is clear that in either case an estimate of the error in the slopes, λ_i, is required. These methods are described in most statistics books. (See, for example, Acton, 1959.)

The standard deviation, σ_λ, of the slope is desired. First, the standard deviation, σ_t, for any experimental value of t, must be obtained. It can be

shown that the "best" estimate for σ_t (in the sense of Maximum Likelihood from a set of data which have been fitted to a line) is s_t where the variance s_t^2 is estimated from

$$(N-2)s_t^2 = \sum t_i^2 - \frac{(\sum t_i)^2}{N} - \frac{\left(\sum x_i t_i - \frac{\sum x_i \sum t_i}{N}\right)^2}{S_{xx}}. \quad (7)$$

This value, s_t^2, is now employed to estimate s_λ by

$$s_\lambda^2 = \frac{s_t^2}{S_{xx}}. \quad (8)$$

An estimate has now been obtained of the uncertainty in the estimate for the slope λ, and a method of stating the significance of this estimate of error is required. In the literature such estimates are presented in a number of ways: standard error, standard deviation, probable error, average deviation, and simply as undefined limits. None of these measures is completely satisfactory. The meaning of standard error is not clear when applied to the estimate of a line parameter, and the numerical values of the standard deviation are frequently misleading when only a few degrees of freedom are available. Average deviation and probable error do not permit application of standard significance tests, and "probable error" is not a clearly defined quantity. The very common use made made of probable error suggests that what is desired is a probability statement about the limits of uncertainty obtained. Such a probability statement is given by the use of confidence limits. Acton (1959) discusses in detail some of the probability statements that can be made.

If ψ is the true value of the slope λ, then $(\lambda-\psi)/\sigma_\lambda$ is distributed according to Student's t distribution. We shall designate Student's distribution by $\mathfrak{Z}$. If the numerical value of $\mathfrak{Z}$ (with $N-2$ degrees of freedom for the desired probability) is employed, confidence limits can be established on $\lambda-\psi$. This yields

$$\psi = \lambda \pm (s_\lambda \mathfrak{Z}_{N-2}). \quad (9)$$

The meaning of the limits (9) is best restated as: If we choose a value of $\mathfrak{Z}_{N-2}$ for probability of 0.1, the true value of the slope will lie in the range $\lambda \pm (s_\lambda \mathfrak{Z}_{N-2})$ nine of every ten times we make such a statement.

Uncertainty of the time intercept

If the time-intercept formula for depth computations is to be used, the limits on the zero distance time intercept are required. To do this it is convenient to use the orthogonal form for the line segments,

$$T = \bar{t} + \lambda(X - \bar{x}) \quad (10)$$

where $\bar{t}$ and $\bar{x}$ are the means of t_i and x_i, respectively.

To find the limits for T for any value of x, say x_0, let the true value be τ for which we have the estimate, T. As before, a relation can be set up in terms of Student's $\mathfrak{Z}$:

$$\mathfrak{Z}_{N-2} = \frac{T-\tau}{S_T}. \quad (11)$$

s_T can be found by noting that the value for T is given by equation (10). Since sampling for $\bar{t}$ and λ is independent (i.e. the covariance is zero) and $\bar{x}$ is without error, the "best" value for s_T is found from

$$s_T^2 = s_t^2 + s_\lambda^2(X - \bar{x})^2. \quad (12)$$

Noting that $s_{\bar{t}}^2 = s_t^2/N$ and substituting the value of s_λ^2 from equation (8), let $T-\tau = d$ and writing an equation involving $\mathfrak{Z}_{N-2}^2$ instead of $\mathfrak{Z}_{N-2}$, we then have

$$\mathfrak{Z}_{N-2}^2 = \frac{d^2}{s_t^2\left[\frac{1}{N} + \frac{(X-\bar{x})^2}{S_{xx}}\right]}. \quad (13)$$

We can employ equation (13) to find limits for the uncertainty in T for $X=0$, for any confidence limits for which $\mathfrak{Z}$ is tabulated, by substituting numerical values.

To clarify the meaning of this, equation (13) can be developed in a slightly different way,

$$\frac{d^2}{\frac{\mathfrak{Z}_{N-2}^2 s_t^2}{N}} - \frac{(X-\bar{x})^2}{\frac{S_{xx}}{N}} = 1, \quad (14)$$

which will be recognized as the standard formula for a hyperbola. The confidence limits on T are portrayed schematically in Figure 1. Finding t_0

is an extrapolation beyond the experimental values (indicated by the solid portion of the line). Hence, it is not surprising to find the uncertainty in T greater at $X=0$ than in the area where experimental points exist. In practice, for long-range refraction, the curvature of the hyperbola is small, but the limits on T for the major layers are of the order of twice as large as $X=0$ as at the value $X=\bar{x}$.

Uncertainty in the crossover distance

If one employs the crossover-distance methods of equation (5) or (6), the uncertainty in the crossover distance is required.

There are now two lines to be dealt with:

$$T_1 = \bar{t}_1 + \lambda_1(X_1 - \bar{x}_1)$$

and

$$T_2 = \bar{t}_2 + \lambda_2(X_2 - \bar{x}_2).$$

The value, X_c, of interest is that which satisfies the condition

$$\bar{t}_1 - \bar{t}_2 + \lambda_1(X_c - \bar{x}_1) - \lambda_2(X_c - \bar{x}_2) = 0. \tag{15}$$

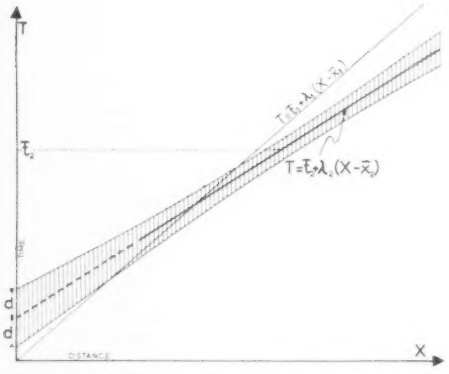

FIG. 1. Confidence region for T (shaded area). The solid portion of the line represents areas where experimental data exist.

Since sampling for $\bar{t}_1$, $\bar{t}_2$, λ_1, and λ_2 are independent; the estimated variance for equation (15) may be written as

$$s_{t_1}^2\left[\frac{1}{N_1} + \frac{(X_c - \bar{x}_1)^2}{S_{xx_1}}\right] + s_{t_2}^2\left[\frac{1}{N_2} + \frac{(X_c - \bar{x}^2)^2}{S_{xx_2}}\right]. \tag{16}$$

From equations (15) and (16) another Student's $\mathfrak{Z}$ equation may be set up with N_1-2+N_2-2 degrees of freedom. Using $\mathfrak{Z}^2$,

$$\mathfrak{Z}^2_{N_1+N_2-4} = \frac{[\bar{t}_1 - \bar{t}_2 + \lambda_1(X_c - \bar{x}_1) - \lambda_2(X_c - \bar{x}_2)]^2}{s_{t_1}^2\left[\frac{1}{N_1} + \frac{(X_c - \bar{x}_1)^2}{S_{xx_1}}\right] + s_{t_2}^2\left[\frac{1}{N_2} + \frac{(X_c - \bar{x}_2)^2}{S_{xx_2}}\right]}. \tag{17}$$

This yields a quadratic equation for X_c in which the roots are the limits on the crossover distance at whatever probability was selected when choosing the numerical value for $\mathfrak{Z}_{N_1+N_2-4}$.

Uncertainty in the crossover distances for multiple layers

Equation (17) could be employed to obtain confidence limits for the crossover distances for any number of layers; but, strictly speaking, these limits would always be too large. To see why this is so, consider two such crossover distances on the same travel-time graph as in Figure 2. There are two conditions of the form of equation (15) to satisfy; so that the lines are

$$T_1 = \bar{t}_1 + \lambda_1(X - \bar{x}_1), \tag{18}$$

$$T_2 = \bar{t}_2 + \lambda_2(X - \bar{x}_2), \text{ and} \tag{19}$$

$$T_3 = \bar{t}_3 + \lambda_3(X - \bar{x}_3). \tag{20}$$

Two points, X_{c1} and X_{c2}, are sought that satisfy

$$\bar{t}_1 - \bar{t}_2 - \lambda_1(X_{c1} - \bar{x}_1) - \lambda_2(X_{c1} - \bar{x}_2) = 0$$

and

$$\bar{t}_2 - \bar{t}_3 + \lambda_2(X_{c2} - \bar{x}_2) - \lambda_3(X_{c3} - \bar{x}_3) = 0. \tag{21}$$

But there exists the additional condition that, for any solution of the two equations (21), X_{c1}

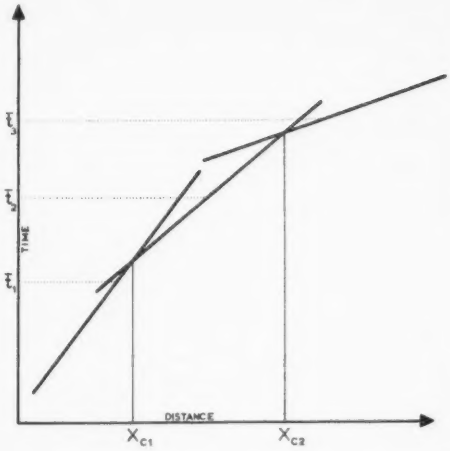

FIG. 2. Schematic travel times for two layers.

and X_{c2} must simultaneously satisfy equation (19). Geometrically, this states the obvious fact that the most uncertain cases cannot be chosen for both X_{c1} and X_{c2}.

This kind of joint-confidence problem is considerably more complex. A matrix method for its solution is available due to Box and Hunter (1954). This method is rather complex, and another method of computing uncertainties in the depths which makes computation of these exact regions unnecessary is given in the section entitled "Uncertainty in the Depths by the Taylor Expansion Method."

LEAST SQUARES AND CONFIDENCE REGIONS FOR DIPPING LAYERS

Least square fitting the line segments

To resolve the case of dipping layers, a "reverse" profile is required consisting of two profiles shot in opposite directions along the line joining the shotpoints, here called A and B. There will now be a line segment on both the A and B profiles for each subsurface layer in the model. Call these line segments for the kth layer; L_{ak}, and L_{bk}.

To preserve reciprocity the two line segments, L_{ak}, and L_{bk}, must have an equal time intercept, t_{Rk}, at $X = R$ where R is the distance from A to B.

Given two sets of points,

$$(x_i, t_i) \in L_{ak} \qquad (i = 1, 2, \cdots, N_a) \text{ and}$$
$$(x_j, t_j) \in L_{bk} \qquad (j = 1, 2, \cdots, N_b),$$

two line segments are to be fitted to equations of the following form:

$$L_{ak}\colon\ T = t_{Rk} + \lambda_{ka}(X - R) \tag{22}$$
$$L_{bk}\colon\ T = t_{Rk} + \lambda_{kb}(X - R),$$

subject to the above constraint.

Three parameters, t_{Rk}, λ_{ka}, and λ_{kb}, need to be obtained from the two sets, (x_i, t_i) and (x_j, t_j). Partially differentiating the sum of squared deviations with respect to each of the parameters in turn and setting these partial derivatives equal to zero, the normal equations are obtained. These are

$$t_{Rk}(N_a + N_b) + \lambda_{ka}(\sum x_i - N_a R) + \lambda_{kb}(\sum x_j - N_b R) = \sum t_i + \sum t_j, \tag{23}$$

$$\sum (x_i - R)(t_j - t_{Rk}) = \lambda_{ka} \sum (x_i - R)^2, \tag{24}$$

and

$$\sum (x_j - R)(t_j - t_{Rk}) = \lambda_{kb} \sum (x_j - R)^2. \tag{25}$$

Defining

$$S_{RRa} \equiv S_{XX_a} + N_a(\bar{x}_a - R)^2 = \sum x_i^2 - \frac{(\sum x_i)^2}{N_a} + N_a(\bar{x}_a - R)^2, \tag{26}$$

$$S_{RRb} \equiv S_{XX_b} + N_b(\bar{x}_b - R)^2 = \sum x_j^2 - \frac{(\sum x_j)^2}{N_b} + N_b(\bar{x}_b - R)^2, \tag{27}$$

and solving for t_R, the least squares estimate for the time intercept is

$$t_{R_k} = \frac{\sum t_i + \sum t_j - \dfrac{N_a(\bar{x}_a - R)(\sum x_i t_j - N_a \bar{t}_a R)}{S_{RRa}} - \dfrac{N_b(\bar{x}_b - R)(\sum t_j x_j - N_b \bar{t}_b R)}{S_{RRb}}}{N_a + N_b - \dfrac{(\sum x_i - R)^2}{S_{RRa}} - \dfrac{(\sum x_j - R)^2}{S_{RRb}}}. \tag{28}$$

To estimate the reciprocal velocities (slopes), λ_{ka}, and λ_{kb}, we first define S_{tRR_a} and S_{tRR_b} as

$$\begin{aligned} S_{tRR_a} &\equiv S_{xt_a} + N_a(\bar{t}_a - t_{R_k})(\bar{x}_a - R) \\ &= \sum x_i t_i - \frac{\sum x_i \sum t_i}{N_a} \\ &\quad + N_a(\bar{t}_a - t_{R_k})(\bar{x}_a - R), \end{aligned} \tag{29}$$

$$\begin{aligned} S_{tRR_b} &\equiv S_{xt_b} + N_b(\bar{t}_b - t_{R_k})(\bar{x}_b - R) \\ &= \sum x_j t_j - \frac{\sum x_j \sum t_j}{N_b} \\ &\quad + N_b(\bar{t}_b - t_{R_k})(\bar{x}_b - R). \end{aligned} \tag{30}$$

The least squares estimates of the slopes are then

$$\lambda_{ka} = \frac{S_{tRR_a}}{S_{RR_a}}, \text{ and} \tag{31}$$

$$\lambda_{kb} = \frac{S_{tRR_b}}{S_{RR_b}}. \tag{32}$$

Uncertainty in the time intercept, t_R

We first define

$$S_{tRtR_a} \equiv \sum t_i^2 - \frac{(\sum t_i)^2}{N_a} + N_a(\bar{t}_a - t_R)^2, \tag{33}$$

$$S_{tRtR_b} \equiv \sum t_j^2 - \frac{(\sum t_j)^2}{N_b} + N_b(\bar{t}_b - t_R)^2; \tag{34}$$

and then estimate the variance s_t^2 of the t observations by

$$(N_a + N_b - 3)s_t^2 = S_{tRtR_a} + S_{tRtR_b} - \frac{(S_{tRR_a})^2}{S_{RR_a}} - \frac{(S_{tRR_b})^2}{S_{RR_b}}. \tag{35}$$

Solving equation (23) for t_R enables us to write the estimated variance $S_{t_R}^2$ as

$$s_{t_R}^2 = \frac{s_t^2}{(N_a + N_b)^2}\left[N_a + N_b - \frac{[N_a(\bar{x}_a - R)]^2}{S_{RR_a}} - \frac{[N_b(\bar{x}_b - R)]^2}{S_{RR_b}}\right]. \tag{36}$$

If τ_R be the true value for which we have the estimate t_R, then $(t_R - \tau_R)/S_{tR}$ is a $\mathfrak{Z}$ variate with $N_a + N_b - 3$ degrees of freedom and we may set the confidence limits as before.

Uncertainty of the apparent slopes, λ_{ka}, and λ_{kb}

The estimated variances of the slopes are

$$s_{\lambda ka}^2 = \frac{s_t^2}{S_{RR_a}}, \qquad s_{\lambda kb}^2 = \frac{s_t^2}{S_{RR_b}}. \tag{37}$$

$(\lambda_{ka} - \psi_{ka})/s_{ka}$ is a $\mathfrak{Z}$ variate with $N_a - 2$ degrees of freedom, so the confidence limits may be obtained.

LIMITS OF UNCERTAINTY ON THE DEPTH BY PROPAGATION OF VARIANCE METHODS

Confidence limits are required on the depths obtained from the above and can be found for all the quantities used. Therefore one could proceed to calculate the depth and estimate the uncertainty in that depth by repeated application of the following identities for the variances:
If

$$C = A + B \text{ or if } C = A - B, \tag{38}$$

then

$$\text{Var}(C) = \text{Var}(A) + \text{Var}(B);$$

and if

$$C = AB \quad \text{or} \quad \text{if} \quad C = \frac{A}{B},$$

then

$$\frac{\text{Var}(C)}{C^2} = \frac{\text{Var}(A)}{A^2} + \frac{\text{Var}(B)}{B^2}. \tag{39}$$

This conventional method is satisfactory, but the arithmetic is tedious. Unless the exact confidence regions are calculated, for instance by the method of Box and Hunter (1954), the estimates for multilayered cases may be subject to substantial errors due to the repeated operations and rounding off. The following Taylor expansion procedure, due to Brunt (1931), answers most of

the difficulties by being simple in application, objective in its estimates, and comparatively free from arithmetic errors of the rounding off and repeated operation type.

UNCERTAINTY IN THE DEPTHS BY THE TAYLOR EXPANSION METHOD

Taylor expansion for horizontal layers

If the equation is written for the depth to interface n; the time-intercept method gives

$$D_n = \frac{t_{0,n+1}}{2(\lambda_n^2 - \lambda_{n-1}^2)^{1/2}} + \sum_{k=1}^{n-1} h_k \left[1 - \frac{(\lambda_k^2 - \lambda_{n+1}^2)^{1/2}}{(\lambda_n^2 - \lambda_{n+1}^2)^{1/2}} \right], \tag{40}$$

and the crossover-distance method gives

$$D_n = \frac{X_{n,n+1}}{2} \left[\frac{\lambda_n - \lambda_{n+1}}{\lambda_n + \lambda_{n+1}} \right]^{1/2} + \sum_{k=1}^{n-1} h_k \left[1 - \frac{(\lambda_k^2 - \lambda_{n+1}^2)^{1/2} - (\lambda_k^2 - \lambda_n^2)^{1/2}}{(\lambda_n^2 - \lambda_{n+1}^2)^{1/2}} \right]. \tag{41}$$

Equation (40) is a function of t_0, h_k, and the λ_k; and equation (41) is a function of $X_{n,n+1}$, the h_k, and the λ_k. Going one step further back, t_0, $X_{n,n+1}$, and the h_k are functions of the parameters of the line segments. Either equation could be written as

$$D_n = F(\bar{t}_i, \bar{x}_i, \lambda_i) \; (i = 1, 2 \cdots, n+1), \tag{42}$$

and a Taylor series expansion of F in the region of any set of experimental values can be obtained.

Let the least squares values for these lines be

$$\begin{aligned} T &= \bar{t}_1 + \lambda_1(X - \bar{x}_1), \\ T &= \bar{t}_2 + \lambda_2(X - \bar{x}_2), \\ &\vdots \\ T &= \bar{t}_{n+1} + \lambda_{n+1}(X - \bar{x}_{n+1}). \end{aligned} \tag{43}$$

An expansion in the region of the experimental values is then of the form

$$\begin{aligned} D_n &= F(\bar{x}, \bar{t}, \lambda,) \\ &= F_n + \sum_{i=1}^{n+1} \left(\frac{\partial F}{\partial \bar{x}} \right)_{\bar{x}=\bar{x}_i} (\bar{x} - \bar{x}_i) \\ &\quad + \sum_{i=1}^{n+1} \left(\frac{\partial F}{\partial \bar{t}} \right)_{\bar{t}=\bar{t}_i} (\bar{t} - \bar{t}_i) \\ &\quad + \sum_{i=1}^{n+1} \left(\frac{\partial F}{\partial \lambda} \right)_{\lambda=\lambda_i} (\lambda - \lambda_i) \\ &\quad + \text{higher order terms} \end{aligned} \tag{44}$$

where F_n is the value of D_n calculated from the experimental values. Since the partial derivatives can be written as numerical values for any particular experimental case, D_n is a linear function of the variables $\bar{t}, \bar{x}, \lambda$ to the extent that it is justifiable to neglect the higher order terms.

Taylor expansion for dipping layers

In the same way a Taylor expansion may be obtained for dipping layers. Using Adachi's (1954) solution for the depths, the depth function for the nth layer on the A end is

$$D_{na} = \frac{t_{R,n+1} - \lambda_{a,n+1}R - \sum_{i=1}^{n-1} h_{ai}\lambda_i(\cos \alpha_i + \cos \beta_i)}{\lambda_n(\cos \alpha_n + \cos \beta_n)} \tag{45}$$

where the α_i and β_i are the refraction angles referred to the vertical for critical refraction at layer n.

Each of the above variables is a function of the parameters of the original line segments. The depth function may be written as

$$D_{na} = F(t_{Ri}, \lambda_{ai}, \lambda_{bi}, R). \tag{46}$$

The expansion is then

$$D_{na} = F(t_R, \lambda_a, \lambda_b, R)$$
$$= F_{na} + \sum_{i=1}^{n+1}\left(\frac{\partial F}{\partial \lambda_a}\right)_{\lambda_a=\lambda_{a_i}}(\lambda_a - \lambda_{ai}) + \sum_{i=1}^{n+1}\left(\frac{\partial F}{\partial \lambda_b}\right)_{\lambda_b=\lambda_{b_i}}(\lambda_b - \lambda_{bi}) + \sum_{i=2}^{n+1}\left(\frac{\partial F}{\partial t_R}\right)_{t_R=t_{R_i}}(t_R - t_{Ri}) + \frac{\partial F}{\partial R}(R - R_i) + \text{higher order terms.} \quad (47)$$

As before, D_{na} is now given as a linear function of the variables t_R, λ_a, λ_b, and R, if the higher order terms may be neglected. This problem is considered in the section entitled *Validity of the linear approximation.*

Variance of a linear function

The variance of a linear function, say $F(x, y, z) = a_0 + a_1x + a_2y + a_3z$, is given by

$$\text{Var}\,(a_0 + a_1x + a_2y + a_3z) = a_1^2\,\text{Var}\,(x) + a_2^2\,\text{Var}\,(y) + a_3^2\,\text{Var}\,(z) + 2a_1a_2\,\text{Covar}\,(xy) + 2a_1a_3\,\text{Covar}\,(xz) + 2a_2a_3\,\text{Covar}\,(yz). \quad (48)$$

Neglecting the higher order terms of the Taylor expansions, equations (44) and (47), the variance of D_n can then be written directly by evaluating the partial derivatives numerically for the range of variation of the $\bar{x}_i$, $\bar{t}_i$, and λ_i for the horizontal case and R, t_{Ri}, λ_{ai}, λ_{bi} for the dipping case.

To abandon the higher order terms in the expansion requires only that the function, D_n, be linear or nearly so in the area of interest. This can be tested by calculating numerically the values of the partial derivatives for the upper and lower limits of the uncertainty and the means of the experimental values in hand. It is possible in this case, however, to state the general validity of the procedure for a wide range of cases.

Validity of the linear approximation

The partial derivatives for $\bar{t}$ and $\bar{x}$ are constant. To show this, it is sufficient to examine the case of two layers. Rewriting equations (40) and (41) in terms of the variables $\bar{t}$, $\bar{x}$, and λ; one gets, for the time-intercept method,

$$D_2 = \frac{\bar{t}_3 - \lambda_3\bar{x}_3}{2(\lambda_2^2 - \lambda_3^2)^{1/2}} + \frac{\bar{t}_2 - \lambda_2\bar{x}_2}{2(\lambda_2^2 - \lambda_3^2)^{1/2}}\left[\frac{1}{(\lambda_1^2 - \lambda_2^2)^{1/2}} - 1\right]; \quad (49)$$

and, for the critical-distance method,

$$D_2 = \frac{\bar{t}_3 - \bar{t}_2 + \lambda_2\bar{x}_2 - \lambda_3\bar{x}_3}{2(\lambda_2^2 - \lambda_3^2)^{1/2}} + \frac{\bar{t}_2 - \bar{t}_1 + \lambda_1\bar{x}_1 - \lambda_2\bar{x}_2}{2(\lambda_1^2 - \lambda_2^2)^{1/2}}\left[1 - \frac{(\lambda_1^2 - \lambda_3^2)^{1/2} - (\lambda_1^2 - \lambda_2^2)^{1/2}}{(\lambda_2^2 - \lambda_3^2)^{1/2}}\right]. \quad (50)$$

It can be seen from inspection that $\partial D/\partial \bar{t}$ and $\partial D/\partial \bar{x}$ are always constant for any fixed values of the λ_i. In the same way it is clear that $\partial D_{na,b}/\partial t_R$ is constant since $D_{na,b}$ is always linear in t_R. Thus, the higher order terms in the expansion involving $\bar{x}$ and $\bar{t}$ are all zero. The partial derivatives, $\partial D_n/\partial \lambda$ and $\partial D_{na,b}/\partial \lambda_{a,b}$, are not constant; but they can be evaluated numerically when the other parameters in the expression for D_n are specified. Study of a number of numerical cases shows, however, that for small changes in the velocities these partial derivatives change slowly enough to justify neglecting higher order derivatives in the expansion, provided only that the ratio V_k/V_{k+1} is not too near 1. Figure 3 shows the behavior, $\partial D_3/\partial V_1$, for two 3-layer cases of interest in crustal studies. These values are for the crossover distance method of computation for horizontal layers. If the derivatives were constant, the lines on Figure 3 would be horizontal. It is clear that, even for relatively large changes in λ_1, the partial derivative changes very little. Typical numerical calculations for velocity ratios, V_k/V_{k+1}, less than 0.95 show the second order terms contribute from 0.01 to 0.001 the amount of the linear term. Thus, the approximation is very good.

If any doubt exists in the experimenter's mind about the linearity of $\partial D/\partial \lambda$, it should be calculated numerically by calculating D_n for the mean and limiting values of λ obtained in the least-

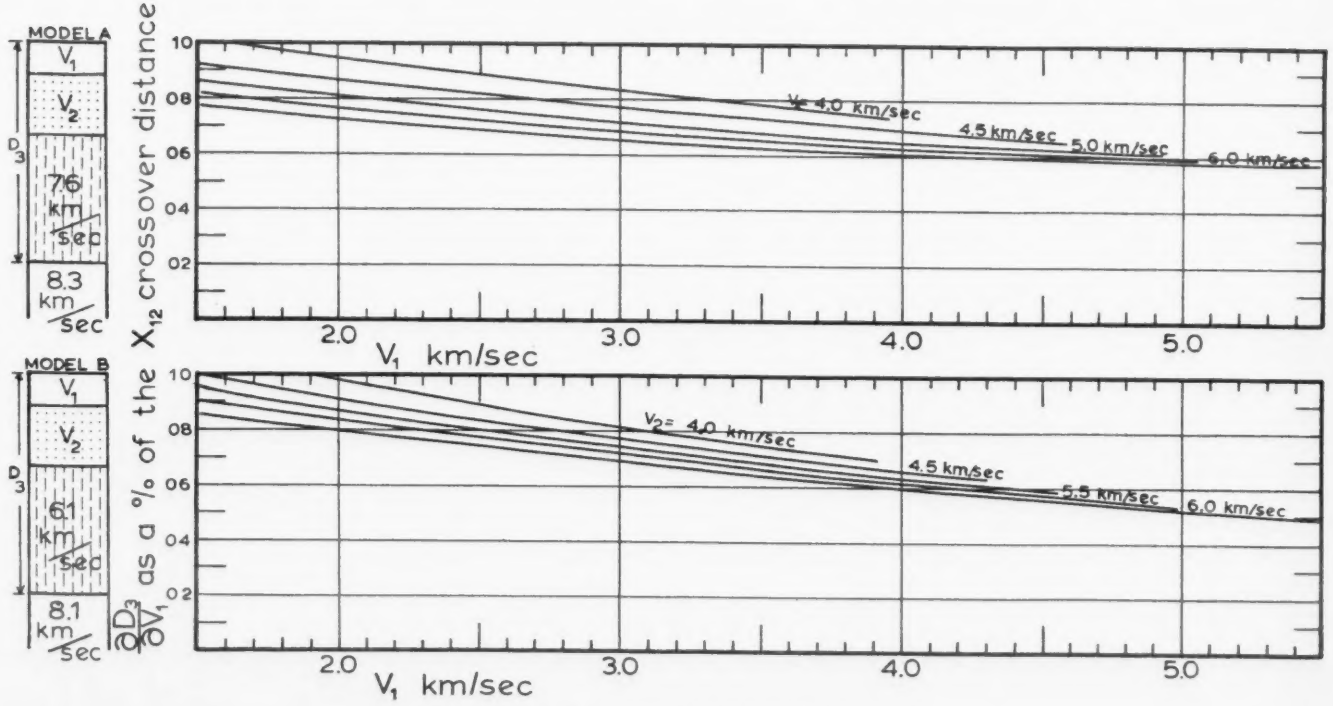

FIG. 3. $\partial D_3/\partial V_1$ for two models for various values of V_2.

square fit. This should always be done if the ratio, V_k/V_{k+1}, approaches 1. In practice, it is necessary to test the linearity of $\partial D/\partial\lambda_k$ if $(V_k/V_{k+1}) \geq 0.95$.

Variance of the computed depths

Utilizing the linear terms of the Taylor expansions, equations (44) and (47), and the variance of the linear function, equation (48), the variance of the depth may be obtained. Since $\bar{x}_1$ is "without error" and the sampling for $\bar{t}_i$ and λ_i is independent, Var $(\bar{x}) = 0$ and the covariance terms in equation (48) are zero. Thus, the variance of D_n may be written as

$$\text{Var}\,(D_n) = \sum_{i=1}^{n+1} A_i^2\,\text{Var}\,(\bar{t}_i) + \sum_{i=1}^{n+1} B_i^2\,\text{Var}\,(\lambda_i) \tag{51}$$

where

$$A_i = \frac{\partial D_n}{\partial \bar{t}_i} \quad \text{and} \quad B_i = \frac{\partial D_n}{\partial \lambda_i} \qquad (i = 1, 2, \cdots, n+1),$$

for the horizontal layer case; and, for the dipping layer case,

$$\text{Var}\,(D_{na}) = \sum_{i=2}^{n+1} A_i^2\,\text{Var}\,(t_{Ri}) + \sum_{i=1}^{n+1} B_i^2\,\text{Var}\,(\lambda_{ai}) + \sum_{i=1}^{n+1} C_i^2\,\text{Var}\,(\lambda_{bi}) \tag{52}$$

where

$$A_i = \frac{\partial D_{na}}{\partial t_{Ri}}, \quad B_i = \frac{\partial D_{na}}{\partial \lambda_{ai}}, \quad C_i = \frac{\partial D_{na}}{\partial \lambda_{bi}}$$

$(i = 1, 2, \cdots, n+1)$.

Numerical values of $\delta D_n/\partial \bar{t}_i$

In an effort to understand which experimentally determined parameters contribute most to the errors in the depths, it is desirable to examine the numerical behaviors of the partial derivatives. Unfortunately, the calculation of the partial derivatives for equations (51) and (52) is complicated enough that in most cases it must be done numerically for a particular case. One such derivative, $\partial D_n/\partial \bar{t}_{n+1}$, is especially simple, however, and may be tabulated for the range of values commonly encountered for the λ_i.

From equation (40) or (41)

$$\frac{\partial D_n}{\partial \bar{t}_{n+1}} = \frac{1}{2(\lambda_n^2 - \lambda_{n+1}^2)^{1/2}} = \frac{V_n}{2\left(1 - \dfrac{V_n^2}{V_{n+1}^2}\right)^{1/2}} \tag{53}$$

which applies to both the time-intercept and critical-distance method. This function is tabulated in Figure 4 for values of V_n and the ratios of V_n/V_{n+1}. The numerical values of

$$\frac{\partial D_n}{\partial \bar{t}_i} \qquad (i \neq n+1)$$

will always be smaller than $\partial D_n/\partial \bar{t}_{n+1}$ for the crossover-distance method since for any other i there is an additional term of opposite sign. The numerical values of $\partial D_n/\partial \bar{t}_i (i \neq n+1)$ for the time-intercept method will be of the same order of magnitude as $D_n/\bar{t}_n$ since there is no such compensating effect. The exception to this is $\partial D_n/\partial \bar{t}_1$ which, for the time-intercept method, is always zero. (This follows from the fact that $\bar{t}_1$ does not enter the equation explicitly.)

It is apparent from Figure 4 that the range of values of the M discontinuity represent the most rapidly changing portion of the graph. This confirms the suspicions raised in a previous section that considerable inaccuracy in calculation of the uncertainty may result from failure to calculate exact confidence regions and using propagation of variance methods. The Taylor expansion method is free from this problem, since numerical values for $\delta D_n/\partial \bar{t}_{n+1}$ are calculated for the case in hand.

Computer applications

The foregoing analysis is iterative in nature and well suited for computation on digital computers. This approach to the variance has been programmed for an IBM 650 computer as a subprogram in general refraction program. The flow chart and SOAP instructions for the program are given by Steinhart (1960).

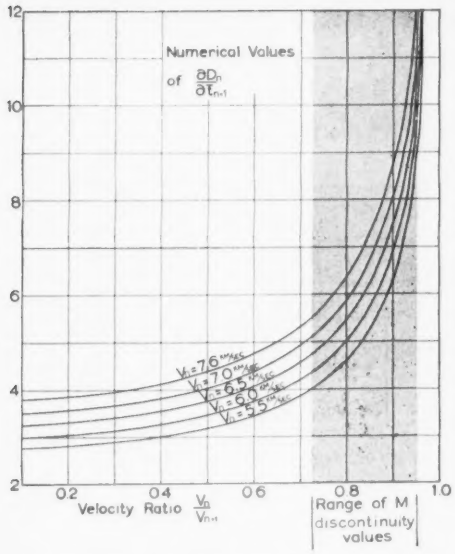

FIG. 4. Numerical values of $\partial D_n/\partial \bar{t}_{n+1}$ as a function of the V_n/V_{n+1} velocity ratio.

THE VALIDITY OF LEAST SQUARES PROCEDURES IN REFRACTION WORK

We now return to the original statistical model to comment on the validity of the least squares estimates of the parameters and their uncertainties. The procedures outlined above will provide a "best" estimate, in the sense of Maximum Likelihood, of the parameters and their variances if

(1) the variance is homogeneous; that is, that it is the same for all values of t;
(2) the distribution of residuals is normal; and
(3) the covariances are zero.

Though these assumptions are necessary to assure a Maximum Likelihood estimate, many of the results of least squares are of more general applicability. In particular, the estimate of the parameters will be unbiased if only the model (i.e. a series of line segments) is appropriate. No other assumptions are required.

The question of the error estimates is not so simple. If the only deviations present were due to the factors listed in the section entitled *The model and sources of error*, the matter would be complex. But we must yet add to the list. Besides the items listed, it may reasonably be supposed that the residuals also include the following:

(1) Deviations due to the difficulty of correctly identifying the first arrival of a wave group at larger distances. (This has been emphasized by many writers.) These should cause the "late" residuals as distance increases and are therefore biased.

(2) Deviations (again biased) caused by the experienced seismologists' efforts to counteract item 1.

(3) Deviations due to the use of arrivals that are near the line; hence, included in the calculations, although they are in fact from a different path (scatterings, conversions, etc.).

(4) Other deviations.

The complete list of sources of the deviations is now formidable indeed, and no comprehensive treatment will be attempted. Items (1) and (2) above will tend to make the variance inhomogeneous; that is, the variance will tend to increase with distance. Examination of published residuals shows that this does occur. A logarithmic transform applied to the time might go a long way towards obviating this effect, but the data may not justify the effort.

The estimated variance obtained from the least squares procedure does not fulfill the requirements for the Maximum Likelihood. Hence, the probabilities associated with the confidence limits cannot be taken as exact. But the estimate of the uncertainty based on least squares is an objective estimate of the uncertainty, taking account of the number of observations and eminently well suited for comparisons of data from different sources.

Figure 5 shows the distribution of all residuals for a number of published crustal refraction profiles. The most important feature of this plot is that the distribution *is* symmetric. Thus, any linear procedure would yield the same estimates for the parameters as least squares.

The distribution itself appears from inspection to be intermediate between the normal distribution and a double-exponential distribution. The double-exponential distribution would lead to the minimization of maximum error to obtain a Maximum Likelihood estimate of uncertainty. The criterion would be very undesirable for seismic studies because of the ever present possibility of including arrivals which have large residuals but which are not associated with the path under consideration. To the extent that the parent distribu-

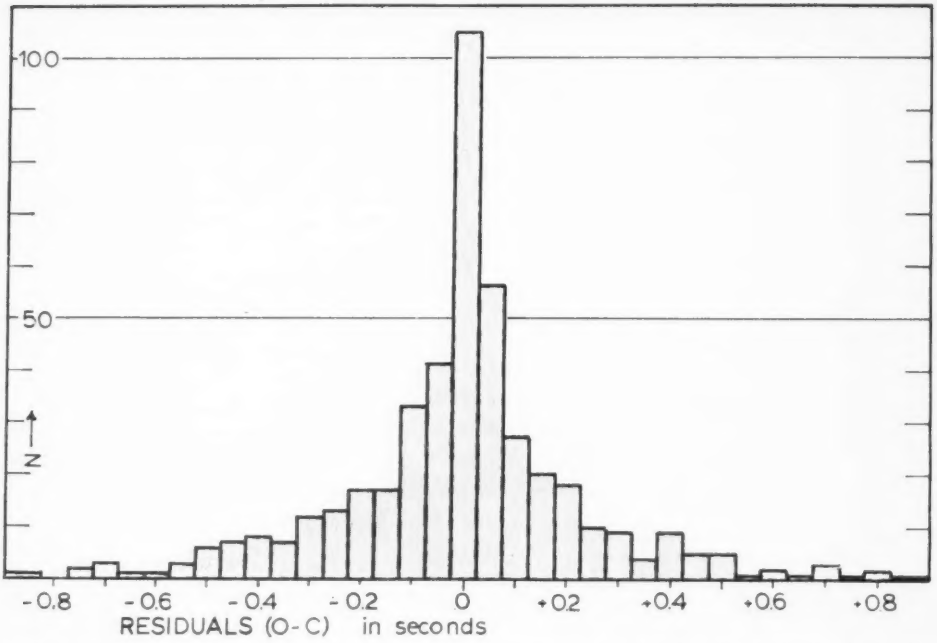

FIG. 5. Histogram of residuals from crustal seismic observations. Data from Bolt et al (1958), Doyle et al (1959), Eiby (1957), Hart (1954), Katz (1955), Matuzawa et al (1959), Slichter (1951), Steinhart (1960), and Usami et al (1958).

tion, giving rise to the observed data, has a sharper peak than the normal distribution, the estimated variance will be somewhat too small. Thus, least squares procedures will still give the minimum estimate of uncertainty sought.

CONCLUSION

It is both tedious and difficult to obtain estimates of uncertainty for refraction depth calculations by the conventional statistical methods. Even when obtained, such estimates may be suspect. Use of the linear terms of a Taylor Expansion yields good approximations of this uncertainty. Equations (51) and (52) may be applied directly unless very small velocity contrasts are being considered. For small velocity contrasts it may be necessary to test some of the partial deviations for linearity.

REFERENCES

Acton, F. S., 1959, Analysis of straight-line data: New York, John Wiley and Sons, Inc..

Adachi, R., 1954, On a proof of fundamental formula concerning refraction method of geophysical prospecting and some remarks: Kumamoto Jour. Sci., Ser. A, v. 2, p. 18–23.

Bath, M., 1956, Some consequences of the existence of low velocity layers: Ann. Geofis., p. 411–450.

Bolt, B. A., Doyle, H. A., and Sutton, D. J., 1958, Seismic observations from the 1956 atomic explosions in Australia: Geophys. Jour., v. 1, p. 135–145.

Box, G. E. P., and Hunter, J. S., 1954, A confidence region for the solution of a set of simultaneous equations with an application to experimental design: Biometrika, v. 41, p. 190–199.

Brunt, D., 1931, The combination of observations: Cambridge Univ. Press.

Bullard, E. C., Gaskell, T. F., Harland, W. B., and Kerr-Grant, C., 1940 Seismic investigations on the Paleozoic floor of east England: Phil. Trans. Roy. Soc., Ser. A, v. 239, p. 29–94.

Dix, C. H., 1952, Seismic prospecting for oil: New York, Harper & Brothers, Inc.

Doyle, H. A., Everingham, I. B., and Hogan, T. K., 1959, Recording of large explosions in southeastern Australia: Australian Jour. Physics., v. 12, p. 222–230.

Eiby, G. A., 1957, Crustal structure project: Geophysical Memoir 5, New Zealand Dept. of Sci. and Indust. Res.

Epinat'eva, A. M., 1948, Accuracy of determination of boundary and layer velocities according to seismic data (in Russian): Akad. Nauk SSSR, inst. geofix. Trudy, No. 1.

———, 1955a, Refracted waves in media with small velocity contrasts (in Russian): Akad. Nauk SSSR, Izv., ser. geofiz., pp. 303–322.
———, 1955b, Experimental data on refracted waves in media with small velocity contrasts (in Russian): Akad. Nauk SSSR, Izv., ser. geofiz., No. 2.
Ewing, M., and Leet, L. D., 1932, Comparison of two methods for interpretation of seismic time-distance graphs which are smooth curves: Trans. Amer. Inst. Min. Met. Eng., Geophys. Prosp., p. 263–270.
Gutenberg, B., 1954, Effects of low velocity layers: Geofis. pura e appl., p. 1–10.
———, 1959, Physics of the earth's interior: New York, Academic Press.
Hales, A. L., and Sacks, I. S., 1958, Evidence for an intermediate layer from crustal structure studies in the Eastern Transvaal: Geophys. Jour., v. 2, p. 15.
Hart, P. J., 1954, Variation of velocity near the Mohorovicic discontinuity under Maryland and northeastern Virginia: PhD thesis, Harvard Univ.
Hoel, P. G., 1954, Introduction to mathematical statistics: 2nd ed., New York, John Wiley and Sons, Inc.
Katz, S., 1955, Seismic study of crustal structure in Pennsylvania and New York: Bull. Seis. Soc. Amer., v. 45, p. 303–325.
Khalevin, N. I., 1956, Evaluation of the accuracy fo interpretation of the data of the refraction method (in Russian): Akad. Nauk SSSR, ser. geofiz., v. 8, p. 912–919.
Kinsman, B., 1957, Proper and improper use of statistics in geophysics: Tellus, v. 9, p. 408–418.
Matuzawa, T., Matumoto, T., and Asano, S., 1959, On the crustal structure derived from observations of the second Hokoda explosion: Bull. Earthq. Res. Inst., Tokyo, v. 37, p. 509–524.
Shima, E., 1957, Note on the depth calculation by the seismic refraction method (in Japanese): Butsuri-Tanko, v. 10, p. 16–18.
Slichter, L. B., 1951, Crustal structure in the Wisconsin area; Office of Naval Research Report, N9onr 86200.
Steinhart, J. S., 1960, Explosion studies of continental structure: PhD thesis Univ. of Wisconsin.
Usami, T., Mikumo, T., Shima, E., Tamaki, I., Asano, S., Asada, T., and Matuzawa, T., 1958, Crustal structure in Northern Kwanto district by explosion-seismic observations, part II: models of crustal structure: Bull. Earthq. Res. Inst., Tokyo, v. 36, p. 349–357.
Zirbel, N. N., 1954, Comparison of break-point and time-intercept methods in refraction calculations: Geophysics, v. 19, p. 716–721.

GEOPHYSICS, VOL. XXVI, NO. 5 (OCTOBER, 1961), PP. 588–600, 5 FIGS.

REFRACTION AND REFLECTION OF SONIC ENERGY IN VELOCITY LOGGING*

V. S. TUMAN†

Abstract: In this paper we have questioned the present accepted concept of straight-line path of the refracted beam (in velocity logging) as the source of energy for the first arrivals recorded by the receivers. The energy considerations and the field data indicate that possibly we are looking at the curved paths, an idea which so far has not been discussed thoroughly in the literature.

Equations are developed for this curve path which are based on Pickett's empirical relation. Some specific cases were analyzed using the IBM 650. It is evident that these curved paths could be utilized in some cases to yield information about the permeability in situ.

In general it is concluded that the field of velocity logging has tremendous potentialities, and there is plenty of room for further research in this area. For example, the development of sonic logging to yield porosity and permeability of the formation in situ is very intriguing. The ideas presented in this paper, after further experimental verification, can also be applied to surface seismic prospecting.

INTRODUCTION

In sonic and other velocity logging a high-frequency pulse traverses the formations around the well-bore. The sonde is normally centered in the middle of the mud column. The beams of acoustic energy travel in all directions, some of them reaching the formation boundary at a critical angle. The interpretation of the velocity logs currently is based on the assumption that only the beams refracted with the critical angle, which presumably travel parallel to the well-bore in a straight line path, are detected.

However, if the formation has a variable refractive index (increasing radially away from the well-bore), then other beams striking the formation boundary at angles smaller than the critical angle entering the formation will follow a curved path back to the well-bore.

Hicks and Berry (1956) and Wyllie, et al (1958) have shown that velocity of acoustic propagation is affected by pressure and the differential pressure.

In a well-bore, there are normal radial stresses which are only related to overburden pressures. However, abnormal or residual radial stresses independent of the overburden pressure do exist in folded formations and possibly in the vicinity of salt plugs. The temperature gradient between the well-bore and formation, due to mud circulation, will superimpose another set of stresses which are also unrelated to the overburden pressure.

In permeable beds, a hydrostatic pressure gradient of several hundred pounds will also exist between the mud column and the formation fluid. Therefore, a "variable effective stress" exists which increases radially and forms a stress envelope away from the well-bore.

In such a system, the sonic velocity will increase radially and thus, continuous refraction is possible. Beams with different angles of incidence will follow different curved paths, and all will eventually arrive back at the well-bore. This would mean that the beam arriving at the first receiver has not necessarily followed the same path as the one detected by the second receiver.

The analysis presented in this paper indicates that, at least in the cases considered, the beams which have followed a curved path will arrive before the beams travelling along a straight line. The theory proposed is based on a variable refractive index medium. In general the curved path beam will provide energy back to the well-bore so long as the energy is transmitted uniformly in all directions. This theory also indicates

† University of Illinois, Urbana, Illinois.

* Presented at the 30th Annual SEG Meeting, Galveston, Texas, November 10, 1960. Manuscript received by the Editor October 25, 1960.

that beams of longer path will penetrate into the high-velocity medium, and thus, they can be affected by the virgin fluids within the pores. This prediction has already been verified by Tixier, et al. At this stage it seems likely that in some cases curved path beams are being detected as first arrivals. The difference between two curved paths detected by two receivers will be larger than that between two straight-line paths. This can explain (at least in part) why the integrated sonic time is frequently longer than the total time recorded by a geophone survey. These questions suggest that the current model has some weaknesses. The proposed curved-path model is capable of explaining some of the points which have been observed in the field and in laboratories.

Now that we have questioned the present accepted theory, let us consider the conditions which will give rise to a curved path. To analyze this phenomena, in general we must know two factors: the effect of temperature and the effect of pressure on the elastic properties of the formations.

THE PRESSURE CONDITIONS AROUND THE WELL-BORE

A. Effect of Temperature Gradient on the Acoustic Velocity

It is a well-known fact that the temperature of various geological beds increases with depth. When a well is drilled, and mud is circulated from a pit at atmospheric temperature, part of the heat from the lower beds is absorbed and transferred to surface. As a result, the drilling fluid in the well reaching the surface is at a higher temperature than its surrounding beds.

The temperature gradient in a well depends on the rate of mud circulation. Normally, this temperature gradient is smaller than the natural gradient in the formations. For example, hardly any temperature gradient will exist in the mud column of a well if mud is circulated at a rate of 20 bbl or more per minute.

In any case, the temperature gradient between the mud and the formation changes from positive to zero, and finally to a negative value (Figure 2).

In this paper we have not attempted to evaluate the effect of temperature gradient on the acoustic impedance. For simplicity we have assumed that the mud column is in thermal equilibrium with its surrounding strata.

According to Hughes and Kelly, acoustic velocity in a consolidated porous medium decreases with rise of temperature when these samples are fully saturated. On the other hand, in an unconsolidated high-porosity formation, the acoustical velocity increases with the temperature (Shumway, 1958). In these highly porous media the effect of temperature on the compressibility of water dominates the other factors in the classical longitudinal velocity equation,

$$V = \left[\frac{K + 4/3\,\mu}{\rho}\right]^{1/2},$$

where

V = the longitudinal velocity,
K = the bulk modulus of elasticity,
μ = the rigidity modulus of the system, and
$C = 1/K$ compressibility of the system.

For a homogeneous, unconsolidated sand and water, we can write:

$$K = \frac{1}{\phi C_w} + \frac{1}{(1-\phi)C_m},$$

where

Cw = compressibility of water,
Cm = compressibility of matrix material, and
ϕ = porosity of the system.

Geertsma, 1960, in his experimental work, has shown that this relation does not apply for consolidated formations.

The density of the system is given by

$$\rho_w\phi + \rho_m(1-\phi),$$

where

ρw = density of water and
ρm = density of matrix.

The compressibility of water (Cw) is reduced by 20.5 percent when we raise the temperature from 0°C. to 50°C., but the compressibility of silica and carbonate increases by 2.2 percent for the same differential temperature. (It must be realized that Shumway's experiments were carried out at atmospheric pressure while Hughes's experiments were carried out under a pressure of 25 bars or more.)

Saunders and Topping have attempted to com-

pute such an effect around the well-bore at 10,000 ft depth. They have indicated that a maximum stress of 3,160 psi will be present at $7\frac{1}{2}$ in away from the well-bore. However, they have assumed a 200°F differential in temperature, which is considerably higher than the average gradient established around the well-bore. Such a stress is obviously time dependent and disappears completely with temperature equilibrium.

Although these authors have considered a rather high temperature gradient, their computations indicate that thermal stresses could be considerable even at lower values and therefore should not be ignored.

B. *The Hydrostatic Radial Pressure Around a Well-Bore*

Hicks (1956) and Wyllie, et al (1958) have already shown experimentally that sonic velocity increases with the differential pressure or the effective stress, $\Delta\sigma$. The effective radial stress is the resultant force of hydrostatic and nonhydrostatic radial stresses around the well-bore.

It is a standard drilling practice to have the hydrostatic pressure of the mud column, *Phm*, higher than that of the fluid pressure, *Phf*, in the formation.

Let

Phm = hydrostatic pressure of mud,
Phf = hydrostatic pressure of formation,
σ_z = overburden pressure,
K_1 = permeability of the mud cake,
K_2 = permeability of the formation,
r_f = radial distance where pressure is *Phf*,
rw = radius of the well,
rmc = *rw* + mud cake thickness, and
$\alpha = K_1/K_2$.

The pressure drop across the mud cake can be written as

$$P_1 = P_{hm} + \left[\frac{P_{hf} - P_{hm}}{\log\frac{r_{mc}}{r_w} + \alpha \log\frac{r_f}{r_{mc}}}\right] \log\frac{r}{r_w} \quad (1)$$

where

$$r_{mc} \geq r \geq r_w.$$

Similarly the pressure drop within the formation is given by

$$P_2 = P_{hf} + \left[\frac{\alpha(P_{hf} - P_{hm})}{\log\frac{r_{mc}}{r_w} + \alpha \log\frac{r_f}{r_{mc}}}\right] \log\frac{r}{r_f} \quad (2)$$

where

$$r_f \geq r \geq r_{mc}.$$ (Muskat, 1949, p. 243)

Equation (2) expresses the radial variation of the hydrostatic stresses away from the well-bore.

C. *The Nonhydrostatic Radial Stresses*

The nonhydrostatic radial stresses can be computed only for special cases. (The term, nonhydrostatic stresses, is used in association with the solid frame work of the porous medium. Only in special, rare occasions will the framework stresses be equal in all directions and thus "hydrostatic.")

Let us consider a semi-infinite bed where the lateral deformation is prevented and the vertical stress, σ_z, is equal to the overburden pressure. In such a case, the radial stress, σ_r, is related to the overburden pressure. We have:

$$\left.\begin{aligned}
&\text{Vertical Strain} && \epsilon_z = \frac{1}{E}\left[\sigma_z - \nu(\sigma_r + \sigma_\theta)\right],\\
&\text{Radial Strain} && \epsilon_r = \frac{1}{E}\left[\sigma_r - \nu(\sigma_z + \sigma_\theta)\right],\\
&\text{Circumferential Strain} && \epsilon_\theta = \frac{1}{E}\left[\sigma_\theta - \nu(\sigma_r + \sigma_z)\right].
\end{aligned}\right\} \quad (3)$$

Since

ϵ_r and ϵ_θ are zero,

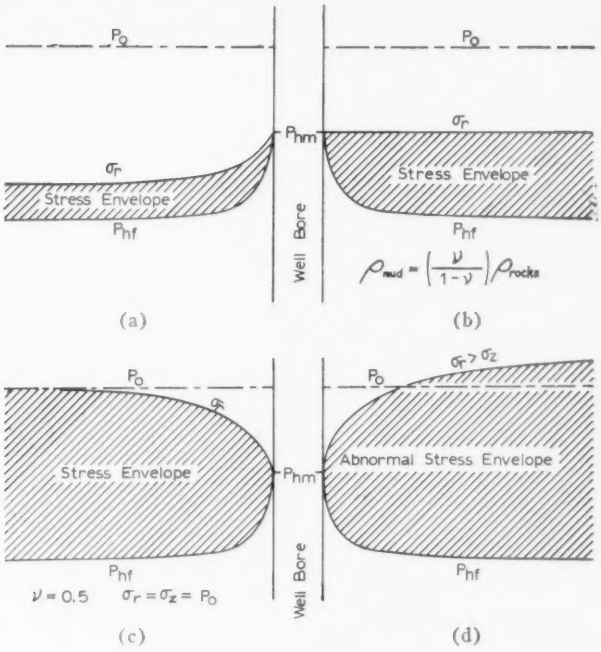

P_0 = overburden pressure
σ_r = radial stress
P_{hf} = hydrostatic pressure
P_{hm} = mud hydrostatic pressure

FIG. 1. (a, b, c, d) radial stress envelopes.

then

$$\sigma_r = \sigma_\theta = \left(\frac{\nu}{1-\nu}\right)\sigma_z. \tag{4}$$

When a well is drilled in such a formation, a stress gradient will be established between the mud hydrostatic pressure (Phm) and the radial stress σ_r . The radial variation of the stress is given by

$$\sigma_r = \sigma_{r_0}\left(\frac{r_w^2}{r^2} - 1\right) - P_{hm}\left(\frac{r_w^2}{r^2}\right), \tag{5a}$$

where

$$\sigma_{r_0} = \left(\frac{\nu}{1-\nu}\right)\sigma_z,$$

the original equilibrium stress condition. Alternatively, we may write

$$\sigma_r = \left[\left(\frac{\nu\sigma_z}{1-\nu}\right) - P_{hm}\right]\frac{r_w^2}{r^2} - \left(\frac{\nu\sigma_z}{1-\nu}\right) \tag{5b}$$

where r_w is radius of the well and r is the radial distance from the center of the well. The relation (5b) defines the radial stress and the shape of the upper curve of the stress envelope (Figure 1a).

When

$$P_{hm} = \frac{\nu\sigma_z}{1-\nu},$$

then relation (5b) is a straight line, indicating that in this case the radial stress remains constant. The Poisson ratio, ν, which varies considerably

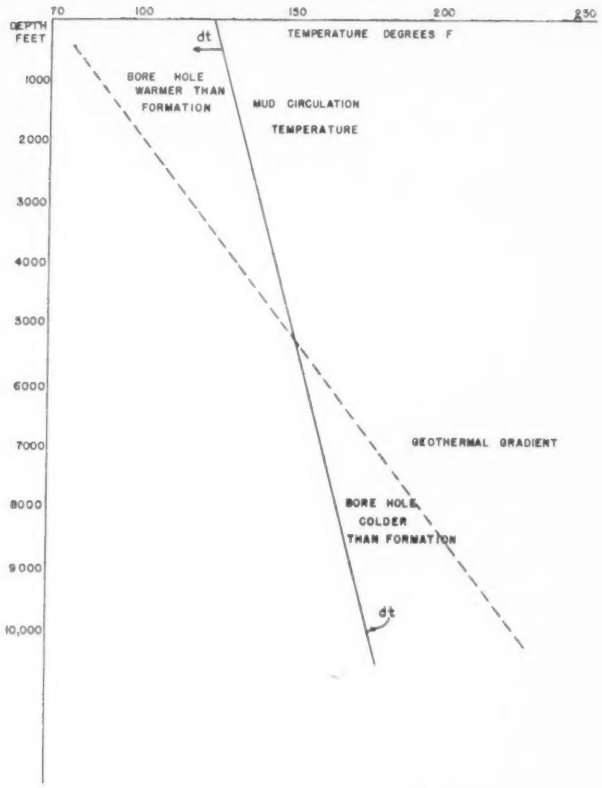

FIG. 2. Temperature distribution in borehole vs formation.

with depth and type of formation, is the controlling parameter of the radial stresses in the example considered.

Laboratory measurements of Fatt, et al Wyllie, et al, and Wuerker indicate that the Poisson ratio of porous sands is normally below 0.5 (average $\nu = 0.2$ to 0.3). However, if $\nu = 0.5$, then the radial stress is equal to σ_z, the overburden pressure. The radial stress curve for this case is given in Figure 1c.

Abnormal radial stresses would exist in folded formations and probability in the vicinity of salt plugs, where $\sigma_r > \sigma_z$ (Figure 1d). The area between nonhydrostatic and hydrostatic radial stress curves is called the stress envelope (Figures 1a, 1b, 1c, and1d).

Thus, the presence of a stress envelope indicates a variable elastic medium with a continu ously changing refractive index. The effective stress (difference between the two curves) increases continuously, and consequently the velocity of propagation would increase radially.

In Figure 3, using relations (3) and (1), we observe that, for $\alpha = 10^{-2}$, only 29 percent of hydrostatic pressure gradient drops across a 0.1-in mud cake. However, if α is reduced to 2×10^{-3}, the pressure drop across the same mud cake becomes 66 percent.

Gassmann (1951) has developed a relation between the differential pressure, ΔP, and acoustic velocity for a hexagonal packing of spheres. Pickett (1960) has modified this relation to fit the known elastic and velocity-porosity data of Hicks and Wyllie. This relation is given below.

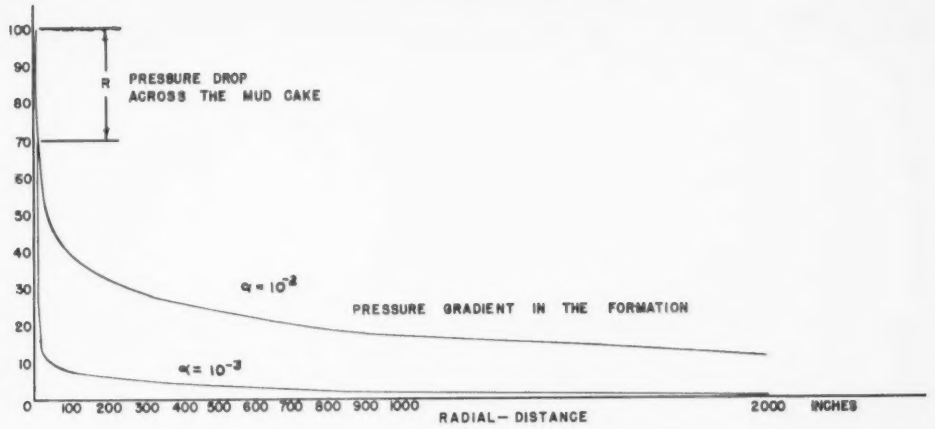

FIG. 3. Pressure distribution in mud cake and formation where

$$\alpha = \frac{K \text{ Mud}}{K \text{ Formation}}.$$

$$\rho V^2 = [1 + q_s(1 - \phi)] \cdot \left[\frac{(1 - 8C_s\overline{C})^2}{C^* - 4C_s^2\overline{C}} + 16\overline{C}\right] \quad (6)$$

where

ρ = the bulk density,
C^* = bulk compressibility,
ϕ = fractional porosity
V = velocity,
C_s = matrix compressibility material,

$$\overline{C} = \frac{5(1 - \phi)^4}{24\sqrt{2}}\left[\frac{18\pi(1 - 2\nu)^2}{C_s^2(1 - \nu^2)^2}\Delta P\right]^{1/3},$$

and

$$q_s = \frac{2(1 - \nu)}{1 + \nu}$$

where ν is Poisson's ratio of silica.

The Pickett equation was used to determine a set of velocity versus porosity curves for different differential pressures, ΔP. These are given in Figure 4. In Figure 5, the transit time ($T = 1/V$) is plotted versus differential pressure for different porosity values. From Figure 5 one can readily observe that the effect of differential pressure cannot be ignored. It is feasible that signals detected at the receivers are those from a curved path and not the one assumed presently.

In any case, we should aim to detect the energy arrivals from the curved path because these beams may reveal useful information, such as the permeability of the formation. (For this technique a patent application has been filed by the University of Illinois.)

EQUATIONS FOR THE CURVED PATHS

It is unfortunate that sonic velocity does not increase linearly in the radial direction because the curved path for such a system has been elegantly determined by Nettleton and others. In a well-bore, however, conditions are more complex. Hence, we use Pickett's empirical relation, which relates ΔP to velocity and porosity, to compute the curved path of the sonic beams. If the velocity of propagation is a function of strains in the direction of propagation, then it is perhaps an oversimplification to use an average stress,

$$\bar{\sigma} = \frac{\sigma_r + \sigma_\theta + \sigma_z}{3}. \quad (7)$$

The equation of a beam travelling in a variable refractive index plane, RZ, is developed below.

From relation (2) and (5b) we have

$$\Delta\sigma = \sigma_r - P_2 \tag{8a}$$

$$\Delta\sigma = \left\{\left[\left(\frac{\nu\sigma_z}{1-\nu}\right) - P_{hm}\right]\frac{r_w^2}{r^2} - \left(\frac{\nu\sigma_z}{1-\nu}\right)\right\} - \left\{P_{hf} + \left[\frac{\alpha(P_{hf} - P_{hm})}{\log\dfrac{r_{mc}}{r_w} + \alpha\log\dfrac{r_f}{r_{mc}}}\right]\log\frac{r}{r_f}\right\}. \tag{8b}$$

Natural logarithm is used throughout these equations. Equations (8b) can be simplified to

$$\Delta\sigma = \left[\frac{K}{r^2} - L\log\psi r\right] \tag{8c}$$

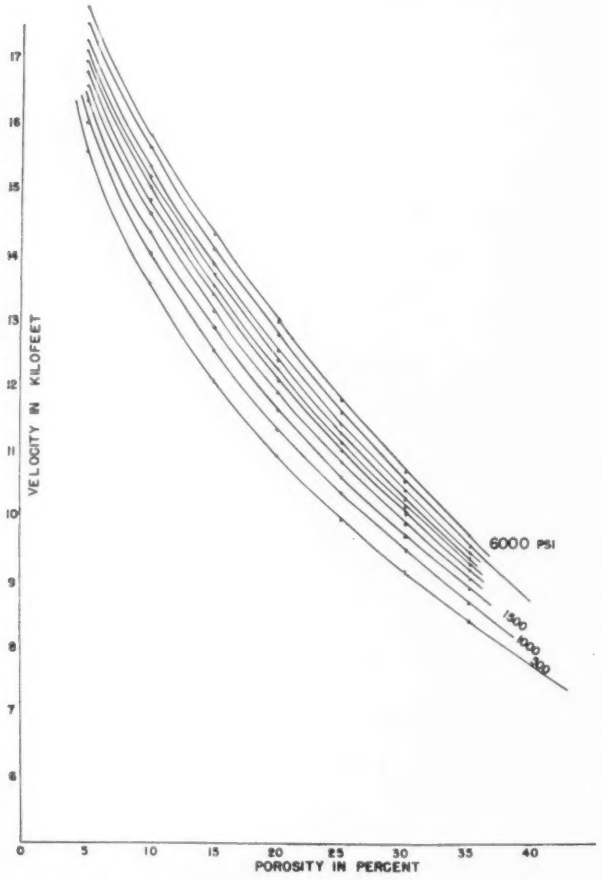

FIG. 4. Velocity vs porosity for different ΔP in PSI.

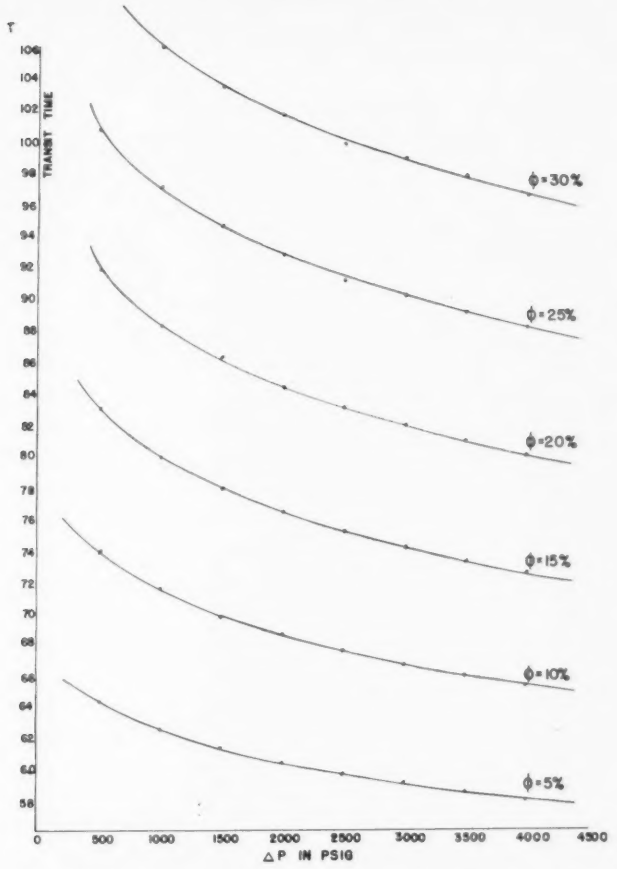

FIG. 5. Transit time vs ΔP for different porosities, sandstone formations only.

where

$$K = \left[\left(\frac{\nu\sigma_z}{1-\nu}\right) - P_{hm}\right] r_w^2,$$

$$L = \left[\frac{\alpha(P_{hf} - P_{hm})}{\log \dfrac{r_{mc}}{r_w} + \alpha \log \dfrac{r_f}{r_{mc}}}\right], \text{ and}$$

$$L \log \psi r_f = \left(P_{hf} + \frac{\nu\sigma_z}{1-\nu}\right).$$

Therefore, the Pickett empirical equation simplifies to

$$V^2 = A\left[\frac{1 - M\left(\dfrac{K}{r^2} - L\log\psi r\right)^{1/3}}{C^* - N\left(\dfrac{K}{r^2} - L\log\psi r\right)^{1/3}}\right]$$

where

$$A = \frac{1}{\rho}\left[1 + q_s(1-\phi)\right],$$

$$M = 16(C_s - C^*)g,$$

$$N = 4C_s^2 g, \text{ and}$$

$$g = \frac{5(1-\phi)^4}{24\sqrt{2}}\left[\frac{18\pi\cdot(1-2\nu)^2}{C_s^2(1-\nu^2)^2}\right]^{1/3}.$$

Let i be the angle of incidence of an acoustic beam, Z represent vertical axis, and r the radial distance; then

$$\cot i = \frac{dr}{dz}. \tag{10}$$

From Snell's law,

$$\frac{V_1}{\sin i_1} = \frac{V_2}{\sin i_2} = \cdots \frac{V_n}{\sin i_n} = V_m, \tag{11}$$

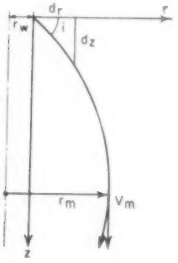

where V_1 and $\sin i_1$ denote the velocity and the angle of incidence at the well-bore, and V_m denotes the maximum velocity attained by the wave along its curved path, i.e. at

$$r = r_m,$$

$$V = V_m \sin i = \frac{V_m}{\sqrt{1+\left(\frac{dr}{dz}\right)^2}}. \tag{12}$$

$$\therefore \frac{dz}{dr} = \left[\frac{A - B\left(\frac{K}{r^2} - L\log\psi r\right)^{1/3}}{\eta - \gamma\left(\frac{K}{r^2} - L\log\psi r\right)^{1/3}}\right]^{1/2} \tag{13}$$

where

$$\eta = (C^* V_m^2 - A) \quad \gamma = (NV_m^2 - AM),$$

$$\text{and } B = AM.$$

Therefore, the length of the curved path of a sonic beam can be expressed as

$$S = 2\int_{r_{mc}}^{r_m}\left[1+\left(\frac{dz}{dr}\right)^2\right]^{1/2} dr \tag{14}$$

or

$$S = 2\int_{r_{mc}}^{r_m}\left[1 + \frac{A - B\left(\frac{K}{r^2} - L\log\psi r\right)^{1/3}}{\eta - \gamma\left(\frac{K}{r^2} - L\log\psi r\right)^{1/3}}\right] dr. \tag{14a}$$

Similarly, by equation (13), Z, the vertical separation between transmitter and receiver as a function of radius of penetration of beam, is given by

$$Z = 2\int_{r_{mc}}^{r_m}\left[\frac{A - B\left(\frac{K}{r^2} - L\log\psi r\right)^{1/3}}{\eta - \gamma\left(\frac{K}{r^2} - L\log\psi r\right)^{1/3}}\right] dr. \tag{15}$$

The travel time, T, is given by

$$T = \int \frac{ds}{V} \tag{16}$$

or

$$T = \frac{2}{\sqrt{A}} \int_{r_{mc}}^{r_m} \left[1 + \frac{A - B\left(\frac{K}{r^2} - L \log \psi r\right)^{1/3}}{\eta - \gamma\left(\frac{K}{r^2} - L \log \psi r\right)^{1/3}} \right]^{1/2} \left[\frac{C^* - N\left(\frac{K}{r^2} - L \log \psi r\right)^{1/3}}{1 - M\left(\frac{K}{r^2} - L \log \psi r\right)^{1/3}} \right]^{1/2} dr. \tag{17}$$

Notice that Vm is the maximum velocity attained by the beam along its path when $r = rm$.

$$V_m^2 = A \left[\frac{1 - M\left(\frac{K}{r_m^2} - L \log \psi r_m\right)^{1/3}}{C^* - N\left(\frac{K}{r_m^2} - L \log \psi r_m\right)^{1/3}} \right]. \tag{18}$$

Since originally we were not aware of the work done by Topping, another set of integrals describing the curved path phenomena were evaluated numerically for the case where nonhydrostatic radial stresses were assumed to vary logarithmically, i.e.

$$\sigma_r = h + b \log \frac{r}{r_f}, \tag{19}$$

and using the assumed boundary conditions,

$$\sigma_r = P_{hm} \quad \text{where} \quad r = 3 \text{ in},$$

$$\sigma_r = \sigma_z \quad \text{where} \quad r = 6 \text{ in}.$$

Then

$$\sigma_r = P_{hm} + \left[\frac{\sigma_z - P_{hm}}{\log_e 2} \right] \log \frac{r}{3}; \tag{20}$$

and

$$\Delta\sigma = \sigma_r - P_2,$$

$$\Delta\sigma = \left\{ P_{hm} + \left[\frac{\sigma_z - P_{hm}}{\log 2} \right] \log \frac{r}{3} \right\}$$

$$- \left\{ P_{hf} + \left[\frac{\alpha(P_{hf} - P_{hm})}{\log_e \frac{r_{mc}}{r_w} + \alpha \log \frac{r_f}{r_{mc}}} \right] \log \frac{r}{r_f} \right\}.$$

If

$$L = \left[\frac{\alpha(P_{hf} - P_{hm})}{\log \frac{r_{mc}}{r_w} + \alpha \log \frac{r_f}{r_{mc}}} \right],$$

$$C = \left[\frac{\sigma_z - P_{hm}}{\log 2} \right].$$

$$\therefore \Delta\sigma = \{ P_{hm} + C \log r - C \log 3 \} - \{ P_{hf} + L \log r - L \log r_f \}.$$

Let

$$D = [P_{hm} - P_{hf} - C \log 3 + L \log r_f],$$

and

$$E = C + L.$$

Thus,

$$\Delta\sigma = (D + E \log r).$$

Also let,

$$P = 16g(C^* - C_s) \quad [= -M],$$

$$m = 4C_s^2 g \quad [= N].$$

Using these constants, equations (2) and (20) were combined as shown above, obtaining the following integrals:

$$S = 2\int_{r_{mc}}^{r_m}\left[1 + \frac{A\{1 + P(D + E\log r)^{1/3}\}}{V_m^2[C^* - m(D + E\log r)^{1/3}] - A[1 + P(D + E\log r)^{1/3}]}\right]^{1/2} dr$$

and

$$T_s = \frac{2V_m}{\sqrt{A}}\int_{r_{mc}}^{r_m}\left[\frac{C^* - m(D + E\log r)^{1/3}}{V_m^2\{C^* - m(D + E\log r)^{1/2}\} - A\{1 + P(D + E\log r)^{1/3}\}}\right]^{1/2} \cdot \left[\frac{1}{1 + P(D + E\log r)^{1/3}}\right]^{1/2} dr.$$

Similarly,

$$Z = 2\int_{r_{mc}}^{r_m}\left[\frac{A\{1 + P(D + E\log r)^{1/3}\}}{V_m^2\{C^* - m(D + E\log r)^{1/3}\} - A\{1 + P(D + E\log r)^{1/3}\}}\right]^{1/2} dr.$$

Results for these integrals are given in table (1).

DISCUSSION OF THE RESULTS

The IBM 650 digital computer on the campus of the University of Illinois was used to evaluate 75 different cases. The length of the path (S), the transmission time for curved path (Ts), and the straight line path (Tz), which are functions of porosity, permeability, and radial penetration into the formation, were studied.

A sand formation of 4,000 ft depth was considered to have a 4,000 psi overburden pressure. If the drilling mud in this well were 10.5 ppg; then the mud hydrostatic pressure (Phm) (opposite the sand) would be 2,174 psi, and sand hydrostatic formation pressure would be 1,800 psi.

To focus the attention on the effect of permeability, next we assumed that a well head pressure of 1,326 psi was applied. Thus , we increased purposely the hydrostatic pressure gradient and reduced the nonhydrostatic radial stresses.

The results for porosity ranges between 5 percent to 30 percent, $\alpha = 10^{-2}$, 10^{-4}, 10^{-6}, and the radius of investigation $r_m = 6''$, $9''$, $12''$, $24''$, and $36''$ were investigated. Some of the results are given in table 1.

It became evident that, in all the cases studied, the curved path time (Ts) was shorter than straight-line path (Tz). It also is evident that the effect of porosity is much more pronounced than the effect of permeability.

For example:

ϕ %	S cms	Z cms	T_s μsec	T_z μsec	$\alpha = \frac{K\text{ mud}}{K\text{ formation}}$	r_m
10	170.54	169.70	395.75	437.11	10^{-4}	6″
10	172.02	171.19	398.74	443.66	10^{-6}	6″
15	181.85	181.06	444.80	484.95	10^{-4}	6″
15	183.41	182.63	448.17	491.66	10^{-6}	6″

REFLECTION OF SONIC ENERGY

In a homogeneous porous formation with oil present behind the invaded front, it is possible to get some of the acoustic energy reflected from this boundary. Theoretically, the energy reflected is about 1 to 4 percent, depending on the porosity and velocity contrast between the virgin and invaded formation. Therefore, with sufficiently sensitive instrumentation it should be possible to detect the hydrocarbons behind the invaded zones. For low-porosity formation, the reflected energy is very small and is further attenuated by deeper invasion. Therefore, the task of detecting a reflected signal from an oil bearing formation should be relatively easier for higher porosity for-

Table I. Summary of the Results

r_m	α	ϕ	S cms	t_s μsec	Z cms	T_z μsec
6	10^{-3}	10	170.54	395.75	169.70	437.17
6	10^{-3}	15	181.85	444.80	181.06	484.95
6	10^{-3}	20	195.90	502.86	195.17	541.21
6	10^{-3}	30	235.95	656.90	235.35	690.16
6	10^{-4}	5	162.77	356.53	161.89	402.30
6	10^{-4}	10	172.03	398.74	171.19	443.66
6	10^{-4}	15	183.41	448.17	182.63	491.66
6	10^{-4}	20	197.57	506.70	196.84	548.19
6	10^{-4}	30	237.91	661.96	237.31	697.88
9	10^{-3}	10	312.53	720.03	310.56	800.06
9	10^{-3}	15	332.96	809.28	331.12	886.89
9	10^{-3}	20	358.38	914.90	356.67	989.06
9	10^{-3}	30	430.86	1,195.01	429.44	1,259.35
9	10^{-4}	5	298.32	648.28	296.26	736.22
9	10^{-4}	10	315.03	725.05	313.08	811.38
9	10^{-4}	15	335.59	814.94	333.76	898.55
9	10^{-4}	20	361.19	921.35	359.49	1,001.17
9	10^{-4}	30	434.16	1,203.52	432.75	1,272.63
12	10^{-3}	10	456.23	1,045.75	453.09	1,167.24
12	10^{-3}	15	485.79	1,175.44	482.84	1,293.27
12	10^{-3}	20	522.57	1,328.90	519.83	1,441.50
12	10^{-3}	30	627.54	1,735.84	625.26	1,833.59
12	10^{-4}	5	435.52	941.15	432.23	1,074.12
12	10^{-4}	10	459.69	1,052.69	456.57	1,183.27
12	10^{-4}	15	489.42	1,183.24	486.50	1,309.75
12	10^{-4}	20	526.45	1,337.82	523.74	1,458.59
12	10^{-4}	30	632.07	1,747.51	629.81	1,852.14
24	10^{-3}	10	1,054.43	2,388.11	1,046.55	2,696.11
24	10^{-3}	15	1,121.40	2,684.84	1,113.99	2,983.79
24	10^{-3}	20	1,204.75	3,035.80	1,197.87	3,321.72
24	10^{-3}	30	1,442.94	3,966.10	1,437.21	4,214.69
24	10^{-4}	5	1,006.75	2,147.10	998.49	2,481.30
24	10^{-4}	10	1,061.43	2,402.10	1,053.60	2,730.52
24	10^{-4}	15	1,128.79	2,700.70	1,121.44	3,019.15
24	10^{-4}	20	1,212.68	3,054.00	1,205.84	3,358.23
24	10^{-4}	30	1,452.30	3,990.20	1,446.60	4,254.16
36	10^{-3}	10	1,680.94	3,781.50	1,668.36	4,298.02
36	10^{-3}	15	1,786.64	4,252.10	1,774.82	4,753.80
36	10^{-3}	20	1,918.05	4,808.40	1,907.06	5,352.63
36	10^{-3}	30	2,294.21	6,283.30	2,285.03	6,700.96
36	10^{-4}	5	1,605.14	339.80	1,591.97	3,956.13
36	10^{-4}	10	1,691.41	380.25	1,678.93	4,351.13
36	10^{-4}	15	1,797.63	427.57	1,785.89	4,807.99
36	10^{-4}	20	1,929.85	483.55	1,918.93	5,344.17
36	10^{-4}	30	2,308.20	631.94	2,299.09	6,761.15

mations. It must be realized that probably this reflected energy will appear as a late arrival. Therefore, special effort should be made to detect the reflected beams.

CONCLUSION

From the theoretical work of Gassman, Brandt, Biot, and Geertsma; the experimental work of Hicks, et al. and Wyllie, et al., it is evident that velocity of sonic propagation is related to a differential stress by a power of $\frac{1}{6}$. There are only two sets of experimental data to verify this phenomenon. Therefore, more experimental work, specifically measurements of velocity along the direction of effective stress, is extremely desirable.

If the velocity of propagation along the x direction is a function of stresses and effective stress in the x direction, then this phenomenon would have a direct application to surface seismic prospecting. By shooting at the center of two concentric circles and spreading the geophones on the circle (surface prospecting), the velocity variation in different directions of propagation can be observed. This would reveal the presence of effective residual stresses, which might be an indication of unforeseen underground folds or salt plugs.

Our views regarding linear variation of velocity with depth may also have to be modified on the basis of such new theoretical and experimental findings.

The idea of measuring permeability is of sufficient importance to warrant more time and effort toward further study of velocity logging.

ACKNOWLEDGMENTS

The author wishes to thank Professor Walter Rose and Professor A. P. Boresi who were kind enough to read this paper. Their comments during many useful discussions have been instrumental in clarifying some of the points on the subjects.

Special thanks go to Mr. M. Anvari for his assistance in the development of the equations of the curved path and to Miss Dorothy Bollman for her work on the IBM 650.

The personnel of the University of Illinois Digital Computer Lab are remembered for their help and cooperation.

The author is also grateful to Mr. T. S. Hutchinson who read the original draft of the paper and made some very constructive suggestions.

Special thanks to Messrs. Harry Fara and Alan Kingery for editing the entire paper, W. L. Magnuson for preparing the diagrams, and Mrs. Madeline Saltarelli for typing and preparing the manuscripts.

REFERENCES

Berry, J. E., 1959, Acoustic velocity in porous media: Journal of Petroleum Technology, v. 11, p. 262.

Biot, M. A., 1956, Theory of propagation of elastic waves in a fluid saturated porous solid; Journal of the Acoustical Society of America, v. 28, p. 179.

Brandt, H., 1955, A study of the speed of sound in porous granular media: Journal of Applied Mechanics, v. 22, p. 479–485.

Gassmann, F., 1951, Elastic waves through a packing of spheres: Geophysics, v. 16, p. 673–685.

Geertsma, J., 1960, Velocity-log interpretation: the effect of rock bulk compressability: paper 1535-G, AIME Symposium, S.P.E.

Hicks, W. G., and Berry, J. E., 1956, Application of continuous velocity logs to determination of fluid saturation of reservoir rocks: Geophysics, v. 21, p. 739–754.

Hueter, T. F., and Bolt, R. H., 1955, Sonics: New York, John Wiley and Sons, Inc.

Hughes, D. S., and Cross, J. H., 1951, Elastic wave

velocities in rocks at high pressures and temperatures: Geophysics, v. 16, p. 577–593.
———, and Kelly, J. L., 1952, Variation of elastic wave velocity with saturation in sandstone: Geophysics, v. 17, p. 739–752.
Lindsay, Robert B., 1960, Mechanical radiation: New York, McGraw-Hill Book Company.
Mann, R. L., and Fatt, I., 1960, Effect of pore fluids on the elastic properties of sandstone: Geophysics, v. 25, p. 433–444.
McCray, A. W., and Cole, F. W., 1959, Oil well drilling technology: Norman, University of Oklahoma Press.
Miles, A. G., and Topping, A. D., 1948, Stresses around a deep well: Journal of Petroleum Technology, T. P. 2411.
Muskat, M., 1949, Physical principles of oil engineering: New York, McGraw-Hill Book Company.
Nettleton, L. L., 1940, Geophysical prospecting for oil: New York, McGraw-Hill Book Company.
Pickett, G. R., 1960, The use of acoustic logs in the evaluation of sandstone reservoirs: Geophysics, v. 25, p. 250–274.
Saunders, K. D., and Topping, A. D., 1951, Thermal stresses around an uncased hole: World Oil, (1950 Part I), p. 167–172, (1951 Part II) p. 155–160.
Shumway, G., 1958, Sound velocity vs. temperature in water-saturated sediments: Geophysics, v. 23, p. 494.
Tixier, M. P. et al, 1959, Sonic logging: Journal of Petroleum Technology, May, p. 106–114.
Topping, A. D., 1951, Elastic, elastic-plastic, and viscoelastic states of stress and strain around a vertical cyclindrical hole in a semi-infinite gravitational body: Urbana, University of Illinois, unpublished thesis.
Wuerker, R. J., 1956, Annotated tables of strength and elastic properties of rocks: Paper 663-G, Petroleum Branch AIME.
Wyllie, M. R., Gregory, A. R., and Gardner, L. W., 1956, Elastic wave velocities in heterogenous and porous media: Geophysics, v. 21, p. 41–70.
———, Gregory, A. R., and Gardner, G. H., 1958, An experimental investigation of factors affecting elastic wave velocities in porous media: Geophysics, v. 23, p. 459–493.

GEOPHYSICS, VOL. XXVI, NO. 5 (OCTOBER, 1961), PP. 601-617, 29 FIGS.

EXPERIMENTAL AND FIELD DATA FOR THE DUAL-FREQUENCY PHASE-SHIFT METHOD OF AIRBORNE ELECTROMAGNETIC PROSPECTING*

NORMAN R. PATERSON†

Abstract: With the growing maturity in airborne electromagnetic instrumentation a transition has taken place from rule-of-thumb application and interpretation methods to a more sophisticated over-all approach. A greatly improved success rate in the location of massive sulphide bodies is illustrated by recent results with the dual-frequency phase-shift airborne electromagnetic method.

Part of the sophistication process has been the improvement of quantitative methods of interpretation, based on both theoretical and model studies. A recent research program has been most useful in this regard. These studies have been carried out within the framework of an active exploration department and have been integrated with field results at various stages.

FOREWORD

The purpose of this paper is to draw attention to work that has been carried out on methods of interpretation of airborne electromagnetic data. Since the writer's experience has been mainly with the system employed by his company, these remarks are based on work carried out with this system. Illustrations apply to this system only, but some of the more general conclusions may have application to situations encountered with other electromagnetic devices.

The paper is not intended as a manual of electromagnetic interpretation. It covers only a few of the important response characteristics of the system and is necessarily limited to the more simple geological situation.

INTRODUCTION

The system under discussion is the dual-frequency phase-shift measuring equipment developed by M. Puranen, A. Kahma, and V. Ronka working under the auspices of the Geological Survey of Finland during the years 1947 to 1953. In 1954, it was put into operational use in Canada by the Hunting organization and since then has been used by Hunting airborne geophysical companies in various parts of the world. The first published description of the system (Engineering and Mining Journal, March, 1956) outlines the basic principles and illustrates some of the early results obtained with the equipment in the field. Since that time improvements have been made which modify the external appearance, sensitivity, and portability of the equipment. The basic design, coil configuration, and frequencies have remained unchanged. All the development work has been done under the direction of V. Ronka.

The instrument consists of a horizontal transmitting coil mounted on an aircraft, generating electromagnetic fields at two frequencies, 400 cps and 2,300 cps., and a vertical receiving coil located in a towed "bird" behind and below the aircraft (Figure 1). Phase detecting circuits in the aircraft allow the phase-shifts of the voltages generated in the receiving coils (relative to the transmitted voltages as reference) to be measured, and these are displayed on a continuous graphical recorder.

Some approximate statistics concerning these main parts of the equipment are listed.

Transmitting coil. Weight 75 lbs., size 540 sq ft, 3 turns.

Power. Low frequency, 80 amps at 500 watts. High frequency, 18 amps at 150 watts. (A lighter transmitter has 6 turns and only 25 percent of the current.)

Receiving coil. Low frequency: 12 lbs, 16,000 turns, size approximately 100 sq inches. High frequency: 6 lbs, 6,000 turns, same size. (The

* Presented at the 30th Annual Meeting, SEG, Galveston, November 10, 1960.

† Hunting Survey Corporation Limited, Toronto, Ontario, Canada.

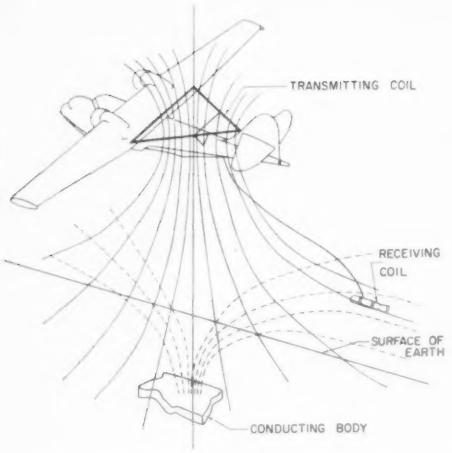

FIG. 1. Geometry of electromagnetic system.

lighter version has a smaller area but roughly the same number of turns.)

Bird. The bird contains the two receiving coils, preamplifier, and battery. (Total weight in the lighter version is 45 lbs.)

Geometry. The bird is normally carried 420 ft behind and 220 ft below the aircraft. At this point the primary field is inclined at about 20° to the axis of the receiving coil.

Compensating coil. A small vertical coil with axis along the direction of flight is fed with a voltage in quadrature with the transmitting voltages (field $\frac{1}{2}$ percent that of primary field) in order to compensate for that quadrature field generated by the skin of aircraft which is at right angles to the primary field at receiver.

Phase Detectors. Use signal correlation to decrease the band width to about 0.2 cps (at 400 cps) at a time constant of 1 sec. Noise level is below 0.05° or less than 1/1,200 of the primary field.

Recorder (radio altimeter). Sanborn 4 channel recorder with dc amplifiers. Used to display A. R. D. (scintillation counter) and A. P. N. 1 data as well as both E. M. frequency channels.

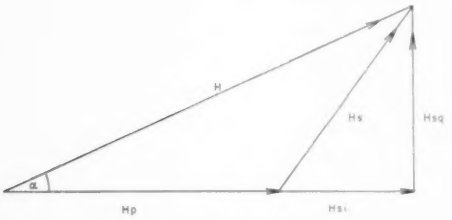

FIG. 2. Vectorial relationships.

Since the measuring system records only the changes in phase of the total field along the axis of the receiver and is effectively compensated for quadrature variations from other than ground sources, normal movements of the bird do not affect the data recorded by the instrument. The vector diagram of Figure 2 illustrates that the quantity measured (α) is proportional, for small phase angles, to the quadrature component (Hsq) of the secondary field generated by ground conductors.

Actual accuracy obtained by the equipment in normal survey operation is about 0.05° or roughly 1 part in 1,200 of the primary field. Normally, anomalies of 0.1° and over are recognizable against the noise background. Excessive turbulence, electrical storms, etc., can, at times, increase the noise level to $\pm 0.1°$ or more; but this is very rare.

Normal flying height for the instrument, mounted in a Canso (PBY) aircraft, is 500 ft above mean terrain. At times this is decreased to 450 ft and on rare occasions to as little as 350 ft. With recent improvements in weight and sensitivity, the equipment can be mounted in a quite small aircraft. Figure 3 shows installations in both a Canso and a Fairchild Husky.

The system has seen its greatest use in Canada, where more than 300,000 line miles have been surveyed by this method. Some of this work is described by MacKay and Paterson (1960). Other surveys which contributed to the discovery of four commercial sulphide deposits are referred to in papers by Springer, Joklik, Cheriton, and Fleming.

Much of the above work was done in the years 1955–1956, a period when airborne electromagnetic prospecting was being applied with great success to exploration for massive sulphide bodies in Canada. During this period alone it is estimated that at least 50 million tons of minable ore were found by the one electromagnetic system at an average survey cost of 5 cents per ton. This is all the more remarkable inasmuch as at that time

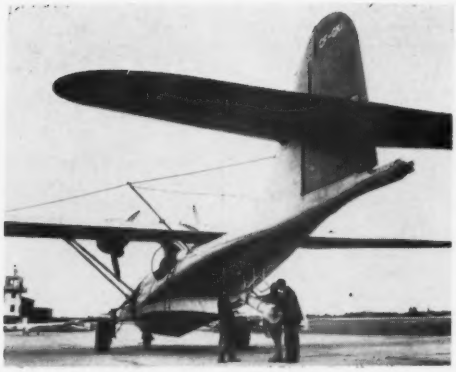

FIG. 3. Electromagnetometer installations in (a) "Canso" (PBY) Amphibian; (b) Fairchild "Husky."

interpretation techniques were in their infancy, and a great deal of money and time was wasted on anomalies which would now be downgraded or eliminated entirely by analysis.

Application of the method in other countries has been only partially successful. Mainly, this has been due to particular geological conditions (deep weathering, shallow conductive layers, etc.) or rugged topography (Tasmania, Cuba, etc.). Partly, again, it has been through confusion arising from inability to recognize and separate the effects of changes in geometry and conductivity, which is sometimes avoidable through careful interpretation.

The writer believes that there is a wealth of information buried in old records of past surveys that could be exploited economically even at this late stage. The same must be true for surveys carried out by other electromagnetic systems. Furthermore, a careful look at those areas previously written off as unsuitable for electromagnetic work might show that new instrumentation and interpretation techniques can operate successfully.

THE REQUIREMENTS OF INTERPRETATION

Any effective electromagnetic system must do two things. First, it must record accurately, and with high sensitivity, the presence and location of a conductor; second, it must provide enough data to enable the interpreter to determine both the shape of the conductor and its width-conductivity factor.

The inventors of the dual-frequency phase-shift electromagnetic system worked under the premise that conductors occur in all conceivable shapes and sizes and in a wide range of effective conductivities. They took extreme care in the choice of coil configuration and frequencies to ensure that the widest possible range of conductors would be detected. This puts an extra burden on the interpreter as he cannot say, as with some systems, that the conductor causing an anomaly must be vertical (or horizontal, etc.). Not only must the interpreter arrive at the right conclusions, but he must do this quickly and economically. It is common in many areas to encounter significant-looking anomalies at the rate of at least one per survey mile. Many of these are caused by noneconomic conductors such as shear-zones, buried river-channels, clay beds and other electrolytic effects. Contrary to what is sometimes stated, it is impossible to eliminate these effects instrumentally from the response of any system and at the same time maintain proper sensitivity to metallic conductors of all shapes and sizes. Unfortunately, the width-conductivity factor for many common electrolytic conductors overlaps well into the range of metallic conductors.

Nor is it normally possible to refly the anomalies at different altitudes, azimuths, or coil spacings. Therefore, the interpreter must be able to unravel the anomalies by analysis and by good geological judgment, quickly and effectively.

Figure 4 illustrates two electromagnetic records from two areas totally different in electrolytic response. In Figure 4(a) a strong background response is caused by a heavy layer of conducting clays. Undulations in this response are difficult to recognize from anomalies originating within the bedrock. In Figure 4(b), on the other hand, the background is relatively low and a lake underlying the left half of the record produces only a very minor change in background level. The inter-

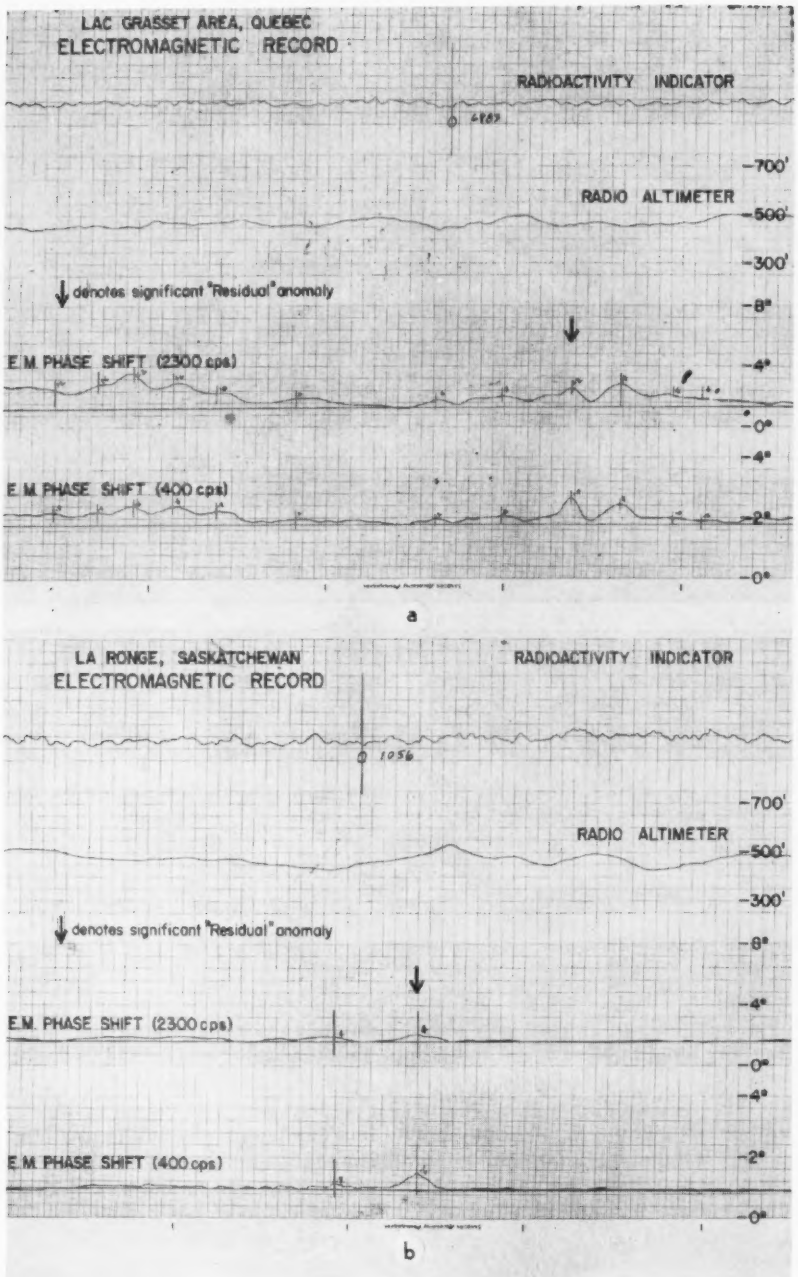

FIG. 4. Electromagnetic Survey Records.

preter has indicated two anomalies, one on each record, which he considers justify further investigation. The processes by which this selection is made are described in the following sections.

GEOMETRICAL FACTORS

If the response of an electromagnetic system to various geometric factors is determined, it is possible to infer certain geometrical properties from the appearance of an anomaly by the reverse procedure. This process, known as indirect interpretation, requires the compilation of type curves through either theoretical or model experimentation.

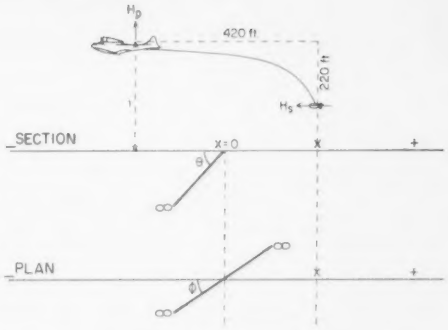

FIG. 5. Configuration used in electromagnetic type curves.

Theoretical Work

Fortunately, the effects of changes in geometry can be studied separately from the more complicated effects of conductivity, width, frequency, and permeability. To do this, the conductor is assumed to have an infinitely high response parameter (for example, infinite conductivity); and the parameters, varied are height, strike, dip, size, and shape are varied. Observations are made of the changes in anomaly size and shape which can then be extrapolated to the finite conductivity case. Since the system under study measures the quadrature response, whereas the infinite conductivity model provides only in-phase anomalies, it is necessary to establish relations between in-phase and quadrature response which can be used to make the extrapolation. This is the subject of the section "Conductivity and Width," below.

One of the important advantages of separating out the geometrical effects is that, by so doing, one can use theoretical solutions for simple models such as the half-plane and the circular disk (West, 1960; Douloff, 1960). These solutions can often be obtained at less than one-tenth the cost of model experiments and in a very small fraction of the time.

Using the theoretical calculations and computer program of West (1960), a large number of type curves was calculated for the dual-frequency phase-shift system during the period 1958–1960. The calculations were done mainly by M. A. Chinnery at the University of Toronto, using the University's IBM 650 computer.

Figure 5 illustrates the geometrical configuration and parameters varied in this series of tests. The half-plane was the only model used. Relative permeability μ is assumed to be unity. Some of the results are now described under the headings of the parameters varied.

Variation with Height.—Figure 6 illustrates electromagnetic profiles over a vertical half-plane at heights varying from 300 to 700 ft above the conductor. Height is measured from the aircraft and the readings are plotted beneath the towed receiver. The profiles illustrate the small secondary peak which develops as the transmitter passes over the conductor.

In Figure 7 the variations of peak response are plotted as a function of height on a logarithmic scale. The slope of the straight lines so derived represents the power at which the anomaly decreases with height. This power is seen to be 4.1. It is interesting to note (also in Figure 7) that the observed response over the Ontario Pyrites Deposit, Sudbury, Ontario, decreases with height

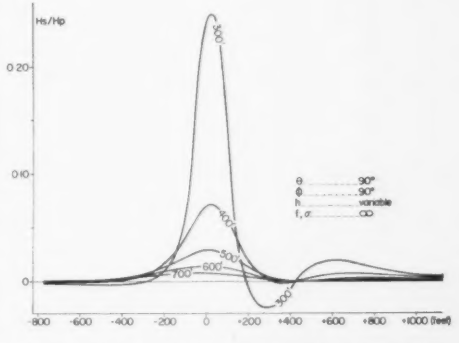

FIG. 6. Variation of in-phase anomaly with height for vertical half-plane (theoretical).

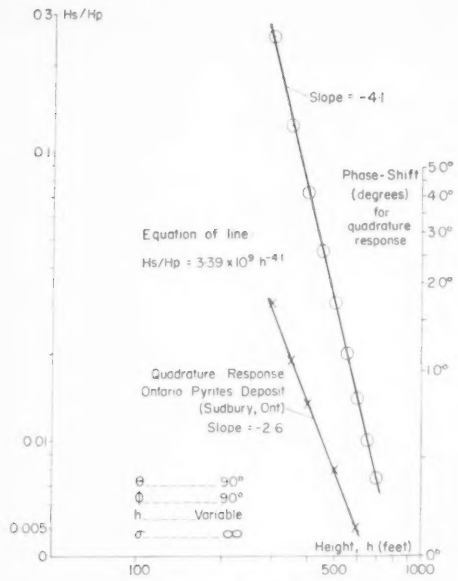

FIG. 7. Variation of peak (in-phase) response of vertical half-plane with height (theoretical).

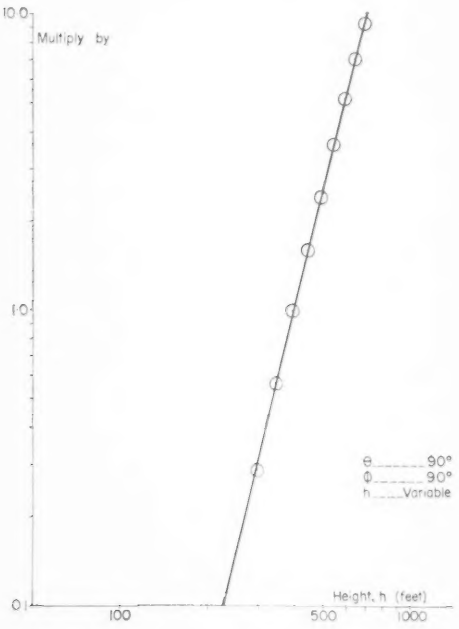

FIG. 8. Normalizing curve to convert response at h feet to equivalent response at 400 feet (vertical half-plane).

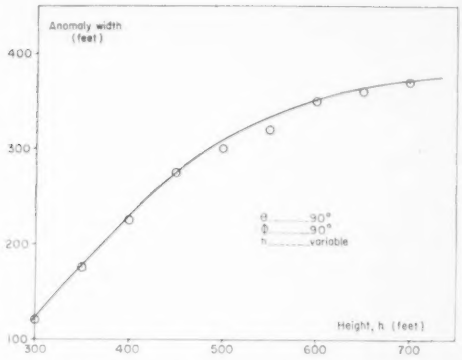

FIG. 9. Variation of anomaly width with height for vertical half-plane (theoretical).

only to the power 2.6. This is believed to be because this particular conducting body is quite broad and is, in fact, made up of several parallel conducting bands. Other observations in the field suggest that a power of approximately 3.5 is appropriate over most geological conductors. For further discussions regarding this point, the reader is referred to an article by the author (1959) and a reply by Hedstrom (1959).

Based on the theoretical results, a normalizing curve has been drawn in Figure 8. This has been found to be useful for comparing the anomaly with type curves obtained at 400 ft elevation.

Figure 9 illustrates the variation of anomaly width (distance between inflection points) with heights as derived from the curves in Figure 6. At normal flying heights of 450 to 500 ft, the width of the anomaly is seen to be 275 to 300 ft. In practice this is seldom observed, probably because of finite conductor width and eddy currents induced in surrounding overburden and in poorly conducting halos around the conductor. However, it illustrates that excessive anomaly width cannot be caused by depth of burial alone and sometimes helps to unravel the effects of dip, height, and width.

Variations with Strike.—The effects of variations in strike angle are illustrated in Figure 10. Erratic behavior of the curves at small strike angles has not been properly explained and in this region the curves were supplemented by model experiments.

The values of peak response from Figure 10 are plotted as a function of strike angle in Figure 11. The rate of fall-off of the anomaly with decrease

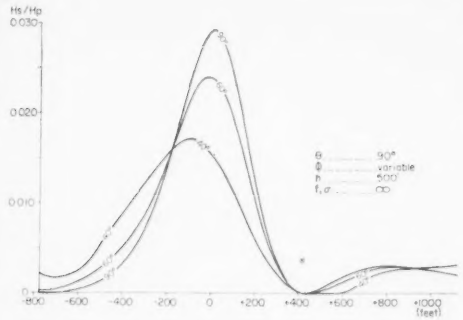

FIG. 10. Variation of in-phase anomaly with strike angle for vertical half-plane (theoretical).

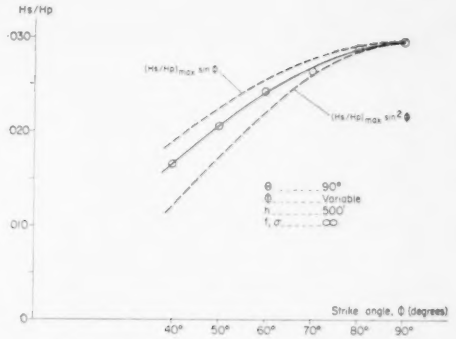

FIG. 11. Variation of peak (in-phase) response of vertical half-plane with strike angle (theoretical).

in strike angle is seen to be roughly midway between a sine and a sine-squared law. This observation has been confirmed in the field.

The variation of anomaly width with strike angle is illustrated in Figure 12. As would be expected, it seems to follow a sine law.

These results confirm that contouring of low-frequency phase angles is a legitimate procedure in areas of steeply dipping conductors. Changes in strike of 45° between adjacent flight lines would cause approximately 30 percent reduction in anomaly. Such a reduction is not large compared with the effects of other geological variations and, in fact, can usually be corrected since such an abrupt change in strike is usually noticeable on the contour plan.

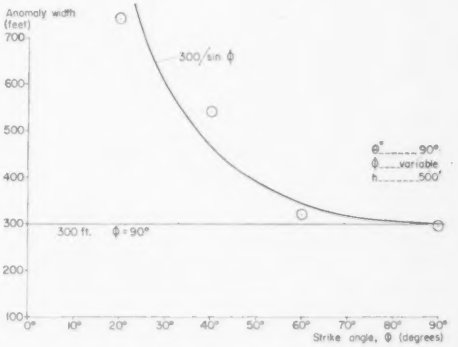

FIG. 12. Variation of anomaly width with strike angle (theoretical).

Variations with Dip.—Of considerably more interest is the effect on the anomaly of variations in dip angle of the conductor, as illustrated in Figure 13. It is noticeable that at dip angles in the range 90° to 180°, a secondary peak develops as the transmitter passes over the upper edge of the conductor. At angles greater than 136°, the secondary peak is stronger than the main peak. This can be confusing in areas of shallow-dipping conductors unless special care is taken. Also, it can cause "herringboning" when alternate lines are flown in opposite directions.

Figure 14 illustrates the variation in peak response with dip angle, as derived from Figure 13. This curve provides a means of correcting a response from a shallow-dipping body to its equivalent over a vertical body for purposes of conductivity comparison.

The variation of anomaly width with dip angle

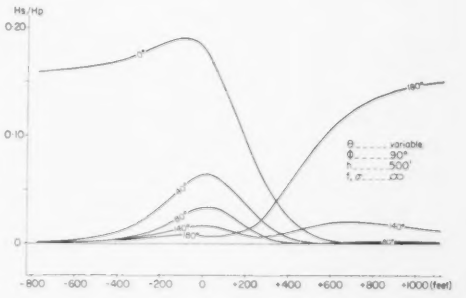

FIG. 13. Variation of in-phase anomaly with dip angle for conducting half-plane (theoretical).

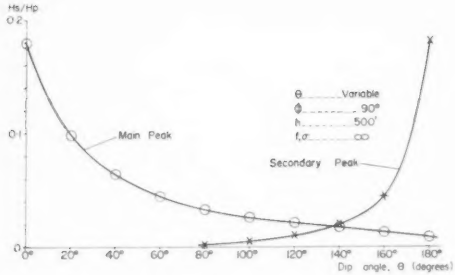

FIG. 14. Variation of peak (in-phase) response with dip angle for conducting half-plane (theoretical).

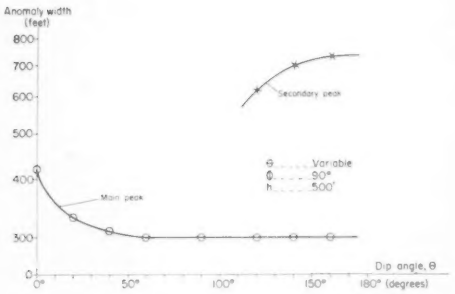

FIG. 15. Variation of anomaly width with dip angle for conducting half-plane (theoretical).

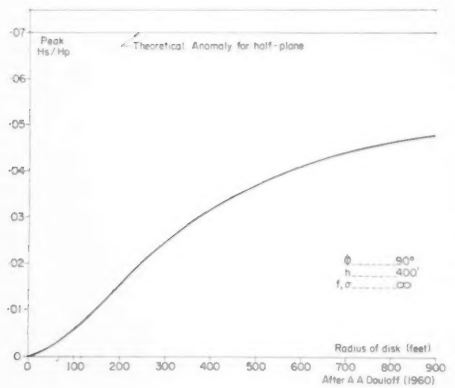

FIG. 16. Peak (in-phase) response over vertical disk as a function of disk radius (theoretical).

is illustrated in Figure 15. It indicates that the secondary peak can usually be recognized by its large anomaly width. The anomaly width of the main peak does not vary much with dip angle and can seldom be used for interpretation.

Variations with Size.—Although it was not part of the same series of tests, some results for bodies of finite size are provided for comparison purposes, These are obtained by means of Douloff's (1960) solution for the circular disk. Figure 16 illustrates the variation in peak response over a vertical disk as a function of disk radius. It is seen that at a radius of 900 ft, the response is still only 68 percent of the response of a vertical half-plane. 50 per cent of the half-plane response is obtained with a disk of radius 450 ft.

Model Work

In order to extend the range of conducting bodies beyond the simple cases that can be treated theoretically, model experiments must be carried out. A large number of these were done by A. A. Douloff, a graduate student at the University of Toronto, during the winter 1959–60. This work was carried out in close conjunction with the theoretical work described above on the model apparatus built by West (1960) and with analyses of field results by the author and his colleagues. Thus, it was possible to arrange models of greatest practical interest to the exploration geophysicist.

The first step in extending theoretical results is to compare theoretical and experimental profiles for a few simple cases. Examples of these are to be found in theses by West (1960) and Douloff (1960). A further example is provided in Figure 17. The agreement between curves is seen to be

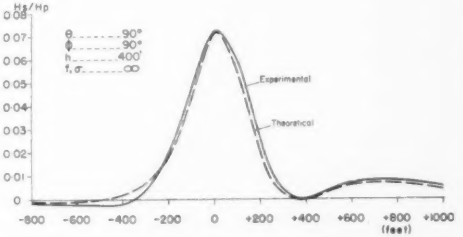

FIG. 17. Comparison between theoretical and experimental profiles over vertical conducting half-plane.

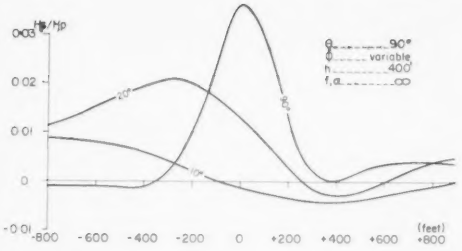

FIG. 18. Variation of in-phase anomaly with strike angle for vertical conducting half-plane (experimental).

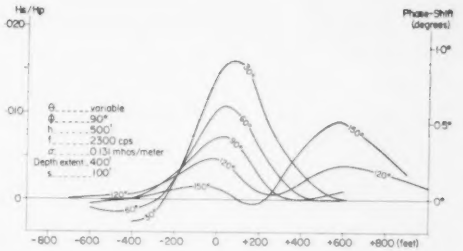

FIG. 19. Variation of quadrature anomaly with dip for conducting sheet (experimental).

rather good as far as amplitude and general shape are concerned. Certainly, it is adequate for practical exploration purposes.

A few illustrations are included to show how these experiments have been used to extend the range of the theoretical work. In all cases relative permeability, μ, can be taken as unity.

Variations with Strike.—It was mentioned above that the theoretical solution gave difficulty at small strike angles. Figure 18 illustrates the anomalies obtained for strike angles of 10° and 20°.

Variations with Dip.—The variations in the anomaly, with changes in dip angle, were studied experimentally for a conducting sheet of limited depth extent. This was a case that could not be treated theoretically. Figure 19 shows profiles over a body of depth extent 400 ft, dipping from 30° to 150°. In comparing these curves with those of Figure 13, it can be seen that the secondary peak is better developed in the case of a conductor of finite depth than for the half-plane.

The results of a series of experiments for sheets of different sizes are shown in Figure 20. In this figure the peak response is plotted as a function of dip angle for the half-plane and for sheets of both 600 ft and 300 ft depth extent. The portion of the half-plane curve from 30° to 90° is seen to agree well with the theoretical curve in Figure 14 for a conductor with an in-phase/quadrature relation of about 3.1.

Variations with Size.—The effect of limiting the depth extent of a rectangular sheet is illustrated in Figure 21. It is seen that the response reaches saturation at a depth extent of about 1,000 ft. At this point the response is over 90 percent of the response of the half-plane. The response falls rap-

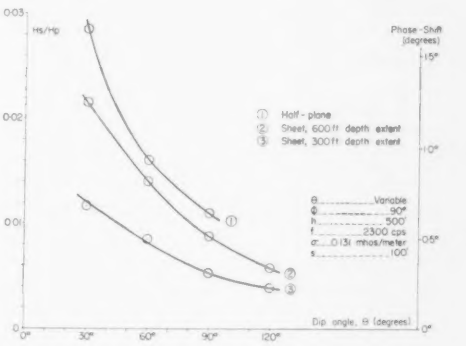

FIG. 20. Variation of peak quadrature response with dip of conducting sheet (experimental).

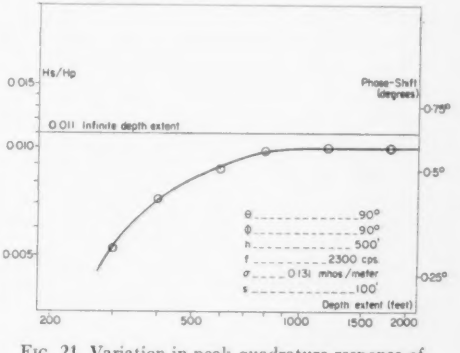

FIG. 21. Variation in peak quadrature response of vertical sheet with depth extent (experimental).

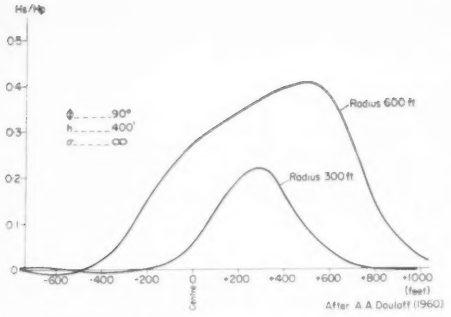

FIG. 22. Anomalies (in-phase) over horizontal disks of different radii (experimental).

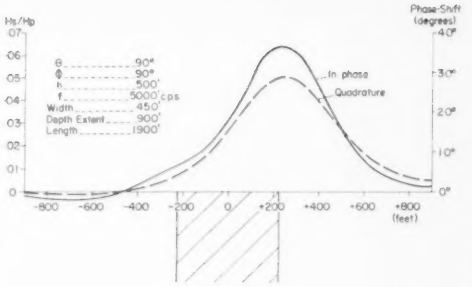

FIG. 24. Response of wide conducting body (dike), (experimental).

idly for depth extents less than the height of aircraft and is only 50 percent of the response from the half-plane at 300 ft.

The anomalies over horizontal disks of two different radii are shown in Figure 22. These curves show how the peak of the anomalies is offset over the edge of the disk nearest to the approaching aircraft. Also illustrated is the similarity between the anomalies of a horizontal disk of small radius and a vertical sheet. When the radius approaches the height of aircraft, two separate peaks develop, accompanied by a widening of the anomaly.

Multiple and Wide Conductors.—The effect of banded or multiple conductors was studied by Burrows (1957) during a program of model work at the University of Manchester in 1956–1957. His results have been converted to conform approximately with the coil geometry currently under study and are shown in Figure 23. It is seen that, as the bands become wider apart, the anomaly first increases in amplitude and widens. As they reach half the flying height apart, it decreases again and splits into two separate peaks. This experiment was done for conductors of very limited depth extent and cannot be extrapolated to the case of the half-plane.

Of particular interest, as will be seen in the next section, is the case of the wide, conducting body or dike. Such a body, of low conductivity, can easily be mistaken for a narrow body of quite high conductivity and the same response parameter. Figure 24 illustrates one profile over such a body and shows certain characteristics that are useful in recognizing bodies of this type. First, the peak is seen to lie over the edge of the body nearest the approaching aircraft. Second, the anomaly width is much larger than for a half-plane. Third, as the body approaches a width equal to the flying height, the anomaly splits into two peaks. An anomaly such as this could be recognized on a contour map by virtue of the "herringbone" pattern when alternate lines reverse in direction.

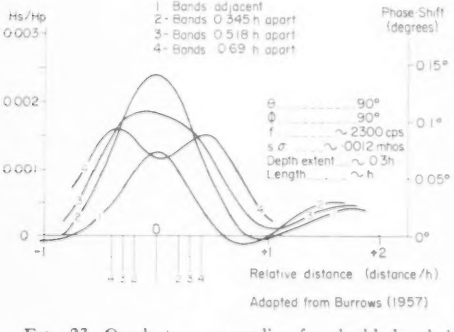

FIG. 23. Quadrature anomalies for double-banded vertical conductors illustrating resolution of bands (experimental).

CONDUCTIVITY AND WIDTH

By means of dimensional analysis (see for example West, 1960) we find that the response of an electromagnetic system can be expressed in terms of a response parameter containing the quantities σ (conductivity), μ (permeability), ω (frequency), and certain geometrical factors. These factors are different for each conductor form and for each prospecting system. For the half-plane and for the system under discussion, the response parameter can be shown to be best chosen as $\sigma\mu\omega sl$, where

s the width of the conductor and l is the horizontal distance between transmitting and receiving coils. The properties of these parameters are such that, providing the value of the parameter is maintained constant and the geometry of the system is unchanged, the individual factors can be varied without affecting the response of the electromagnetic system.

Thus, it is possible through scale reductions to make determinations in the laboratory which will be exactly equivalent to those observed at different frequencies, conductivities, and dimensions in the field.

It was stated that theoretical solutions for electromagnetic response have been limited to the infinite conductivity case. This is equivalent to an infinitely high response parameter and results in the disappearance of the quadrature component, which is the one actually measured in the phase-shift method of prospecting. For purposes of studying the effects of changes in conductivity and width for the half-plane, sheets, and disks, it has been necessary, therefore, to rely entirely on model experiments. These were carried out by Burrows in 1956–1957 and by A. A. Douloff in 1959–1960. The profile in Figure 25 is typical of such experiments. This profile is similar in form to those, for example, in Figure 6, but permits an accurate prediction of phase-shift for a body of given conductivity and width in the field.

By choosing a particular model and by varying the frequency, it is possible to plot the response as a function of the response parameter over a very wide range. By holding certain quantities constant, the response can be expressed as a function of whatever quantity or combination of quantities is desired. In Figure 26 the quadrature response of a vertical half-plane is expressed as a function of $s\sigma$, the conductivity-width factor, at two frequencies, 400 cps and 2,300 cps. Again, permeability, μ, is taken as unity. These curves are extremely useful as they provide an estimate of conductivity-width factor from a measurement of response at either frequency. It can also be noted that, regardless of the value of the response parameter, the quadrature response cannot exceed 0.0282, corresponding to a phase-shift of 1.62°. If stronger responses are noted in the field, this must be due to the conductor having a flatter dip or the height being less than 400 ft. It should also be noted that the range of conductivity-width factors which provides a 400 cps response greater than twice the maximum noise-level of the equipment (0.1°) extends from at least 0.6 to 250. For bodies 100 ft wide, this would be equivalent to a range of conductivities of from 0.018 mhos per meter to 7.6 mhos per meter. The peak 400 cps response is obtained at a conductivity-width factor of 12.8, corresponding to a body of width 100 feet and conductivity 0.39 mhos per meter. For bodies of limited size, the entire response curve is shifted to higher values of the conductivity-width factor, thus, increasing the upper limit of conductivities detectable by the system.

It was noted in deriving these curves that changes in width had the same effect as changes in the other factors in the response parameter in

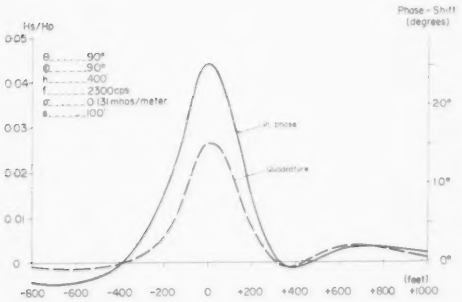

FIG. 25. Experimental profile over vertical half-plane (in-phase and quadrature).

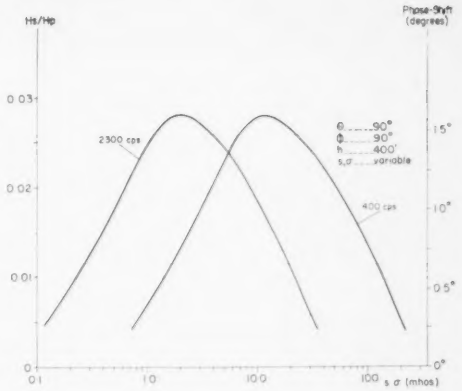

FIG. 26. Variations of quadrature response with conductivity-width factor for vertical half-plane (experimental).

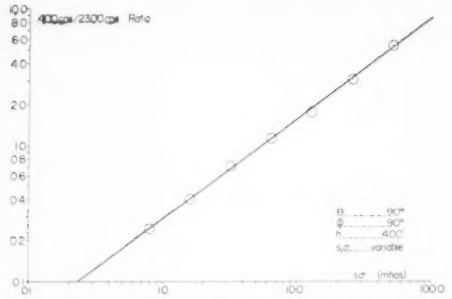

FIG. 27. Variation in 400 cps/23,000 cps ratio with conductivity-width factor for vertical half-plane (experimental).

the range $0 < s < 0.5h$. For greater conductor widths, the half-plane becomes a tabular body and the curves no longer apply.

From curves such as these, it is possible to derive relations between the ratio of responses at two frequencies and the conductivity-width factor. The straight-line curve in Figure 27 is derived for the vertical half-plane from the curves in Figure 26. This curve is, for all practical purposes, independent of height and is therefore more useful in estimating the conductivity-width factor than are the response curves when the depth of burial is unknown.

A useful relation between ratio and response has been derived from the above curves and plotted in Figure 28. If the 400 cps response and the corresponding ratio of an anomaly are plotted on this graph and the point falls on or near the calculated curve, that the anomaly is possibly caused by a vertical half-plane. If the plotted point falls to the left of the curve, it is because the conductor has limited size or occurs at a depth greater than 400 ft. If the point falls to the right, the conductor is not vertical or eddy currents in the overburden are contributing. The various possibilities can often be eliminated by studying curves such as those in Figure 7, Figure 14, Figure 16, and Figure 21.

EXAMPLES

Possibly the most valuable criterion in the interpretation of anomalies is the 400 cps/2,300 cps ratio. Referring to Figure 27, it can be seen that a ratio of greater than 0.5 corresponds to a conductivity-width factor greater than 2.1. Assuming an overburden less than 200 ft thick, this would correspond to a conductivity greater than .032 mhos per meter or a resistivity less than 31 ohm-meters. This can be true in certain areas, and in these areas other criteria are necessary. But in a large portion of the world, overburden conductivities are seldom less than 5 or even 10 times this value for a vertical distance of 200 ft. It is, therefore, reasonable to conclude, and it has found to be valid in the field, that a value of ratio can often be established above which it is safe to assume that conductors cannot be due to overburden.

Other criteria for recognizing overburden are, the peak response, the anomaly width, and the form of the anomaly, particularly on adjacent lines flown in opposite directions.

To illustrate some of these factors, the reader is referred back to Figure 4. First consider the anomaly indicated as significant in Figure 4(a). The peak 400 cps response and ratio are respectively 0.7° and 1.0. Correcting the response to 400 ft elevation by means of the normalizing curve in Figure 8, we obtain figures of 1.2° and

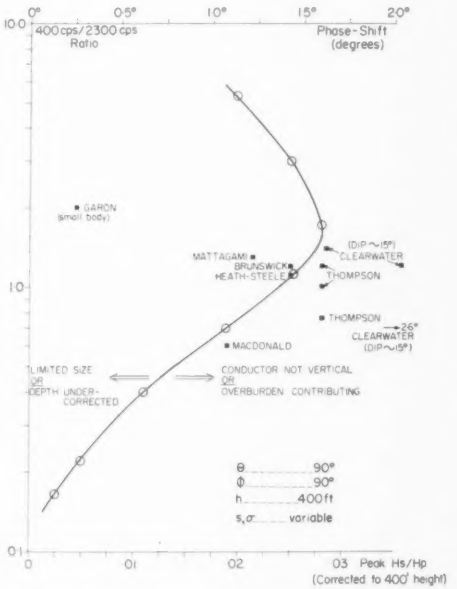

FIG. 28. Relation between ratio and peak quadrature response at 400 cps for vertical half-plane at 400 ft. height (experimental).

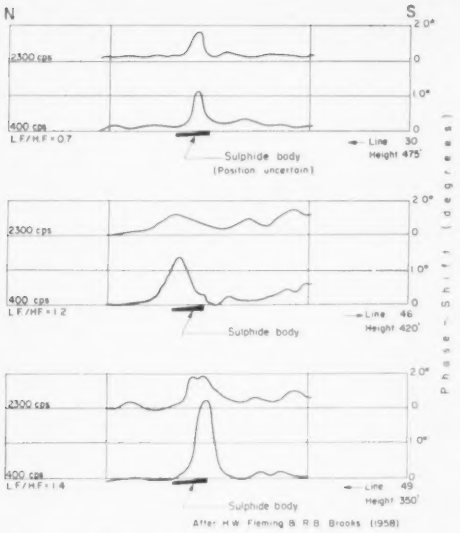

FIG. 29. Electromagnetic profiles over Clearwater Deposit, New Brunswick.

1.0. The value of 1.0 indicates a conductivity-width factor of 5.5 mhos. This is well within the range of metallic conductors. Plotting the two values in Figure 28, the point is seen to lie slightly to the left of the theoretical line for the half-plane. To bring the points exactly on the theoretical line would require a normalizing factor of 2.4 or a depth below aircraft of 500 ft. This implies an overburden thickness of 40 ft. Alternatively, the body must have finite dimensions. From the appearance of the anomaly and other geological factors, the 40-ft depth seems the more reasonable alternative. Finally, the width of the anomaly is seen to be approximately 340 ft. This is reasonable for a narrow, near-vertical sheet. It is concluded that the anomaly is caused by a steeply dipping, conducting sheet of considerable lateral and vertical dimensions, having conductivity typical of massive sulphides.

Referring now to the anomaly adjacent to the latter, we obtain values of 0.4° and 0.45 for 400 cps response and ratio, respectively. The latter value is just borderline between electrolytic and disseminated metallic conductors and must be considered on other grounds. Fortunately, it is noted that the anomaly has a width of 850 ft. Referring to curves in Figures 21 to 24 and Figure 15, it is seen that the body must have either very great width or a dip approaching 180°. In the former case, the conductivity would have to be too low to be of economic interest. The latter case implies very limited areal extent. The anomaly is most probably caused by a bedrock depression filled with conducting clays.

Figure 4(b) illustrates a straightforward case of a high conductivity-width factor coupled with a wide anomaly, suggesting a banded, near-vertical, metallic conductor.

The 400 cps response and ratio for eight different economic sulphide deposits are plotted in Figure 28. Most of these are grouped quite close to the theoretical curve for the vertical half-plane. The Garon deposit is considerably displaced due to its restricted lateral and vertical dimensions (Joklik, 1960). Three profiles over the Thompson deposit show rather large amplitudes which are attributed to the secondary effects of eddy currents generated in conducting overburden and, in one instance, an overlying body of water. The Clearwater deposit is a somewhat more interesting case, indicating quite clearly the effects of small dip angles.

Figure 29, taken from Fleming and Brooks (1960), shows electromagnetic profiles over the Clearwater deposit. This deposit is described by the authors as a replacement body of massive sulphides containing about 75 percent sulphides and 25 percent quartz. The sulphide portion contains pyrite, sphalerite, pyrrhotite, galena, and chalcopyrite in the ratios 75:10:5:5:5. The body consists of a massive core approximately 80 ft thick, having horizontal dimensions roughly 700 ft by 500 ft, surrounded by a disseminated zone of about twice these dimensions. The body occurs in a quartz-chlorite-sericite schist within the gently dipping north limb of a major east-west anticline. The body occurs near the flattest part of a synclinal cross-fold which plunges to the northwest at about 15°.

The exact position of the airborne anomalies with respect to the sulphide body is unknown, particularly in the case of the discovery line, Line 30, which traversed the anomaly quite by accident outside the limits of the planned survey area. However, certain characteristics of the anomaly are demonstrated by the profiles and the rough location of the ore body shown in Figure 29 that are pertinent to the present study.

Referring first to Line 30, we find an anomaly

indicating a conductivity-width factor of 3.4 mhos and an amplitude (corrected to 400 ft elevation assuming 25 ft of overburden) of 2.6°. The high amplitude and an anomaly width of 500 ft both suggest a body dipping in the direction of flight. Referring to curves similar to those in Figure 14, the dip is found to be less than 30° in the direction of the flight line. Because of the uncertainty in positioning, it is impossible to say how the anomaly correlates with the sulphide body. From experiments such as those in Figure 13, Figure 19, and Figure 24, it would be expected that the peak would occur over the up-dip edge of the body. Analyses of Flight Lines 46 and 49 provide similar results. The higher ratios on these lines are indicative of conductivity-width factors on the range 7 to 9. For a body 80 ft thick, this implies a conductivity of roughly 0.3 mhos per meter. Assuming 25 ft of overburden, we obtain corrected amplitudes of 2.1° and 1.7°. In both cases a flat dip is suggested and is confirmed by the shape of the profiles on the two lines. On both lines the anomaly appears over the edge of the body towards the approaching aircraft. The width of the anomaly (800 ft to 900 ft) confirms its shallow dip, and this is also confirmed by the appearance of the small anomaly over the opposite edge of the body. The actual depth to the body is unknown, so it is not possible to use curves such as those in Figure 14 to obtain a more accurate dip angle. It seems probable that the effective overburden depth is in the order of 500 ft under these flight lines.

The authors of this paper draw slightly different conclusions from the above results, principally with regard to the displacement of the anomaly and the significance of the ratio. Specifically, they attribute the displacement of the anomaly partly to the fact that it may be the outer, poorly conducting zone which is causing most of the anomaly. The writer considers that this conclusion is supported only in the case of the second, high-frequency peak on Line 49, there being little or no evidence for it elsewhere. Also, the authors draw attention to the increase in ratio with decrease in flight elevation, a phenomenon which is certainly valid for bodies of finite strike length. The writer concurs in principal but considers that the ratio is more closely related in this instance to changes in width and conductivity of the central core of the conductor. Further model studies with disks and plates would help clarify this situation.

FIELD OBSERVATIONS OF CONDUCTIVITY

Seventeen anomalies over known ore bodies have been studied to obtain estimates of conductivity-width factors. In some cases, the effective flying height (including depth of burial) has been

Table 1

Ore Body	400 cps* Response (Degrees)	Ratio	Conductivity-Width Factor (Mhos)
Thompson Mine, Manitoba	1.2	0.75	3.7
Thompson Mine, Manitoba	1.2	1.0	5.6
Thompson Mine, Manitoba	1.2	1.2	7.1
Anacon-Leadridge, New Brunswick	1.9?	1.85?	12.8?
Campbell-Chibougamau, Quebec	?	1.0	5.6
LaReine Mines, Desmesloizes Twp., Quebec	?	1.3	8.0
Heath-Steele Mines, New Brunswick	1.5	1.1	6.3
MacDonald Mine, Ontario	1.1	0.6	2.8
Geco Mine, Mantiouwadge Ontario	?	0.5	2.2
New Bidlamaque Quebec	?	0.9	4.8
Brunswick Mine New Brunswick	?	1.2	7.1
Mattagami Lake Mine Quebec	1.4	1.3	8.0
Clearwater Deposit, New Brunswick	2.6	0.7	3.4
Clearwater Deposit, New Brunswick	2.1	1.2	7.1
Clearwater Deposit, New Brunswick	1.7	1.4	8.8
Caribou Deposit, New Brunswick	?	1.0	5.6
Middle River Deposit, New Brunswick	?	0.8	4.1

* Corrected for elevation and depth of burial to a flying height of 400 ft.

Table 2

Ore Body	Conductivity-Width Factor (Mhos)	True Width Assumed (Feet)	Conductivity (Mhos/Meter)
Mattagami Lake Mine, Quebec	8.0	150	0.16
Clearwater Deposit, New Brunswick	8.0	80	0.3
Caribou Deposit, New Brunswick	5.6	50	0.34
Middle River Deposit, New Brunswick	4.1	85	0.15

known approximately and the results are therefore plotted in Figure 28. In the remainder of cases, only conductivity-width can be obtained.

The average value of conductivity-width, so obtained, is 6.0 mhos. The total range is 2.2 to 12.8? mhos. The average ratio is 1.05 and the range is 0.5 to 1.85. In general, we might say that the range of ratios over known commercial sulphide deposits is 0.5 to 2.0 with an average value of about 1.0.

Unfortunately, because of lack of information on conductor width, it is impossible, in most cases, to derive a value of conductivity. In a few cases, however, an approximate value can be obtained. These values are plotted in Table 2.

The average conductivity of these four bodies. so obtained, is 0.23 mhos per meter.

In an effort to obtain more reliable information on conductivity, ten examples of airborne and ground surveys with corresponding drill results have been compiled from recent surveys and are plotted in Table 3.

In the cases of Anomalies 5 and 7, conducting overburden of 170 ft and 100 ft respectively account for the high ratios. (It can be shown, for example, that a depth of burial of 170 ft in a medium of conductivity 10^{-2} mhos per meter will roughly double the ratio.) In the case of Anomaly 10, the drill did not completely cross the conducting zone and only a maximum conductivity can be derived. Leaving out these three cases, the average conductivity obtained from these examples is 0.37 mhos per meter. The range is 0.11 mhos per meter to 0.93 mhos per meter. Ratios vary from 0.7 to 2.0 with average of 1.5. Conductivity-width factors vary from 3 to 14 with an average of 10.1. It is noted that, generally speaking, the graphitic conductors have lower conductivities than those containing massive sulphides. However, the disseminated sulphides extend well into the range of the graphitic conductors. It is of further interest that in-phase/quadrature ratios obtained with horizontal loop ground electromagnetic equipment were 1.5, 2.5, and 2.0 for Anomalies 1, 2, and 10, respectively.

The above examples were chosen mainly from Northwestern Quebec. While they are not necessarily representative of conductors in other areas, they do illustrate certain facts. The most notable conclusion is that conductivity is more than three orders of magnitude less than that of hand specimens of similar material. This was the observation referred to by the writer in his discussion with Hedstrom (1959). The same conclusion was drawn by West (1960) through analyses of ground survey results over sulphide bodies. It is worth-

Table 3

Anomaly No.	Airborne Ratio	Conductivity-Width Factor (Mhos)	Conductivity (Mhos/Meter)	Drill Results
1	1.5	9.6	0.17	Three bands, 160, 20, and 7 ft of graphitic shale.
2	1.7	11.5	0.43	90 ft 20 percent py. and po. with bands up to 90 percent
3	0.7	3	0.11	90 ft graphitic schists with py. in two bands.
4	1.5	9.2	0.15	200 ft 10–15 percent py. and po. in numerous bands.
5	>5	>50	>2	80 ft 5–50 percent py. with one zone 30 ft with 40 percent.
6	2.0	14	0.61	75 ft oxidized zone with hematite and py.
7	>3	>25	>0.83	100 ft graphite plus 5–20 percent py. in bands.
8	2.0	14	0.93	50 ft 85 percent py. plus minor bands up to 98 percent.
9	1.0	5.5	0.18	100 ft graphite and 10–30 percent py. in bands.
10	2.0	14	<0.93	50 ft (plus) silicified graphite with py.

while to quote one of the conclusions of his thesis. "The most important conclusion that can be drawn from the examples is about the bulk conductivity of the conductors examined. These all consist of sulphide minerals in high concentration. The measurements of the conductivity of hand specimens of similar material . . . indicate that values of 10^3 mhos per meter might be expected from material of this type. The electromagnetic survey results give values of the order of 1 mho per meter. This gives conclusive evidence in support of the widely held theory that sulphides are usually very badly connected." It is probable that the conductivities obtained by West are slightly higher than those derived from airborne surveys because of the more restricted volume of conductor responding to the electromagnetic system. At a height of 500 ft above the conductor, the entire width of the conductor usually is effective in generating the electromagnetic response. This includes the bad, as well as the good, conductivity portions, and the bulk conductivity is affected largely by the former.

The relative roles of width and conductivity in the conductivity-width factor are not known. However, the restricted range of conductivities obtained over sulphide bodies by the writer, West, and others seems to suggest that, once interconnection has been established in a body, relatively little change in conductivity takes place by increasing the concentration of the sulphide particles. It might be argued, therefore, that width is all-important in deciding the electromagnetic response. However, a comparison of Tables 2 and 3 shows that the average conductivity of the graphite and sulphide bodies is higher than that of the ore bodies by the same factor that relates the two conductivity-width factors. The only notable conclusion, supported by Table 1, is that ore bodies in general have lower conductivity-width factors than most massive sulphide bodies. It has been the experience of the writer that the exceptionally high conductivity-width factors are usually related to salt water, wide graphitic zones, and wide sulphide bodies of sedimentary origin. In these instances, it seems certain that width is the dominant factor.

THE ROLE OF INTERPRETATION IN EXPLORATION

It is not sufficient to be able to recognize the more attractive anomalies in a given airborne electromagnetic survey. An effective interpretation must include a systematic grading of anomalies in order of likelihood of their representing massive sulphide bodies. By means of this discrimination, not only is the follow-up work directed advantageously (an important factor in the competitive mining market), but an economic cut-off point can be established after which further investigation of anomalies would yield less chances of profit than would primary exploration in another area.

The writer can recall examples of both intelligent and unintelligent use of interpretation within his own experience. In the one case, anomalies were investigated unsuccessfully on the ground for almost two years at considerable cost, despite the fact that they had been classified as extremely poor "bets" by the interpreter. In the other case, an area of 1,700 sq miles of exceptionally high surface conductivity provided at least one discrete anomaly per square mile. Detailed interpretation reduced the number of anomalies considered significant to 250. These were classified with the aid of aeromagnetic data according to likelihood of representing sulphide bodies. In addition, it was stated whether the cause of the anomaly was suspected to be due to electrolytic conduction. Of 120 anomalies so far investigated by ground geophysical methods, 80 percent of the 87 interpreted as metallic conductors were confirmed as such, whereas only 36 percent of the 33 doubtful anomalies were substantiated. Gravity methods were used to help select the 22 most favorable anomalies for drilling. All 22 intersected metallic conductors and 20 of these found massive sulphides.

CONCLUSIONS

There is nothing new about theoretical calculations, model experiments, or field tests. The work described in this paper must be similar to work being carried out by numerous organizations in the exploration business.

The main conclusion that the writer would like to draw from the work described in this paper is that practical operating factors and geological experience must be used in all phases of instrument design, operation, and interpretation.

The inventors of the dual-frequency phase-shift method of electromagnetic prospecting are to be congratulated on their early comprehension of these factors. It is impossible to build equipment which is optimum for each factor, but the system

described is believed to be a happy compromise.

In the operation of a successful survey program, intelligent use must be made of the advantages of the system being employed. The weaknesses of the system must be recognized and, if possible, avoided.

Interpretation must take into consideration both the physical and geological factors involved as well as the economics of exploration.

Finally, the geophysicist should be on guard against over-simplification of an interpretation problem and a feeling of complacency that a handful of type curves may inspire. When the solution to a problem seems most certain, this is the time to be most alert for the manifestations of geological caprice.

REFERENCES

Burrows, Keith, 1957, An investigation into the interpretation of airborne electromagnetic data by means of scale model experiments: M.Sc. Thesis, University of Manchester.

Cheriton, C. G., 1960, Anaconda exploration in the Bathurst District of New Brunswick, Canada: A.I.M.E. Mining Transactions.

Douloff, A. A., 1960, The Response of a conducting disk in a dipolar magnetic field: M.A. Thesis, University of Toronto.

Fleming, H. W., and Brooks, R. B., 1960, Geophysical case history of the Clearwater deposit, Northumberland County, New Brunswick, Canada: A.I.M.E. Mining Transactions.

Hedstrom, E. H., and Parasnis, D. S., 1959, Reply to comments by N. R. Paterson: Geophysical Prospecting, v. 7, n. 4.

Joklik, G. F., 1960, The discovery of a copper-zinc deposit at Garon Lake, Quebec: Econ. Geol. v. 55, n. 2.

MacKay, D. G., and Paterson, N. R., 1960, Geophysical discoveries in the Mattagami District, Quebec: Can. Inst. of Min. & Met. Bull. v. 53, n. 581.

New airborne geophysical methods speeds prospecting: Engineering and Mining Journal, 1956.

Paterson, N. R., 1959, Comments on paper entitled "Some model experiments relating to electromagnetic prospecting with special reference to airborne work" by E. H. Hedstrom and D. S. Paranis: Geophysical Prospecting, v. 7, n. 4.

Springer, K. J., 1959, Organization, planning and operation in the location of the Mattagami Orebody: C.I.M. Annual Meeting, Montreal.

West, G. F., 1960, Quantitative interpretation of electromagnetic prospecting measurements: Ph.D. Thesis University of Toronto.

GEOPHYSICS, VOL. XXVI, NO. 5 (OCTOBER, 1961), PP. 618-625.

RADIOACTIVITY OF VOLCANIC SEDIMENTS IN BRAZOS COUNTY, TEXAS*

WILLIAM L. RUSSELL† AND R. O. STEINHOFF‡

Abstract: The relation between the field unit of gamma radiation intensity, microroentgen per hour, and the laboratory units, expressed in concentration of radioactive elements, was determined by measuring the radiation intensity over a level rock surface and measuring the gamma radioactivity of the same rocks in the laboratory. The available data indicate that one percent potassium equivalent of gamma radioactivity is 1.25×10^{-12} radium equivalents, 3.5×10^{-6} potassium equivalents, 4.4×10^{-6} thorium equivalents, and produces a gamma radiation intensity of 0.57 microroentgen per hour over a flat surface.

Measurements of volcanic sediments of Upper Eocene and Miocene age in Brazos County, Texas, show gamma-ray emissivities of 4.5 to 10.9 percent potassium equivalents of gamma-ray emissivity. This is about the same as ordinary shales. The mixture of volcanic particles with clastic sediments in these samples suggests that the radioactivity of the original volcanic matter may possibly have been reduced by weathering.

INTRODUCTION

The published data on the radioactivities of rocks do not give conclusive information on several important points. One of these is the relation between the units of measurement giving the results of field surveys of gamma-ray intensity and the units expressing the results of laboratory tests. Definite information is also needed on the radioactivity of sediments of volcanic origin. Some bentonites have been shown to be of very high radioactivity compared to ordinary sedimentary rocks, and there is a widespread belief that all volcanic sediments are highly radioactive. Determinations are especially needed to show the radioactivity of volcanic tuff and ash which are in many places interbedded with sediments. The present paper presents new data bearing on these problems.

PREVIOUS WORK

Russell (1944) has published the results of 510 determinations of the gamma radioactivity of sedimentary rocks. The results are expressed in radium equivalents; but the relation of these units to potassium, uranium, and thorium equivalents is also given. These determinations include two measurements of volcanic ash which show a gamma radioactivity of 13.9 and 11.4 percent potassium equivalents. Osmond (1954) measured the uranium and thorium contents of some Ordovician and Cretaceous bentonites. Let it be assumed that the average potassium content of bentonites is 4 percent. By reducing the uranium and thorium concentrations obtained by Osmond to percent potassium equivalents and adding, 4 values of 18 percent potassium equivalents are obtained for the Ordovician bentonites and of 41 percent for the Cretaceous bentonites. Since the average radioactivity of shales of medium-to-light shades is about 7 percent potassium equivalents, according to Russell (1944), these bentonites are of very high radioactivities compared to average sedimentary rocks.

The relation between various concentration equivalents has been given by Russell (1944). According to the data furnished, one percent potassium equivalent of gamma radiation intensity is equivalent, in grams per gram, to the following concentrations: 1.25×10^{-12} radium, 3.5×10^{-6} uranium, and 4.4×10^{-6} thorium.

The relation between field and laboratory units for expressing gamma radioactivity has been discussed by Russell and Scherbatskoy (1951). The methods used in measuring the gamma radiation

* Manuscript received by the Editor April 20, 1961.

† Texas A. & M. College, College Station, Texas.

‡ Tulane University, New Orleans, Louisiana.

of rocks and expressing the results have been described by Curtiss (1949), Johnson (1954), Russell (1955), Russell and Scherbatskoy (1951), and Stead (1956).

CALIBRATION

Field and Laboratory Units

Unfortunately, the results of many surveys of gamma-ray intensity at the surface are expressed in terms of counts per minute or other units which apply only to the particular instruments used. Some results have been expressed in multiples of background radiation. However, this is an unreliable unit because the intensity of the background radiation varies greatly from place to place. The best unit for expressing the results of surface gamma-ray surveys appears to be microroentgen per hour. This unit has the disadvantage that variations in the energy of the gamma-rays measured effect the response of varied types of instruments in different manners. Thus, if the gamma radiation due to thorium and to uranium was the same in microroentgen per hour when measured by a Geiger counter, it might not be the same when measured by a scintillometer. However, the disadvantages of this unit appear to be less serious than those of any other field unit proposed.

The gamma radiation of samples, on the other hand, is best expressed by gamma-ray equivalents. These units indicate the concentration of a radioactive element needed to give the observed gamma radiation intensity if all the radiation were produced by that element or its family. In the case of thorium, radium, and uranium equivalents, all the members of the radioactive family are assumed to be in equilibrium.

Calibration of Laboratory Instruments

The calibration of laboratory instruments is made by noting the increase in radiation intensity measured when the concentration of a radioactive element in the sample emitting gamma rays is increased by a known amount. In order to avoid errors due to differences in the amount of absorption of gamma rays in the sample, the changes in the concentration of radioactive elements in the samples should not be accompanied by appreciable changes in density. The laboratory instrument used in making the measurements described in the present paper was calibrated by chemically pure potassium chloride. It was found that the counting rate of this particular instrument increased by 2.74 counts per minute for a one-percent increase in potassium content in the sample.

Calibration of Field Instruments

The calibration of field instruments involves two steps, eliminating the effect of cosmic radiation and determining the effect of known changes in gamma radiation intensity. The effect of cosmic rays on different instruments varies greatly, and some are specially designed to be insensitive to cosmic rays. The percentage of the background radiation due to cosmic rays may be determined with reasonable accuracy by reading the instrument at a locality on a lake or pond where the water is more than 8 ft deep and where the shores are either so distant or so low that the gamma radiation from them has no appreciable effect. The readings obtained in this manner should be subtracted from the readings observed on land to obtain the radiation intensity due to the rock and soils. Since the intensity of the cosmic radiation increases upwards, new measurements of its intensity must be made for each large change in elevation.

The calibration of field instruments in microroentgens per hour has been described by Russell and Scherbatskoy (1951). Gamma radiation is increased by 5 microroentgen per hour by bringing a source containing 50 micrograms of radium up from a great distance to a distance of 108 inches.

APPARATUS

The apparatus used for measuring gamma-ray intensity in the field and in the laboratory were lent for the investigation by Geophysical Measurements Corporation. The laboratory instrument for detecting gamma rays was a Geiger counter of relatively high efficiency of absorption, 1.1 inches in diameter, and 13 inches long. The samples to be measured were placed in an annular space about 0.4 inch wide surrounding the Geiger counter. Each sample weighed about 0.4 lb. The pulses of the Geiger counter were counted automatically, and time was measured with a stop watch.

The field instrument consisted of Geiger counters of a similar type, equipped with a counting rate meter and three time constants.

ACCURACY

The statistical accuracy of the measurements was calculated in the usual manner. Let A be the total number of pulses of the counter recorded with the sample in the container, B the number of pulses recorded during the background measurement, Mb the duration of the background measurement in minutes, Ms the duration of the sample measurement in minutes, and C the standard deviation of the sample measurement in counts per minute; then

$$C = \sqrt{\frac{\sqrt{A}}{Ms} + \frac{\sqrt{B}}{Mb}}.$$

The standard deviation is given after the $\mp$ sign in Table II. The standard deviation applies only to the purely statistical error and does not indicate errors due to the apparatus and conditions of measurement.

COLLECTION AND DESCRIPTION OF SAMPLES

In the southern part of Brazos County, Texas, there are many fine exposures of volcanic sediments in the Whitsett formation (Upper Eocene) and in the Catahoula formation (Miocene). Over 100 samples were collected from the uppermost 100 ft of the Whitsett formation and the basal 100 ft of the Catahoula formation. These samples were from localities listed as A, B, and C in Table II. Locality A is 1 to 2 miles northeast of Millican, locality B is 1 to 2 miles north-northeast of Millican, and locality C is at Dunlap Quarry, 2.4 miles southeast of Millican. The stratigraphy of this area has been described by Russell (1957). Measurements of radioactivity were made on 54 of these samples which are listed in Table II. Over 30 thin-sections were made of the samples measured in order to facilitate the identification and description of the rock types. The presence of bentonite was determined by benzidene solutions.

RELATION OF LABORATORY AND FIELD UNITS

The relation of laboratory and field units is a problem of major importance in determining the concentration of radioactive elements in rocks and in prospecting for radioactive ores. The determination of this relation would enable the results of field surveys to be evaluated in terms of concentrations of the radio-active elements and would also indicate the intensities of surface radiation to be expected from rocks having known concentrations of radioactive elements.

Table I

Sample No.	Gamma radiation over flat surface in microroentgen per hour (cosmic ray effects eliminated)	Laboratory, measurement, percent potassium equivalent	Number of microroentgen per hour produced by 1 percent potassium equivalent	Number of percent potassium equivalents producing microroentgen per hour
1	18.7	9.2	2.03	0.49
2	18.7	10.6	1.76	0.57
3	18.7	9.7	1.93	0.52
4	20	9.4	2.13	0.47
5	31.2	18.0	1.73	0.58
6	32.5	21.4	1.52	0.66
7	13.8	8.9	1.55	0.65
8	20.0	11.3	1.77	0.57
9	10	7.5	1.33	0.75
10	20.0	11.4	1.76	0.57
Average			1.751	0.583

The localities and description of these samples are as follows:

Samples 1 to 4. From granite dome just off granite quarry west of Marble Falls, Texas. Coarse pink granite.

Sample 5. Northwest exposure at Malotte's house, west side of Buchanan Lake, Texas, about 1 mile from dam. Fine-grained granite dike, gray, weathered.

Sample 6. Same location, same character. About 30 ft northwest of fence corner at Malotte's house.

Sample 7. Fine-grained granite dike cutting granite in park east of low granite dome, on west side of Buchanan Lake, Texas, about 2 miles from dam.

Sample 8. On north side of Colorado River just below Buchanan Dam, Texas. Coarse pink granite, much weathered.

Sample 9. Coarse pink granite about 15 miles south from Llano, Texas, on Highway 16 and thence 4 miles on road towards Enchanted Rock.

Sample 10. Eleven miles towards Mason on Highway 29 from Llano Texas. Coarse pink granite, much weathered.

The relation between gamma radiation at the surface, expressed in microroentgen per hour, and the concentration, expressed in gamma-ray equivalents, may be determined when several conditions are fulfilled. The field instrument is read on a level surface at a point where there are no projections above this surface near enough to produce an appreciable effect. It must be possible to break off samples for testing. A high radioactivity, absence of weathering, and uniform distribution of radioactive elements would be desirable. Unfortunately, practically all natural level surfaces of rock are weathered, and appreciable variations in the concentration of radioactive elements are generally present.

In the area accessible to field work it was possible to find suitable level exposures of rock of relatively high radioactivity, but all these exposures are weathered.

The results of measurements to determine the relation between microroentgen per hour and potassium equivalents are shown in Table I. The irregular variations in the fourth and fifth column of Table I are doubtlessly due to the effects of weathering as well as to irregular variations in

Table II. List of Radioactivity Determinations of Rock Samples

Sample number		Description*	Radioactivity in percent potassium equivalents
		Samples 1–26 are from locality *A*	
		(top of section)	
1	Miocene Catahoula formation Chita member	Sandstone, very light gray, fine- to medium-grained, friable to hard, massive, and bentonitic.	6.2± .39
2	Eocene Whitsett formation	Tuff, white, massive, tough, bentonitic, and iron-stained	5.6± .42
3		Tuff, white, massive, tough, bentonitic, and iron-stained.	6.7± .39
4		Ash, very light gray, very fine, loose and powdery, massive, and bentonitic†	10.5± .37
5		Ash, very light gray, very fine, loose and powdery, massive, and bentonitic.†	8.7± .43
6		Ash, very light gray, very fine, cross-bedded, loose, bentonitic, and iron-stained. Thin-section contains mostly isostropic material, index of refraction lower than balsam. Glass shards make up three-fourths of slide. Some very small angular quartz noted. Small amount of mineral and clayey matter present.†	10.9± .41
7		Tuff, white, massive, tough bentonitic, and iron-stained.†	5.0± .45
8		Sandstone, yellowish-gray, massive, loose to friable, fine-grained, bentonitic, and having some iron stains.	8.3± .41
9		Tuff, white, massive, friable, bentonitic, light, smooth to the touch, and having conchoidal fracture.	5.7± .33
10		Ash, very light gray, very fine, slightly friable, thinly bedded and bentonitic. Thin-section shows almost three-fourths of slide to be glass shards. Some very small and angular quartz present. Small amount of clayey material and some mica noted.†	7.1± .39
11		Sandstone, yellowish-gray, loose to friable, fine-grained, bentonitic, massive, and iron-stained.	6.3± .38
12		Sandstone, very light gray, very fine-grained, massive, loose to friable, bentonitic, and having some iron stains.	10.1± .39
13		Sand, yellowish-gray, massive, loose to friable, and bentonitic.†	9.9± .38
14		Sandstone, yellowish-gray, fine-grained loose to friable, and bentonitic.†	8.5± .35
15		Sandstone, yellowish-gray, fine, loose to friable, massive, and bentonitic.†	5.8± .34
16		Sandstone, yellowish-gray, fine-grained, loose to friable, massive bentonitic, and iron-stained.	6.0± .35
17		Tuff, white, massive, bentonitic, light in weight, smooth to the touch, and having conchoidal fracture. Thin-section consists of particles that are elongated and angular with an index of refraction lower than balsam. Most of specimen consists of curved, glassy materials. Very little kaolin present. Some of the small mineral grains noted may be quartz. Also present are some anisotropic minerals having an index of refraction higher than balsam.†	5.4± .38
18		Tuff, white, massive, bentonitic, tough, light in weight, smooth to the touch, and having conchoidal fracture. Appears to be channel filling in underlying siltstone.	5.7± .37
19		Siltstone, yellowish-gray, friable, massive bentonitic, and iron-stained.	5.6± .34
20		Sandstone, yellowish-gray, fine-grained, loose to friable, massive, bentonitic, and iron-stained.	4.9± .35
21		Siltstone, white, tough, massive, bentonitic, and iron-stained. Thin-section shows mostly angular quartz having a great variation of grain size. Some kaolinitic matter and glass shards were identified. Curved rod-like bodies having spines are clearly fossil remains. A few fragments of pumice were noted.†	5.6± .43

(*Continued on next page*)

* All colors are from the National Research Council (1948) Rock-Color Chart, Washington, D. C.
† Thin-section made of sample and used as an aid in the classification of the rock.

Table II. (*continued*)

Sample number		Description*	Radioactivity in percent potassium equivalents
22		Sand, yellowish-gray, very fine, loose to friable, massive, bentonitic, and iron-stained. Thin-section shows mostly quartz grains and some glassy fragments that are unusually large, thick, and have a conchoidal fracture. The few grains of feldspar noted were mostly kaolinized. A few fossil, spiny tubes are present and have been replaced by opal. Touramline and magnetite grains and a small amount of bleached biotite were also noted.†	9.4± .38
23		Tuff, white, massive, bentonitic, friable, light in weight, smooth to the touch, and having conchoidal fracture.	5.4± .42
24		Sandstone, yellowish-gray, very fine, loose to friable, massive, bentonitic, and iron-stained.	6.1± .31
25		Siltstone, yellowish-gray, tough, massive, bentonitic, and iron-stained.	5.2± .39
26		Siltstone, yellowish-gray, tough, bentonitic, and iron-stained. (bottom of section)	6.7± .39
		Total thickness of section is approximately 100 ft.	
		Samples 27–48 are from locality *B* (top of section)	
27	Miocene Catahoula formation Chita member	Sandstone, very light gray, fine- to medium-grained, very hard, massive, and iron-stained. Forms resistant hill.	4.1± .31
28		Sandstone, very light gray, fine-grained, friable to hard, massive, bentonitic, and iron-stained.†	8.9± .23
29		Sandstone, yellowish-gray, fine-grained, friable to hard, massive, bentonitic, and iron-stained. Forms resistant ledge and waterfall in creek.	5.4± .33
30	Eocene Whitsett formation	Tuff, yellowish-gray, massive, bentonitic, and tough.	6.1± .34
31		Tuff, white, massive, bentonitic, tough, and rough to the touch.†	6.9± .40
32		Ash, yellowish, laminated, benonitic, and iron-stained. Thin-section contains mostly glass shards. Some kaolinized material and small quartz grains present.†	10.5± .40
33		Shale, yellowish-gray, fine, tough, platy, bentonitic, and iron-stained. Worm boring present at outcrop.	7.4± .36
34		Ash, yellowish-gray, massive, bentonitic, and iron-stained.	7.4± .42
35		Sandstone, yellowish-gray, fine-grained, hard, bentonitic, and in places iron-stained. Forms a massive layer 2 feet in thickness.	8.2± .40
36		Ash, grayish-yellow, fine, massive, loose, bentonitic, and iron-stained.	10.4± .43
37		Ash, yellowish-gray, fine, loose, massive, bentonitic, and iron-stained.†	9.2± .36
38		Sandstone, yellowish-gray, massive ledge several feet thick and steeply dipping, fine-grained, friable, and bentonitic.†	7.7± .40
39		Siltstone, very pale orange, tough, massive, bentonitic, and iron-stained.†	7.2± .38
40		Sandstone, yellowish-gray, very fine, loose to friable, massive, bentonitic, and iron-stained.	7.2± .39
41		Sand, yellowish-gray, fine, very loose, massive, bentonitic, and iron-stained.†	7.8± .31
42		Sand, yellowish-gray, fine, very loose, massive, bentonitic, and iron-stained.	4.9± .32
43		Ash, very light gray, massive, fine, loose, and bentonitic.	8.0± .39
44		Ash, very light gray, massive, fine, loose, bentonitic, and iron-stained.†	9.3± .35
45		Claystone, grayish-orange, tough, shaly, muscovitic, bentonitic, and iron-stained.†	4.9± .36
46		Sand, yellowish-gray, fine, very loose, massive, bentonitic, and iron-stained. Thin-section shows mostly quartz grains with some kaolinized material present. A few glass shards were noted.†	11.0± .53

Table II. (*continued*)

Sample number		Description*	Radioactivity in percent potassium equivalents
47		Sandstone, yellowish-gray, fine, loose to friable, massive, muscovitic, bentonitic, and iron-stained.	5.9±.32
48		Sandstone, yellowish-gray, fine, loose to friable, massive, bentonitic, and iron-stained. Some muscovite flakes noted. Total thickness of section is approximately 100 ft. (bottom of section)	5.2±.28
		Samples 49–54 are from locality *C* (top of section)	
49	Miocene Catahoula formation Dunlap member	Sandstone, yellowish-gray, fine- to medium-grained, slightly quartzitic, chiefly massive but with some flaggy and cross-bedded layers.†	1.0±.25
50		Sandstone, light greenish-gray, very fine, to friable, finely bedded, tuffaceous, and bentonitic. Thin-section has mostly quartz with smaller amounts of feldspar (some with definite albite twinning) present. Feldspar is mostly kaolinized but is partly unaltered. Glass shards are present, some having rounded edges.†	6.7±.34
51	Miocene Catahoula formation	Siltstone, yellowish-gray, tough, massive, siliceous, bentonitic, iron-stained, forming a resistant ledge 3 to 5 ft thick across a creek. Thin-section contains mostly quartz with some feldspar, largely kaolinized. Well-rounded garnet grains were noted.†	7.2±.33
52		Bentonite, yellowish-gray, soft, massive, jointed, having conchoidal fracture, and iron-stained. Thin-section shows a highly altered glass. Considerable angular mineral matter, probably quartz, is present. Some pumice, apatite, and zircon were noted.†	6.2±.36
53	Miocene Catahoula formation Chita member	Sandstone, very light gray, fine- to medium-grained, slightly quartzitic, chiefly massive but with some flaggy and cross-bedded layers. Thin-section contains grains that are chiefly quartz and feldspar, both being angular and subangular in shape. Some glass shards are present and all are slightly decomposed. The feldspar is all kaolinized.†	7.2±.33
54		Sandstone, very light gray, fine- to medium-grained but with some rice-sized grains, conglomeratic in places, chiefly massive but having some cross-bedding, friable to hard, muscovitic, jointed, and bentonitic. Total thickness of Section is 101 ft. (bottom of section)	4.5±.27

concentration. Because of the solid angle effect, the radiation intensity in an empty borehole would be about twice the radiation on a flat surface if the effects of weathering and cosmic rays were eliminated. Russell and Scherbatskoy (1951) estimated from rather inaccurate data that one microroentgen per hour would be produced by about 2×10^{-12} radium equivalents or 1.6 percent potassium equivalents. This agrees very well with the average of 1.75 percent potassium equivalents given by Table I. According to the figures previously mentioned, one microroentgen per hour is produced by the following concentrations of radioactive elements: potassium, 1.75×10^{-2}, radium 0.72×10^{-12}, uranium 2.0×10^{-6}, and thorium 2.5×10^{-6}. These figures refer to the increases in concentration required to cause the gamma radiation produced by the rocks to increase by one microroentgen per hour when measured over a flat surface.

RADIOACTIVITY OF VOLCANIC SEDIMENTS

The results of determinations of the gamma radioactivity of 54 samples from Brazos County, Texas, are given in Tables II and III. Table II gives the lithologic descriptions and the results of measurements of each sample. Table III gives the average radioactivities and ranges of the determinations of the different rock types. With two exceptions, all these samples contained volcanic

Table III. Average Radioactivities of Various Lithologic Types

Lithologic Type	Number of samples	Range	Average radioactivity in percent potassium equivalents
Sand, bentonitic	1		7.4
Sand, bentonitic and tuffaceous	1		9.4
Sandstone, nonbentonitic	2	1.0- 4.1	2.6
Sandstone, tuffaceous	1		7.2
Sandstone, bentonitic	17	4.5-10.1	6.8
Sandstone, bentonitic and tuffaceous	1		6.7
Siltstone	5	5.2- 7.2	6.4
Siltstone, bentonitic and tuffaceous	1		5.6
Shale, bentonitic	1		7.4
Claystone, bentonitic	1		4.9
Ash	10	7.1-10.9	9.2
Tuff	9	5.0- 6.9	5.8
Bentonite	1		6.2

matter in the form of ash, tuff, or bentonite. The two nonvolcanic samples were sandstone, having an average gamma radioactivity of 2.6 percent potassium equivalents. The average radioactivity of the 21 samples of sand and sandstone containing volcanic material is 7 percent potassium equivalents. Clearly bentonitic, ashy, or tuffaceous sandstones have a much higher radioactivity than sandstones that are free from volcanic matter. In fact, sandstones containing volcanic sediments show about the same radioactivity as light-colored shales. The average radioactivity of 10 samples of volcanic ash is 9.2 percent potassium equivalents; and of 9 samples of tuff, 5.8 percent potassium equivalents. Since the average radioactivity of shale of medium-to-light shades is about 7 percent potassium equivalents, according to Russell (1944), these volcanic sediments also have about the same radioactivity of shales of the same shade.

The bentonites analyzed by Osmond (1954) were much more radioactive, most of the radioactivity being due to thorium. These bentonites occur as thin, persistent beds intercalated with marine strata. The lower radioactivity of the volcanic sediments from Brazos County, Texas, may be due to the original nature of the volcanic material or to greater weathering. The latter explanation is supported by the fact that the volcanic particles in these rocks are commonly mixed with clastic deposits.

APPLICATION TO INTERPRETATION OF RADIOACTIVITY WELL LOGS

The common occurrence of volcanic matter in sediments makes it important to determine how it is expressed on radioactivity well logs. There has been a tendency to assume that volcanic sediments would be expressed on the logs by radioactivities higher than those of ordinary shale. The results of the present investigation suggest that many volcanic sediments have about the same radioactivity as common shales. This is true of the Eocene - Miocene tuffs and ashes measured. Sandstones containing volcanic matter may also have about the same radioactivity as shales. When this is the case, natural gamma-ray logs alone cannot distinguish them from shales. Some bentonites, on the other hand, have very high radioactivity compared to shales. Although thin, these bentonites make prominent peaks on radioactivity well logs and may be very useful for correlation.

In marine sedimentary rocks, conspicuous peaks produced by thin beds may be produced either by bentonites or by organic marine shales. Samples may be required to distinguish between these two rock types. However, in nonmarine strata, thin, highly radioactive beds are probably due to bentonites or other types of volcanic sediments.

CONCLUSIONS

1. Field and laboratory measurements suggest that the intensity of the gamma radiation over a flat surface is increased by 1 microroentgen per hour by an increase of about 1.75 percent potassium equivalents of gamma-ray intensity in the rocks. Data previously published indicate that 1.75 percent potassium equivalents of gamma-ray intensity are equal to the following equivalents of gamm-ray intensity, expressed in grams per gram: 0.72×10^{-12} radium, 2×10^{-6} uranium, and 2.5×10^{-6} thorium.

2. Volcanic sediments collected from the upper 100 ft of Eocene strata and basal 100 ft of Miocene strata in southern Brazos County, Texas, have ranges of about 5 percent to about 11 percent potassium equivalents of gamma radioactivity.

3. The radioactivities of the volcanic sediments of southern Brazos County are about the same as

those of shales of medium-to-light shade. Sandstones containing considerable volcanic matter were also found to have about the same radioactivity as shales.

4. Thin beds of high radioactivity which appear on logs of natural gamma-ray intensity may, in marine strata, be due to either bentonites or to organic marine shales. In nonmarine strata these thin, highly radioactive beds are likely to be produced by volcanic sediments. Ashy and bentonitic sandstones look like shales on natural gamma-ray logs.

ACKNOWLEDGMENTS

The work of the senior author was supported in part by the Texas Engineering Experiment Station.

Grateful acknowledgment is made to Carl Lausen for his help in the description of many of the thin sections. The junior author also wishes to thank the University Council for research at Tulane University for a research grant for the summer of 1959.

REFERENCES

Curtiss, Leon F., 1949, Measurements of radioactivity: U.S. Bureau of Standards Circular 476, p. 1–84.

Johnson, D. H., 1954, Geophysical exploration by nuclear methods, in Nuclear Geology: New York, John Wiley & Sons, pp. 219–250.

Osmond, John Kenneth, 1954, Radioactivity of bentonites, thesis submitted in partial fulfillment of requirements for degree of doctor of philosophy: Madison, University of Wisconsin.

Russell, William L., 1954, The total gamma-ray activity of sedimentary rocks as indicated by Geiger counter determinations: Geophysics, v. 9, p. 180–216.

———, 1955, The use of gamma-ray measurements in prospecting: 50th Anniversary Volume, Economic Geology, p. 835–866.

———, 1957, Faulting and superficial structures in east-central Texas: Trans. Gulf Coast Assoc. Geol. Soc. v. 7, p. 165–172.

———, and Scherbatskoy, S. A., 1951, The use of sensitive gamma-ray detectors in prospecting: Economic Geology, v. 46, p. 427–446.

Stead, Frank R., 1956, Instruments and techniques for measuring radioactivity in the field: U.S. Geological Survey Prof. Paper 300, p. 705–713.

GEOPHYSICS, VOL. XXVI, NO. 5 (OCTOBER, 1961), PP. 626–634

THE DIRECTIVITY PROBLEM FOR A BURIED LINE SOURCE*

FREEMAN GILBERT† AND LEON KNOPOFF‡

Abstract: A method based on the first motion approximation is presented for determining the radiation pattern of a buried line source. If measurements at the surface are used to obtain the P and S components of the source, the multipolar distribution of the source may be determined. The multipolar distribution is not unique since several distributions can have the same radiation pattern. Some examples are presented for simple sources. The method is applicable to real sources or virtual sources such as centers of diffraction or scattering.

INTRODUCTION

The existence of an anomalous elastic condition at depth within the earth results in a suite of anomalous seismic disturbances at detectors on the surface of the earth. Seismic observations can be divided into normal and anomalous pulses. An anomalous pulse is defined as a pulse that appears to emanate from a point (a line in two dimensions) although there is no source of elastic energy at that point. In this context we say that an anomalous pulse is due to a virtual source. It has been demonstrated that the incidence of a seismic pulse upon a diffracting half-plane (deHoop, 1958) results, at a point of observation in the illuminated zone, in a seismic record consisting of the direct pulse, a diffracted P pulse, and a diffracted S pulse appearing to come from the edge of the half-plane. By the definition above these diffracted pulses are the anomalous pulses. Similarly, when we consider the scattering of a seismic pulse by a sphere or cylinder (Gilbert, 1960; Knopoff and Gilbert, 1960; Gilbert and Knopoff, 1960; Gilbert and Knopoff, 1959), we observe at each point in space a direct or normal pulse corresponding to the incident wave and scattered P and S pulses appearing to originate at the sphere or cylinder. These latter are again the anomalous pulses. Actually the scattered P and S pulses come from the surface of the sphere or cylinder, but for a small sphere or cylinder we may assume that the anomalous pulses come from the center of the sphere or cylinder. We confine our attention to the anomalous pulses.

Let us assume that observations of the distribution of the anomalous pulses have been made over the entire, free, plane surface of an elastic solid. Let us further assume that the physical anomaly has only one singular point or line. As examples; the singular line for the half-plane is its edge, the singular point for a sphere is its center, for a cylinder the singular line is its center. At the singular point in two or three dimensions we propose to place a fictitious, line or point, virtual source whose properties are such that we can replace the scattering or diffraction problem by the superposition of two problems: (1) the incidence of the normal pulse system upon the half-space; and (2) the problem of a point or line source, having complicated directional and amplitude properties, located at the anomaly and providing exactly the distribution of anomalous pulses observed at the surface to the half-space. We shall consider only the problem of the incidence of pulses where the seismic wave lengths are short compared with the dimensions of the anomaly.

Inverse boundary value problems are well known in many aspects of geophysical exploration (Langer, 1933; Pekeris, 1934; Slichter, 1933, 1951, 1952, 1954; Stevenson, 1934, 1935). In these problems the distribution of observations on the surface is used to reconstruct the distribution of physical parameters within the earth (the anomaly). In the present inverse problem we recon-

* Institute of Geophysics Publication No. 184. Manuscript received by the Editor June 5, 1960.

† University of California, La Jolla, California.

‡ University of California, Los Angeles, California.

struct not the anomaly itself, but the virtual source to be placed at the singular point of the anomaly. It has not yet been determined whether this will have the "signature" of the anomaly, that is to say, whether to each anomaly there will correspond a unique virtual source for a given system of direct or normal waves.

The problem of multiple anomalies is simply treated from the travel-time data in terms of a superposition of results for the isolated anomalies if the anomalies are far apart compared with the pulse wave length. The problems of multiple scattering and pulse overlap are too complicated for this elementary analysis.

We restrict ourselves to two-dimensional problems. The case when the scattering center is infinitely far away from the surface of the half-space has already been treated (Knopoff, et al, 1957). It has been shown that it is possible, from surface observations of the motion, to deduce what the motion is in the interior of the solid in regions remote from the boundary of the half-space. In this paper we develop the procedure whereby the directivity pattern of a buried line source can be determined from measurements of displacement on the surface of a half-space.

RESPONSES FOR UNIFORM SOURCES

In this section we reproduce the solutions given elsewhere (Garvin, 1956; Gilbert, 1956) for the motion of the surface of a half-space in which first, a line source of pure compression waves is buried; and second, a line source of pure shear (in the SV polarization) is buried. The procedures, as outlined in the above references, are simplified by the application of the reasoning developed previously for the deformation of the contours in the complex domain (deHoop).

Consider a line source of compression located at $z=h$, $x=0$, and extending to infinity in the y direction. The half-space is the region $z>0$. We write the displacement of a particle U in terms of the two potentials ϕ and ψ.

$$U = \nabla\phi + \nabla x\psi j, \tag{1}$$

where j is the unit vector in the y direction.

The Laplace transform of the potential ϕ satisfies the differential equation

$$\nabla^2\bar{\phi} - (s^2/\alpha^2)\bar{\phi} = -\delta(x)\delta(z-h)F(s); \tag{2}$$

and the Laplace transform of the potential ψ satisfies the differential equation

$$\nabla^2\bar{\psi} - (s^2/\beta^2)\bar{\psi} = 0, \tag{3}$$

where α is the velocity of P waves, β is the velocity of S waves, and $F(s)$ is the Laplace transform of the source function with respect to time. The solutions to equations (2) and (3) are

$$\bar{\phi} = \frac{F(s)}{2\pi i}\int_{c-i\infty}^{c+i\infty}\frac{e^{spx}}{2\eta_p}\left(e^{-s\eta_p|z-h|} + A(p,s)e^{-s\eta_p z}\right)dp, \text{ and} \tag{4}$$

$$\bar{\psi} = \frac{F(s)}{2\pi i}\int_{c-i\infty}^{c+i\infty}\frac{e^{spx}}{2\eta_p}B(p,s)e^{-s\eta_s z}dp, \tag{5}$$

where $\eta_p=(\alpha^{-2}-p^2)^{1/2}$, $\eta_s=(\beta^{-2}-p^2)^{1/2}$. The first term of equation (4) is , of course, a particular solution to the inhomogeneous equation, (2).

The functions $A(p,s)$ and $B(p,s)$ are to be determined from the boundary conditions on the normal stresses, $\tau_{zz}=\tau_{xz}=0$ at $z=0$. These are

$$\bar{\tau}_{zz} = \lambda\nabla^2\bar{\phi} + 2\mu(\partial\overline{U}_z/\partial z) = 0 \text{ and} \tag{6}$$

$$\bar{\tau}_{xz} = \mu(\partial\overline{U}_z/\partial x + \partial\overline{U}_x/\partial z) = 0, \tag{7}$$

where the barred quantities are the Laplace transforms of the corresponding unbarred quantities. Applying the boundary conditions, solving for $A(p,s)$ and $B(p,s)$, and writing the two components of the displacement at the surface $z=0$; we have, from equation (1),

$$U_x = \frac{sF(s)}{2\pi i}\int_{c-i\infty}^{c+i\infty}e^{spx}\frac{2p\eta_s e^{-s\eta_p h}}{\beta^2 R(p)}dp \text{ and} \tag{8}$$

$$U_z = \frac{sF(s)}{2\pi i}\int_{c-i\infty}^{c+i\infty}\cdot\frac{e^{spx}(\beta^{-2}-2p^2)e^{-s\eta_p h}}{\beta^2 R(p)}dp, \tag{9}$$

where

$$R(p) = (2p^2-\beta^{-2})^2 + 4p^2\eta_p\eta_s.$$

The integrands have branch points at $p=\pm 1/\alpha$ $\pm 1/\beta$ and simple poles at $p=\pm p_R$ (a real quantity) where $R(p_R)=0$. Branch cuts at Im $p=0$, $\alpha^{-1}<|\text{Re } p|<\infty$, and Im $p=0, \beta^{-1}<|\text{Re } p|<\infty$ insure Re $\eta_p\geq 0$ and Re $\eta_s\geq 0$ everywhere in the p-plane. We require s to be a real number, sufficiently large to permit the application of Jordan's lemma in equations (8) and (9).

In equations (8) and (9) we set

$$t = -px + \eta_p h, \tag{10}$$

a real positive number. The resulting contour of integration in the p-plane is a hyperbola opening to the left if x is positive and opening to the right if x is negative. And it is equivalent to the original contour since Jordan's lemma is applicable.

We define $r=(x^2+h^2)^{1/2}$, $\tan\theta=x/h$ and note that the path of integration is given by

$$p = -(t/r)\sin\theta \pm i(t^2/r^2 - \alpha^{-2})^{1/2}\cos\theta \tag{11}$$

(Knopoff, 1958(a); Knopoff, Gilbert and Pilant, 1960). Since the path of integration in equation (11) is symmetric with respect to the real axis, the value of the integral is twice the imaginary part of the integral taken along the path

$$p = \omega_p(t) = -(t/r)\sin\theta + i(t^2/r^2 - \alpha^{-2})^{1/2}\cos\theta, \quad t \geq r/\alpha. \tag{12}$$

Remembering that both s and t are real numbers, we change the variable of integration in equations (8) and (9) from p to t with the results,

$$\overline{U}_x = \frac{sF(s)}{\pi}\int_{r/\alpha}^{\infty} e^{-st} \cdot \mathrm{Im}\left\{\frac{d\omega_p}{dt}\,\frac{2\omega_p\eta_s}{\beta^2 R(\omega_p)}\right\} dt, \tag{13}$$

$$\overline{U}_z = \frac{sF(s)}{\pi}\int_{r/\alpha}^{\infty} e^{-st} \cdot \mathrm{Im}\left\{\frac{d\omega_p}{dt}\,\frac{(\beta^{-2} - 2P^2)}{\beta^2 R(\omega_p)}\right\} dt. \tag{14}$$

We set $F(s)=s^{-1}$ in equations (13) and (14) and see that the transient response for a step function source of P waves is given by the expressions:

$$U_x = \frac{1}{\pi\beta^2}\,\mathrm{Im}\left\{\frac{d\omega_p}{dt}\,\frac{2\omega_p\eta_s}{R(\omega_p)}\right\} H(t - r/\alpha), \tag{15}$$

$$U_z = \frac{1}{\pi\beta^2}\,\mathrm{Im}\left\{\frac{d\omega_p}{dt}\,\frac{(\beta^{-2} - 2\omega_p^2)}{R(\omega_p)}\right\} \cdot H(t - r/\alpha). \tag{16}$$

The problem of a buried uniform line source of SV waves is treated in a manner similar to that given above. We require that the motion be given by the solution to the pair of differential equations

$$\nabla^2\bar{\phi} - (s^2/\alpha^2)\bar{\phi} = 0, \tag{17}$$

$$\nabla^2\bar{\psi} - (s^2/\beta^2)\bar{\psi} = -\delta(x)\delta(z-h)F(s). \tag{18}$$

Again we obtain integral representations for the particular solution and solve for the two undetermined kernels by the technique using the two boundary conditions above. The Laplace transforms of the two components of motion can be written as follows:

$$\overline{U}_x = \frac{sF(s)}{2\pi i}\int_{c-i\infty}^{c+i\infty} e^{spx} \cdot \frac{(\beta^{-2} - 2p^2)e^{-s\eta_s h}}{\beta^2 R(p)}\, dp, \tag{19}$$

$$\overline{U}_z = \frac{sF(s)}{2\pi i}\int_{c-i\infty}^{c+i\infty} e^{spx}\,\frac{2p\eta_p e^{-s\eta_s h}}{\beta^2 R(p)}\, dp. \tag{20}$$

In equations (19) and (20) we set

$$t = -px + \eta_s h,$$

a real positive number. For $0 \leq |\sin\theta| \leq \beta/\alpha$, the resulting contour of integration in the p-plane is a hyperbola opening to the left if x is positive and opening to the right if x is negative. For $\beta/\alpha \leq |\sin\theta| \leq 1$, the contour described above is complemented by a lancet with a real turning point at $p=-1/\alpha$ if x is positive and at $p=+1/\alpha$ if x is negative. In either case, the contour is equivalent to the original contour by Jordan's lemma. In terms of r and θ, the path of integration analogous to equation (10) is

$$\omega_s(t) = -(t/r)\sin\theta + i(t^2/r^2 - \beta^{-2})^{1/2}\cos\theta, \quad t \geq r/\beta, \tag{21}$$

$$\omega_{sp}(t) = -(t/r)\sin\theta - (\beta^{-2} - t^2/r^2)^{1/2}\cos\theta, \quad t_{sp} \leq t \leq r/\beta; \tag{22}$$

where

$$t_{sp} = (r/\alpha)\sin\theta + (r/\beta)(1 - \beta^2/\alpha^2)^{1/2}\cos\theta, \quad \beta/\alpha \leq |\sin\theta| \leq 1. \tag{23}$$

We set $F(s)=s^{-1}$ in equations (17) and (18). Using the contours given in equations (21) and (22), we see that the transient response for a step function source of SV waves is

$$U_x = \frac{1}{\pi\beta^2}\,\mathrm{Im}\left\{\frac{d\omega_s}{dt}\,\frac{(\beta^{-2}-2\omega_s^2)}{R(\omega_s)}\right\}H(t-r/\beta) + \frac{1}{\pi\beta^2}\,\mathrm{Im}\left\{\frac{d\omega_{sp}}{dt}\,\frac{\beta^{-2}-2\omega_{sp}^2}{R(\omega_{sp})}\right\}\left[H(t-t_{sp})-H(t-r/\beta)\right], \tag{24}$$

$$U_z = \frac{1}{\pi\beta^2}\,\mathrm{Im}\left\{\frac{d\omega_s}{dt}\,\frac{2\omega_s\eta_p}{R(\omega_s)}\right\}H(t-r/\beta) + \frac{1}{\pi\beta^2}\,\mathrm{Im}\left\{\frac{d\omega_{sp}}{dt}\,\frac{2\omega_{sP}\eta_p}{R(\omega_{sp})}\right\}\left[H(t-t_{sp})-H(t-r/\beta)\right]. \tag{25}$$

FIRST MOTIONS FOR UNIFORM P AND SV SOURCES

If we assume that the motions observed at the surface of the half-space consist of a suite of pulses whose duration is short compared with the travel time of P and S waves through a distance equal to the depth of burial of the sources, then a convenient representation of the distribution of the amplitudes on the surface can be obtained by computing the first motions from the general solution obtained above (Knopoff, 1958b).

Near the arrival time of the P wave, r/α, the following approximations hold:

$$\omega_p \approx -(\sin\theta)/\alpha,\qquad \eta_p \approx (\cos\theta)/\alpha,\qquad \frac{d\omega_p}{dt} \approx \frac{(i/\alpha)\cos\theta}{(t^2-r^2/\alpha^2)^{1/2}},\qquad \eta_s \approx (1/\beta)(1-k^2\sin^2\theta),\quad k=\beta/\alpha. \tag{26}$$

Substituting equations (26) into equations (15) and (16), we obtain the initial behavior of the P arrival,

$$U_x = U_{xp}^0 = U_{xp}(\theta)\,\frac{H(t-r/\alpha)}{(t^2-r^2/\alpha^2)^{1/2}}, \tag{27}$$

$$U_z = U_{zp}^0 = U_{zp}(\theta)\,\frac{H(t-r/2)}{(t^2-r^2/\alpha^2)^{1/2}}. \tag{28}$$

Here,

$$U_{xp}(\theta) = \frac{-2\sin\theta\cos\theta(1-k^2\sin^2\theta)^{191}}{\pi\alpha^2\beta^3R(-\alpha^{-1}\sin\theta)}, \tag{29}$$

$$U_{zp}(\theta) = \frac{(1-k^2\sin^2\theta)\cos\theta}{\pi\alpha\beta^4R(-\alpha^{-1}\sin\theta)}. \tag{30}$$

This result is a satisfactory approximation to the solution given in the preceding section for times close to the arrival time of the P wave.

Near the arrival time of the S wave, r/β, the following approximations hold:

$$\omega_s \approx -(\sin\theta)/\beta,\qquad \eta_s \approx (\cos\theta)/\beta,\qquad \frac{d\omega_s}{dt} \approx \frac{(i/\beta)\cos\theta}{(t^2-r^2/\beta^2)^{1/2}},\qquad \eta_p \approx \alpha^{-1}(1-k^{-2}\sin^2\theta)^{1/2} = \beta^{-1}(k^{-2}-\sin^2\theta)^{1/2}. \tag{31}$$

Substituting equation (31) into equations (24) and (25), we find the first motion of the SV waves, for points on the surface for which $|\sin\theta| \leq \beta/\alpha$, to be

$$U_x = U_{xs}^0 = U_{xs}(\theta)\,\frac{H(t-r/\beta)}{(t^2-r^2/\beta^2)^{1/2}}, \tag{32}$$

$$U_z = U_{zs}^0 = U_{zs}(\theta)\,\frac{H(t-r/\beta)}{(t^2-r^2/\beta^2)^{1/2}}, \tag{33}$$

where

$$U_{xs}(\theta) = \frac{\cos\theta(1-2\sin^2\theta)}{\pi\beta^3R(-\beta^{-1}\sin\theta)}, \tag{34}$$

$$U_{zs}(\theta) = \frac{-2(1-k^{-2}\sin^2\theta)^{1/2}\sin\theta\cos\theta}{\pi\alpha\beta^4R(-\beta^{-1}\sin\theta)}.$$

In the case of the buried SV source, for stations at coordinates exceeding the critical angle $\sin^{-1}\beta/\alpha$, there are three discrete events having discontinuities in the response for impulsive excitation. At these more remote points there is an onset which we call the event sP, an event whose onset time corresponds to the travel of the wave over the ray path emerging from the source at the critical angle, traveling with the velocity of S, thence along the surface with the velocity of P. This event is frequently called the "head wave" or the "conical wave."[1] The conical wave has a tail. The tail becomes infinite in amplitude immediately *before* the arrival of S. Immediately following the arrival of S, the normal discontinuity in S is observed. Thus, the S events at stations beyond the critical angle have discontinuities occurring at either side of the time r/β, and both are preceded by the event occurring at the sP refraction time. The discontinuity in S immediately before r/β will be associated with the sP event.

In order to compute the motions immediately before the time r/β, we consider the sP contributions in equations (24) and (25). The following approximations are valid:

$$\begin{aligned} \omega_{sp} &\approx -(\sin\theta)/\beta, \\ \eta_s &\approx (\cos\theta)/\beta, \\ \frac{d\omega_{sp}}{dt} &\approx -\beta^{-1}(r^2\beta^{-2} - t^2)^{-1/2}\cos\theta, \\ \eta_p &\approx i\beta^{-1}(\sin^2\theta - k^2)^{1/2}. \end{aligned} \tag{36}$$

Substituting these expressions into equations (24) and (25), we find the sP behavior near r/β to be

$$\begin{aligned} U_x &= U^{f}_{xsp}(\theta)\frac{H(r/\beta - t)}{(r^2\beta^{-2} - t^2)^{1/2}}, \\ U_z &= U^{f}_{zsp}(\theta)\frac{H(r/\beta - t)}{(r^2\beta^{-2} - t^2)^{1/2}}, \end{aligned} \tag{37}$$

where

$$\begin{aligned} U^{f}_{xsp}(\theta) &= \begin{cases} 0 & |\sin\theta| \le \beta/\alpha \\ \dfrac{4}{\pi\beta^9}\dfrac{\cos^2\theta\sin^2\theta(1 - 2\sin^2\theta)(\sin^2\theta - k^2)^{1/2}}{R(\omega_{sp})\overline{R}(\omega_{sp})} & |\sin\theta| \ge \beta/\alpha, \end{cases} \\ U^{f}_{zsp}(\theta) &= \begin{cases} 0 & |\sin\theta| \le \beta/\alpha \\ \dfrac{-2}{\pi\beta^9}\dfrac{\cos\theta\sin^2\theta(1 - 2\sin^2\theta)(\sin^2\theta - k^2)^{1/2}}{R(\omega_{sp})\overline{R}(\omega_{sp})} & |\sin\theta| \ge \beta/\alpha. \end{cases} \end{aligned} \tag{38}$$

The motion immediately following the time r/β at stations $\sin\theta \ge \beta/\alpha$ is given by the conditions obtained in equation (31). For this case, we obtain motions as in equations (32) and (33) but where

$$U_{zs}(\theta) = \frac{\cos\theta(1 - 2\sin^2\theta)^3}{\pi\beta^9 R(-\beta^{-1}\sin\theta)\overline{R}(-\beta^{-1}\sin\theta)}$$

and

$$U_{xs}(\theta) = \frac{8(1 - k^{-2}\sin^2\theta)\sin^3\theta\cos^2\theta}{\pi\alpha^2\beta^7 R(-\beta^{-1}\sin\theta)\overline{R}(-\beta^{-1}\sin\theta)}. \tag{35}$$

[1] The conical wave front in two dimensions has the shape of a two-dimensional cone. Hence it takes the form of a wedge or inhomogeneous plane wave.

The quantity $\overline{R}(p)$ is the expression conjugate to $R(p)$,

$$\overline{R}(p) = (2p^2 - \beta^{-2})^2 - 4p^2\eta_s\eta_p.$$

To compute the motion near the onset of sP we note that the sP motion is given by the integral around the branch cut ($-\infty < \mathrm{Re}\ p < -\alpha^{-1}$). The integrands decrease exponentially along the negative real axis beyond $p = -\alpha^{-1}$. We approximate the contribution of the branch line integral by letting

$$\begin{aligned} \eta_p &= \pm i\gamma \begin{matrix} \text{Top} \\ \text{Bottom} \end{matrix} \text{ of branch line}, \\ p &\approx -\alpha^{-1} - \tfrac{1}{2}\gamma^2\alpha, \\ \eta_s &= (\beta^{-2} - \alpha^{-2})^{1/2} - \tfrac{1}{2}\gamma^2(\beta^{-2} - \alpha^{-2})^{-1/2}; \end{aligned} \tag{39}$$

then $pdp=\gamma d\gamma$ and

$$R(p) \approx (2\alpha^{-2} - \beta^{-2})^2 \pm i\gamma 4\alpha^{-2}(\beta^{-2} - \alpha^{-2})^{1/2} = R_0 \pm i\gamma R_1.$$

In equations (19) and (20) we retain terms to the second order in γ in the exponents and retain terms to the first order in γ elsewhere. For $F(s)=1$ we have, approximately,

$$\overline{U}_z = \frac{1}{\pi}\int_0^\infty \gamma^2 d\gamma \frac{\alpha(\beta^{-2} - 2\alpha^{-2})R_1}{\beta^2 R_0^2} \exp\left\{-st_{sp} - \tfrac{1}{2}s\gamma^2\left[x\alpha - h(\beta^{-2} - \alpha^{-2})^{-1/2}\right]\right.,$$
$$\overline{U}_z = -\frac{1}{\pi}\int_0^\infty \gamma^2 d\gamma \frac{2}{\beta^2 R_0} \exp\left\{-st_{sp} - \tfrac{1}{2}s\gamma^2\left[x\alpha - h(\beta^{-2} - \alpha^{-2})^{-1/2}\right]\right. . \tag{40}$$

The expression for U_x becomes, after integrating over γ,

$$\overline{U}_x = \frac{\alpha(\beta^{-2} - 2\alpha^{-2})R_1}{2^{1/2}\beta^2 R_0\left[x\alpha - h(\beta^{-2} - \alpha^{-2})^{-1/2}\right]^{3/2}\pi^{1/2}S^{3/2}} e^{-st_{sp}}. \tag{41}$$

The inverse transform of equation (41) with respect to s is

$$U_x = \frac{2^{1/2}(\beta^{-2} - 2\alpha^{-2})R_1}{\pi\beta^2 R_0^2 \alpha^{1/2} x_{sp}^{3/2}} \cdot (t - t_{sp})^{1/2} H(t - t_{sp}), \tag{42}$$

where $x_{sP}=x-h\alpha^{-1}(\beta^{-2}-\alpha^{-2})^{1/2}$ is the distance from the point of observation to the point of emergence of the critical ray at the surface. The corresponding expression for U_z is

$$U_z = -\frac{1}{\pi R_0 \beta^2 \alpha^{3/2}}(t - t_{sp})^{1/2} H(t - t_{sp}). \tag{43}$$

We rewrite equations (42) and (43) in the form,

$$U_x = U_{xsp}^{i}(t - t_{sp})^{1/2} H(t - t_{sp}), \qquad U_{xsp}^{i} = \frac{2^{1/2}(\beta^{-2} - \alpha^{-2})R_1}{\pi\beta^2 R_0^2 \alpha^{1/2} x_{sp}^{3/2}}, \qquad |\sin\theta| \geq \beta/\alpha \text{ and}$$
$$U_z = U_{zsp}^{i}(t - t_{sp})^{1/2} H(t - t_{sp}), \qquad U_{zsp}^{i} = -\frac{1}{\pi\beta^2 R_0 \alpha^{3/2}}, \qquad |\sin\theta| \geq \beta/\alpha. \tag{44}$$

THE RADIATION PATTERN OF A DIRECTIONAL SOURCE

We may construct elastodynamic multipoles by means of the same artifice used in electricity. An elastodynamic multipole source of compression will be derived from the scalar potential ϕ for a cylindrically symmetric line source of compression. A similar procedure yields multipolar SV sources when we operate upon the shear potential function ψ.

A directional line source of P waves with a radiation pattern $\sin^m\theta\cos^n\theta$ is given by the potential

$$\bar{\phi}_{mn} = \frac{1}{2\pi}\left(\frac{\alpha}{s}\right)^{m+n}\frac{\partial^{m+n}}{\partial x^m \partial h^n} K_0(sr/\alpha)F(s) = \frac{F(s)}{2\pi i}\int_{c-i\infty}^{c+i\infty}\frac{1}{2}\, p^m \eta_p^{n-1}\alpha^{m+n} \cdot e^{spx - s\eta p(z-h)}dp. \tag{45}$$

Comparing equation (45) with the particular solution to equation (2) which is given as in the first term of equation (4), we see that the first

motion of the P event is, when the source is the potential function ϕ_{mn},

$$U_{xp}^{mn} = (-1)^m \sin^m \theta \cos^n \theta U_{xp}^0,$$
$$U_{zp}^{mn} = (-1)^m \sin^m \theta \cos^n \theta U_{zp}^0. \quad (46)$$

When the source radiation pattern is the result of the super-position of several multipolar sources of the type given in equation (45), the first motion for the P arrival is the corresponding superposition of first motions given by equation (46). Let $f(\theta)$ be the radiation pattern of the source,

$$f(\theta) = \sum_{m,n} a_{mn} \sin^m \theta \cos^n \theta = \sum_{m,n} f_{mn}(\theta). \quad (47)$$

The source potential must be

$$\bar{\phi}_f = \sum_{m,n} a_{mn} \bar{\phi}_{mn}; \quad (48)$$

and the first motion is, by superposition,

$$U_{xp}^f = \sum_{m,n} a_{mn} U_{xp}^{mn},$$
$$U_{zp}^f = \sum_{m,n} a_{mn} U_{zp}^{mn}. \quad (49)$$

The first motions due to an SV multipolar source are treated in exactly the same way as the solution for the multipolar P source.

THE INVERSE PROBLEM

From measurements of the displacements corresponding to the first motion events on the surface of the elastic half-space, we wish to determine the source radiation pattern, $f(\theta)$. The procedure is straightforward. We note that a buried P source contributes only P events on the surface of the half-space. A buried SV source contributes both S events and sP events. Thus, in the inverse problem, if we wish to determine the multipolar source distribution which produces the motion at the surface, the amplitudes of the P events must be related only to a distribution of compressional sources. Similarly, the amplitudes of the S and sP events must be related only to a distribution of shear potential functions. We can thus obtain the multipolar distribution functions separately by correlating the P sources with the P amplitudes and the S sources with the S or sP amplitudes. We describe the solution to the determination of the P distributions in some detail.

First, the first motion amplitudes of horizontal and vertical displacement components of the P amplitudes at the surface of the half-space are written as functions of θ. We next divide these distribution functions by the expressions, $U_{xp}(\theta)$ and $U_{zp}(\theta)$, respectively. The quotients are equal to the series,

$$\sum_{m,n} (-1)^m f_{mn}(\theta) = g(\theta) = \frac{A_{xp}(\theta)}{U_{xp}(\theta)} = \frac{A_{zp}(\theta)}{U_{zp}(\theta)}. \quad (50)$$

The quantities, $A_{xp}(\theta)$ and $A_{zp}(\theta)$, are the measured horizontal and vertical amplitudes of the P events. If the two ratios in equation (50) are not the same, there must be interference caused by more than one virtual source. The effects of interference must be eliminated, and the two ratios in equation (50) must be the same before the following procedure can be applied.

Rather than expand $g(\theta)$ in a trigonometric power series directly, we use a Fourier series expansion. We express $g(\theta)$ as the sum of its even and odd parts,

$$g(\theta) = g_e(\theta) + g_0(\theta). \quad (51)$$

These two terms are expanded in series as follows:

$$g_e(\theta) = \sum_{n=0}^{\infty} A_n \cos n\theta, \qquad A_n = \frac{\epsilon_n}{\pi} \int_{-\pi/2}^{\pi/2} g_e(\theta) \cos n\theta d\theta,$$
$$\frac{g_0(\theta)}{\sin \theta} = \sum_{n=0}^{\infty} B_n \cos n\theta, \qquad B_n = \frac{\epsilon_n}{\pi} \int_{-\pi/2}^{\pi/2} g_0(\theta) \frac{\cos n\theta}{\sin \theta} d\theta. \quad (52)$$

Obviously, a trigonometric power series expansion is not unique because the identity,

$$\sin^2 \theta + \cos^2 \theta = 1,$$

may be employed to rearrange the power series without affecting its value. For example, the vertical dipole, $\sin^2 \theta$, may be written as the difference between a simple pole and a horizontal di-

pole, $1-\cos^2\theta$. Thus, the multipolar distributions are not unique. Similarly, using the identity,

$$\cos n\theta = 2\cos(n-1)\theta\cos\theta - \cos(n-2)\theta,$$

we can recast equation (52) into a trigonometric power series. We avoid this ambiguity by taking the uniform source ($m=0$) and the horizontal dipole source ($m=1$) as the two fundamental sources. This selection is arbitrary. All other multipolar sources can be represented as differentiations of these two fundamental sources with respect to the vertical direction. By restricting the integer, m, in the multipolar expressions to the values, $m=0$ and $m=1$; we see that $f(\theta)=g(\theta)$ if $g(\theta)$ is even, $f(\theta)=-g(\theta)$ if $g(\theta)$ is odd, and $f(\theta)=g_e(\theta)-g_0(\theta)$ if $g(\theta)$ is mixed.

The solution for the multipolar shear sources follows in exactly the same way. It is evident that the motions corresponding to the shear sources are even more seriously overdetermined than those due to the P sources. In the examples which follow, we shall use only the S motions and not the sP motions because of the complexity of the latter. Beyond the critical angle, the S motions themselves consist of two wavelets. The distributions of the two wavelets with their two spatial components represent four quantities whose ratios to the theoretical amplitudes must be constant in order that the half-space be homogeneous. Within the critical angle there are, of course, only two quantities describing the motion since there is only a single S wavelet in this region. There ratios to the theoretical amplitudes must also conform to the theoretical ratios predicted. From the value of $g(\theta)$ computed for the ratio of the S amplitudes to the theoretical values, we can expand in a series of the multipoles derived from poles and horizontal dipoles, and compute in this way the directivity of the shear sources in complete analogy with the result obtained earlier for compressional sources.

APPLICATIONS OF THE METHOD

Consider a line source of the stress component $\tau_{zz}=-\delta(x)\delta(z-h)(2\pi)^{-1}$. The Laplace transforms of the potential functions are

$$\bar{\phi} = -\frac{\beta^2}{2\pi i\mu s}\int_{c-i\infty}^{c+i\infty} e^{spx-s\eta_p(h-z)}dp,$$
$$\bar{\phi} = -\frac{\beta^2}{2\pi i\mu s}\int_{c-i\infty}^{c+i\infty} e^{spx-s\eta_s(h-z)}\frac{pdp}{\eta_s}, \tag{53}$$

for $0\le z\le h$. The solution to this problem has been obtained by Pekeris (1955) for the motions at the surface due to a point source. We do not need the solutions for the motions at the surface in order to perform the inversion as indicated in the preceding section. Rather, we may compare the integral expressions for the potential functions given in equation (53) with the potentials for the point P and S sources. In this case, we observe that the directivity of the P source is $-\cos\theta$, and the directivity of the S source is $\sin\theta$.

In a similar way we consider the source of the stress component, $\tau_{xz}=-\delta(x)\delta(z-h)(2\pi)^{-1}$. The potentials are

$$\bar{\phi} = \frac{\beta^2}{2\pi i\mu s}\int_{c-i\infty}^{c+i\infty} e^{spx-s\eta_p(h-z)}\frac{pdp}{\eta_p},$$
$$\bar{\psi} = \frac{\beta^2}{2\pi i\mu s}\int_{c-i\infty}^{c+i\infty} e^{spx-s\eta_s(h-z)}dp, \tag{54}$$

for $0\le z\le h$. Again avoiding the problem of evaluating the motions at the surface, it is apparent that the directivity pattern for the virtual P source is $-\sin\theta$ while for the S source it is $\cos\theta$.

It is evident that, from these two kinds of sources, we can obtain the motions at the surface for the direct problem merely by superimposing the appropriate solutions for the pure compression and shear sources obtained earlier, applying the appropriate directivity.

REFERENCES

deHoop, A. T., 1958, Representation theorems for the displacement in an elastic solid and their applications to elastodynamic diffraction theory: Thesis, Delft.

Garvin, W. W., 1956, Exact transient solution of the buried line source problem: Proc. Roy. Soc., London, v. A, 234, p. 528–541.

Gilbert, J. F., Jr., 1956, Seismic wave propagation in a two-layer half-space: Ph.D. Thesis, Massachusetts Institute of Technology, Cambridge, Mass.

Gilbert, F., 1960, Scattering of impulsive elastic waves by a smooth convex cylinder: Jour. Acoust. Soc. Amer., v. 32, p. 841–857.

——— and Knopoff, L., 1959, Scattering of impulsive elastic waves by a rigid cylinder: Jour. Acoust. Soc. Amer., v. 31, p. 1169–1175.

——— 1960, Scattering of impulsive elastic waves by a rigid sphere: Jour. Acoust. Soc. Amer.

Knopoff, L., 1958a, Love waves from a line SH source: Jour. Geophys. Res., v. 63, p. 619–630.

——— 1958 b, The surface motions of a thick plate: Jour. Appl. Phys., v. 29, p. 661–670.

——— Fredricks, Gangi, and Porter, 1957, Surface amplitudes of reflected body waves: Geophysics, v. 22 p. 842–847.

——— Gilbert, and Pilant, 1960, Wave propagation

in a medium with a single layer: Jour. Geophys. Res., v. 65, p. 265–278.
——— and Gilbert, F., 1960, Diffraction of elastic waves by the core of the earth: Bull. Seismol. Soc. Amer., In press.
Langer, R. E., 1933, An inverse problem in differential equations: Bull. Am. Math. Soc., v. 39, p. 814–820.
Pekeris, C. L., 1934, An inverse boundary value problem in seismology: Physics, v. 5, p. 311–316.
——— 1955, The seismic buried pulse: Proc. Nat. Acad. Sci., v. 41, p. 629–639.
Slichter, L. B., 1933, An inverse boundary value problem in electrodynamics: Physics, v. 4, p. 411–418.
——— 1951, An electromagnetic interpretation problem in geophysics: Geophysics, v. 16, p. 431–449.
——— 1952, An electromagnetic interpretation problem for the sphere: Proc. Roy. Soc., London, v. A, 214, p. 356–370.
——— 1954, Seismic interpretation theory for an elastic earth: Proc. Roy. Soc., London, v. A, 224, p. 43–63.
Stevenson, A. F., 1934, On the theoretical determination of earth resistances from surface potential measurements: Physics, v. 5, p. 114–124.
——— 1955, On the theoretical determination of earth resistances from surface potential measurements: Phil. Mag., v. 19 p. 297–306.

GEOPHYSICS, VOL. XXVI, NO. 5 (OCTOBER, 1961), PP. 635–642, 1 FIG.

RADIATION RESISTANCE OF A VERTICAL MAGNETIC DIPOLE OVER AN INHOMOGENEOUS EARTH*

JANARDAN G. NEGI†

Abstract: The expressions for the energy radiated per second from an oscillating vertical magnetic dipole situated above a two-layer earth are derived. Of the three important cases to which particular attention has been given, the first and the second involve the presence of a conducting and insulating substratum, respectively. The third deals with a dipole placed over a thin conducting sheet of infinite extent. Appropriate approximations have been made such that the results may be useful for geoelectrical exploration.

INTRODUCTION

It was shown by Sommerfeld (1949) and Wait (1953) that the expressions for the radiation resistance of the electric and magnetic dipoles are considerably modified due to the proximity of the earth. The extent of modification depends upon the geological conditions as well as on the values of the electrical constants of the ground. It was suggested that this property can be utilized for geoelectrical exploration. With this motivation Tikhonov and Chitaev (1956) computed theoretical curves from Sommerfeld's expressions for the radiation resistance of an electric dipole over a homogeneous earth.

The growing importance of aeroelectromagnetic surveys demands the study of the influence of inhomogeneous earth. For many practical purposes the earth may be taken as a horizontally stratified medium consisting of electrically homogeneous and isotropic layers. The simplest, yet useful, case is that of a two-layer earth. This paper gives a theoretical analysis of the problem of the power flow from a vertical magnetic dipole in the presence of a two-layer earth. The general results are simplified to computable forms for certain cases of interest in exploration geophysics.

FORMULATION OF THE PROBLEM

Let an oscillating vertical magnetic dipole be placed at a point $(0, 0, -h)$. At sufficiently low frequencies this is equivalent to a small circular loop of area dA carrying a current $Ie^{i\omega t}$ and having its axis perpendicular to the ground surface. The whole space under consideration is divided into four regions with specified values of conductivity (σ) and permittivity (ϵ), as shown in Figure 1. The magnetic permeability (μ) is assumed to be the same all over.

The time average of the power radiated in the z-direction can be calculated from the z-component P_z of the Poynting vector, which is given by

$$P_z = \tfrac{1}{2}\ \mathrm{Re}\ E_\phi H_\rho^* \qquad (1)$$

where Re means "real part of" and H_ρ^* is the complex conjugate of H_ρ.

Denoting the total power radiated through horizontal planes at $Z=-(h\pm\delta h)$, $\delta h\to 0$ by S_+ and S_- respectively, one has

$$S_\pm = 2\pi \int_0^\infty P_z \rho d\rho \Big]_{z=-(h\pm\delta h)} . \qquad (2)$$

The total effective radiation resistance R of the magnetic dipole in the presence of layered earth may be defined by an expression,

$$R = \frac{2S}{[I]^2}, \qquad (3)$$

where the total power flow S is equal to $(S_+ - S_-)$.

Now it is obvious that, to calculate R, one must first determine E_ϕ and H_ρ as functions of the ground constants.

CALCULATION OF E_ϕ AND H_ρ

It will be more convenient if electric and magnetic vectors E and H are expressed everywhere

* Manuscript received by the Editor April 12, 1961.

† Department of Geology and Geophysics, Indian Institute of Technology, Kharagpur, West Bengal, India.

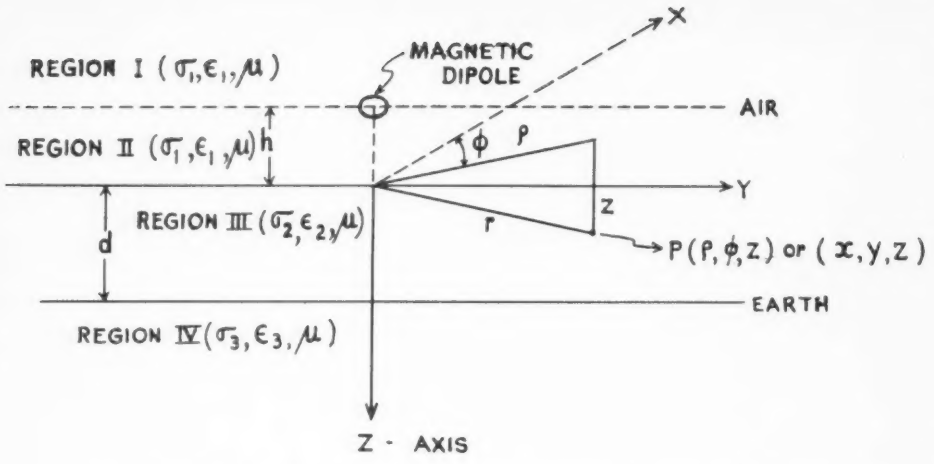

FIG. 1. Magnetic dipole located at a height, h, above the surface of a plane two-layer earth.

in terms of a single vector potential F, which is defined as

$$E = -\text{ Curl } F \tag{4}$$

and

$$H = -(\sigma + i\omega\epsilon)F + 1/i\omega\mu \text{ grad div } F. \tag{5}$$

The symmetry considerations clearly indicate that all electromagnetic field quantities except F_z, H_ρ, H_z, and E_ϕ will be zero. With the customary time dependence factor $e^{i\omega t}$ suppressed throughout, the resulting vector F_k (where k=I, II, III, or IV) in the four regions will satisfy the wave equation

$$\frac{1}{\rho}\frac{\partial}{\partial\rho}\left(\rho\frac{\partial F_k}{\partial\rho}\right) + \frac{1}{\rho^2}\frac{\partial^2 F_k}{\partial\phi^2} + \frac{\partial^2 F_k}{\partial z^2} - \gamma_k^2 F_k = 0 \tag{6}$$

subject to appropriate boundary conditions and the radiation condition at infinity. Here

$$\gamma_k^2 = (i\sigma_k\mu\omega - \epsilon_k\mu\omega^2). \tag{7}$$

Following Wait (1951) the general expressions for the vector potentials in the different media will be

$$F_{\text{I}} = i\alpha\int_0^\infty \Big[\lambda u_1^{-1}\exp\left[u_1(z+h)\right] + A_0\exp\left[u_1(z+h)\right]\Big]J_0(\lambda\rho)d\lambda, \tag{8}$$

$$F_{\text{II}} = i\alpha\int_0^\infty \Big[\lambda u_1^{-1}\exp\left[-u_1(z+h)\right] + A_1\exp\left[u_1(z+h)\right] + B_1\exp\left[-u_1(z+h)\right]\Big]J_0(\lambda\rho)d\lambda, \tag{9}$$

$$F_{\text{III}} = i\alpha\int_0^\infty \left[A_2\exp\left(u_2 z\right) + B_2\exp\left(-u_2 z\right)\right]J_0(\lambda\rho)d\lambda, \text{ and} \tag{10}$$

$$F_{\text{IV}} = i\alpha\int_0^\infty B_3\exp\left(-u_3 z\right)J_0(\lambda\rho)d\lambda \tag{11}$$

where the factors α and u_k are given by

$$\alpha = IdA\mu\omega/4\pi \text{ and} \tag{12}$$

$$u_k^2 = \lambda^2 + \gamma_k^2. \tag{13}$$

These A's and B's are still undetermined funtions of λ. They will be evaluated from the boundary conditions which require that the tangential electric and magnetic fields are continuous across the plane interfaces. These tangential components $E_{\phi k}$ and $H_{\rho k}$ are connected to the vector potential F by the equations,

$$E_{\phi k} = \frac{\partial F_k}{\partial \rho} \text{ and} \tag{14}$$

$$H_{\rho k} = \frac{1}{i\mu\omega} \frac{\partial^2 F_k}{\partial \rho \partial z}. \tag{15}$$

So at any point on the plane $z=-h$ the functions F_I and F_{II} must satisfy the conditions

$$\left.\begin{aligned} \partial F_{\mathrm{I}}/\partial \rho &= \partial F_{\mathrm{II}}/\partial \rho \\ \text{and} \\ \partial^2 F_{\mathrm{I}}/\partial \rho \partial z &= \partial^2 F_{\mathrm{II}}/\partial \rho \partial z \end{aligned}\right]_{z=-h}. \tag{16}$$

These relations hold for all values of λ. This behavior along with the radiation condition at ∞ reduces the above conditions to

$$\left.\begin{aligned} F_{\mathrm{I}} &= F_{\mathrm{II}} \\ \text{and} \\ \partial F_{\mathrm{I}}/\partial z &= \partial F_{\mathrm{II}}/\partial z \end{aligned}\right]_{z=-h}. \tag{17}$$

Two more sets of similar equations will be at the planes $z=0$ and $z=d$.

The six equations so obtained can be solved for A_0, A_1, B_1, A_2, B_2, and B_3. The result of the algebraic process is

$$B_1 = 0 \text{ and} \tag{18}$$

$$A_0 = A_1 = -\frac{\lambda}{u_1} e^{-2u_1 h} G \tag{19}$$

where

$$G = \frac{(u_1+u_2)(u_3-u_2)e^{-2u_2 d} + (u_2-u_1)(u_2+u_3)}{(u_2-u_1)(u_3-u_2)e^{-2u_2 d} + (u_1+u_2)(u_2+u_3)}. \tag{20}$$

This agrees with the result of Wait (1951). On utilizing the results of equations (18), (19), and (20), we obtain

$$\begin{aligned} F_{\substack{\mathrm{I} \\ \mathrm{II}}} &= i\alpha \int_0^\infty \lambda u_1^{-1} e^{\pm (h+z)u_1} J_0(\lambda\rho) d\lambda \\ &\quad - i\alpha \int_0^\infty G\lambda u_1^{-1} e^{(z-h)u_1} J_0(\lambda\rho) d\lambda. \end{aligned} \tag{21}$$

The positive and the negative signs in equation (21) are for $z<-h$ and $0\geq z>-h$, respectively.

Equations (14) and (15) with (21) lead to

$$\begin{aligned} E_\phi = i\alpha \int_0^\infty &\left[e^{\pm (h+z)u_1}\right. \\ &\left. - Ge^{-(h-z)u_1}\right] \lambda^2 u_1^{-1} J_1(\lambda\rho) d\lambda \end{aligned} \tag{22}$$

and

$$\begin{aligned} H_\rho = \frac{\alpha}{\mu\omega} \int_0^\infty &\left[\pm e^{\pm (h+z)u_{1m}}\right. \\ &\left. - G_m e^{-u_{1m}(h-z)}\right] m^2 J_1(m\rho) dm. \end{aligned} \tag{23}$$

Here again positive and negative signs correspond to the above mentioned regions. The fact that in equation (23) we used a variable of integration different from λ, and hence had to replace u by $u_m=(m^2+\gamma_k^2)^{1/2}$, will prove useful in what follows.

CALCULATION OF TOTAL POWER RADIATED

On using equations (22) and (23), equation (2) can be rewritten as follows

$$\begin{aligned} S_\pm = \mathrm{Re} \frac{i\alpha^2\pi}{\mu\omega} \int_0^\infty f_1(\lambda)\lambda^2 d\lambda \int_0^\infty f_2^*(m) m^2 dm \\ \cdot \int_0^\infty J_1(\lambda\rho) J_1(m\rho) \rho d\rho \end{aligned} \tag{24}$$

where

$$f_1(\lambda) = \frac{1}{u_1}\left(e^{-u_1 \delta h} - Ge^{-2u_1(h \pm (\delta h/2))}\right) \tag{25}$$

and

$$f_2^*(m) = \pm e^{-u_{1m}^* \delta h} - G_m^* e^{-2u_{1m}^*(h \pm (\delta h/2))}. \tag{26}$$

Here we can apply the orthogonal integral property of Bessel functions, viz.

$$\int_0^\infty J_1(\lambda\rho) J_1(m\rho) \rho d\rho = \frac{\delta\left(\frac{\lambda}{m}\right)}{m}, \tag{27}$$

where

$$\delta\left(\frac{\lambda}{m}\right) = \begin{cases} 0 & \text{for } \lambda \neq m \\ \infty & \text{for } \lambda = m \end{cases} \qquad (28)$$

with

$$\int_{m-\epsilon}^{m+\epsilon} \delta\left(\frac{\lambda}{m}\right)\lambda d\lambda = 1 \quad (\epsilon \to 0). \qquad (29)$$

Hence, the latter integral in equation (24) vanishes for all values of m except for $\lambda = m$, so that the middle integration yields $\lambda f_2^*(\lambda)$. Thus, equation (24) reduces to the simple integral,

$$S_{\pm} = \mathrm{Re}\,\frac{i\alpha^2\pi}{\mu\omega}\int_0^{\infty} \lambda^3 f_1(\lambda) f_2^*(\lambda) d\lambda. \qquad (30)$$

A further simplification is obtained if we let the planes $z = -(h \pm \delta h)$ approach the position of magnetic dipole, that is

$$|z + h| = \delta h, \quad |z - h| \leqq 2h.$$

The total power radiated, S, which is supplied by the dipole to its surrounding, is now

$$S = S_+ - S_-$$
$$= \mathrm{Re}\,\frac{2i\alpha^2\pi}{\mu\omega}\int_0^{\infty} \frac{\lambda^3}{u_1}\left[e^{-\delta h(u_1+u_1^*)} - Ge^{-2hu_1}\right]d\lambda \qquad (31)$$

where, due to $\delta h \ll h$, we may neglect $u_1^* dh$ as compared to $2hu_1$ in the exponential function under the second integral sign. A result equivalent to equation (31) has also been found by Wait (1958) using a different method.

The rigorous evaluation of this integral for a general case is rather difficult and may not be so useful. We shall focus our attention on applying these results in the few cases of practical importance from the geophysical point of view. The cases considered are

(1) the lower layer is a perfect conductor,
(2) the lower layer an insulator, and
(3) the dipole is kept over a thin conducting sheet of infinite extent situated in a poorly conducting, infinite, homogeneous medium.

CASE I: PERFECTLY CONDUCTING SUBSTRATUM

In geoelectrical exploration the frequencies used are usually so low that the displacement currents can be safely neglected everywhere. Here we have $\sigma_1 = 0$ (for air) and $\sigma_3 = \infty$ (for a perfectly conducting layer). In this particular case,

$$\begin{aligned} u_1 &= (0 + \lambda^2)^{1/2} = \lambda, \\ u_2 &= (\lambda^2 + i\omega\mu\sigma)^{1/2}, \text{ and} \\ u_3 &= \infty. \end{aligned} \qquad (32)$$

The corresponding value of G on combining equations (20) and (32) will be equations given by

$$G = e^{-2u_2 d} + \frac{u_2 - \lambda}{u_2 + \lambda}. \qquad (33)$$

With this value of G, the expression for power in equation (31) can be rewritten as

$$S = \frac{2\alpha^2\pi}{\mu\omega}\left[\mathrm{Re}\, i\int_0^{\infty} e^{-\delta h(u_1+u_1^*)}\lambda^2 d\lambda + \mathrm{Re}\, i\int_0^{\infty}\frac{\lambda - u_2}{\lambda + u_2}e^{-2h\lambda}\lambda^2 d\lambda - \mathrm{Re}\, i\int_0^{\infty}\lambda^2 e^{-2(u_2 d + h\lambda)}d\lambda\right]. \qquad (34)$$

Since here u_1, u_1^* and, of course, $u_1 + u_1^*$ are real, the first term in equation (34) vanishes completely. The second term is exactly the same. This was obtained and discussed in detail by Wait (1953) as an expression for power flow by a magnetic dipole placed over a homogeneous ground. We shall call that part of our equation (34) as S_0 and the remaining part as S_1. This S_1 can be interpreted as the contribution from this particular inhomogeneity.

Now it is quite obvious that the contribution S_1 from this inhomogeneity will be quite appreciable if $h\lambda \ll u_2 d$, i.e. if the dipole is kept at low heights such that d is much larger than h. In this case, the expression for S_1 reduces to

$$S_1 = -\,\mathrm{Re}\,\frac{2i\alpha^2\pi}{\mu\omega}\int_0^{\infty}\lambda^2 e^{-u_2 d}d\lambda. \qquad (35)$$

On writing $\lambda^2 = u_2^2 - \gamma_2^2$ with the abbreviation $\beta = 2d$, equation (35) becomes

$$S_1 = \mathrm{Re}\,\frac{2i\alpha^2\pi}{\mu\omega}\int_0^{\infty}(\gamma_2^2 - u_2^2)e^{-\beta u_2}d\lambda, \qquad (36)$$

$$= \mathrm{Re}\,\frac{2i\alpha^2\pi}{\mu\omega}\left(\gamma_2^2 - \frac{\partial^2}{\partial\beta^2}\right)\int_0^{\infty} e^{-\beta u_2}d\lambda, \qquad (37)$$

and

$$I_1 = \int_0^\infty e^{-\beta u_2} d\lambda = 2\gamma_2 K_1(\gamma_2\beta) \quad (38)$$

(see appendix I)

where $K_1(\gamma_2\beta)$ is a Bessels modified function of the second kind. Finally we have

$$S_1 = \mathrm{Re}\frac{4i\alpha^2\pi}{\mu\omega}\left(\gamma_2^2 - \frac{\partial^2}{\partial\beta^2}\right)\gamma_2 K_1(\gamma_2\beta). \quad (39)$$

CASE II: INSULATING SUBSTRATUM

In this case, since $\sigma_1=\sigma_3=0$ and displacement currents again are negligible, we shall have

$$u_1 = u_3 = \lambda$$

and

$$u_2 = (\lambda^2 + i\omega\mu\sigma_2)^{1/2}. \quad (40)$$

With these values of u's in equation (20) we have

$$G = \frac{(u_2-\lambda)(u_2+\lambda)(1-e^{-2u_2 d})}{(u_2+\lambda)^2 - (u_2-\lambda)^2 e^{-2u_2 d}}. \quad (41)$$

Since the second term in the denominator of equation (41) is small compared to the first, we get,

$$G \approx \frac{u_2-\lambda}{u_2+\lambda}(1-e^{-2u_2 d}). \quad (42)$$

Inserting this value of G in equation (33) and also noting that the term associated with $\delta(u_1+u_1^*)$ vanishes completely, the expression for the total power radiated now becomes

$$S = \mathrm{Re}\frac{2i\alpha^2\pi}{\mu\omega}\left[\int_0^\infty \lambda^2 \frac{\lambda-u_2}{\lambda+u_2} e^{-2h\lambda} d\lambda + \int_0^\infty \lambda^2 \frac{u_2-\lambda}{u_2+\lambda} e^{-2(h\lambda+u_2 d)} d\lambda\right] \quad (43)$$

The above formula is a sum of two terms of the type

$$S = S_0 + S_2. \quad (44)$$

Our interest lies in the second term S_2 which is the effect of the inhomogeneity in the ground.

In useful practice, when the dipole is kept at low heights such that $h\lambda \ll u_2 d$, we have

$$S_2 = \mathrm{Re}\frac{2i\alpha^2\pi}{\mu\omega}\left[\int_0^\infty \lambda^2 e^{-2du_2} d\lambda - \int_0^\infty \frac{\lambda^3}{u_2+\lambda} e^{-2du_2} d\lambda\right] \quad (45)$$

$$= S_1 + S_2'. \quad (46)$$

It turns out, therefore, that S_2, itself, may be considered as the sum of two effects. The first term is familiar and arose in Case I when the substratum was a perfect conductor.

The second term, S_2', may be interpreted as the correction accounting for the partial penetration of the waves in the lower layer.

The expression for S_2' can be rewritten as

$$S_2' = \mathrm{Re}\frac{4i\alpha^2\pi}{\mu\omega}\frac{1}{\gamma_2^2}\cdot\left[\int_0^\infty \lambda^3(\lambda-u_2)e^{-2u_2 d} d\lambda\right]. \quad (47)$$

Expressing equation (47) as a sum of two integrals and also using the relation $\mu_2^2=\lambda^2+\gamma_2^2$, equation (47) becomes

$$S_2' = \mathrm{Re}\frac{4i\alpha^2\pi}{\mu\omega}\frac{1}{\gamma_2^2}\cdot\left[\int_0^\infty (u_2^2-\gamma_2^2)^2 e^{-2u_2 d} d\lambda + \int_0^\infty u_2(\gamma_2^2-u_2^2)\lambda e^{-2u_2 d} d\lambda\right]. \quad (48)$$

Putting again $\beta=2d$, one gets

$$S_2' = \mathrm{Re}\frac{4i\alpha^2\pi}{\mu\omega}\frac{1}{\gamma_2^2}\cdot\left[\left(\frac{\partial^4}{\partial\beta^4} - 2\gamma_2^2\frac{\partial^2}{\partial\beta^2} + \gamma_2^4\right)\int_0^\infty e^{-\beta u_2} d\lambda - \frac{\partial}{\partial\beta}\left(\frac{\partial^2}{\partial\beta^2} - \gamma_2^2\right)\int_0^\infty \lambda e^{-\beta u_2} d\lambda\right]. \quad (49)$$

From Appendix I and II, we have

$$I_1 = \int_0^\infty e^{-\beta u_2} d\lambda = 2\gamma_2 K_1(\gamma_2\beta)$$

and

$$I_2 = \int_0^\infty \lambda e^{-\beta u_2 d}\,d\lambda = e^{-2\gamma_1 d}\left(\frac{1 + 2\gamma_2 d}{4d^2}\right). \tag{50}$$

Finally we obtain

$$S_2' = \mathrm{Re}\,\frac{4\pi i\alpha^2}{\mu\omega}\,\frac{1}{{\gamma_2}^2} \cdot\left[\left(\frac{\partial^4}{4\beta^4} - 2{\gamma_2}^2\frac{\partial^2}{\partial\beta^2} + {\gamma_2}^4\right)\cdot 2\gamma_2 K_1(\gamma_2\beta) - \frac{\partial}{\partial\beta}\left(\frac{\partial^2}{\partial\beta^2} - {\gamma_2}^2\right)e^{-2\gamma_2 d}\frac{(1 + 2\gamma_2 d)}{4d^2}\right] \tag{51}$$

and

$$S_2 = S_1 + S_2' = \mathrm{Re}\,\frac{2i\alpha^2\pi}{\mu\omega}\left[\left(\frac{\partial^2}{\partial\beta^2} - {\gamma_2}^2\right)2\gamma_2 K_1(\gamma_2\beta) + \frac{2}{{\gamma_2}^2}\left\{\left(\frac{\partial^4}{\partial\beta^4} - 2{\gamma_2}^2\frac{\partial^2}{\partial\beta^2} + {\gamma_2}^4\right)\cdot 2\gamma_2 K_1(\gamma_2\beta) - \frac{\partial}{\partial\beta}\left(\frac{\partial^2}{\partial\beta^2} - {\gamma_2}^2\right)e^{-2\gamma_2 d}\,\frac{(1 + 2\gamma_2 d)}{4d^2}\right\}\right]. \tag{52}$$

CASE III: DIPOLE ABOVE A THIN CONDUCTING SHEET OF INFINITE EXTENT

In this case, we assume that the conductivity of all regions outside the conducting sheet of thickness d is practically zero. On neglecting displacement currents we have

$$u_1 = u_3 = \lambda$$

and

$$u_2 = (\lambda^2 + {\gamma_2}^2)^{1/2}. \tag{53}$$

When these values are substituted in the expression for G in equations (20) we obtain, after some rearrangements,

$$G = 1 - \frac{2\lambda\left(1 + \dfrac{\lambda}{u_2}\right) + \left(1 - \dfrac{\lambda}{u_2}\right)2\lambda e^{-2u_2 d}}{\dfrac{1}{u_2}\left[(\lambda + u_2)^2 - \{(\lambda + u_2)^2 - 4u_2\lambda\}e^{-2u_2 d}\right]}. \tag{54}$$

Now, following Wait (1951) and (1953b), we consider a special form of a slab with thickness d and conductivity σ, correspondingly small and large in such a way that σd remains finite. This is true even in practice for geometrically thin sheets of high conductivities.

Under these assumptions the following simplifying approximations may be used:

$$e^{-2u_2 d} = 1 - 2u_2 d + \cdots \tag{55}$$

$$u_2{}^2 d = d(\lambda^2 + i\omega\mu\sigma) \approx i\omega\mu\sigma d, \tag{56}$$

$$\frac{\lambda}{u_2} \ll 1 \quad \text{and also} \quad u_2 d \ll 1. \tag{57}$$

Thus,

$$G \cong 1 - \frac{\lambda}{\lambda + iq} \quad \text{where} \tag{58}$$

$$q = \frac{\omega\mu\sigma d}{2}. \tag{59}$$

Combining equations (58) and (31) the nonvanishing term is

$$S = \mathrm{Re}\,\frac{2i\alpha^2\pi}{\mu\omega}\int_0^\infty \lambda^2\,\frac{\lambda}{\lambda + iq}\,e^{-2h\lambda}d\lambda, \tag{60}$$

$$= \mathrm{Re}\,\frac{2i\alpha^2\pi}{\mu\omega}\left[\int_0^\infty (\lambda^2 - iq\lambda - q^2)e^{-2h\lambda}d\lambda + \int_0^\infty iq^3\,\frac{1}{\lambda + iq}\,e^{-2h\lambda}d\lambda\right] \tag{61}$$

$$= \mathrm{Re}\,\frac{2i\alpha^2\pi}{\mu\omega}\,[I_{01} + I_3 + I_{02} + I_4] \tag{62}$$

where

$$I_{01} = \int_0^\infty \lambda^2 e^{-2h\lambda} d\lambda, \tag{63}$$

$$I_3 = -iq \int_0^\infty \lambda e^{-2h\lambda} d\lambda, \tag{64}$$

$$I_{02} = -q^2 \int_0^\infty e^{-2h\lambda} d\lambda, \text{ and} \tag{65}$$

$$I_4 = iq^3 \int_0^\infty \frac{e^{-2h\lambda}}{\lambda + iq} d\lambda. \tag{66}$$

It is evident that integrals I_{01} and I_{02} are real, so they won't contribute any real part on being multiplied by i. On leaving corresponding terms we have

$$S = \text{Re} \frac{2i\alpha^2\pi}{\mu\omega} (I_3 + I_4). \tag{67}$$

Putting their values from Appendix III, one gets

$$S = \text{Re} \frac{2i\alpha^2\pi}{\mu\omega} \left[-\frac{iq}{4h^2} + iq^3 e^{2hqi} \Gamma(0, 2hqi) \right] \tag{68}$$

where $\Gamma(0, 2hqi)$ is an incomplete gamma function.

CONCLUSION

The problem of radiation resistance of a magnetic dipole over a layered earth is interesting from a theoretical as well as an experimental point of view. We have derived expressions for a simple two-layer earth which are in agreement with results of Wait (1951, 1953, 1953b, 1958). The results have been applied to three important special cases. From the analysis it is evident that the radiation resistance is modified considerably by the closeness of the ground and its inhomogeneous character. It is believed that this property can be very conveniently utilized in a method of prospecting in which a small circular loop may be fixed on a low-flying aircraft, as suggested by Wait (1953). It may be mentioned that this possibility has also drawn the attention of U.S.S.R. exploration geophysicsts (Semenov & Korneev, 1957).

ACKNOWLEDGMENTS

The study was supported by the Council of Scientific and Industrial Research, India. The author takes this opportunity and pleasure of thanking Professor P. K. Bhattacharya for his kind interest and guidance throughout the work. He is also thankful to Dr. A. Roy for many valuable suggestions.

APPENDIX I

Evaluation of integral I_1.

$$I_1 = \int_0^\infty e^{-\beta u_2} d\lambda \tag{1}$$

$$= \int_0^\infty e^{-\beta u_2} (u_2^2 - \gamma_2^2)^{-1/2} u_2 du_2 \tag{2}$$

$$I_1 = \left[(u_2^2 - \gamma_2^2)^{1/2} e^{-\beta u_2} \right]_{\gamma_2}^\infty + \beta \int_{\gamma_2}^\infty e^{-\beta u_2} (u_2^2 - \gamma_2^2)^{1/2} du_2 \tag{3}$$

$$= \beta \int_{\gamma_2}^\infty e^{-\beta u_2} (u_2^2 - \gamma_2^2)^{1/2} du_2. \tag{4}$$

If we put $u_2 = t + \gamma_2$ so that $du_2 = dt$, the limits in equation (4) again become 0 to ∞. Then we have

$$I_1 = \beta e^{-\beta\gamma_2} \int_0^\infty e^{-\beta t} (t^2 + 2\gamma_2 t)^{1/2} dt \tag{5}$$

$$= \beta e^{-\beta\gamma_2} \frac{2\gamma_2}{\beta} e^{\gamma_2\beta} K_1(\gamma_2\beta) \tag{6}$$

$$= 2\gamma_2 K_1(\gamma_2\beta). \tag{7}$$

APPENDIX II

Evaluation of integral I_2.

$$I_2 = \int_0^\infty \lambda e^{-\beta u_2} d\lambda \tag{8}$$

$$= \int_{\gamma_2}^\infty e^{-\beta u_2} u_2 du_2 \tag{9}$$

$$= \left[\frac{u_2 e^{-\beta u_2}}{-\beta} \right]_{\gamma_2}^\infty + \frac{1}{\beta} \int_0^\infty e^{-\beta u_2} du_2 \tag{10}$$

$$= \frac{\gamma_2}{\beta} e^{-\beta\gamma_2} + \frac{1}{\beta^2} e^{-\beta\gamma_2}. \tag{11}$$

Resubstituting $\beta = 2d$, we have

$$I_2 = e^{-2\gamma_2 d}\frac{(1 + 2\gamma_2 d)}{4d^2}. \qquad (12)$$

APPENDIX III

$$I_3 = \int_0^\infty \lambda e^{-2h\lambda} d\lambda = \frac{1}{4h^2} \qquad (13)$$

and

$$I_4 = \int_0^\infty \frac{1}{\lambda + iq} e^{-2h\lambda} d\lambda. \qquad (14)$$

If we put

$$2h(\lambda + iq) = x,$$

then

$$2hd\lambda = dx.$$

Corresponding limits for x become $2hqi$ to ∞, and I_4 may be rewritten as

$$I_4 = e^{2hqi}\int_{2hqi}^\infty \frac{e^{-x}}{x} dx \qquad (15)$$

$$= e^{2hqi}\Gamma(0, 2hqi). \qquad (16)$$

REFERENCES

Erdelyi, A., et al, 1954, Tables of integral transforms: v. 1, McGraw-Hill, New York.

Sommerfeld, A., 1949, Partial differential equations in physics: Academic Press, New York.

Semenov, A. A., and Korneev, G. A., 1957, On the possibility of using radiation resistance of antennae in electrical exploration: (In Russian) Information Bulletin VITP, n. 3

Tikhonov, A. N., and Chitaev, D. N., 1956, On possible use of radiation resistance of an antenna for electrical mapping: (In Russian) Izv. Geophy. n. 3, p. 346–348.

Wait, J. R., 1951, The magnetic dipole over the horizontally stratified earth: Can. Jour. Physics, v. 29, p. 577–592.

Wait, J. R., 1953a, Radiation resistance of a circular loop in the presence of a conducting ground: Jour. of Applied Physics, v. 24, p. 646–649.

Wait, J. R., 1958, Induction by an oscillating dipole over a two-layer earth: App. Sci. Research. Sec. B, v. 7, p. 73–80.

Wait, J. R., 1953b, Induction in a conducting sheet by a small current carrying loop: App. Sci. Research Sec B, v. 3, p. 230–235.

DEPARTMENTS

DISCUSSIONS AND COMMUNICATIONS

FAULTS AND EARTH TIDES

DANILO A. RIGASSI*

It can be assumed that the effect of luni-solar attraction depends, to a certain extent, upon the geological structure. For instance, this effect should not be equal on the two sides of a fault separating rocks of different densities and competencies. If, on two geologically different blocks separated by a fault, two different values of the earth tidal motion can be measured, there is an *earth tidal anomaly* evidencing the presence of the fault. In other words, measuring and comparing earth tidal motions can be considered as a new geophysical prospecting method.

Instruments such as the extensometer or the horizontal pendulum cannot be used as field prospecting tools, due to their complexity. The accuracy of field gravity meters is not sufficient for detecting small anomalies of a few mms. Consequently, we tried to use a theodolite. The first experiment was made on June 8, 1960 across a vertical fault bordering to the SSW the Mormont Horst, Canton, of Vaud, Switzerland. The direction of the fault is about W 35°N–E 35° S. The vertical throw of the fault ranges from 150 to 200 m. To the SSW, there are shales and sandstones of Chattian (Oligocene) age; to the NNE, Urgonian (L. Cretaceous) limestones are exposed. The density contrast between the lighter Oligocene series and the heavier limestones is probably from 0.1 to 0.2. A Wild T-3 theodolite was set on the Oligocene downthrown block, approximately at Lat. 46°39′08″ N and Long. 6°31′44″ E, at a distance of about 300 m from the fault. A stadia was set on the Cretaceous upthrown block, to the N 37°E and at a distance of about 450 m from the theodolite or about 150 m from the fault. The following differences in elevation between the theodolite and the stadia were then measured (average of six readings):

Hour:		*Difference in elevation, meters:* (corrected for refraction)
A.M.	4.25	99.319±0.002
	6.00	99.311
	8.00	99.312
	10.00	99.293†
	12.00	99.313
P.M.	14.00	99.316
	16.00	99.316
	18.00	99.321
	20.00	99.324

† The reading at 10.00 A.M. was probably distorted by refraction effects due to the warming by the sun of a concrete surface located just in front of the theodolite.

We believe that the observed changes in elevation are due to tidal motions. It seems that during the night the moon, being approximately at the zenith, is pulling the Cretaceous horst above the surrounding Oligocene regions. During the day, on the contrary, the moon, being approximately at the nadir, is pulling down the Cretaceous horst.

Whether this explanation is entirely true or not, whether measurements of earth tidal motions do constitute a prospecting method, and whether the theodolite is a suitable instrument for such measurements cannot be decided upon the restricted experiment described in this paper. For answering these questions, numerous measurements on several faults and also on other structural types are necessary. The author has no opportunity to carry out further investigations. The scope of this short note is thus not to present undeniable scientific facts and figures, but to promote the interest of geophysicists in what could become a new prospecting method.

* Rue du Vioux College, Geneva, Switzerland.

EXCERPTS FROM AN ADDRESS GIVEN BEFORE THE ANNUAL CONFERENCE OF THE DIVISION OF EARTH SCIENCES, NATIONAL RESEARCH COUNCIL.

CHARLES C. BATES*

It is a striking fact that this country has no single major center, governmental, industrial, or academic, possessing the breadth required for handling all the concurrent work needed in Vela Uniform. As a result, the Advanced Research Projects Agency (ARPA) has several agents handling the forty major contracts in the Vela Uniform program, each agent being assigned a specific technical area. For those of you not familiar with the ARPA concept, the actual management mechanism includes the following.

(1) ARPA defines the specific problem area.

(2) An ARPA Order is issued describing the work to be done, the funds available, the reporting procedure, and the Order's effective period. These Orders are usually directed to an agent, who may undertake the task internally. In other cases, the agent may contract for the work with a university, a nonprofit agency, or an industrial concern.

(3) The agent is made responsible for the detailed technical supervision and administration of the assigned work. The agent maintains contact with the scientists doing the work, receives the reports, comments on them, and takes appropriate action. ARPA also receives a copy of each report, and it is reviewed by the staff. When guidance is needed, ARPA provides it to the agent; if ARPA is immediately responsible for the work, the guidance is given directly to the contractor.

(4) The ARPA staff periodically reviews all work under the Project. The findings are also summarized for ARPA's Ad Hoc Group on Nuclear Test Detection, which provides further technical guidance. In addition, one general summary of the Project was held in the form of a symposium. The response was very good and the symposium *Proceedings* have been widely distributed. A second symposium is planned for late summer or early fall of this year.

The Air Force Technical Applications Center (AFTAC) of Alexandria, Virginia, is ARPA's major technical advisor. AFTAC is also ARPA's technical agent for the systems and on-site inspection technique development tasks, as well as for certain aspects of improved seismic instrumentation, data display, and teleseismic field measurement techniques.

In the important nuclear-chemical research explosion series, the conduct of which has not yet been authorized, AFTAC codifies the technical requirements for the entire measurements program and also directs the acquisition of off-site seismic measurements. In this shot series, the Atomic Energy Commission (AEC) is responsible for providing the nuclear devices, the sites and cavities in which to fire the devices, the actual firing, and the making of measurements directly associated with such firing. In addition, similar support will be provided by the AEC for all chemical detonations at the Nevada Test Site. The third key activity in the shot program is the Defense Atomic Support Agency (DASA) with headquarters in Washington, D. C., which coordinates all Department of Defense activities at the various shot sites, manages the necessary close-in measurement programs to observe the conversion of shock waves to elastic waves, and executes all chemical explosions required outside the Nevada Test Site. In addition, DASA has accepted the responsibility to conduct research studies aimed at developing a comprehensive theory of the generation of seismic wave spectra by a theoretical and experimental study of close-in phenomena associated with large-scale detonations under various types of containment. DASA also provides the public and technical information service for this portion of Vela Uniform. In addition to the government agencies previously mentioned, the Air Force Cambridge Research Laboratories, Bedford, Massachusetts, is the agent for applied seismology, the Air Force Office of Scientific Research, Washington, D. C., for basic seismology and allied sciences, and the Rome Air Development Center, Rome, New York, is an agent for underground electromagnetic pulse investigations. Foreign seismic research has been arranged through the European Office of the U. S. Army in Frankfurt, Germany, the European Office of the Air Force Office of Aerospace Research in Brussels, Belgium, and the Office of the Secretary of Defense. The United States Geological Survey has also undertaken for ARPA a major investigation of seismic propagation paths in southern California and Nevada. In addition, limited investigations pertinent to the detection of subsurface nuclear explosions at sea are being conducted under the auspices of the Office of Naval Research, Washington, D. C., and the Bureau of Ships' Naval Electronics Laboratory and Naval Radiological Defense Laboratory in San Diego and San Francisco, California, respectively.

A brochure describing the Advanced Research Projects Agency and the manner in which unsolicited research proposals may be submitted to it can be obtained by writing the Agency at the Pentagon, Washington 25, D. C.

* Vela Uniform Branch, Nuclear Test Detection Office, Advanced Research Projects Agency, Washington, D. C.

RAPID COMPUTATION OF GRAVITY ANOMALIES FOR IRREGULARLY SHAPED THREE-DIMENSIONAL BODIES

AMALENDU ROY*

So much has been written (Levine, 1941, Gassman, 1951, Baranov, 1953, Talwani and Ewing, 1960, Goguel, 1941, etc.) on the above subject that any further publication on this theme seems to be of doubtful value. The only justification of printing this note lies in the genuine simplicity of both derivation and use of the method outlined herein. While this may be of particular interest to those who have to undertake manual computation, some simple scheme of programming on digital computors may perhaps also be devised.

The body is broken up into vertical prisms of small cross-section (Figure 1), each of which contributes

$$\gamma\rho dx dy\left(\frac{1}{(x^2+y^2+z_1^2)^{1/2}}-\frac{1}{(x^2+y^2+z_2^2)^{1/2}}\right)$$

to the gravitational effect at the origin. (This is numerically the same as the difference in gravitational potential due to surface distributions of matter, ρ gms/cm², on the two ends of the prism.) One has to compute only one term like

$$\frac{1.073}{(r^2+z^2)^{1/2}} \text{ gravity units,}$$

where, in particular,

$$dx(\Delta x) = dy(\Delta y) = 0.1 \text{ mile}$$

ρ = density contrast = 1 cgs unit

r and z are expressed in miles.

The constant, 1.073, includes the gravitational constant, changes units from cm to miles, specifically for $\Delta x = \Delta y = 0.1$ mile and for effects in "gravity units," i.e. 10^{-4} gals.

Figure 2 is a chart thus obtained and is valid as long as $z \gg \Delta x$ or Δy. This is why the chart is drawn only for $z \geq 1$ mile. Where shallower depths are involved, smaller values of Δx and Δy need to be considered, but the same chart of Figure 2 can be used with a correction factor. For example, if $\Delta x \Delta y$ is 0.0025 square mile instead of 0.01 square mile, one simply divides the anomaly by 4. However, in such a case, it will be necessary to add one or more curves to Figure 2 for lower values of z. This is a matter of hardly one or two hours.

Figure 3 is a part of a quadrant of a transparent template drawn to the scale of the available map with one dot for every elementary area, $\Delta x \Delta y$. For every dot

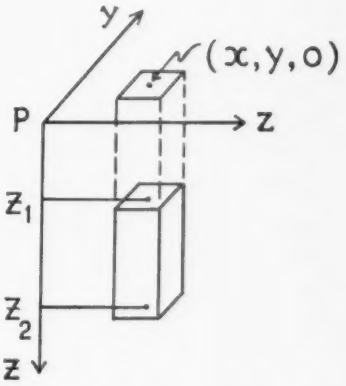

FIG. 1. An elementary prism.

enclosed by the depth contours of the gravitating body, one value of r and two values of z (the deeper value being usually constant for all dots) are read off from the template (properly positioned) and the contours re-

(*Figure 2 is on next page*)

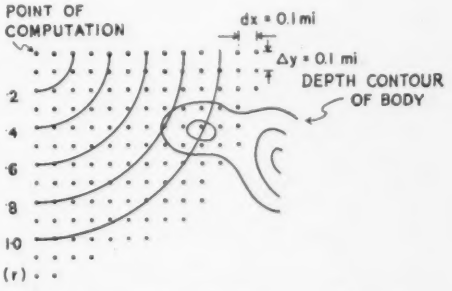

FIG. 3. Portion of computation template. To be drawn to the scale of available map with one dot for every $\Delta x \Delta y$. Circles are for different values of r (miles).

* Indian Institute of Technology, Kharagpur, India.

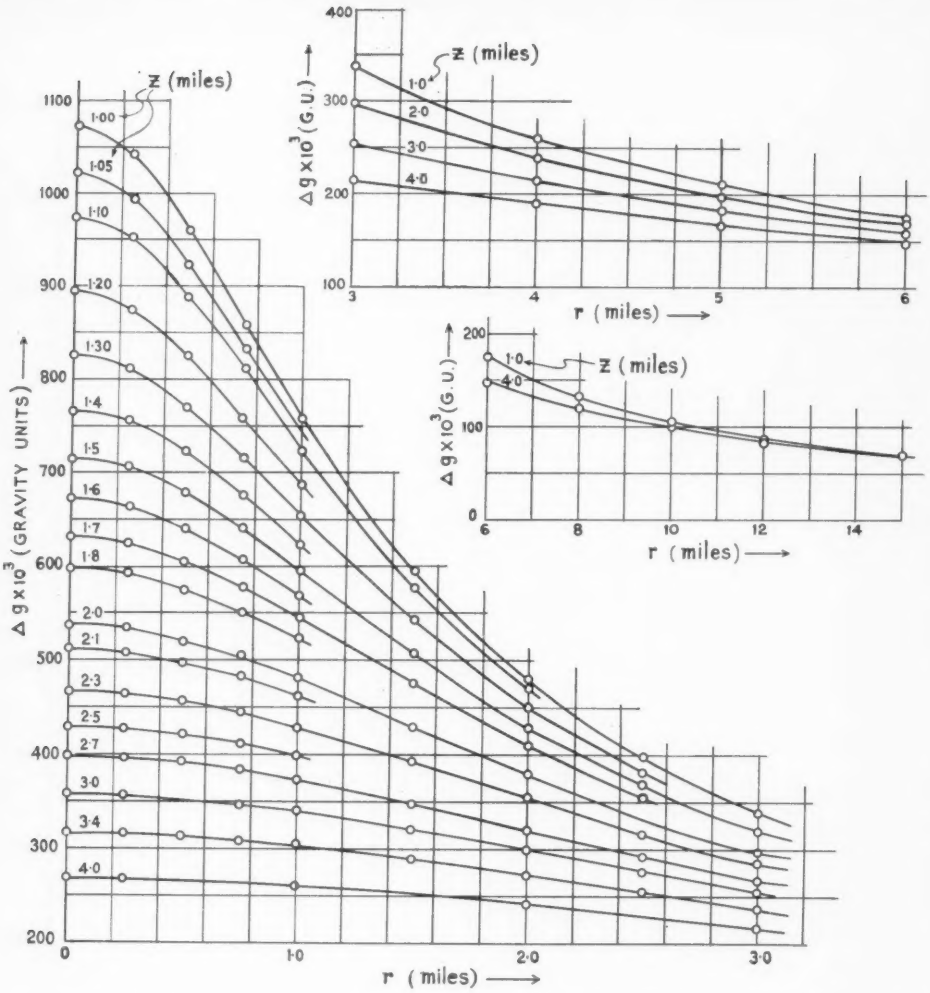

FIG. 2. Chart for rapid computation of gravitational anomalies. Gives the vertical component of attraction due to vertical columns of square cross-section (0.01 square mile). r is the horizontal distance of the prism from the point of computation and z is the depth of the prism top. The lower end extends to infinity.

spectively. Their gravitational contributions are determined from Figure 2, added and multiplied by the actual density contrast.

REFERENCES

Baranov, V., 1953, Sur le calcul de l'influence gravimetrique des structures defines par les isobathes: Geophysical Prospecting, v. 1, no. 1, p. 36–43.

Gassman, F., 1951, Graphical evaluation of anomalies of gravity and of magnetic field caused by three-dimensional bodies: Proc. Third Petr. World Congress (Section I), p. 613–623.

Goguel, J., 1961, Calcul de l'attraction d'un polygone horizontalede densit'e uniforme: Geophysical Prospecting, v. 9, n. 1, p. 116–127.

Levine, S., 1941, Calculation of gravity anomalies due to bodies of finite extent: Geophysics, v. 6, no. 2, p. 180–196.

Talwani, M., and Ewing, M., 1960, Rapid computation of gravitational attraction of three-dimensional bodies of arbitrary shape: Geophysics, v. 25, n. 1, p. 203–225.

VELA UNIFORM RESEARCH PROGRAM IN SEISMOLOGY*

Organization	*Nature of Project*
a. *Seismic Source Mechanisms*	
University of California (Berkeley)	Seismic Waves from small Earthquakes; Nature of Aftershocks (2 yrs)
St. Louis University	Shear Waves from Small Explosions (1 yr)
	Source Mechanism Using Other than *P* Waves (2 yrs)
Columbia University	Generating Mechanisms Using Intermediate and Long-Period Waves (2 yrs)
University of Michigan	High-frequency Noise in Wells (1,500 ft Depth) (1 yr)
United Electrodynamics	Variation of Seismic Noise and Signals with Geologic-Geographic Environment (6 mo)
St. Louis University	S-Wave Studies of Focal Mechanisms (1 yr)
Stanford Research Institute	Dynamic Properties of Rocks with Respect to Prediction of Stress Waves Produced by an Explosion in Earth (1 yr)
Sandia Corporation	Research and Analysis of Close-in Data (1 yr)
United Electro-Dynamics, Inc.	Field Study at the Variation in Characteristics of Seismic Noise & Signals with Geologic and Geographic Environment—Phase II (9 mo)
University of Oklahoma	Study of Absorption of Supersonic Elastic Waves in Solid Bodies and in Granular Media (2 yrs)
b. *Seismic Propagation Phenomena*	
California Institute of Technology	Transfer Functions Typical Crustal Structure (2 yrs)
California Institute of Technology	Inverse Transforms for Long-period Waves (2 yrs)
Penn State University	Model Studies of Radiation Patterns around Simulated Faulting and Exposive Sources (1 yr)
Weizmann Institute (Israel)	Research Project on Theoretical Seismology (1 yr)
California Research Corporation	Theoretical Study on the Determination of Depth of Source (2 yrs)
Columbia University	Support of Seismological Research (1 yr)
c. *Propagation Paths*	
U. S. Geological Survey	Western U. S. Crustal Structure by Refraction Shooting (1 yr)
St. Louis University	Phase Velocities Central U. S. (2 yrs)
California Institute of Technology	Phase Velocities Various Mtn. Regions (2 yrs)
Uppsals University (Sweden)	Seismic Investigation of Crustal Structure (1 yr)
U. S. Geological Survey	A Study of Seismic Propagation Paths and Regional Traveltimes in Calif-Nev Region (1 yr)
University of Alberta (Canada)	Seismological Study of the Crust in Western Canada (1½ yrs)
University of Witwatersrand (S. Africa)	Extended Programme of Crustal Structure Research (2 yrs)
d. *Seismic Signal Detection*	
Columbia University	Improved Long-period Detectors Discriminating Against 4–10 Sec. Microseisms
California Institute of Technology	Direct Digitizing Seismograph
	More Stable Long-Period Seismograph
Geotech Corporation	Improved General Purpose Seismographs
	Special Purpose Seismographs for Remote Operation or Rapid Deployment (1 yr)

* Refer to Geophysics, v. 26, n. 4, p. 504–505, Vela-Uniform, The Nation's Quest for Better Detection of Underground Nuclear Explosions, by Charles C. Bates.

Jersey Production Research Company	Distant Explosion Detection by Seismic Measurements in Deep Boreholes (6 mo)
Texas Instruments, Inc.	Design and Development of an Unattended Marine Seismic Monitoring and Recording System (6 mo)
Southeastern Industrial Electronics Company	Development of Improved Long-period Seismometer (6 mo)
Rensselaer Polytechnic Institute	Use of Shallow and Deep Wells for Earthquake and Explosion Detection (2 yrs)
Columbia University	Project to Measure the Motion of the Floor of the Deep Ocean in the Frequency Range of Seismic Waves (1 yr)
Electro-Mechanics Company	Electronic Seismograph Using Variable Electric Reactance Transducer (1 yr)

e. *Signal Analysis and Data Display*

University of California (La Jolla)	Characteristics Microseismic Noise and Ocean Bottom Signals (2 yrs) Methods for Distinguishing Seismic Signals in Noise (2 yrs)
University of Michigan	Spectrum and Attenuation of Waves from Small Earthquakes & Explosions (yr)
California Institute of Technology	Development Hi-Speed Digital Techniques (2 yrs)
Columbia University	Development Hi-Speed Computation Techniques (2 yrs)
Massachusetts Institute of Technology	Cross-correlation Techniques for First Motion of *P* waves (1 yr)
Texas Instruments, Inc.	Study and Development of Specific & Practical Method of Presenting Information Derived from an Array of Seismometers (Phase I, 6 mo)
Texas Instruments, Inc.	Digital Analysis of Project COWBOY Data (2 mo)
Texas Instruments, Inc.	Seismometer Array Data Processing Phase II and III (1 yr)
Armour Research Foundation	Discriminatory Analysis Applied to Classification of Seismic Phenomena
Bell Telephone Labs	Develop Data Analysis and Display Techniques for VELA UNIFORM Applications Using Research Type Hydroacoustic Data analysis equipment (1 yr)

CORRECTION

Corrections to "Theoretical Horizontal Resistivity Profiles Over Hemispherical Sinks," by Kenneth L. Cook and Russell L. Gray, GEOPHYSICS, v. 26, n. 3, p. 342–354; also published as special reprint, including complete album of curves, pages 1–48 (June, 1961).

	GEOPHYSICS Page no.	Special Reprint Page no.	Now reads	Should read
Second equation in equation set (3)	345	4	$\left(\frac{r}{r}\right)^n$	$\left(\frac{r}{r_0}\right)^n$
Caption to Figure 7	350	12	(b) 8*a* (c) 6*a*	(b) 6*a* (c) 8*a*
Distance from center of sink to traverse 3 in "Plan View" diagram in Figure 19	351	24	1.5	1.75

REVIEWS

REVIEWS COMMITTEE

CARL H. SAVIT, Chairman, Western Geophysical Company of America, Los Angeles, California
JAMES AFFLECK, Gulf Research & Development Company, Pittsburgh, Pennsylvania
WILLIAM L. BASHAM, Standard Oil Company of California, La Habra, California
F. G. BLAKE, California Research Corporation, La Habra, California
PIERRE L. GOUPILLAUD, Continental Oil Company, Ponca City, Oklahoma
ROLAND G. HENDERSON, U. S. Department of the Interior, Washington, D. C.
HYMAN KAUFMAN, McGill University, Montreal, Canada
NORMAN H. RICKER, The University of Oklahoma, Norman, Oklahoma
JOSHUA L. SOSKE, Stanford University, Stanford, California
S. H. WARD, University of California, Berkeley, California
ISIDORE ZIETZ, U. S. Department of the Interior, Geophysics Branch, Washington, D. C.

CONTENTS

The Rotation of the Earth, Walter H. Munk and Gordon J. F. MacDonald, By *Roland G. Henderson* 649
On Thermonuclear War, Herman Kahn, By *Carl H. Savit* 650
A Hole in the Bottom of the Sea, Willard Bascom, By *Carl H. Savit* 651
Submarine Exploration for Oil, A Symposium by Members of B. P. Exploration Co., Ltd., By *William L. Basham* 651
Classics in Science, Philosophical Library, By *Jennings G. Smith* 652

The Rotation of the Earth, Walter H. Munk and Gordon J. F. MacDonald, Cambridge University Press, London, 1960, xx+323 pp., $13.50.

This book is an enlightening account of the irregularities in the rotation of the Earth as indicated by variations in observations of latitude (wobble) and length of day (l.o.d.). Such irregularities are largely due to phenomena on and within the Earth and are used as an effective means of studying a number of geophysical problems. Although the purpose, modestly stated, is "to make this method of study readily accessible to geophysicists," the book achieves considerably more. The authors examine critically the present state of the study and challengingly point out areas of no progess and areas where the theory could be advantageously tidied.

The reading is facilitated by a first chapter preview of the entire book and an excellent summary at the close of each essentially non-mathematical chapter. After a qualitative discussion of wobble and length of day in Chapter 2, there follows in Chapters 3 through 6 the mathematical formulation for quantitative discussion. The tensor notation is used, but this poses no difficulty once one has familiarized himself with the index notation and the summation convention.

The irregularities in rotation are discussed in terms of solutions to a Liouville equation satisfying appropriate stress-strain relations. The stress-strain relations are simplified by the introduction of dimensionless Love numbers discussed in Chapter 5. For problems involving periods greater than one year, deviations from perfect elasticity must be accounted for. Anelastic deformation is discussed as well as a specific dissipation function $1/Q$ applicable to observational data without regard to the detailed mechanism for energy dissipation.

A perturbation scheme valid for all problems except polar wandering is used to reduce the Liouville equation to a simple form. The rotational parameters (direction cosines of the rotation axis and rotation rate) are expressed in terms of an "excitation function," the evaluation of which is the principal task of the book. Solutions are given for wobble due to various types of excitation functions. Included among the idealized illustrations, is the excitation function for the wobble induced by a hula dancer performing at the North Pole. In a footnote the authors, inspired by an obscure Jules Verne fiction, make a calculation which shows the drollery of an election campaign speech.

A historical sketch of the search for a predicted 10-month variation in latitude that was found to have a period of 14 months by Chandler, mentions prominently the roles of Kelvin and Newcomb. After a discussion of instruments, methods of observation and reduction, the main features of analyses of the observations of the International Latitude Service are summarized in a power spectrum showing an annual line and

a Chandler peak. The precision in length of day determinations is discussed in terms of the power spectrum of the errors involved in the various methods of measurement. The bulwark of the book's treatment of stationary time series is Tukey-type power spectra, the fundamentals of which are quite clearly presented in an appendix.

Seasonal and other short period variations in rotation are treated in Chapter 9. Annual variation in latitude is due to shifts in air mass; annual variation in length of day is due to winds. Semi-annual change in l.o.d. is apparently caused by the atmosphere and by tidal distortion, while monthly and forthnightly variations are caused by bodily tides.

The cause of the 14-month Chandler wobble is still a matter of speculation; however, the irregular variations in the atmosphere provide a possible mechanism. The Q of the Chandler band is poorly determined and the interpretation of the damping, apparently closed when Bondi and Gold referred it to the mantle, is considered an open problem in this book. Another "solved" problem likewise regarded by the authors as quite open is the dissipation of energy in tides.

After removal of the annual term and the Chandler wobble from latitude variations there is inconclusive evidence of polar drift in the residual. There is possibly a 10-ft displacement of the pole towards Greenland during the 20th century, but observations at Greenwich and Washington neither contradict nor support it.

Nontidal variations in length of day are characterized by a decrease in the last 2,000 years with large amplitude decade fluctuation superimposed. The authors are inclined towards the core as an explanation of the decade fluctuations in l.o.d. and find a faint hint in magnetic data that motions in the core are associated with the 20th century wiggle.

The authors consider use of paleomagnetic results to determine the ancient axis of rotation unreliable because the origin of the natural remanent magnetization in many rocks is unsolved; the stability of NRM under changing chemical and physical conditions is not understood, and magnetic reversals are enigmatic. Paleoclimatic and paleontological data offer little positive evidence in support of the kind of polar wandering suggested by paleomagnetic observations. Paleo-wind methods are even more tenuous than paleomagnetic and paleontological methods. If there must be continental drift and polar wandering, the authors, having misgivings about existing theories and methods, discuss some of the rules by which the game is to be played.

The book is unique in the literature in that it gives a unified account of the spectrum of both wobble and rotation rate. Although it touches many branches of geophysics, the book is well within the grasp of the unspecialized reader.

ROLAND G. HENDERSON
U. S. Geological Survey
Washington, D. C.

On Thermonuclear War, Herman Kahn, Princeton University Press, Princeton, 1961, xx+668 pp., $10.00.

No recent book has evoked more emotional objections than has *On Thermonuclear War*. While laudatory, or at least dispassionate, reviews have appeared, all too many are hysterical attacks typified by the three-page tirade by James R. Newman in the March 1961 issue of *Scientific American*. Newman professes to doubt the very existence of any such person as Herman Kahn, the book's author. Newman cannot bring himself to believe than any human could coldly and rationally discuss the possible conduct and results of an H-bomb war. Such objectors on emotional and compassionate grounds seem to imply, however, that if we ignore the problems of "The Bomb," they will go away.

Every thinking person must realize that if we, as members of the human race, are to survive, we must have some plan or set of alternative plans for coping with the very real menance of modern, thermonuclear war. Furthermore, if our plans are to have any meaning, they must be based on sober, thoughtful analysis, not on wishful thinking or emotional bias.

On Thermonuclear War examines many hypotheses concerning modern war threats together with the strategies and probable results arising from each situation. In particular, the concept that because thermonuclear war is too horrible to contemplate, it thus will not deliberately or even "accidentally" be initiated by either side is critically examined. This conclusion becomes invalid if only *one* of the two contestants disagrees with the premise. In other words, if only one side believes that war is too horrible to start, the other side can and probably will start if it has strong enough reasons.

A portion of the book is devoted to examining post-war conditions, recovery rates, and comparative economic status, based on various premises. It is, for example, shown that the United States could return to its present standard of living in 50 years in the face of the 80 million dead which would result from an all-out attack occurring now with no civil defense measures. On the other hand, the 40 million dead which might ensue if a bare minimum fallout-shelter program is added, would entail a recovery time of 20 years. If reasonable steps are taken to provide for evacuation in times of extreme tension or before making ultimatums, the casualties could be held to below 20 million and a 10-year recuperation period would suffice. Even under some of the most drastic situations mentioned above, if pre-war plans are made for recuperation, recuperation time can be greatly shortened.

Other considerations carefully examined by the author are those having to do with common concepts concerning international blackmail, ultimatums, Munich-type situations, etc. It is shown that the side which properly protects itself and which understands and can distinguish between post-war states will necessarily

be in a superior bargaining position in international crises. Some very astute comparisons between international bargaining and the juvenile-delinquent game of "chicken" are made. Various degrees or gradations can be shown to exist in this type of game as applied to international affairs.

Deterrence or "massive retaliation" as a national policy is the prime concern of the author throughout the bulk of the book. It is shown that it is necessary to distinguish among various types of deterrents as being applicable to a variety of situations. The ability to destroy or to inflict extreme damage upon the enemy may be a suitable deterrent against a direct attack. It is probably totally ineffective against minor provocations, particularly if an all-out attack on the enemy in retaliation for the minor provocation would bring on an all-out counter-retaliation against our own country by the enemy. Deterrence is carefully examined and subdivided into several major types, each of which requires its own military capability and war plan.

In a series of appendices Kahn proposes specific programs and lines of action. The body of the text prior to the appendices is thus devoted only to a discussion of the present and future situations and questions arising from various hypotheses. Whether or not one agrees with Kahn's recommendations, the questions he raises must be answered.

While this book is long and involved and perhaps ununduly repetitious, it is mandatory reading for every citizen of the free world. In addition, *On Thermonuclear War* furnishes invaluable background material for those geophysicists who are becoming involved in civil defense, nuclear detection, and allied fields.

CARL H. SAVIT
Western Geophysical Company of America
Los Angeles, California

A Hole in the Bottom of the Sea, Willard Bascom, Doubleday & Company, Inc., Garden City, New York, 1961, 352 pp., $4.95.

Willard Bascom is a dedicated man and, naturally, as Director of the Mohole Project, his interests are intimately tied up with that scientific deep drilling program. His involvement is, however, both older than the directorship and intensely personal. While the Mohole was first being seriously discussed, Bascom was participating in IGY activities in the South Seas. He returned just as a formal organization was about to be established. In his own words, " . . . on hearing what had happened while I was away . . . I vowed to become associated with the project somehow and before long was invited to become its part-time executive secretary."

Crusading zeal and scientific interests are not normally conducive to simple or lucid writing. Willard Bascom has nevertheless succeeded in producing a highly readable book that conveys the feelings of the visionary men who are fathering the Mohole. In clear, simple, authoritative prose, Bascom leads the reader through history, mythology, science-fiction, geology, geophysics, naval architecture, and deep drilling techniques.

Written for the "popular science" audience, *A Hole in the Bottom of the Sea*, cuts across diverse sciences and technologies in its broad scope. Experts in any field will find the discussions in their own field to be somewhat elementary but few people, perhaps only the Director of the Mohole Project, are experts in all the disciplines involved in that Project. As a result, anyone interested in man's quest for knowledge will read with fascination this account of knowledge and speculation concerning the earth's interior and methods to probe it.

Beginning with two introductory chapters which summarize the technical and administrative histories of the Mohole Project, the author covers in succession: fictional and pseudo-scientific theories, geologic evidence of the internal constitution of the earth, gravitational evidence, and seismic evidence. A chapter on oceanography is followed by chapters on "Magnetism, Heat, and Pressure" and one on the cosmological approach and theories concerning the planets and asteroids. Finally, there are six chapters on the selection of a drill site and on the techniques of drilling a hole, particularly from a ship.

Illustrated with photographs, drawings, and diagrams, *A Hole in the Bottom of the Sea* is required reading for all of us in the earth sciences particularly as we are, and increasingly will be, called upon by laymen and scientists of other disciplines to comment on the Mohole Project.

This reviewer feels free to commend Willard Bascom's book to readers of all shades of technical background as both the reviewer and his secretary read it with pleasure and profit.

CARL H. SAVIT
Western Geophysical Company of America
Los Angeles, California

Submarine Exploration for Oil, A Symposium by Members of B. P. Exploration Co., Ltd., *Journal of the Institute of Petroleum*, Vol. 45, No. 429, September 1959, pp. 263–286.

The *Journal* is printed in Great Britain. This article furnishes considerable historical detail for its short 23-page length.

1. *Introduction*, by C. V. Crostwaithe, describes offshore development originating in shallow water Lake Maracaibo in 1923. Peak offshore drilling occurred in Louisiana in 1957, with 100 deepwater units active to make 665 well completions. Thirty-nine percent of Louisiana

offshore rank wildcats have produced oil or gas compared to the U. S. onshore ratio of 11 percent. Offshore drilling is also discussed in Borneo, Trinidad, and particularly in the Persian Gulf which promises to rival the Gulf of Mexico as the world's most active offshore area.

2. *Geology*, by S. Elder, states that marine exploration originated in areas where submerged borders were an offshore continuation of proved oil provinces. Now, offshore extensions of areas are being explored where oil has not yet been found. The Continental Shelf, generally defined as extending to the 100 fathom line, has an area of approximately 10 million square miles and varies from one to 700 miles in width. Estimates of potential oil reserves on the Continental Shelf are given as 150 to 200 billion barrels.

3. *Geophysics*, by A. B. Malone, discusses in a general way the uses and history of the three main offshore geophysical prospecting tools, magnetic, gravimetric, and seismic. Mention is made of surface vessel and airborne gravity meters, the former is now operational with accuracy better than ± 5 mg, and the latter is being tested. Reflection seismograph outputs of 10 to 20 times those on land are achieved with costs per mile of about $\frac{1}{3}$ land costs. The problem of handling the large data output was mentioned together with the suggested solution of digital computers to speed up data processing. The Sonoprobe was discussed as a high-frequency (4,000 cps), shallow penetration seismograph. Subsequent to the article, the gas exploder, using signals of 50–100 cps to obtain penetration of several thousand feet under ideal conditions, has been developed.

4. *Drilling Barges*, by W. A. Roy, discusses the wide variety of designs available, ranging from self-contained platforms to drilling in very deep water from a surface vessel.

5. *Drilling*, by V. P. Baker, argues that the special offshore problems are how to spud in and how to keep the sea out of the well. Subsequent to the article, ocean bottom completions have been made off Peru, California, and Louisiana. A new method utilizing an ocean floor mast with its top 90 ft below the ocean surface is being used to drill a well off California at the present time.

6. *Testing*, by W. J. Baker, states that completion tests are difficult because many problems exist in locating testing gear and disposal of any oil produced. Safety is even more important than on land.

7. *Economics*, by C. V. Crostwaithe, points out that while offshore seismic monthly costs are higher than onshore, the per profile offshore is about one-third the onshore cost. Offshore gravity is considerably more costly than onshore, with a per station cost of about $100, compared to $17 onshore. Offshore drilling costs are about 4 times the onshore cost of a similar well. Offshore exploration is attractive in spite of higher exploration costs, because onshore areas have been so much more thoroughly explored, especially Continental U.S.A.

The articles will be of general interest to anyone concerned with offshore exploration.

William L. Basham
Standard Oil Company of California
La Habra, California

Classics in Science, a Course of Selected Reading by Authorities, Philosophical Library, Inc., New York, 1960, xxiii+322 pp., $6.00.

Classics in Science is a well-arranged collection of essays, lectures, etc., of historical significance and importance, covering writings of most of the masters from Pythagoras of Samos to Dr. J. Bronowski's delightful description of Dr. Einstein and his work.

The volume is arranged into four parts or "books," appropriately designated "The Origin and Meaning of Science," "The Universe," "Matter and Energy," and "Science and Everyday Life." The Introduction, by Professor E. M. da C. Andrade, followed by a series of "leading questions," affords a fitting prelude to the various essays, which are themselves sufficiently prefaced to lend a pleasant continuity to the whole.

Aside from its importance as a collection of historical writings, the book is composed of articles whose authors were well versed in that peculiar ability to present in quite simple terms many entirely new, and sometimes strange concepts.

A list of detailed biographical sketches is included at the end of the volume covering each author represented in the body of the text.

Jennings G. Smith
Western Geophysical Company of America
Los Angeles, California

PUBLICATIONS RECEIVED

BOOKS

Descriptive Palaeoclimatology, edited by A. E. M. Nairn, Interscience Publishers, New York, $11.00.

The Earth Today, edited by A. H. Cook and T. F. Gaskell, Oliver and Boyd, Edinburgh, 80s ($19.47).

Waves in Layered Media, Applied Mathematics and Mechanics: Vol. 6, by Leonid M. Brekhouskikh, Academic Press, New York, $16.00.

Mathematical Handbook for Scientists and Engineers, by Granino A. Korn and Theresa M. Korn, McGraw-Hill, New York, $20.00.

The Genesis Flood, by Henry M. Morris and John C. Whitcomb, Jr., The Presbyterian and Reformed Publishing Co., Philadelphia, Pa., $8.95.

Progress in Very High Pressure Research, editors: F. P. Bundy, W. R. Hibbard, Jr., and H. M. Strong, John Wiley and Sons, Inc., New York, $12.00.

Field Geology, 6th ed., Frederic H. Lahee, McGraw-Hill, New York, $10.75.

Physics of the Aurora and Airglow, Vol. 2, Joseph W. Chambelain, Academic Press, New York, $16.50.

PERIODICALS

American Journal of Science, v. 259, nos. 6 & 7 (June & Summer, 1961).

Boletin de la Associacion Mexicana de Geolgos Petroleros, v. 12, nos. 11 & 12 (Nov., & Dec., 1960).

Bulletin of the Seismological Society of America, v. 51, n. 2 (April, 1961).

Canadian Geophysical Bulletin, v. 13 (December, 1960).

I' U.G.G. Chronicle, nos. 35 & 36 (May & June, 1961).

Disaster Prevention Research Institute Bulletin, nos. 34–41 (June–Dec., 1960).

Deutsches Hydrographisches Institu Jarbuch, v. 11 (1957 & 1958).

Deutsche Hydrographische Zeitschrift, v. 13, n. 6 (1960).

Economic Geology, v. 56, nos. 3 & 4 (May–July, 1961).

Erdöl and Kohle, v. 14, nos. 5 & 6 (May & June, 1961).

Freiburger Forschungshefte, v. C88 (1960).

Gerlands Beiträge zur Geophysik, v. 70, n. 2 (1961).

Infrared Physics, v. 1, n. 1 (March, 1961).

The Journal of Earth Sciences Nagoya University, v. 8, n. 2 (December, 1960).

Journal of Geophysical Research, v. 66, nos. 6 & 7 (June & July, 1961).

Mines Magazine, v. LI, nos. 6 & 7 (June & July, 1961).

Mining Engineering, v. 13, nos. 5, 6, & 7 (May, June, & July, 1961).

Physics Today, v. 14, nos. 6 & 7 (June & July, 1961).

Quarterly Journal of the Geological Society of London, v. 117, Part 2, n. 466 (June, 1961).

The Science Reports of the Tohoku University, 5th Series, Geophysics, v. 12, nos. 1, 2, & Supplement (Dec. & March, 1961).

Seismische Registrierungen in Jena, Heft 64–1956 (1961).

Transactions American Geophysical Union, v. 42, n. 2 (June, 1961).

PATENTS

O. F. RITZMANN*

ELECTRICAL PROSPECTING

U. S. No. 2,973,811. A. S. Rogers. Iss. 3/7/61. App. 11/25/57. Assign. Phillips Petroleum Co.

Process for Detecting Underground Water. A system for detecting the dewatered zone after air is injected into a formation to displace water preparatory to an in-situ combustion project in which a surface electrical resistivity survey is made before the air is injected and subsequently repeated and the results compared.

U. S. No. 2,974,276. R. L. Davis. Iss. 3/7/61. App. 8/16/57. Assign. The Superior Oil Co.

Method of and Apparatus for Use in Measuring Earth Potentials. An earth potential surveying device having a wheel with an electrolyte-soaked rim connected to a buried pipeline through a self-balancing potentiometer whose indications are recorded on a chart moved in accordance with cable paid out.

See also Patent No. 2,974,273 listed under WELL LOGGING.

GRAVIMETRIC PROSPECTING

U. S. No. 2,977,799. L. J. B. LaCoste. Iss. 4/4/61. App. 9/23/55. Assign. LaCoste & Romberg.

Force Measuring Apparatus. A gravity meter for use on a submarine having a horizontal pendulum on a horizontal axis with an adjustable zero-length supporting spring whose adjustment is digitalized and recorded, the pendulum being heavily overdamped and having a photoelectric position indicator, the recorder also indicating the time between zero transits of the beam so that a gravity value can be computed from the integrated torque applied to the pendulum during its swing.

U. S. No. 2,978,906. F. Haalck. Iss. 4/11/61. App. 4/2/58 and 4/14/58. Assign. Askania-Werke A.G.

Gravimeters. A gravity meter having a mass on a spring and with the indicating light beam reflected from two pendulously mounted prisms so as to effect tilt compensation.

See also Patent Nos. 2,976,378; 2,976,733; 2,976,734; 2,979,959; and 2,979,960 listed under MISCELLANEOUS.

* Gulf Oil Corporation, Patent Department

MAGNETIC PROSPECTING

U. S. No. 2,974,277. D. A. Wales. Iss. 3/7/61. App. 12/16/58. Assign. Maico Electronics, Inc.

Magnetic Field Sensing Device. A magnetic detector having a closed oblong loop of low reluctance material with coils wound on opposite legs of the loop connected in parallel to an oscillator through rectifiers so that one half-wave energizes one coil and the alternate half-wave energizes the other coil to produce flux in the same direction in the core, and with unbalance in the waves detected.

U. S. No. 2,975,360. W. E. Bell. Iss. 3/14/61. App. 7/5/56. Assign. Varian Associates.

Magnetoabsorption Flux Meter and Gradiometer. A magnetometer having a high-permeability core in a coil excited at *r-f* whose absorption is observed while current in auxiliary coils apply a sweep field to the core, current in a buck-out coil being used to neutralize the ambient field and the buck-out current measured when the core shows zero-field conditions.

U. S. No. 2,976,483. W. H. Moore and D. P. Burcham. Iss. 3/21/61. App. 11/30/56. Assign. U.S.A.

Gradiometer for Underwater Missile Warhead. A magnetic gradiometer having a rod of high-permeability material wound with coils at each end and with the coils connected in series opposition and shunted by a capacitor to tune the system to a low frequency.

U. S. No. 2,981,885. E. O. Schonstedt. Iss. 4/25/61. App. 7/21/58.

Saturable Measuring Device and Magnetic Core Therefor. A flux-valve core having a ceramic tube on which two thin ribbons of high permeability alloy are helically wound in opposite directions, excitation being produced by a toroidally wound exciting coil and second harmonic picked up by a coil wound coaxially with the ceramic tube.

RADIOACTIVITY PROSPECTING

U. S. No. 2,974,247. N. Anton. Iss. 3/7/61. App. 8/4/55.

Geiger-Mueller Counter Tube. A cylindrical Geiger-Mueller tube having a cylindrical cathode with coaxial anode supports at each end, and a central anode wire fastened at one of the end supports and held under tension by an enlargement centering in a small opening in the other end support through which the tube is evacuated.

U. S. No. 2,974,248. J. A. Auxier, G. S. Hurst, and R. E. Zedler. Iss. 3/7/61. App. 9/10/57. Assign. U.S.A.

Neutron-Insensitive Beta-Gamma Dosimeter. A counter for measuring beta and gamma radiation in the presence of fast neutrons having an inner cylinder of wall thickness greater than the range of secondary electrons and containing a gas at low pressure, the dimensions of the cylinder being smaller than one-tenth of the mean free path of ionization for primary electrons of 30,000 volts, and having a conductive layer on the cylinder and an inner electrode.

U. S. No. 2,975,287. P. E. Ohmart. Iss. 3/14/61. App. 3/23/56. Assign. The Ohmart Corp.

Low Noise Level Ionization Chamber. An ionization chamber in which the applied potential is such that the ion collection efficiency is less than 85 percent and less than the potential at which gas multiplication occurs in order to reduce current fluctuations.

U. S. No. 2,975,288. W. Minowitz and J. F. Grimm. Iss. 3/14/61. App. 3/11/58. Assign. Tung-Sol Electric Inc.

Ion Chamber and Circuit Therefor. An ionization chamber having a sealed conducting envelope as one electrode and a series of concentric discs of different sizes with separate leads selectively employed as the other electrode, the envelope also containing a constant-current diode for calibrating the external circuit.

U. S. No. No. 2,976,443. L. E. Johnson. Iss. 3/21/61. App. 11/22/57.

High Sensitivity Ionization Chamber. A neutron detector for use at high temperature having two concentric chambers, the inner one containing $B^{10}F_3$ gas and the outer one containing nitrogen to provide pressure balance and protection against oxidation.

U. S. No. 2,976,445. R. P. Mazzagatti. Iss. 3/21/61. App. 6/24/54 and 12/15/58. Assign. Texaco Inc.

Radiation Detector. A radioactivity detector of the gas-amplification pulse-producing type for use at high temperature whose housing is constructed of welded stainless steel type No. 304.

U. S. No. 2,979,617. A. Somerville. Iss. 4/11/61. App. 11/29/57. Assign. General Motors Corp.

Scintillation Detector Circuit. A radioactivity detector having a scintillating crystal and photomultiplier energized by a low frequency a-c and with a condenser and a-c amplifier connected across the cathode load, the midband frequency of the amplifier corresponding to the energizing frequency.

U. S. No. 2,979,619. J. Bosch. Iss. 4/11/61. App. 12/7/54 and 12/6/55. Assign. Frieseke and Hoepfner, G.m.b.H.

Ionization Chamber Circuitry with Temperature Compensation. A radioactivity thickness gauge in which the ionization chamber is in series with a resistor having a negative temperature coefficient of resistance which corrects for the effect of temperature variation of the air intervening between the ionization chamber and the specimen being tested.

See also Patent Nos. 2,974,303; 2,978,585; and 2,979,618 listed under WELL LOGGING.

SEISMIC PROSPECTING

U. S. No. 2,973,739. N. N. Estes. Iss. 3/7/61. App. 10/6/49.

Underwater Transducer. An underwater sound source having a pair of flat triangular sheets of rubber whose edges are clamped together along two sides of the triangle with a mixture of steam and air introduced between the sheets at the apex.

U. S. No. 2,974,743. R. B. Rice. Iss./3/14/61. App. 9/15/53. Assign. Phillips Petroleum Co.

Method of Seismic Prospecting. A method of seismic shooting where there is a high-velocity layer close to the surface and in which a shot hole is drilled to below the high-velocity layer and the shot is fired at a depth of about one-fourth wave length in the material below the high-velocity layer.

U. S. No. 2,975,398. A. E. Melhose. Iss. 3/14/61. App. 5/5/51. Assign. Bell Telephone Laboratories, Inc.

Hydrophone. A hydrophone having two diaphragms one of which is fastened to one end of a frictionally mounted rod that moves when static pressure deflects the diaphragm, the rod also carrying a transducer element whose movable element is connected by a light linkage to the second diaphragm.

U. S. No. 2,975,399. K. N. Burns. Iss. 3/14/61. App. 4/8/58. Assign. Jersey Production Research Co.

System for Processing Seismic Data. A seismogram reading apparatus employing on synchronized drums a visual record on which reflected events are marked with electrically conducting ink and a reproducible record that is played back, the marked record controlling a gate circuit that passes only play-back signals near the

marked time, with the time of the gated signals printed out on paper tape.

U. S. No. 2,976,106. R. G. Piety. Iss. 3/21/61. App. 1/23/56. Assign. Phillips Petroleum Co.

Seismic Signal Recording Apparatus. A system for removing step-out of events in seismic recording by employing two galvanometers for each light beam with their axes at right angles, one galvanometer being used for the seismic signal in the usual way and the other galvanometer carrying a time-varying direct current that deflects the beam longitudinally of the trace to compensate for step-out.

U. S. No. 2,976,107. W. W. Klein, Jr. and A. E. Tilley. Iss. 3/21/61. App. 4/3/57. Assign. California Research Corp.

Seismic Section Plotter. Apparatus for making a seismic section from reproducible records in which the record is placed on a rotating drum and the play-back signals fed to galvanometers on a carriage that moves downward on the section being plotted, with motion of the carriage synchronized with rotation of the drum by means of a servo system that counts timing lines on the record.

U. S. No. 2,976,108. J. F. Johnson. Iss. 3/21/61. App. 2/20/59. Assign. Sinclair Oil & Gas Co.

Portable Oscillograph. A recorder for making seismic record sections having a drum on the inside of which a sheet of photographic recording paper is placed and having an axial mount for a bank of oscillographs that can be moved axially for recording the respective seismograms, the drum being rotated by a motor geared to the drum.

U. S. No. 2,977,571. B. Bernstein and J. Chervenak. Iss. 3/28/61. App. 3/26/52.

Split Ring Electroacoustic Transducer. A high-frequency electroacoustic transducer having a C-shaped core with a small air gap and an extension on the core opposite the air gap so that when excited the core vibrates as a short tuning fork.

U. S. No. 2,977,572. T. J. Pope. Iss. 3/28/61. App. 12/12/51. Assign. Bell Telephone Laboratories, Inc.

Hydrophone. An electrostrictive transducer having a a stack of barium titanate rings in a cylindrical housing with a spring holding an end diaphragm against the stack of rings.

U. S. No. 2,977,573. E. E. Mott. Iss. 3/28/61. App. 12/30/52. Assign. Bell Telephone Laboratories, Inc.

Pressure Compensated Underwater Transducer. A fluid filled underwater sound source having a domed sound-transparent outer diaphragm with a weakened edge portion so that the diaphragm can assume an annular re-entrant shape when subjected to static pressure, and having an electromagnetic transducer with an inner domed diaphragm, the inner chamber having an annular air-filled rubber tube to permit pressure equalization.

U. S. No. 2,978,673. R. H. Graham. Iss. 4/4/61. App. 2/21/55. Assign. Jersey Production Research Co.

Seismic Surveying Method and System. A system for analyzing a seismic signal in which a pulse generator produces a pulse each time the geophone signal crosses the zero-signal axis, and the pulses are fed into a frequency meter whose output indication is recorded, with a constant relatively-high frequency indicating presence of a reflection.

U. S. No. 2,979, 692. W. W. Grannemann and G. A. W. Trorey. Iss. 4/11/61. App. 12/16/55. Assign. California Research Corp.

Elimination of Multiple Frequency Components in Seismic Records. A system for eliminating multiple frequency ringing by filtering the signal through narrow band-pass filters each with a long time-constant avc, generating auxiliary signals of the same frequency as the filter pass band, and combining the auxiliary signals with the filtered signal to cancel the ringing frequencies.

U. S. No. 2,980,042. B. McCollum. Iss. 4/18/61. App. 2/21/57.

Method for Planting Seismic Detectors. A method of detector planting using a machine that lays the cable with a little slack and at each detector location digs a trench into which the detectors are placed and covered with tamped earth.

U. S. No. 2,980,884. R. A. Kaasa. Iss. 4/18/61. App. 11/1/57. Assign. Geophysical Specialties Co.

Apparatus for Measuring the Time Between Seismic Events with a Counter. A seismic travel time counter having a crystal-controlled oscillator that feeds pulses to a counter through two gate circuits the first of which is opened by a signal from a hammer blow or by a seismic signal arrival at a first detector and the second controlled by a seismic signal arrival at a second detector.

U. S. No. 2,980,885. D. D. Mize, P. C. Sundt, and M. A. Drews. Iss. 4/18/61. App. 11/25/57. Assign. Mandrel Industries, Inc.

Seismic Recording and Playback Apparatus. A seismograph re-recording apparatus having a flat bed support for the recording medium and in which the dynamic corrections are made by cams moving the playback heads and with the cam shaft driven by a spring with its speed controlled by a worm-geared synchronous motor.

U. S. No. 2,981,357. W. B. Huckabay and C. D. McClure. Iss. 4/25/61. App. 2/1/55. Assign. Socony Mobil Oil Co., Inc.

Submerged Strata Acoustic Probe System. A subbottom acoustic exploration system using a magnetostrictive transducer immersed in an impedance-matching fluid and an electrostatic recorder whose drum is synchronized with a single cycle impulse in the transducer, and having a time-controlled logarithmic gain variation.

U. S. No. 2,981,358. R. G. Piety and R. S. Marsden, Jr. Iss. 4/25/61. App. 11/16/55. Assign. Phillips Petroleum Co.

Signal Generator. A seismograph gain control system in which the gain is controlled as a desired function of time by using a glow transfer tube with a plurality of cathodes connected to potentiometers that control the seismograph gain, and transferring the glow discharge to successive cathodes in a programmed sequence.

U. S. No. 2,981,927. V. G. McKenney. Iss. 4/25/61. App. 4/4/46. Assign. U.S.A.

Underwater Sound Transmitter. An underwater noise transmitter having a disc recorder that continuously records received noise and when a sound exceeds a preset threshold, the reproducer is connected to an amplifier and transducer to re-transmit the previously recorded noise.

U. S. No. 2,981 928. J. M. Crawford and W. E. N. Doty. Iss. 4/25/61. App. 10/20/54. Assign. Continental Oil Co.

Method for Eliminating Undesired Components of Composite Received Signals. A system for reducing the effect of an interfering wave in a varying frequency continous signal seismic system by using two detectors whose outputs are combined in opposition or using two generators having half wave length spacing for the undesired component.

WELL LOGGING

U. S. No. 2,973,583. D. E. Stolle and N. O. Cross. Iss. 3/7/61. App. 9/12/58. Assign. Standard-Vacuum Oil Co. and Esso Research and Engineering Co.

Tube Calipering Device. A calipering device having feelers that emerge from slots in the body of the apparatus to contact the hole wall and whose inner ends engage a plunger that moves the slider of a rheostat whose resistance is measured and indicated.

U. S. No. 2,974,273. C. B. Vogel and D. Weiser. Iss. 3/7/61. Appl. 1/28/57. Assign. Shell Oil Co.

Method and Apparatus for Investigating Earth Formations. A permeability logging method and apparatus in which a section of borehole wall is irradiated with high-frequency sound waves by means of an electrically insulated sound generator, with the sound passing through an electrically insulated sound-transparent grid and the flow potential measured after the mud cake has been dispersed by the sound waves.

U. S. No. 2,974,303. D. R. Dixon. Iss. 3/7/61. App. 2/8/57. Assign. Schlumberger Well Surveying Corp.

Electrical Systems for Borehole Apparatus. A single-conductor radioactivity logging system in which d-c is supplied over the conductor to a Geiger-Mueller tube and amplifier in the sonde, and the output of the amplifier is transformer-coupled to the conductor and the signal separated at the surface by a high-pass filter and counting-rate meter and recorded.

U. S. No. 2,974,523. A. Z. Bendar. Iss. 3/14/61. App. 11/12/53. Assign. Star Recorder Corp.

Depth and Operation Recorder for Earth Bore Drilling Rigs. A drilling rate recorder having two pens one of which records penetration and the other records rig operations, the penetration pen being engaged by a clutch and marking the record at each foot drilled.

U. S. No. 2,977,680. D. U. Halverson. Iss. 4/4/61. App. 7/11/57. Assign. Texaco Inc.

Apparatus for Use in Correlating Oil Well Logs. A device having a number of parallel slideable strips on which well logs may be mounted, the strips being longitudinally adjusted with respect to each other and marker horizons being identified by pins that are connected with elastic thread.

U. S. No. 2,977,792. C. N. Simm. Iss. 4/4/61. App. 6/21/57. Assign. California Research Corp.

Method for Detecting Fluid Flow in or Near a Well Bore. A well flow detecting system in which a pyrotechnic source of heat is ignited in the well and the resulting temperature distribution above and below the heat source observed with a thermister-type thermal logging device, flow of well fluid producing an asymmetric temperature distribution at successive times.

U. S. No. 2,978,585. W. R. Rabson. Iss. 4/4/61. App. 5/2/55 and 3/13/58. Assign. PGAC Development Co.

Neutron Calibration Method and Apparatus. A calibration device for a neutron logging sonde having a cylinder of neutron-attenuating material into which the sonde is placed so that its indication can be adjusted to a standard value, and a hollow annular container that may be placed between the sonde and the absorbing material and filled with fluids to simulate the effect of well fluid

U. S. No. 2,978,634. J. J. Arps. Iss. 4/4/61. App. 8/31/50, 1/17/57, and 4/2/57.

Apparatus for Logging Wells. A detector for picking up acoustic signals in the drilling fluids when logging while drilling, the detector having two pressure-equalized chambers separated by a diaphragm whose motion is detected by an electromagnetic transducer.

U. S. No. 2,979,618. J. A. Rickard. Iss. 4/11/61. App. 12/7/56. Assign. Jersey Production Research Co.

Helium 3 Logging Method. A neutron logging system using neutron spectroscopy and having a source of neutrons and a proportional counter type of neutron detector containing He^3 in which induced fast neutrons produce protons and tritons whose effect over a selected energy range is detected by a discriminator and recorded.

U. S. No. 2,980,486. J. O. Melton. Iss. 4/18/61. App. 4/5/56. Assign. The Geolograph Co.

Recorder. A drilling rate recorder having a manually operated clutch which engages the recorder pen with a shaft to record drilling rate and when disengaged returns the pen to zero, and also having a second pen that records the derrick load.

U. S. No. 2,981,102. J. O. Melton. Iss. 4/25/61. App. 3/23/56. Assign. The Geolograph Co.

Well Depth Recorder. A drilling rate recorder in which the chart is advanced by a Geneva movement with each unit of depth drilled and deflections of the recording pen are proportional to the length of time required to drill each unit.

MISCELLANEOUS

U. S. No. 2,974,318. B. W. Koeppel. Iss. 3/7/61. App. 10/16/56. Assign. Seismograph Service Corp.

Radio Location System. A hyperbolic c-w phase comparison type of radio location system using three transmitting stations each of which heterodynes the other two to obtain a reference signal.

U. S. No. 2,974,629. J. A. Rickard. Iss. 3/14/61. App. 12/10/58. Assign. Jersey Production Research Co.

Alarm for Detection of Pressure Surges in a Borehole. A device for indicating excessive acceleration of drill pipe in a well having a cable from the traveling block to a pulley that monitors pipe movement and has a mass mounted on a radial elastic arm, the mass normally being centered between two gongs but striking one of the gongs upon excessive rotational acceleration.

U. S. No. 2,974,739. C. A. Dean. Iss. 3/14/61. App. 3/31/58. Assign. G. C. Dean.

Core Orienting Apparatus. A wire line core barrel in which a record of the core orientation is made by firing a bullet into the bottom of the hole prior to cutting the core and the orientation of the gun and core barrel is recorded and the record recovered with the core.

U. S. No. 2,975,361. C. E. Holaday. Iss. 3/14/61. App. 3/5/58. Dedicated to the Public.

Apparatus for Determining the Moisture Content of Granular and Fibrous Material. A moisture testing device having a cup-shaped container for the material and a plunger hydraulically pressed into the cup, the plunger having a central pointed electrode with a flat coaxial insulated annular collar, the resistance through the material between the point and the collar being measured.

U. S. No. 2,975,397. H. E. Edgerton. Iss. 3/14/61. App. 6/6/55. Assign. Edgerton Germeshausen & Grier, Inc.

Surface-Indicating Apparatus. An underwater exploration device having a camera with a flash illumination device and an acoustic transmitter with a switch suspended below the assembly so that when the switch reaches bottom, the switch turns off the transmitter to signal the operator that the assembly is in proper position to photograph the water bottom.

U. S. No. 2,975,417. B. Alexander, M. Rogoff, and M. C. Vosburg. Iss. 3/14/61. App. 6/27/57. Assign. International Telephone and Telegraph Corp.

Long Range Radio Navigation System. A radio position determining system using three spaced transmitters operating at different frequencies and the mobile craft having three separate receivers whose local oscillators are slaved to the received signals so that hyperbolic bearing loci can be determined, and with the transmitters operating on a time schedule so that differential distances can also be determined.

U. S. No. 2,976,378. R. W. Goddard. Iss. 3/21/61. App. 6/3/58. Assign. Lockheed Aircraft Corp.

Acceleration Responsive Devices. An acceleration switch having a magnet suspended on a spring and immersed in damping fluid in a case with external magnetic reeds that close electric contacts when the magnet approaches and deflects the reed.

U. S. No. 2,976,733. B. Litman, M. Pavalow, P. H. Savet, and J. Statsinger. Iss. 3/28/61. App. 4/29/55. Assign. American Bosch Arma Corp.

Accelerometer. A servo accelerometer operating in two directions and having a magnetic system with perpendicular axes and a pendulously supported armature, part of the magnetic system being used to detect displacement of the armature and provide a signal to an operational amplifier whose output is fed to coils on another part of the system to set up counterforces that hold the armature in place.

U. S. No. 2,976,734. P. Gindes and A. C. Hughes, Jr. Iss. 3/28/61. App. 12/18/57. Assign. Genisco, Inc.

Accelerometer. An accelerometer having a mass supported on E-shaped springs with a circular enlargement at the base of the E slots and with the metal dimpled to prevent cracking.

U. S. No. 2,979,134. E. E. Reed and C. T. Brandt. Iss. 4/11/61. App. 5/20/55. Assign. Phillips Petroleum Co.

Core Hole Testing Apparatus. A core hole testing device having spaced upper and lower inflatable packers and a conduit to supply fluid under pressure, and also a conduit to the space between the packers and a conduit to the hold space below the lower packer so that samples of formation fluid can be obtained and permeability tests made through the conduits.

U. S. No. 2,979,955. P. R. Shepler. Iss. 4/18/61. App. 4/12/57. Assign. Schlumberger Well Surveying Corp.

Pressure Responsive Systems. A differential pressure guage having two sets of bellows connected to the two pressure points with the pressure inside each bellows applied to the outside of the other and the deflection of the bellows detected by strain guages in a bridge circuit.

U. S. No. 2,979,959. S. P. Clurman. Iss. 4/18/61. App. 6/3/59.

Magnetic Accelerometer. An accelerometer having a steel ball free to roll in a concave recess so that acceleration displaces the ball from the center of the concavity and with motion of the ball detected by a magnetic circuit from under the ball to two opposing pole pieces having coils in an indicating circuit.

U. S. No. 2,979,960. G. W. Johnson. Iss. 4/18/61. App. 6/16/58. Assign. International Business Machines Corp.

Acceleration Measuring Means. An oscillating pendulum accelerometer in which pendulum displacements are detected and actuate a torque-producing means on the pendulum axis to effect an opposing displacement, the average torque-producing current being a measure of the linear acceleration normal to the plane of the pendulum and its axis.

U. S. No. 2,981,221. J. Gillois and H. W. Gehlen. Iss. 4/25/61. App. 6/4/56 and 6/3/57. Assign. Dipl. Ing. H. W. Gehlen.

Self Propelled Amphibious Vehicles. An amphibious vehicle whose body has a broad platform with a hinged loading ramp and has sealed housings for retractable wheels and inflatable pontoons on each side of the body.

SELECTED LIST OF U. S. PATENTS ISSUED DURING MARCH AND APRIL OF 1961

Patent No.	*Subject**	*Patent No.*	*Subject**	*Patent No.*	*Subject**
2,973,583[a]	44	2,974,296	484	2,975,017	368
2,973,585	180	2,974,303[a]	516	2,975,046	136
2,973,641	428	2,974,317	316	2,975,236	224
2,973,643	16	2,974,318[a]	312	2,975,238–242	224
2,973,647	4	2,974,368	324	2,975,243	484
2,973,649–651	16	2,974,521	492	2,975,277–279	236
2,973,662	68	2,974,523[a]	100	2,975,280	196
2,973,739[a]	436, 484	2,974,525	148	2,975,281	308
2,973,811[a]	124	2,974,526	200	2,975,283	196
2,973,897	68	2,974,529	4, 68	2,975,284	16, 196
2,973,919	40	2,974,531–532	4	2,975,286	308
2,974,056	224	2,974,536	76, 380	2,975,287[a]	308
2,974,202–204	484	2,974,589	48	2,975,288[a]	308
2,974,231–232	308	2,974,590	196	2,975,360[a]	232
2,974,247[a]	308	2,974,629[a]	528	2,975,361[a]	88
2,974,248[a]	308	2,974,727	48	2,975,369–370	68
2,974,254	68	2,974,739[a]	84	2,975,397[a]	108, 280
2,974,256	416	2,974,743[a]	360	2,975,398[a]	436, 492
2,974,273[a]	8, 276	2,974,868	68	2,975,399[a]	352
2,974,276[a]	124	2,974,891–892	224	2,975,409	68
2,974,277[a]	232	2,974,960–961	484	2,975,411	68

* A key to the subject classification system will be found in GEOPHYSICS, v. 12, pp. 256–264 (April, 1947).

[a] Abstracted on preceding pages of this issue.

Patent No.	*Subject**
2,975,413	16, 312
2,975,414	316
2,975,416	316
2,975,417[a]	312
2,975,418	316
2,975,634–635	148
2,975,638	188
2,975,641	4
2,975,669	416
2,975,672	224
2,975,765	148
2,975,972	68
2,976,102–103	324
2,976,106[a]	364
2,976,107[a]	352
2,976,108[a]	160, 352, 364
2,976,109	324
2,976,354	224, 324
2,976,371	324
2,976,372	224
2,976,373	484
2,976,378[a]	4
2,976,413	236
2,976,414	196
2,976,418	308
2,976,419	196
2,976,420–423	308
2,976,430	68
2,976,433	308
2,976,434	484
2,976,442	308
2,976,443[a]	308
2,976,445[a]	308
2,976,483[a]	232
2,976,506	288
2,976,525	68
2,976,528	68
2,976,529	316
Re.24,956	224
2,976,618	16
2,976,721	492
2,976,722	188
2,976,727	200
2,976,728	188
2,976,731	288
2,976,732	492
2,976,733[a]	4
2,976,734[a]	4
2,976,763	200
2,976,765	224
2,976,865	428
2,976,940	392
2,977,046	148
2,977,070–071	16
2,977,177	16, 324
2,977,423–425	484
2,977,462	68
2,977,470–471	236
2,977,472	324
2,977,473–474	168, 308
2,977,477	196
2,977,478	308
2,977,480	484
2,977,495	236
2,977,534	68
2,977,544	68
2,977,568	316
2,977,569	484
2,977,571[a]	436, 484
2,977,572[a]	436, 484
2,977,573[a]	436, 484
2,977,579	224
2,977,582	68
2,977,586	16
2,977,587–589	316
2,977,592	316
2,977,680[a]	520
2,977,752	16
2,977,790	496
2,977,791	288
2,977,792[a]	148
2,977,794–796	148
2,977,799[a]	180
2,977,804	16, 444
2,977,806	16
2,977,878	136
2,977,925	308
2,977,990	288
2,978,102	188
2,978,174	308
2,978,175	68
2,978,177–180	68
2,978,198	224
2,978,210	16
2,978,287	324
2,978,414	224
2,978,543	484
2,978,545–546	224
2,978,581	308
2,978,583	308
2,978,585[a]	304
2,978,586–587	308
2,978,602	308
2,978,634[a]	208
2,978,636–637	140
2,978,668	108
2,978,669–672	436, 484
2,978,637[a]	360
2,978,674	16
2,978,688	484
2,978,691	200
2,978,693	68
2,978,701	312
2,978,816	68
2,978,899	12
2,978,901–902	428
2,978,906[a]	180
2,978,909	412
2,978,910	180
2,978,912–913	16
2,978,945	484
2,978,947	136
2,978,954	444
2,978,956	196
2,978,968	324
2,978,977	324
2,979,006	16
2,979,134[a]	276
2,979,256	16, 68
2,979,257	68
2,979,261–263	68
2,979,277	224
2,979,289–290	16
2,979,382	196
2,979,467	196
2,979,557–558	224
2,979,562	224
2,979,572	224
2,979,582	4
2,979,617[a]	308
2,979,618[a]	304
2,979,619[a]	308
2,979,620	308
2,979,654–655	228
2,979,656	140
2,979,657	324
2,979,680	288
2,979,681	68
2,979,690	436, 484
2,979,691	288, 484
2,979,692[a]	352
2,979,708	68
2,979,713–715	316
2,979,718	316
2,979,807	428
2,979,821	316
2,979,940	12
2,979,948	148
2,979,949	200
2,979,950	188
2,979,952	460
2,979,955[a]	288
2,979,959[a]	4
2,979,960[a]	4
2,980,017–018	48

Patent No.	*Subject**
2,980,019	136
2,980,042[a]	360
2,980,069	68
2,980,126	68
2,980,330	68
2,980,332	68
2,980,486[a]	100
2,980,513	168
2,980,768	224
2,980,798	416
2,980,799	308
2,980,811	484
2,980,812	428
2,980,850	228
2,980,860	228
2,980,871	68
2,980,884[a]	360
2,980,885[a]	360, 364
2,980,895	16
2,980,899	68
2,980,902	16
2,980,905–906	316
2,980,907	312
2,981,096	12
2,981,100–101	428
2,981,102[a]	100
2,981,104	148
2,981,105	200
2,981,111	412
2,981,113	16
2,981,147	444
2,981,185	48
2,981,186	136
2,981,221[a]	490
2,981,240	148
2,981,357[a]	108, 360
2,981,358[a]	360, 372
2,981,470	68
2,981,472–473	68
2,981,587	324
2,981,805	224
2,981,839	236
2,981,841	200
2,981,844	68
2,981,885[a]	232
2,981,905	12
2,981,909	484
2,981,911	288
2,981,912	484
2,981,913	196
2,981,927[a]	8, 360, 436
2,981,928[a]	360
2,981,942–943	316
2,981,944	312

CONTRIBUTORS

IRA H. CRAM, JR.

IRA H. CRAM, JR., received a B.S. in Mathematics from Beloit College in 1952 and a Ph.D. in Geology from Rice in 1961.

He served as a Field Artillery Officer in the U. S. Army from 1952–1954. From 1954 to 1957 he was employed by Western Geophysical Co. He is now Senior Research Geophysicist for The Pure Oil Co. Research Center.

Mr. Cram is a member of the SEG, AGU, Seismological Society of America, Houston Geophysical Society, Houston Geological Society, Sigma Xi, and Sigma Gamma Epsilon.

FRED HEFER

FRED HEFER attended Staatliche Ingenieurschule, Cologne, Germany and received a M.S. in E.E. in 1947. He was a technician in the German Air Force, and is now a U. S. Citizen. Mr. Hefer holds several patents on amplifier circuits. He was part owner of the Engineering Bureau in Bonn, Germany, doing consulting and design on amplifiers, filters, and tape recording equipment. He was manager of the Electronics Division for Electrodynamic Instrument Corp., and worked as design engineer for SIE Research and Development, designing auxiliary geophysical equipment. He is now SIE Division Engineer and Manager of Geophysical Systems Engineering.

LOUIS B. MCMANIS

LOUIS B. MCMANIS, Marketing Manager, Geophysical Division of Dresser Electronics, SIE Division, received his B.S. in E.E. from Kansas State College and his M.S. in E.E. from Oklahoma A & M College. While employed by Halliburton Oil Well Cementing Co. he was concerned chiefly with well logging instrumentation design. His work in this capacity was interrupted by service in the USAAF where he instructed radar and radio schools. Later he joined Stanolind Oil and Gas Company as a Senior Research Engineer in the development of geophysical equipment.

At SIE, Mr. McManis is responsible for such projects as electromechanical data processing systems and field recording equipment. He holds numerous U. S. patents, both issued and pending, on subjects such as

gain attenuators, gain expanders, limited phase distortion, two-channel phase modulation, and similar instrumentation circuits. He is a member of SEG and a Senior Member of the Institute of Radio Engineers.

ROBERT P. MEYER attended Carleton College, the University of Oregon, and the University of Wisconsin. He received B.S. and M.S. degrees in physics in 1948 and 1950 respectively, and a Ph.D. in geology in 1956.

He was an instructor in the geology department of the University of Wisconsin from 1956–1959 and since then has been Assistant Professor of Geology and a Program Director of the Geophysical and Polar Research Center at the University.

From 1954–1957 his principal research involved the regional offshore-onshore seismic program for basement depth determination in the southeastern United States. Since 1957 he has been responsible for the crustal seismic program of the University.

ROBERT P. MEYER

Mr. Meyer is a member of the SEG, AGU, Seismological Society of America, Geological Society of America, and Sigma Xi.

WILLIAM L. RUSSELL received the degrees of B.A., M.S., and Ph.D. from Yale University in 1920, 1922, and 1927, respectively. He had previously been employed by South Dakota Geological Survey (1924–1926), Tidewater Oil Co. (1935–1938), Standard Vacuum Oil Co. in South Africa (1938–1940), Well Surveys, Inc. (1940–1943), Stanolind Oil and Gas Co. (1943–1946), and was Associate Professor and Professor of Geology, Texas A. & M. College (1946 to date). He has been appointed lecturer in petroleum geology at the University of Cairo, U.A.R., for 1961–1962. His scientific interests are in petroleum geology, structural geology, determining incipient metamorphism from physical properties of sedimentary rocks, deep hydrocynamic circulation, and radioactivy of sedimentary rocks. He has published two books, *Principles of Petroleum Geology* (McGraw-Hill Book Co., 1951, new edition, 1959), and *Structural Geology for Petroleum Geologists* (McGraw-Hill Book Co., 1955), and about 45 scientific papers.

WILLIAM L. RUSSELL

John S. Steinhart received an A.B. degree from Harvard University in 1951. Upon graduation he served four years with the U. S. Navy. In 1955 he began graduate work at the University of Wisconsin and was awarded a Ph.D. degree in 1960. In 1957–58 and 1958–59 he held SEG scholarships, and in 1959–60 and 1960–61 he held predoctoral and postdoctoral fellowships of the National Science Foundation. In 1961 he joined the staff of the Department of Terrestial Magnetism, Carnegie Institution of Washington, as a seismologist. Dr. Steinhart is a member of SEG, AGU, SSA, and Sigma Xi.

JOHN S. STEINHART

VLADIMIR S. TUMAN

VLADIMIR S. TUMAN is an associate professor in the Department of Mining and Metallurgical Engineering at the University of Illinois. A native of Iran, he holds an Hon. B.S. degree in physics from Birmingham University, England, and received his DIC in advanced geophysics from the Imperial College in London in 1949. In 1950 he joined the Anglo-Iranian Oil Company. Later, upon the nationalization of the industry he was appointed Acting Chief Petroleum Engineer for the National Iranian Oil Company. Immigrating to the United States in 1957, he worked for the Atlantic Refining Company as a research physicist. In November, 1959, he joined the faculty at the University of Illinois.

FREEMAN GILBERT is a graduate of M.I.T. where he received his B.S. in geophysics in 1953 and his Ph.D. in geophysics in 1956. After a short time at the University of Cambridge as a NSF post doctoral fellow he joined the staff of the Institute of Geophysics, UCLA. He became assistant Professor of Geophysics in 1958 and associate Professor in 1960. In 1960 he went to Geophysical Service Inc. as Senior Research Geophysicist. In October, 1961, he became Professor of Geophysics, University of California at San Diego.

Dr. GILBERT is a member of Sigma Xi, Seismological Society of America, Acoustical Society of America, AGU, SEG, American Association for the Advancement of Science, and a Fellow of the American Academy of Arts and Sciences.

Biographies of the following authors appear in earlier issues of GEOPHYSICS as follows: Leon Knopoff, v. 25, p. 1295; N. R. Paterson, v. 26, p. 530.

MEMBERSHIP APPLICATIONS RECEIVED

Applications for active membership have been received from the following candidates. This publication does not constitute an election but places the names before the membership at large, in accordance with By-laws, Article III, Section 4. References are listed in parentheses following the names of each candidate. If any member has information bearing on the qualifications of these candidates he should sent it to the president within thirty days.

APPLICATIONS FOR ACTIVE MEMBERSHIP

Allen Robert Banks (G. R. Hess, A. A. M. Van Dijk, Dr. N. C. Steenland)

Charles R. Bentley (G. P. Woollard, John E. Nafe, J. Lamar Worzel, A. P. Crary)

A. E. Bluestone (B. B. Robinson, Jr., C. N. Page, Charles Kimbell, Ed. M. Handley)

Richard L. Brenan (Judson B. Hughes, Jr., Flint Agee, Bart Sorge)

John Kendall Costain (Kenneth L. Cook, A. J. Eardley, Peter Mandel, Jr.)

Doak C. Cox (M. King Hubbert, Joshua L. Soske, J. H. Swartz, Frank Press)

J. Espersen (S. Werner, L. V. B. Denslow, G. Tornquist, A. Lundbak)

Alvin R. Gregory (Sigmund Hammer, Lewis W. Gardner, Edsel K. Darby, Paul C. Wuenschel)

Charles Edmund Harr (F. R. Reeves, D. R. Dobyns, J. B. Bellican, H. G. Wilmot)

Moruja Hyodo (Hayashi Hajime, Nagumo Shozaburo, T. Kaneko, Kawashima Takeshi)

Lewis William Kidd (Prof. John D. Isaacs, Dr. H. W. Menard, Dr. Edward D. Goldberg, F. W. Outler)

Yves Bernard Ledoux (L. Migaux, R. Desaint, H. Richard, P. Giraud)

Dominique Michon (R. Desaint, P. Geraud, J. M. Vallet, H. Richard)

Charles H. Mims, Jr. (B. F. McPherson, S. O. Patterson, F. H. Agee, Dr. R. A. Peterson)

Leo W. Pfitzner (Robert B. Galeski, James A. Smith, N. H. Miller, J. Hodgkinson)

Tsuneo Sasaki (Hayashi Hajime, Nagumo Shozaburo, T. Kaneko, Kawashima Takeshi)

Frederick Lee Schenck (Robert H. Ray, Robert S. Duty, Milton C. Born, Frank T. Allen)

William Ronald Wright (J. A. Cathey, D. H. Hammond, C. R. Nigh)

APPLICATIONS FOR TRANSFER TO ACTIVE MEMBERSHIP

Wm. E. Bennett (Leland Snow, S. O. Patterson, T. J. Mouche, B. H. Flusche)

Richard Wallin Boebel (Gordon Mace, Raleigh Upsaw, A. L. Morgan, III)

John B. Cameron (M. A. Knock, J. G. Jones, O. G. Gross, E. F. K. Zarvdzki)

A. A. Dame (W. Gordon Smith, H. C. Maliphant, A. Junger, J. J. S. Hamilton)

Sylvester P. Gay, Jr. (W. H. Westphal, J. L. Soske, Ralph Holmer, W. Bourret (not member))

Walter Kostra (W. H. Merrill, A. J. Christman, K. B. Mickleson)

Robert K. Merritt (J. A. Long, John C. Baxter, S. W. Freuhling, L. A. Martin)

Lawrence S. Morrison (H. W. Kasiske, R. F. Weichert, Marvin Romberg, John C. Hollister)

Norman Paterson (Prof. J. T. Wilson, L. W. Morley, D. J. Salt, James Affleck)

J. B. Prendergast (F. C. McConnell, P. J. Farrell, J. A. C. Keefe)

V. Bhaskara Rao (B. S. R. Rao)

George D. Simmons (William T. Gilland, John C. Hoffman, Artemio S. Maureira)

John Stanley (C. P. Hartmann, Dick M. W. teGroen, Garrett Bakker, A. Helmer)

John F. Weyer (A. J. Barthelmes, N. K. Moody, R. D. Hilliker, R. L. Whitaker)

ANNOUNCEMENTS

Cecil H. Green Receives Honorary Degree from The University of Tulsa

Introduction to Dr. Ben Henneke, President of the University of Tulsa, by Mr. John Rogers, Member of Board of Trustees

"America's strengths and weaknesses in science and in education have been much discussed since September, 1957, when Russia launched the first earth satellite. The sciences and education have been undergoing a rigorous appraisal, since that date. The companies with which Cecil Green has been associated have long been leaders in developing programs of scientific endeavor appropriate to this country's needs and its future.

"Therefore, Mr. President, I have the honor to present to you CECIL H. GREEN, honorary chairman of the board and director, Geophysical Service, Inc.

"Dr. Green's educational background and business experience are known to this audience. He has pioneered programs of cooperative education between his company and universities, and programs of continuing education for the employees of his companies. The research and development activities of the companies which he directs are making available to our society the products which the new science discovers.

"Because of Dr. Green's stature as a scientist, an engineer, explorer for petroleum, and industrialist; because of his leadership in the cause of higher education, and most particularly in the fields of research and scientific enquiry, I am honored, Mr. President, to present to you for the degree of Doctor of Science, Dr. Cecil H. Green."

SEG Foundation Scholarships

EDWARD F. CHIBURIS has received a scholarship from the Society of Exploration Geophysicists Foundation, according to Maynard W. Harding, Chairman of Scholarship Administration for the Foundation. Chiburis will be a second-year graduate student at Texas A&M, where he will be working on his Ph.D. in geophysics.

His scholarship was made possible by a grant from Grant Body Manufacturing Corporation, of Tulsa, to the SEG Foundation.

Chiburis, born in Omaha, Nebraska, in 1933 moved to Fresno, California in 1946. He attended Fresno High School, then spent four years in the Air Force. He graduated from Texas A&M in May, 1960. There he received the George P. Mitchell Award for scholastic achievement, was elected President of the A&M Chapter of SEG in the fall of 1959, and was elected to Tau Beta Pi. In September, 1960, he was offered a part-time assistantship and a Mobil Oil Company scholarship to do graduate work in geophysics. His Master's thesis, to be completed this summer, is concerned with the LaCoste-Romberg S-9 ocean surface gravity meter.

MURLI MANGHNANI has received a scholarship from the Society of Exploration Geophysicists Foundation. Manghnani will be a graduate student at Washington University, where he will study geophysics.

His scholarship was made possible by a grant from the Society of Exploration Geophysicists to the SEG Foundation.

Manghnani, born in Karachi, West Pakistan, is the son of Mr. and Mrs. Hukumal M. Manghnani. He attended school in India, graduating from the Modern High School, Jodhpur, standing second in order of merit. He received his B.S. and M.S. degrees, with honors, in Applied Geology from the Indian School of Mines and Applied Geology, Dhanbad, India. He will received a Ph.D. in Geology at Montana State University in 1961 before entering Washington University. During summers he has been employed as a geologist and geophysicist in Montana.

Awards from the SEG Foundation are made as scholarships to outstanding students majoring in fields of interest to petroleum exploration, and as grants-in-aid for teaching and research. The Foundation's trust fund is made up of contributions from organizations and individuals interested in the earth sciences.

A college scholarship sponored by the Petty Geophysical Engineering Company, San Antonio, has been awarded to ROGER M. STEWART for 1961–1962. Stewart, a 20 year old junior, will use the Petty scholarship at the University of California where he will study geophysics.

Roger, son of Mr. and Mrs. Roy P. Stewart of Oklahoma City, has attended the University of Oklahoma the past two years. As a freshman he was a member of their honor society and one of 10 outstanding freshmen.

This summer, as in 1960, Roger is aboard the research ship, Stephen F. Baird of the Scripps Institution of Oceanography, working in the Pacific Ocean making sediment and core studies.

The scholarship is made available through the Society of Exploration Geophysicists Foundation and Harry Mayne, Petty Vice-President, commended the foundation for their choice of students. Petty for the past several years has sponsored scholarships through

the foundation which awards them to outstanding students majoring in fields of interest in petroleum exploration.

Yellowstone-Bighorn Research Association Meets

The Yellowstone-Bighorn Research Association held its annual meeting in Red Lodge, Montana, on July 8, and elected the following slate of officers:

William E. Bonini, Princeton University, Princeton, N. J., Past President; George Darrow, Consulting Geologist, Billings, Mont., President; George McGill, University of Massachusetts, Amherst, Mass., Vice-President; Vincent T. Larsen, Phillips Petroleum Co., Billings, Mont., Secretary; James Brophy, Brophy Coal Company, Red Lodge, Mont., Treasurer.

Marvin Kauffman, Franklin and Marshall, Lancaster, Pa., Howard Cramer, Emory University, Atlanta, Ga., Edgar Spencer, Washington & Lee Univ., Lexington, Va., William McMannis, Montana State College, Bozeman, Mont., Arie Poldervaart, Columbia University, N. Y., N. Y., Councilors.

The Y.B.R.A. is a nonprofit educational organization which has been actively engaged in teaching and research on the geology of the Northern Rocky Mountain region for over 31 years. Permanent facilities a few miles from Red Lodge provide food and lodging for research parties and serve as a base camp for an undergraduate summer field course. Members of the Y.B.R.A. include academic and industrial geologists from all parts of the United States.

The summer field course this summer has 23 students representing seven schools. Mr. Marvin Kauffman, Franklin and Marshall, field course chairman, was assisted by Dr. G. E. McGill, University of Massachusetts, Dr. R. R. Dutcher, Penn. State University, Dr. J. R. Butler, University of North Carolina, Dr. E. W. Spencer, Washington and Lee, Dr. W. H. Parsons, Wayne State University, Dr. F. B. VanHouten, Princeton University and Dr. H. R. Cramer, Emory University.

Geophysics Research Board

The Geophysics Research Board was established in 1960 by Detlev W. Bronk, President of the National Academy of Sciences—National Research Council, in concert with the Governing Board of the Academy. This was partly in response to a request from the International Council of Scientific Unions (which has called upon all Academies to establish a means for their cooperation with its International Geophysics Committee [C.I.G.]), and partly in response to expressions of interest by many members of the geophysical community. The American Geophysical Union, for example, strongly urged that the Board be established and pledged its cooperation and assistance.

Discussions, during the past year, involving many geologists and geophysicists, have led President Bronk to define the basic functions of the Board as follows:

(1) to effect participation by American scientists in the new International Committee on Geophysics of the International Council of Scientific Unions; and

(2) to stimulate and encourage research interest in the United States in geophysics and related fields, particularly those of an interdisciplinary character.

Membership of the Board consists largely of the chairmen or representatives of existing committees within the Academy; this will serve not only to bring together the geophysical interests of the Academy but also to minimize the burdens on the Board itself. These individuals and their committee activities are as follows:

Merle A. Tuve, Carnegie Institution of Washington, Chairman

L. V. Berkner, Space Science Board

Henry G. Booker, United States National Committee—International Scientific Radio Union

Harrison S. Brown, Committee on Oceanography

Michael Ference, Jr., Committee on Atmospheric Sciences

Laurence M. Gould, Committee on Polar Research

Joseph Kaplan, United States National Committee—International Geophysical Year

Martin A. Pomerantz, United States National Committee—International Union of Pure and Applied Physics

Francis W. Reichelderfer, United States Weather Bureau

Walter O. Roberts, United States National Committee—International Astronomical Union

George P. Woollard, United States National Committee—International Union of Geodesy and Geophysics and American Geophysical Union.

The Board has approved the establishment of the following four panels to deal with problems immediately before it:

World Magnetic Survey, E. H. Vestine, Chairman; Interchange of geophysical data. A. H. Shapley, Chairman; Proposed sunspot minimum program (now called the International Year of the Quiet Sun and scheduled for 1964–65), M. A. Pomerantz, Chairman; The solid earth, consisting of two working groups under the chairmanship of G. P. Woollard and H. A. Yoder, Jr.

In each of the above areas the Board has before it international proposals stemming from the C.I.G. and is called upon to examine the nature and prospects of American contributions to these worldwide efforts. In addition, the Panel concerned with the solid earth will discuss opportunities to advance the knowledge of our planet on a long term basis. A short meeting of the Board is scheduled during the time of the Academy's Annual Meeting to discuss a few problems in preparation for a full meeting later in the year.

ABSTRACTS

Bulletin (*Izvestiya*) December, 1960, Academy of Sciences, U.S.S.R., Geophysics Series.

Multiple Reflected and Transmitted Waves

YU. V. RIZNICHENKO AND O. G. SHAMINA

A theoretical discussion is given in this paper of a problem on dispersed summarized multiple waves, reflected and transmitted refracted seismic waves in a multilayered medium with thin dispersion layers. Experiments are described on ultrasonic pulse modeling of reflection and transmission of seismic waves in a medium having thin layers. A comparison of the experimental results with theoretical computations are discussed.

On the Experimental Analysis of Interferences and of the Reliability of the Results of the Grouping of Signals

F. M. HOLZMANN

The author investigates the fundamental characteristics of x- and t-expressions of a signal and of an interference. Some methods of the experimental analysis of these properties are examined. It is demonstrated that the results of the groupiug of signals appear to be reliable only on the condition that the spectra of the x-expressions of an effective signal and of the interference are separated. Some qualitative criteria of reliability evaluation are suggested.

Statistical Evaluation of the Reliability of the Results of the Grouping of Signals

F. M. HOLZMANN

The author suggests a probability evaluation of the reliability of the axes of cophasality obtained in the grouping of signals. Some practical methods for the calculation of the reliability are examined. The dependence of the reliability of the axes isolated on the conditions of the experiments is investigated.

On the Theory of Grouping

The theory of directed action of various types of grouping is discussed for an impulse system which is characteristic for seismic prospecting.

Determination of the Parameters of Attenuation of the Waves P_n and S^*

I. P. PASSECHNIK

The exponent "n" of the divergence function and the amplitude coefficient of absorption "a" are evaluated from amplitude curves of the waves P_n and S^*, obtained on a longitudinal profile during underground nuclear explosions of 5 and 19 kilotons, and also in the Arys' TNT explosion, by two independent methods. For the P_n waves, which have periods of oscillation from 0.6 to 0.8 sec, the average values are $n \approx 2.0$, $a = 0.0022$ km^{-1}; for the S^* waves, which have periods of 1.0–1.2 sec, $n \approx 1.7$, $a = 0.0023$ km^{-1}.

On the Question of the Determination of the Energy of Earthquakes

V. L. BELOTELOV AND N. V. KONDORSKAYA

We present the results of the determination of the energy of longitudinal and transverse waves for ten Far-Eastern earthquakes, using a method which had been suggested earlier by the authors. The results that were obtained agree with the energy values that had been calculated by means of the formula of Gutenberg and Richter which is based upon the determination of the magnitude M for the earthquakes in question.

An attempt is made to construct an "energy hodograph"; there is a general tendency for the increase of lg E with epicentral distance for P and S waves which is estimated.

The Investigation of the Elastic Properties of Rock Samples Taken from a Deep Borehole at High Pressures

E. I. BAYUK

The elastic parameters of rocks taken from the Novo-Alekseevskaya deep borehole were determined by the supersonic impulse method under pressures up to 4000 kG/cm^2. The obtained values of the velocities of longitudinal waves are compared to the data of the seismic logging of the above-mentioned borehole.

Distortions During the Recording of Elastic Pulses in Rocks

A. G. KONSTANTINOVA

The Interpretation of Results Obtained by Measuring the Angle of Inclination of the Plane of Polarization of the Variable Natural Magnetic Field

YU. B. SCHAUB

The Application of Electronic Computers in the Interpretation of Gravitational and Magnetic Anomalies

E. G. Bulakh

Experimental Dependence of the Energy of Seismic Waves on the Explosive Conditions

E. I. Luecke

The Field of a Point Source Located on the Boundary of a Half-Plane in the Presence of a Dividing Surface in the Form of a Paraboloid

A. M. Gluzmann

Numerical Calculation of Heat Inversions in Media with Phase Shifts as a Criterion for Determining the Temperature Shift

V. A. Kudryavtsev and V. G. Melamed

Time of Reestablishing the Thermal Conditions Disturbed by Drilling a Borehole

G. A. Cheremenski

Determination of the Surface Heat Flow at Stary Matsesta

E. A. Lyubimova, L. N. Lyusova, F. V. Firsov, G. N. Starikova and A. P. Shushpanov

Bulletin (*Izvestiya*), January, 1961, Academy of Sciences, U.S.S.R., Geophysics Series.

On the Nature of the Lg_1 Wave and of Its Propagation in Northeast Asia

N. G. Waldner and E. F. Savarensky

Statistical Distribution of Earthquakes and Tectonic Structure of Seismic Zones

S. L. Solov'ev

The statistical distributions of earthquakes in space and time may depend on the tectonic structure of the seismic zones. Such distributions consits of relationships between the frequency of weak and strong earthquakes and of the arrangement of the earthquakes with depth in the upper layers in the earth's mantle.

On the Internal Structure of the Earth

L. V. Altschuler and S. B. Kormer

Conclusions on the internal structure of the Earth derived from data on the percussive and isentropic compressibility of metals are given and new results on the measurements of the percussive compressibility of olivine and iron pyrites are presented. A comparison of the speed of sound in iron at high pressures and the velocities of seismic waves confirms Bullen's hypothesis of the solid nature of the inner core and points to the chemical uniformity of the core. The dependence of the density of iron and nickel on pressure in a region corresponding to the outer core does not coincide with Bullen's calculated dependencies, nor does it fall within the Rado-Molodenski limits at the boundary of the outer core.

Their studies of the percussive compression of olivine did not lead the authors to conclude that phrase transformation in it was possible, as is assumed by Lodochnikov and Ramsey. Preference should therefore be accorded to the hypothesis that the core of the Earth is composed of iron ore.

Relationship Between Earthquake Energy and Maximum Velocity of the Oscillations in Body Waves

V. L. Belotelov and N. V. Kondorskaya

The present paper examines the relationship between the energy of an earthquake, as determined by the authors, and the maximum oscillation velocity of the longitudinal and transverse waves. The energy differences of deep-focus and shallow earthquakes of equal magnitude are discussed.

The Screening of an Anomalous Field by Sediment

V. I. Dmitriev

A rigorous solution is obtained for the diffraction of an electromagnetic wave at a perfectly conducting half-plane embedded vertically in a homogeneous conducting half-space that is covered by a conducting layer with different resistivity.

Some Results of Paleomagnetic Investigations of Primary Igneous Rocks in Czechoslovakia

V. Bouha

A Graphic Method for Determining the Depth of Magnetized Bodies

A. K. Weinberg

The proposed graphic method for determining the upper boundary of disturbing bodies from the form of the anomalies of ΔT, Z_a and H_a is theoretically capable of a wide range of application.

An Instrument for Acoustical Investigations in Boreholes

N. I. Khalevin and D. D. Barykin

A diagram of a station for the study of the variation in intensity of the dominant harmonic elastic waves in boreholes is described in this paper. It can be utilized in the generally accepted modification of seismic logging of average velocities. The first parameter is utilized in the study of the physical properties of rocks cut by the drill, the second is necessary for improving the accuracy of interpretation of seismic prospecting results. Examples of measurements in the boreholes are given in this paper.

PERSONAL ITEMS

THEODOR H. BRAUN has been appointed Vice-President and Director of Plans and Operations for the System Development Corporation of Santa Monica, Calif., according to M. O. Kappler, Corporation President. Mr. Braun, who was in the oil exploration business for 23 years, joined SDC in 1960. He first served as Special Assistant to Mr. Kappler, then as Director of Operations and recently was named Director of Plans and Operations.

EDDIE ROE, formerly with Jersey Production Research Co., is now a development engineer for United Geophysical Corp. in Pasadena. Mr. Roe had been with Jersey Research for 13 years and had been employed by Esso divisions for 22 years.

L. B. RAY, formerly a field engineer in Midland, has been transferred to the engineering department of United Geophysical Corp. In Pasadena.

ROBERT N. HARDING has been appointed Assistant to the Senior Vice-President in Texaco's New York Production Department.

G. A. BOLLINGER has returned to St. Louis University to begin graduate work in Geophysics. For the last five years he had been with The California Oil Co. primarily concerned with Gravity and Magnetics.

H. V. W. DONOHOO is now Assistant Manager of Exploration and Chief Geophysicist for Texas Gulf Sulphur Co. He is in charge of company exploration on the Gulf Coast and will continue to be responsible for other geophysical activities of the company outside The Gulf Coast region.

ROBERT JASTROW, an Associate Editor of Geophysics, has been appointed Director of the recently established Institute for Space Studies in New York. The Institute is a part of the Theoretical Division of the Goddard Space Flight Center. Mr. Jastrow will continue to serve as chief of the Theoretical Division.

P. EDWARD BYERLY has joined the staff of the California Research Corporation, La Habra, California as Research Geophysicist. He was formerly with the U. S. Geological Survey in Denver, Colorado.

WALTER HAYS graduated from Washington University in St. Louis in June with a Ph.D. degree in Geology. He has been hired as a Geophysicist by the California Company and will be located in New Orleans, Louisiana.

M. DAVID ROSTOKER has accepted a position on the Research & Development staff of Arthur D. Little, Inc., Cambridge, Massachusetts.

LOYAL H. WELLS joined Cities Service Petroleum Company as District Geophysicist in the South Louisiana District on January 1, 1961.

ROY O. SMITH announces the opening of his Geophysical Consulting Office in Houston, Texas. With twenty-one years experience in Geophysics he has worked with Robert H. Ray Company, Southern Geophysical Company, and States Exploration Company. Since 1953 he has served as supervisor and area manager for States Exploration Company in the Gulf Coast Area. He has a wide range of experience in the Mid-Continent and Canadian Areas as well as on the Gulf Coast. His office is located at 525 San Jacinto Building, Houston 2, Texas.

M. KING HUBBERT, Consultant in General Geology, Shell Development Company, Houston, Texas, has been appointed as Visiting Professor of Geology and Geophysics of Stanford University for the winter quarters of the academic years 1961–1962 and 1962–1963. While maintaining his affiliation with Shell Development Company, Dr. Hubbert will be in residence at Stanford University during the above-mentioned periods, and will give a course entitled "Physics of underground fluids."

STANLEY L. SMITH, formerly Regional Exploration Manager of the West Texas Region for The Atlantic Refining Company, is now District Manager of Atlantic's Rocky Mountain District in Denver.

EDWARD A. GRIBI, JR., has announced his return to full time consulting geological practice at 229 Vivian Street, King City, California. Most recently with Westates Petroleum Company in Los Angeles, he has been a geologist for Sinclair in Ethiopia, for General Petroleum in California, and was a consultant in Great Falls, Montana, from 1953 through 1956. He is a 1948 Stanford graduate.

GEORGE L. LAIRD has been named manager of the newly-opened Denver office and processing center of

Robert H. Ray Company, Inc., Houston-based geophysical company.

Head of Ray's Midland office since 1956, Laird, 48, has been in geophysics for more than 27 years. He heads a seven-man office that will offer all four geophysical services of the Ray company—weight dropping, conventional seismic, gravity, magnetic—plus complete tape processing facilities.

Laird, married with three children, attended Lon Morris Junior College and the University of Texas. He joined RHR when the McCollum Exploration Company was purchased by the Ray company in 1959.

The Denver center occupies the seventh floor of the Terminal Building, 1730 Glenarm Place.

JOHN OHMAN has been appointed as Head, Physical Sciences, by Bay State Electronics Corporation, Boston Massachusetts.

Since 1958, Mr. Ohman has been Head of the Physics Laboratory at Melpar's Applied Science Division. For seven years prior to that, he was associated with Southwest Research Institute, San Antonio, Texas, in several Technical management positions, the most recent being Vice-Chairman, Department of Physics. His total twenty-nine years of responsible technical work and publication have included comprehensive experience in many phases of instrumentation and geophysical experimentation.

Mr. Ohman will be active in Bay State's expanded research and development program in the Earth environmental sciences, emphasizing oceanography and geophysical experimentation.

HAROLD F. PATTERSON has been appointed division geophysicist for Pan American Petroleum Corporation's North Texas-New Mexico Division at Fort Worth, according to an announcement by W. T. Smith, division exploration superintendent.

The announcement says that Mr. Patterson replaces CLARENCE J. LONG who has been named division geophysicist for the company's Canadian division at Calgary.

A native of Nebraska, Mr. Patterson graduated from high school at York, Nebraska. He holds a B.S. degree in geology from the University of Nebraska.

Hired by Pan American in February, 1946, as a junior computer, he worked on seismograph crews in Mississippi, Louisiana, Oklahoma, and Texas. He was named field seismograph supervisor in 1949 and worked at Forth Worth, Sweetwater, and San Angelo. He was district geophysicist at Midland from November, 1954 to May, 1955.

In June, 1955, Mr. Patterson was appointed division geophysicist for the company's gulf coast division at Houston. Since July, 1958, he has been district exploration superintendent at Lafayette, Louisiana.

Mr. Patterson is a member of the Society of Exploration Geophysicists, and Sigma Gamma Epsilon fraternity.

OTTO HACKEL, ROY W. TURNER and WILLIAM W. WHITLEY have resigned from Intex Oil Company to engage in independent consulting work. Otto Hackel was formerly Manager of Exploration, Roy Turner and Bill Whitley were District Geologists in California and the Rocky Mountains, respectively. The Association will have offices at 1414 "Q" Street, Bakersfield, California; mailing address: P. O. Box 968; telephone: Fairview 5-4682, and at 401 Patterson Bldg., 1706 Welton Street, Denver 2, Colorado; telephone: Alpine 5-9911.

BRODRICK F. DUNLAP, contract landman, will office with the group and will make his headquarters for petroleum land service in Bakersfield.

JAMES L. O'NEILL, former Chief Geologist for Oceanic Oil Company, with a background of geological experience in the majority of the oil provinces of the Western United States, will also be affiliated with the organization at the Bakersfield address.

F. R. ROSENLIEB, recently Assistant Treasurer and Chief Accountant of Intex Oil Company will have his office with the association in Bakersfield and will provide accounting services as well as income tax consultations.

The group will be known as "Otto Hackel and Associates" and petroleum consulting services will be available in geology, land and accounting.

FRANK PRESS, Professor of Geophysics at the California Institute of Technology was named California Scientist of the Year by the California Museum of Science and Industry Foundation. The annual award carries a prize of $5,000.

ROBERT A. PHINNEY and Stewart W. Smith have been appointed as Assistant Professors of Geophysics and Ari Ben-Menahem as a research fellow at Caltech.

JAMES RYAN WALKER, Staff Geophysicist for Murphy Corporation since December 1958, died in an El Dorado (Ark.) hospital on July 6 after a brief illness.

A graduate of the University of Oklahoma in 1931, his former employers included National Geophysical Company and Arkansas Fuel Oil Corporation. He was born in Charleston, S. C., on October 25, 1907.

M. B. DOBRIN, formerly with Triad Oil Company, is now Chief Geophysicist for United Geophysical Corporation, Pasadena, California.

Whether you hit the right spot or go astray may be determined by the accuracy of your aim.

Gravity surveys

based on practical application of the latest proven scientific methods, you can benefit from our broad experience and acquaintance with oil provinces throughout the world.

Call, wire or write for prompt, accurate geophysical surveys.

E. V. McCOLLUM & CO.

WE WEIGH THE EARTH

E. V. McCOLLUM
515 Thompson Bldg.

CRAIG FERRIS
Ph. LUther 2-3149

TULSA, OKLAHOMA

Foreign Affiliate: namco INTERNATIONAL

PROFESSIONAL DIRECTORY

ARIZONA

PHIL P. GABY

Geophysical Consultant

• *International* •

401 PIMA BUILDING TUCSON, ARIZONA

HEINRICHS GEOEXPLORATION CO.

Mining Oil & Water Consultants & Contractors

Geophysics Geology & Geochemistry

Examination-Interpretation-Evaluation

MOBILE MAGNETOMETER SURVEYS

Walter E. Heinrichs, Jr.

P.O. Box 5671 Tucson, Ariz. Phone: MAin 2-4202

CALIFORNIA

H. WAYNE HOYLMAN

Consultant

Petroleum and Mining Exploration

Aerogeophysics Company 816 W. 5th St.

MAdison 8-6428 Los Angeles 17, Calif.

L. F. IVANHOE

Consulting Geologist and Geophysicist

Domestic and Foreign Exploration

Phone: GE 9-7924 221 Nieto Avenue

CABLE: IVANHOE LONG BEACH 3, CALIFORNIA

CURTIS H. JOHNSON

Geophysical Consultant

Domestic & Foreign

816 WEST 5TH STREET, LOS ANGELES 17, CALIFORNIA

Phone: MAdison 6-0020

WILLIAM CROWE KELLOGG

Geological Engineer

Kellogg Exploration Company

Geologists — Geophysicists

Electrical — Magnetic — Gravity — Radioactivity

Air-Ground Surveys Interpretation

3301 NORTH MARENGO ALTADENA, CALIFORNIA

CALIFORNIA

HENRY SALVATORI

Western Geophysical Company of America

933 North La Brea Ave.

LOS ANGELES 38, CALIFORNIA

JOSHUA L. SOSKE

Geologist and Geophysicist

Dept. of Geophysics

SCHOOL OF MINERAL SCIENCES

Stanford University

STANFORD, CALIFORNIA

ELLIOTT SWEET

Gravity Meter Surveys

Gravity and Seismic Interpretation

SWEET GEOPHYSICAL CO.

21544 Rambla Vista Drive

MALIBU, CALIFORNIA

COLORADO

Milt Collum Wes Morgan

PETROLEUM GEOPHYSICAL COMPANY

Contract Seismograph Crews

Seismic Review and Interpretations

Rocky Mountain Area

KEystone 4-0253

2011 Glenarm Denver 5, Colorado

KENTUCKY

WM. DUCHSCHERER, JR.

Consulting Petroleum Geologist-Geophysicist

4324 Rudy Lane TW 3-2852

Louisville 7, Ky.

NEW YORK

ROLAND F. BEERS
ROLAND F. BEERS, INC.
Petroleum and Minerals Exploration Consultants
Ground and Airborne Surveys
Data Reduction and Analysis
P.O. Box 1019 Troy, New York
AShley 2-6478; 2-2351

OKLAHOMA

THOMAS J. BEVAN
Geophysicist
914 American Airlines Bldg. Phone LUther 2-7508
TULSA 3, OKLAHOMA

CRAIG FERRIS
Geophysicist
E. V. McCollum & Co. GeoSeis, Inc.
Namco, International
515 Thompson Bldg.
TULSA 3, OKLA

TOM D. MAYES
Mayes-Bevan Co.
Gravity Meter Surveys
and Interpretations
345 Kennedy Building
TULSA, OKLAHOMA

E. V. McCOLLUM
Geophysicist
E. V. McCollum & Co. Geo Seis, Inc.
Namco, International
515 Thompson Building
TULSA, OKLAHOMA

RICHARD A. POHLY
Gravity Surveys and Re-interpretation
POHLY EXPLORATION COMPANY
1135 E. 38th St. RIverside 2-2009
TULSA 5, OKLAHOMA

BEN F. RUMMERFIELD
Geologist and Geophysicist
6787 Timberlane Dr.
Tulsa, Oklahoma RI 7-7082

OKLAHOMA

JOHN J. RUPNIK
Petroleum Exploration Consultant
GEOPHYSICAL & GEOLOGICAL COORDINATION
J. J. RUPNIK AND COMPANY
730 BEACON BLDG., Telephone LU 4-6355
TULSA 3, OKLAHOMA

HUGH M. THRALLS
Consulting Geophysicist
Box 9577 GIbson 7-3921
TULSA, OKLAHOMA

TEXAS

JOHN F. ANDERSON
ANDERSON & COOKE
Oil Exploration Consultants
Geological Consulting
Seismic Surveys & Interpretations
665 San Jacinto Bldg. Houston 2, Texas

WALTER D. BAIRD
Consulting Geophysicist
NEIL P. ANDERSON BUILDING
PHONE EDison 6-8400 FORT WORTH 2, TEXAS

JOHN L. BIBLE
Gravity-Magnetic-Surveys-Interpretations
Bible Geophysical Co., Inc.
1045 Esperson Bldg. Houston 2, Texas

HART BROWN
Brown Geophysical Company
Gravity-Meter-Surveys
Interpretations
5300 Brownway Rd. Houston 19, Texas

R. A. CRAIN
Texas Seismograph Company
1502 Eighth St.
WICHITA FALLS, TEXAS

TEXAS

R. H. DANA

Dana Explorations, Inc.

1301 W. T. Waggoner Bldg.
Fort Worth, Texas

PAUL FARREN
Geophysical Consultant

Specializing in Seismic Interpretation, Review, and Supervision

1528 Bank of the Southwest
HOUSTON 2, TEXAS FA 3-1356

L. F. FISCHER
Petroleum Exploration Consultant
Geologist and Geophysicist

L. F. Fischer & Company
3636 Richmond Ave. Houston 27, Texas

J. F. FREEL
GEOSONIC CORPORATION

5134 Westheimer Road
Houston, Texas

JOHN A. GILLIN
National Geophysical Company, Inc.
Namco International, Inc.
2345 West Mockingbird Lane
Dallas, Texas

T. I. HARKINS
Independent Exploration Company

1973 West Gray
P.O. Box 13237
Houston 19, Texas

W. B. HOGG
Geophysical Consultant

619 Fidelity Union Life Bldg.
DALLAS 1, TEXAS

TEXAS

JOHN S. IVY

Niels Esperson Building
HOUSTON, TEXAS

J. C. KARCHER
Geophysicist

Adolphus Tower
DALLAS, TEXAS

MARTIN C. KELSEY
Rayflex Exploration Company

6923 Snider Plaza Dallas 5, Texas

H. KLAUS
Geologist and Geophysicist
Klaus Exploration Company
Gravimetric and Magnetic Surveys and Interpretations
P.O. Box 1617 Lubbock, Texas

PAUL H. LEDYARD
Mid-Continent Geophysical Co.

Contract Seismograph Crews
Seismic-Reinterpretations
2509 West Berry Fort Worth, Texas

C. T. MACALLISTER
Geophysical Consultant

Seismic Interpretations and Field Supervision

6327 Vanderbilt, Telephone:
Houston 5, Texas MA 3-4181

HAYDON W. McDONNOLD
Geologist & Geophysicist
Keystone Exploration Company

2813 Westheimer Road
HOUSTON, TEXAS

TEXAS

A. E. "SANDY" McKAY
Geologist and Geophysicist
Continental Geophysical Company
Namco International, Inc.
FORT WORTH, TEXAS
1409 Continental Life Bldg., Phone EDison 2-9231

GEORGE D. MITCHELL, JR.
Geologist and Geophysicist
4021 Marquette Ave. DALLAS 25, TEXAS

P. E. NARVARTE
Consulting Geophysicist
Seismic Interpretations
Current Supervision and Review
Frost National Bank Building
San Antonio, Texas

L. L. NETTLETON
Gravity Meter Exploration Co.
Interpretation of Gravity Surveys
Interpretation of Aeromagnetic Surveys
3621 W. Alabama
HOUSTON 27, TEXAS

W. W. (IKE) NEWTON
Geophysicist
823 Corrigan Tower
DALLAS, TEXAS

C. W. PAYNE
Exploration Consultant
Geology—Geophysics
812 Continental Life Bldg.
FORT WORTH TEXAS

H. B. PEACOCK
Consulting Geophysicist
9746 Audubon Place
DALLAS 20, TEXAS

TEXAS

J. C. POLLARD
GEOPHYSICAL ENGINEERING
•
SEISMIC . . . GEOGRAPH . . . GRAVITY
MAGNETIC SURVEYS
•
2500 Bolsover Rd., P.O. Box 6557, Houston 5, Tex.

ROBERT H. RAY
GEOPHYSICAL ENGINEERING
•
SEISMIC . . . GEOGRAPH . . . GRAVITY
MAGNETIC SURVEYS
•
2500 Bolsover Rd., P.O. Box 6557, Houston 5, Tex.

SAM D. ROGERS
Rogers Geophysical Company
Rogers Explorations, Sociedad Anonima
3616 West Alabama Houston 6, Texas

C. WHITNEY SANDERS
Consulting
Petroleum Geologist-Geophysicist
U. S. and European Exploration
1132 Bank of the Southwest Building
HOUSTON 2, TEXAS

RAYMOND L. SARGENT
Magnetometer Surveys
Interpretations
M & M Bldg.
HOUSTON 2, TEXAS

SIDNEY SCHAFER AND COMPANY
Geophysicists and Geologists
EXPLORATION CONSULTANTS
Domestic and Foreign
Sidney Schafer 2200 Welch Avenue
Jack C. Weyand Houston 19, Texas

HUBERT L. SCHIFLETT
States Exploration Company
Seismic, Gravity and Magnetic Surveys
5313 Richmond Road Highway 75 North
HOUSTON, TEXAS SHERMAN, TEXAS

TEXAS

HERBERT C. SMITH
Consulting Geophysicist and Geologist
Seismic Interpretations, Reviews and Current Supervision
Specializing in the Gulf Coast Area
320 Pinehaven Drive OV 6-5153
HOUSTON 24, TEXAS

H. B. SMYRL
Portable Seismograph, Inc.
706 Frost National Bank Bldg.
San Antonio 5, Texas

NELSON C. STEENLAND
Gravity Meter Exploration Company
Geophysicist
3621 W. Alabama Houston 27, Texas

R. C. SWEET
Geophysicist
1111 Bering Dr. Houston, Texas

Seismic Reviews Field Supervision
KIRBY J. WARREN
Geophysical Consultant
909 Continental Life Building
Fort Worth, Texas ED 2-9073

E. DARRELL WILLIAMS
Geophysicist
Specializing in Radiometric Exploration for Oil
3114 PRESCOTT ST., HOUSTON 25, TEXAS
PHONE MA 3-3991

JOHN H. WILSON
Exploration Consultant
1201 Sinclair Bldg.
FORT WORTH, TEXAS

TEXAS

CHARLES C. ZIMMERMAN
Geologist & Geophysicist
Keystone Exploration Company
2813 Westheimer Road
HOUSTON, TEXAS

WYOMING

Exploration Geology Seismic Reviews
Evaluations Seismic Supervision
JOHN F. PARTRIDGE, JR.
Consulting Geologist—Geophysicist
P.O. Box 258 Room 211 O-S Building
Phones 2-6485 and 2-3328 CASPER, WYOMING

CANADA

R. E. DAVIS
Geophysical Consultant
Farney Exploration Company, Ltd.
Specializing in Seismic Interpretation
830-8th Avenue West
CALGARY, Alberta, Canada

JOHN O. GALLOWAY
Petroleum Consultant
805 Eighth Avenue South West
AMherst 2-9018 CALGARY, ALBERTA

THEODORE KOULOMZINE
Geologist & Geophysicist
Koulomzine & Brossard Ltd.
P.O. Box 880, VAL D'OR Que. Canada.
Rm 905, 80 Richmond St. W. Toronto, Ont. Can.
Rm 1014, 132 St. James St. W. Montreal, Que. Can.

W. F. STACKLER
Consulting Geophysicist
Phone CHery 4-7303
1937 25th Avenue S.W.
CALGARY, ALBERTA

ENGLAND

WM. P. OGILVIE
Geophysicist and Geologist
GEOPROSCO LIMITED
20, ALBERT EMBANKMENT LONDON S.E.11

It takes a world of men, equipment and experience . . .

. . . to be successful in today's world-wide search for oil. In geophysical work, no report is worth more than the weakest link in its preparation. That's why Rogers Companies use only the best men and equipment—backed by world-wide experience—to give you the best in geophysical prospecting. Remember Rogers for results!

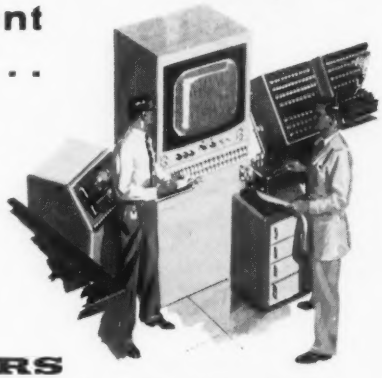

ROGERS
Geophysical Companies

3616 WEST ALABAMA • HOUSTON, TEXAS

FOREIGN OFFICES

Edificio Republica • Caracas, Venezuela
Mogadiscio • Somalia
34 Ave. des Champs Elysees • Paris, France
1-3 Arlington St., St. James's • London 1, England
Madrid, Spain
Tripoli, Libya • Algeria

ROGERS' CREWS GO EVERYWHERE

HIGH RESOLUTION CONTINUOUS SEISMIC PROFILING

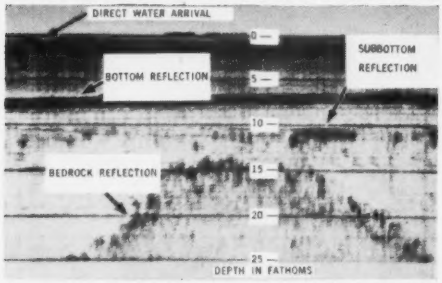

Representative reflection profile across irregular bedrock overlaid by several sediment layers — Narragansett Bay.

The broad tone shade response of **Alfax papers** and wide range of writing speeds of Alden "flying spot" **Helix Recorders** have been used to build an extremely flexible sonar recording and control instrument for the most rigorous all around high resolution deep sea recording. Designed by the scientists of Woods Hole Oceanographic Institute specifically for oceanographic research, the keying, record gating, drives and amplifiers chosen are now available in the **Alden #419 Precision Graphic Recorder**. Typical uses are:

- **PRECISION ECHO SOUNDING or RANGING**
- **SCATTERING LAYER and BIOLOGICAL STUDIES**
- **BOTTOM MAPPING and HYDROGRAPHY**
- **SEISMIC PROFILING**
- **PRECISE TRACKING of LOWERED or TOWED VEHICLES**
- **SALVAGE, OCEAN MINING and CONSTRUCTION PROJECTS**

ALFAX PAPER and unique ALDEN techniques provide these exclusive features:

• 12-speed operation. Provides 12 discrete intervals from 20 fm to 3000 fm full scale • Manual or Automatic Programming for Keying and Recording. Independent each channel. Discrete recording via programming for selected intervals • 5-speed precision paper feed provides variable resolution or integration of recorded signals • Fumeless, permanent, rf interference free, smudge-proof recordings with broad dynamic tone shade response proportional to marking signal • Single or dual channel operation. • Variable scale lines, adjustable keying pulse length, edge or center keying select, automatic time indication, event marker and half wave — full wave selectivity • **Alfax Papers** and **Alden Recorders** combined in other specific oceanographic recording systems are available from:

- **Alpine Geophysical Services** Houston, Texas, U. S. A.
- **Hunting Survey Corporation** Toronto, Ontario, Canada

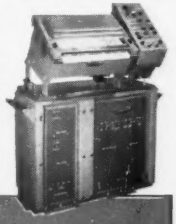

ALDEN ELECTRONIC & IMPULSE RECORDING EQUIPMENT CO., INC. Westboro, Mass.
Att: L. A. Farrington, Dept. E-1

1962

32nd ANNUAL MEETING

SEG

will be held in

CALGARY, ALBERTA

where

your hosts will be

THE CANADIAN SOCIETY OF EXPLORATION GEOPHYSICISTS

for

further details, look in at

BOOTH 41

at

the forthcoming

SEG ANNUAL MEETING

in

DENVER

GEOPHYSICIST

Civil Service Career

with the
Bureau of Mines
U. S. Department of the Interior

• • •

Qualifications needed: Experimental research in elastic wave propagation in rock. M.S. in geophysics or physics preferred. Some knowledge of electronics essential.

• • •

Working conditions: New modern Research Center, Minneapolis, Minn. Opportunity to work independently with good promotion possibilities. Publications encouraged.

• • •

Starting salary: $6,435 per year or more, depending upon education and experience. Numerous fringe benefits including paid vacation, sick leave, retirement, life and health insurance, and others. Write to Personnel Office, Bureau of Mines, Minneapolis Mining Research Center, East 58th Street at Mississippi River, Minneapolis 17, Minn.

Harper announces a monumental work—"the fruition of many years of sustained and strenuous effort"
(Carey Croneis, Editor of Harper's Geoscience Series)

GEOLOGY of the ATLANTIC and GULF COASTAL PROVINCE of NORTH AMERICA

by Grover E. Murray
Louisiana State University

This is the only geologic summary of present knowledge about the entire coastal region between Newfoundland and Spanish Honduras. The book gives a three-dimensional picture of the continental shelf, coastal plain, and certain plateau and mountain elements once part of the Mesozoic and Cenozoic coast. Important economic products are discussed. Many maps, sections, photographs, and charts; extensive bibliography.

postpaid in U.S.A. . . . no handling charges . . .
50¢ foreign postage
when purchased from

SOCIETY OF EXPLORATION GEOPHYSICISTS
Shell Bldg. *Tulsa 19, Okla.*

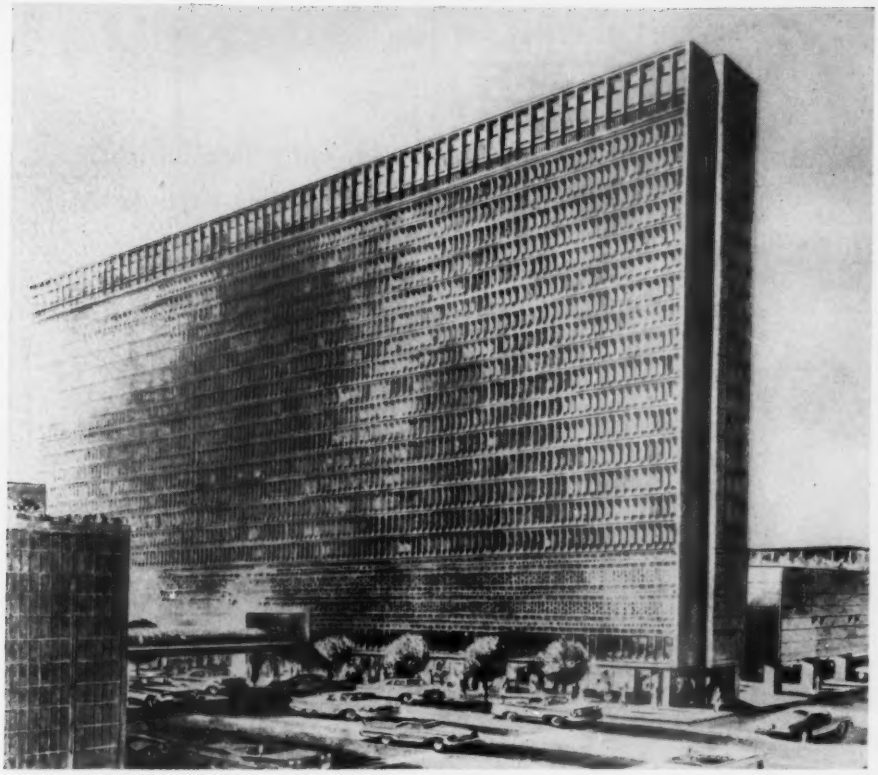

This is the Denver Hilton . . .

Site of the 31st Annual International

Meeting of the

S. E. G.

November 5-9, 1961 • Make Your plans!!

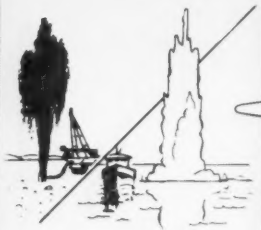

AMERICAN CYANAMID EXPLOSIVES

. . . for safe, dependable seismic exploration!

THE CYANAMID SEISMOGRAPH LINE*:

Dynamites
Hi-Speed
Geogel®
Ajax® S

Blasting Agents
Cyamon® OS
Cyamon® S
Cyamon® S Primer

40% Pattern Powder

DISTRIBUTOR SALES OFFICES AND MAGAZINES:

Dixie Dynamite Distributors, Inc.
Jackson, Mississippi
Lafayette, Louisiana
Hattiesburg, Mississippi
Houma, Louisiana

Southwestern Pipe, Inc.
Alice, Texas
Brookhaven, Mississippi
Houma, Louisiana
Lafayette, Louisiana
Lake Charles, Louisiana
Shreveport, Louisiana

Beeville H. & T. Sales Company
Beeville, Texas

Southwestern Explosives and Supply, Inc.
Midland, Texas

Deupree Distributing Company
Oklahoma City, Oklahoma
Tulsa, Oklahoma
Albuquerque, New Mexico

Milne Explosives Company
Great Bend, Kansas

Ashton Supply Company
Vernal, Utah

Carbon Transfer & Supply Co.
Helper, Utah

W. H. Burt Explosives Company
Aztec, New Mexico
Farmington, New Mexico
Moab, Utah

Wycoff Company, Inc.
Salt Lake City, Utah

Archie L. Bowman
Denver (Littleton), Colorado

Ted Andrus Explosives Co.
Billings, Montana
Sidney, Montana
Casper, Wyoming
Rock Springs, Wyoming

Fowler Engineering & Sales Co.
Ashland, Oregon
Burns, Oregon
Eugene, Oregon
John Day, Oregon
Medford, Oregon

Economical prospecting?

use AJAX® S DYNAMITE!

When high density is not essential, this 60% bulk strength semi-gelatin can replace gelatin dynamites at substantial savings. It offers good performance but should not be used under excessive water conditions.

It is supplied in rigid, spiral wound, glued shells in standard sizes of 2″ x 2 lbs., 2″ x 2½ lbs., 2¼″ x 5 lbs. and 3″ x 10 lbs. All sizes are available plain or with Fast Coupler or E-Z Lok® coupling sleeves for joining units to form long, rigid columns.

Cyanamid offers the industry a complete line of seismograph explosives and blasting agents. All are stocked for prompt delivery by leading distributors.

For complete information and recommended uses, contact our Sales Department or the distributor nearest you.

AMERICAN CYANAMID COMPANY
EXPLOSIVES AND MINING CHEMICALS DEPARTMENT
30 ROCKEFELLER PLAZA, NEW YORK 20, N. Y.

CJ-10 seismic amplifier system

The CJ-10 is an all-transistor seismic amplifier system with performance more than adequate for the most demanding truck-mounted instrument application yet possessing the physical size, weight and construction essential to remote and rugged portable jobs. Twenty-four complete amplifier channels plus all control and test functions are included in a single lightweight rugged unit. Output circuits will drive all types of photographic and magnetic recorders.

- Differential amplifiers with high gain stability and reliability
- Unique AGC—130-db dynamic range, one microvolt to 3-volt input
- Total weight — 62 lbs.
- Low distortion — Input filter ahead of any gain
- Programmed gain control
- AGC recovery rates faster than attack rates at all settings
- Power consumption — less than 50 watts

Other instruments and complete systems for earth-motion sensing and recording are available. Call or write for further information on the CJ-10 and our Press-Ewing and Lehner-Griffith products.

United GeoMeasurements — a division of

United ElectroDynamics, Inc.

422 SOUTH PASADENA AVE., PASADENA, CALIFORNIA, SY 5-8694

Interesting Career Opportunities for Scientific Personnel are Now Available

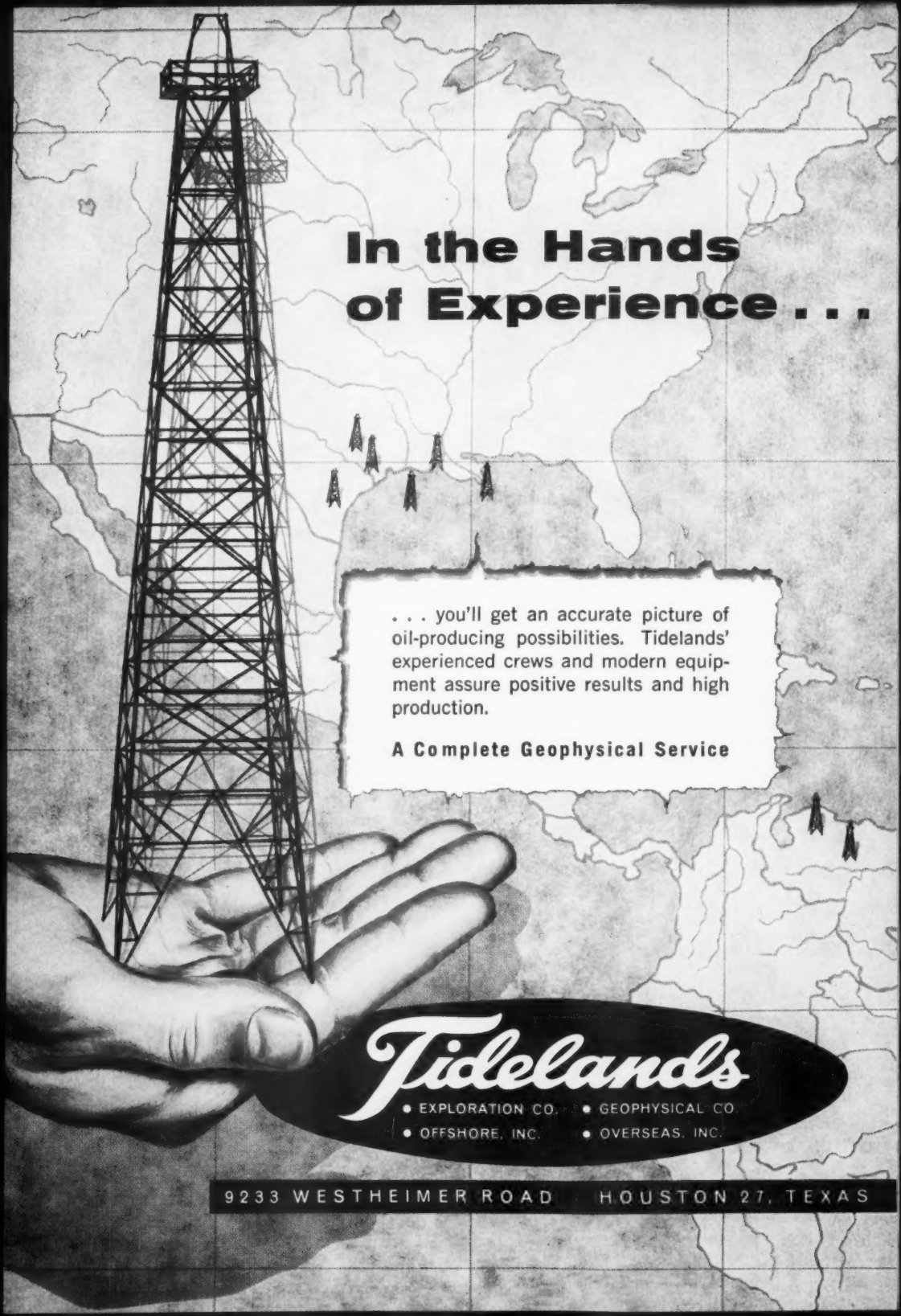
In the Hands of Experience . . .
. . . you'll get an accurate picture of oil-producing possibilities. Tidelands' experienced crews and modern equipment assure positive results and high production.
A Complete Geophysical Service
Tidelands
• EXPLORATION CO. • GEOPHYSICAL CO.
• OFFSHORE, INC. • OVERSEAS, INC.
9233 WESTHEIMER ROAD HOUSTON 27, TEXAS

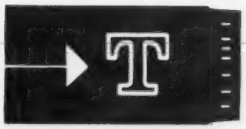

VISIT BOOTH 30 SEG

and ask about *new instrumentation economies* available from the leader and most experienced manufacturer of direct recording systems.

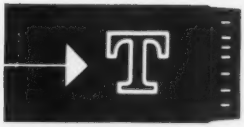

VISIT BOOTH 30 SEG

and be introduced to the NEW TI-554 CONTROL UNIT (transistorized) equipped with fork controlled timing signal generator, synchronous motor power supply, bias oscillator, record networks, reproduce networks, auxiliary channel reproduce amplifiers, metering, level adjustments and complete record-reproduce switching. Provides facilities for TI-401 Recorder similar to those incorporated in TI-551 Portable Recorder.

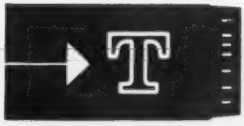

VISIT BOOTH 30 SEG

and discuss the latest applications of dual and triple drum assemblies providing recording, reproducing, static and moveout correction, stacking, integrating, compositing, transcribing, drum phasing and other facilities to meet the most demanding data processing requirements.

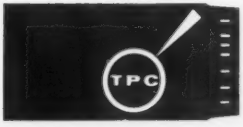

VISIT BOOTH 30 SEG

and be introduced to the application of wave analysis systems to seismic data problems. The TP-625 WAVE ANALYZER SYSTEM is a product of our associate company, TECHNICAL PRODUCTS COMPANY INSTRUMENT DIVISION.

TECHNO

TECHNO INSTRUMENT COMPANY / 6666 LEXINGTON AVENUE, LOS ANGELES 38, CALIFORNIA / HOLLYWOOD 2-7492 / TWX LA 191
Technical Products Company Instrument Division / 6670 Lexington Avenue, Los Angeles 38, Calif. / HOllywood 4-8121 / TWX LA 191

Affiliated with
Technical Products Company

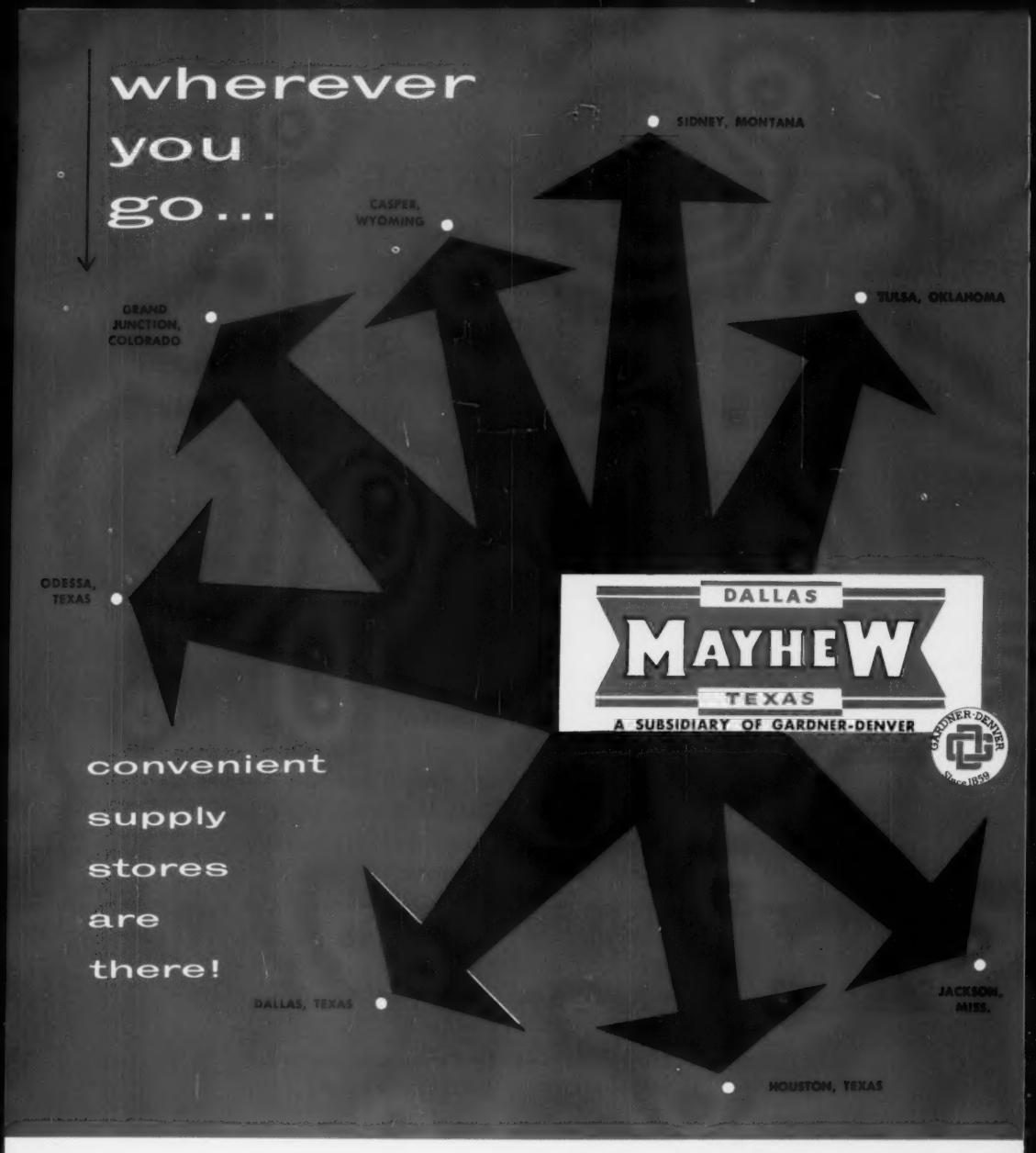

- Located in all active oil areas, Mayhew assures you of continuous operation with a complete line of supplies and replacement parts. So wherever you are located contact your convenient Mayhew Supply Store... You get the most with a Mayhew!

HOME OFFICE	**MAYHEW SUPPLY CO., INC.** 4700 SCYENE ROAD • DALLAS, TEXAS
SALES AND SERVICE	CASPER, WYOMING • TULSA, OKLAHOMA • SIDNEY, MONTANA • ODESSA, TEXAS • GRAND JUNCTION, COLORADO JACKSON, MISS. • HOUSTON, TEXAS
CANADA	SEISMIC SERVICE SUPPLY, LTD., CALGARY AND EDMONTON, ALBERTA
EXPORT	GARDNER-DENVER INTERNATIONAL DIV. NEW YORK, N. Y.

Standard of the Industry

MAGNETIC TAPE RECORDING SYSTEMS FOR GEOPHYSICAL EXPLORATION

Individual Components • Complete Systems • Transistorized FM or Conventional

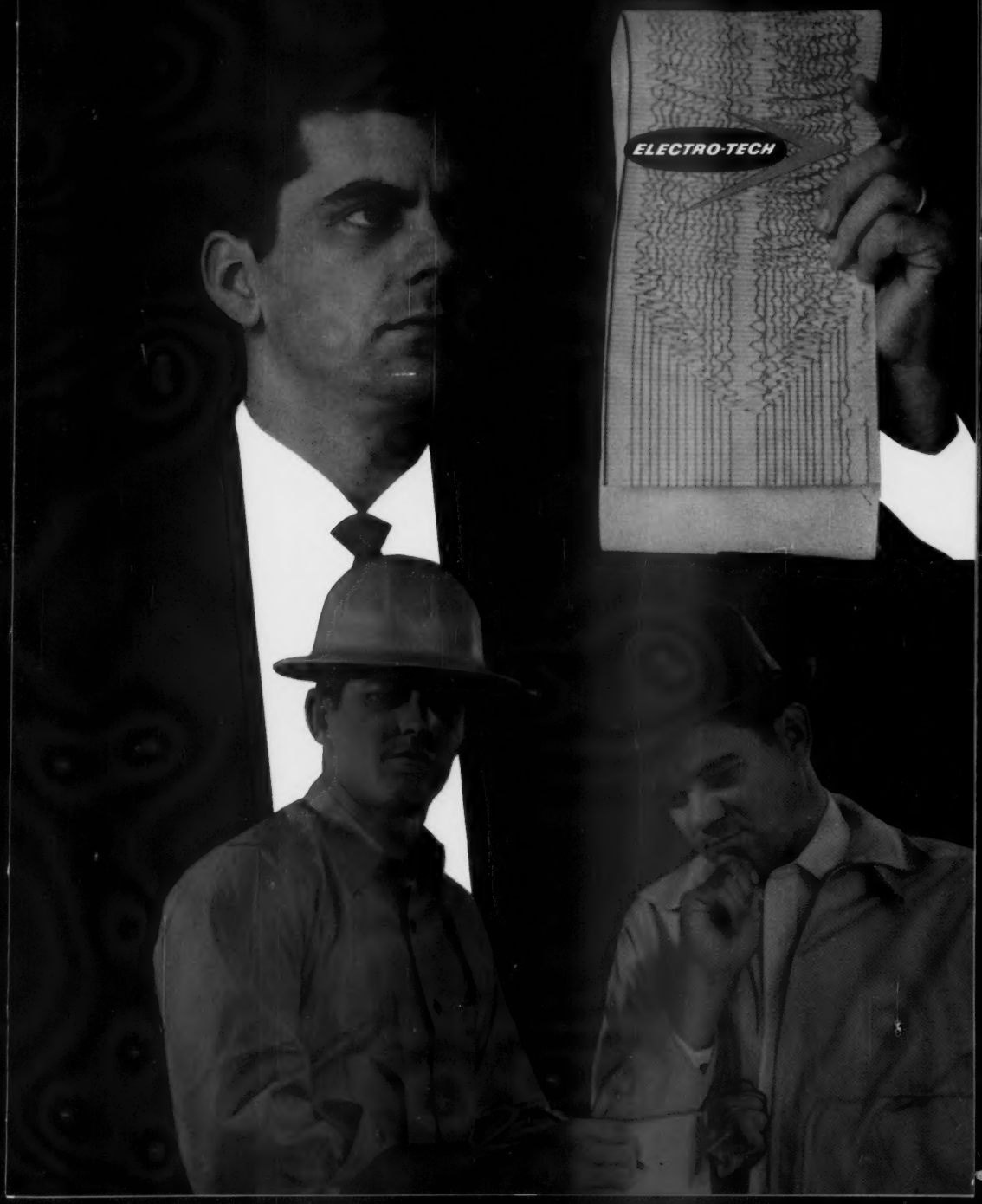

ELECTRO-TECH

MFR•1

TRANSISTORIZED FM FIELD RECORDER SYSTEM

Designed for maximum portability and minimum power drain, the MFR-1 preserves the highest figures of merit in linearity, signal to noise ratio and frequency spectrum. Extremely stable and reliable, it is built to maintain laboratory performance without continuous adjustment or repair. The three units of the system are housed in fiber glass carrying cases for lighter weight and ease of handling.

The drum, heads, tape and speed of the MFR-1 are completely compatible with existing FM systems.

The tape transport's steel belt drive eliminates much of the noise generated by other types of drives. The 28 channel recording heads are accessible through the front panel and are individually mounted for easy alignment and replacement. An auxiliary power pack contains the time standard, phase comparator, motor drive oscillator and power amplifier.

Very low harmonic distortion and negligible phase shift are exhibited by the completely transistorized, MTM-2 modulator-demodulator. Individual "plug-in" printed circuit boards are used for the mods and demods, providing ready access to all components. A test meter, with center frequency and level controls, is mounted on the front panel for ease of adjustment.

When combined with quality seismic amplifiers, the MFR-1 provides the most modern high fidelity FM magnetic recording system in the field.

CONDENSED SPECIFICATIONS

Input to Modulator: 0.5v rms at 40,000 ohms
Center Frequency: 4 kc
Tape: 4" center punched alignment holes
Tape Speed: 7.5 in/sec
Recording Current: 2½ milliamps
Frequency Range: 1-500 cps
Signal to Noise Ratio: 60 db
(rms 1-500 cps with noise cancellation)
Distortion: Less than 1%
Power Requirements:
Tape Transport: 4 amps 12v DC
Modulator-Demodulator: 1.25 amps 24v DC
System Weight: 115 pounds

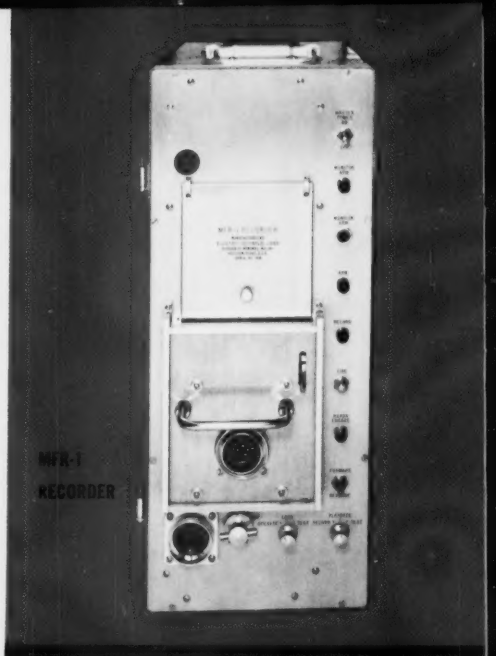

MFR-1 RECORDER

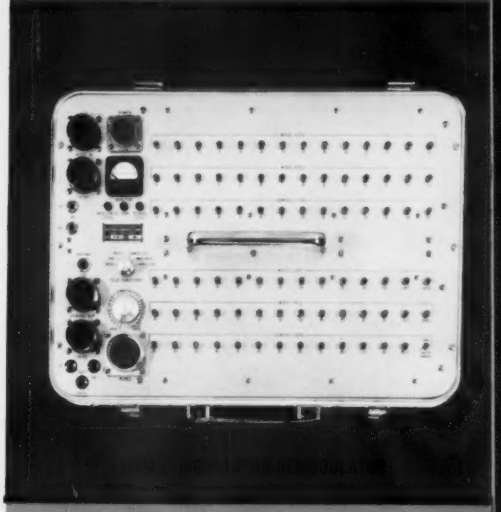

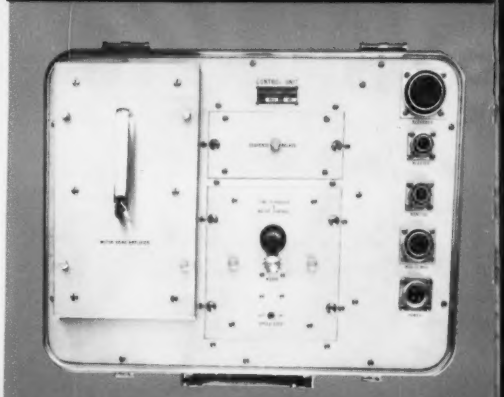

CU-1 CONTROL UNIT

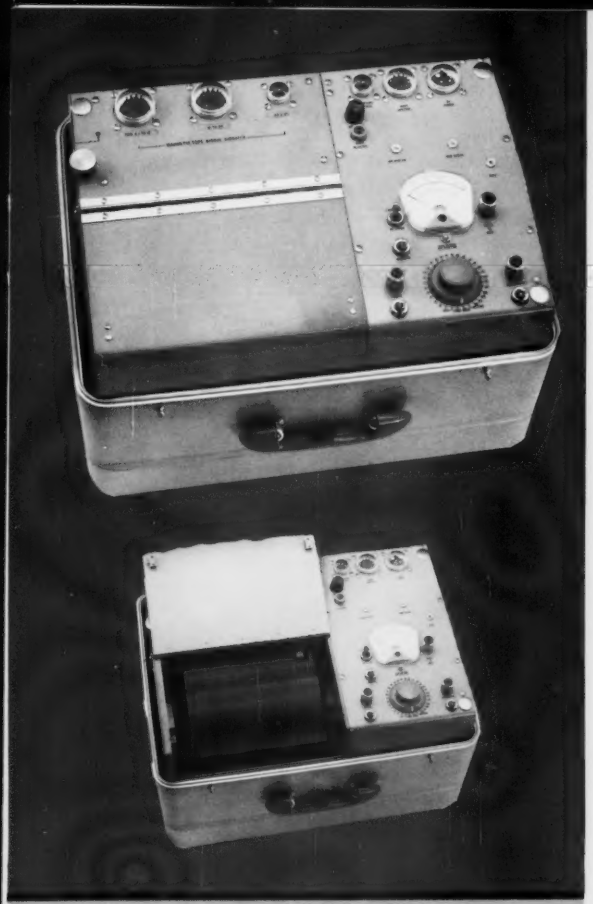

ELECTRO-TECH

DS·9

DRUM TYPE DIRECT RECORDER

The DS-9, direct recording, drum type, magnetic recorder is a completely self-contained unit that has been exactingly engineered for dependable service anywhere geophysical crews must operate.

The unit contains 28 magnetic heads and has a recording speed of 3.59 inches per second. The drive system operates from a 400 cps hysteresis synchronous motor and utilizes a speed monitor gear for continuous drum speed monitoring.

The compact, single case design combines all units and circuits into a complete tape recorder. Mechanically, it features rugged castings for the drum and transport, with an equally rugged fixed head rack assembly. Fully transistorized, the unit operates from a single 12 volt battery. The circuitry is of modular construction for ease of maintenance.

At the beginning of each recording cycle a pulse circuit is actuated to record a permanent indication of the head alignment on each magnetic track.

External controls are also brought out for automatic playback operation and auxiliary switching.

Manufactured under license of Western Geophysical Company

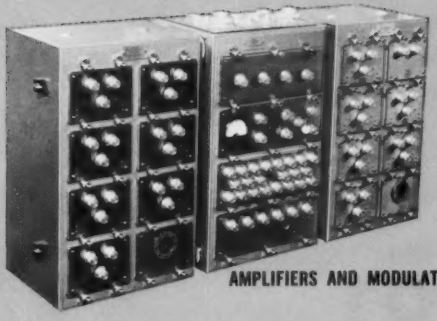

AMPLIFIERS AND MODULATORS

ELECTRONIC POWER SUPPLIES

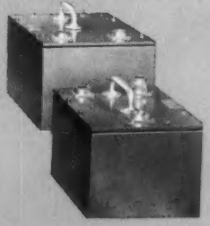

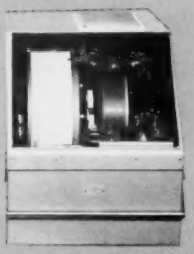

TAPE DRUM AND FIELD CAMERA

FR·1

FIELD RECORDER SYSTEM

The FR-1 is a complete system — no additional amplifiers, oscillographs, or power supplies are required — for obtaining permanent, reproducible seismic records in the field. Its dependability and simplicity of operation have been proven in years of field use. In addition to the high quality, 30 channel tape recorder, the FR-1 is equipped with a field camera for transferring information from tape to electrosensitive paper immediately after firing is completed, and without the photographic process.

Recording amplifiers are combined geophone signal amplifiers and pulse-width modulators with automatic gain control and gain expander. Input signal threshold is 1 microvolt and overall control range is 6,000,000:1.

Tape Size: 2¼" x .003"
Tape Speed: 7½ in/sec
Signal to Noise: 46 db, Peak Ratio
Power Required: 12v DC, Record: 45 amps, Playback: 21 amps
Frequency Response: 7 to 220 cps
Weight: 325 pounds

Licensed under patent rights of the Esso Research and Engineering Co.

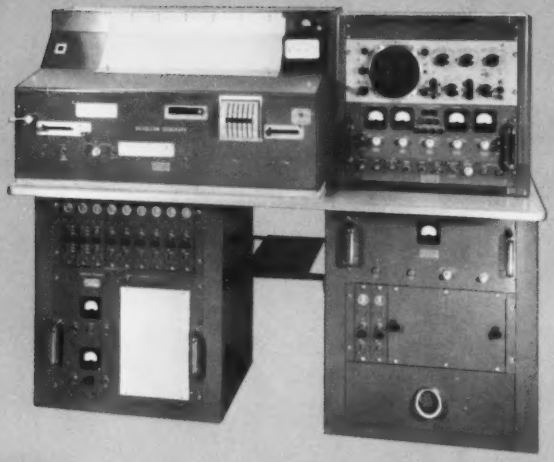

E•313

WEIGHT DROPPING GEOGRAPH FIELD RECORDER

The dual purpose, multiple drum Geograph Field Recorder can simultaneously record up to four channels of seismic data, and can store six groups of this data on the 24 primary tape tracks of the primary drum. The utility of this unit has been proved through years of field experience.

In addition to the four recording drums, the E-313 provides a field camera for recording on electro sensitive paper and an oscilloscope for visual monitoring either record or transfer signals.

Power for the unit is converted by self-contained, transistorized power supplies. The tape is 4 inches wide and records at 10 in/sec or 6⅔ in/sec. Signal to noise ratio is 46 db.

Licensed under patent rights of Robert H. Ray Co.

DS•7

FLATBED TAPE TRANSPORT AND PLAYBACK UNIT

Extremely simple in design and operation, the DS-7 is an inexpensive direct recording magnetic tape recorder and playback unit, completely self-contained. Reliable operation under all field and office conditions is provided by the simplified plane-surface head carriage system. The great flexibility of the unit and unlimited record time allows it to be successfully integrated with any existing seismic equipment.

Tape Size: 7½ in wide
Tape Speed: 7½ in/sec
Traces: 27
Weight: 48 pounds

Signal to Noise: Greater than 46 db rms-to-rms at peak magnetization, at 30 cps.
Power: 12v DC, Record: 5.5 amps; Playback: 4 amps

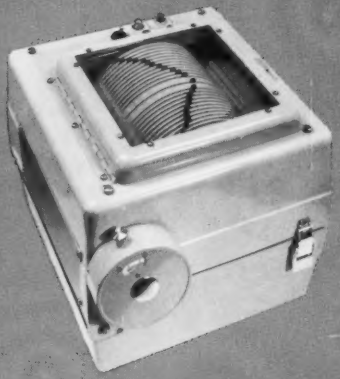

DS•8

FLATBED TAPE TRANSPORT AND PLAYBACK UNIT

The DS-8 recorder is a fixed head version of the DS-7 unit and has a tape speed of 3.59 in/sec. A highly useful assembly of the DS-8 is shown with storage and tape takeup spools capable of holding 500 feet of magnetic tape. Special configurations and tape speeds are available upon request.

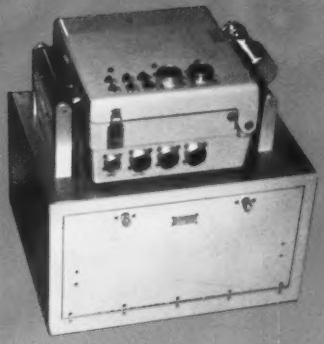

ELECTRO-TECH

Leaders in the Field of Exploration Instrumentation

ELECTRO-TECHNICAL LABS

Division of Mandrel Industries, Inc.

5234 Glenmont • Houston 36, Texas

Cable Address: ELECTROTEX

OFFICES • U.S.A. Houston • Lafayette • Tulsa EUROPE Annecy, France CANADA • Calgary, Alberta

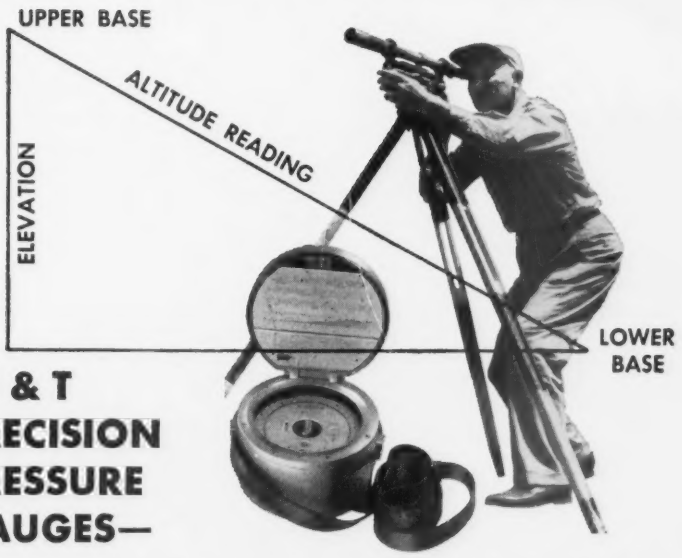

W & T PRECISION PRESSURE GAUGES—

THE KEY TO ACCURATE MEASUREMENT

Among the wide range of Wallace & Tiernan precision pressure instruments, the W&T Altimeter shown here is one of the most popular. Its versatility, accuracy, and sensitivity make it ideal for prospecting, topographic surveying, aerial mapping, pipeline location, and conservation studies.

W&T Altimeters come in three ranges—1200, 2100, and 4800 meters. Dials are readable within 15.2 to 60.8 cms., depending on range. The altimeters always balance with the atmosphere . . . there is no need for adjustment. Individually calibrated dials give accurate, direct, quick reading. And the shockproof mechanism provides dependability under rugged field conditions.

Two or more W&T Altimeters can be simultaneously calibrated to assure identical characteristics in the two-base method of altimetry. With this method, a wider area can be covered in far less time than with conventional surveying techniques. Full details are available on request. Write Dept. F-122.42

WALLACE & TIERNAN INC.
25 MAIN STREET, BELLEVILLE 9, NEW JERSEY

A NEW METHOD OF IMPROVING THE PRESENTATION AND THE INTERPRETATION OF SEISMIC RECORDS

THE COMPLETE SYNTHETIC SEISMOGRAM with multiple reflections

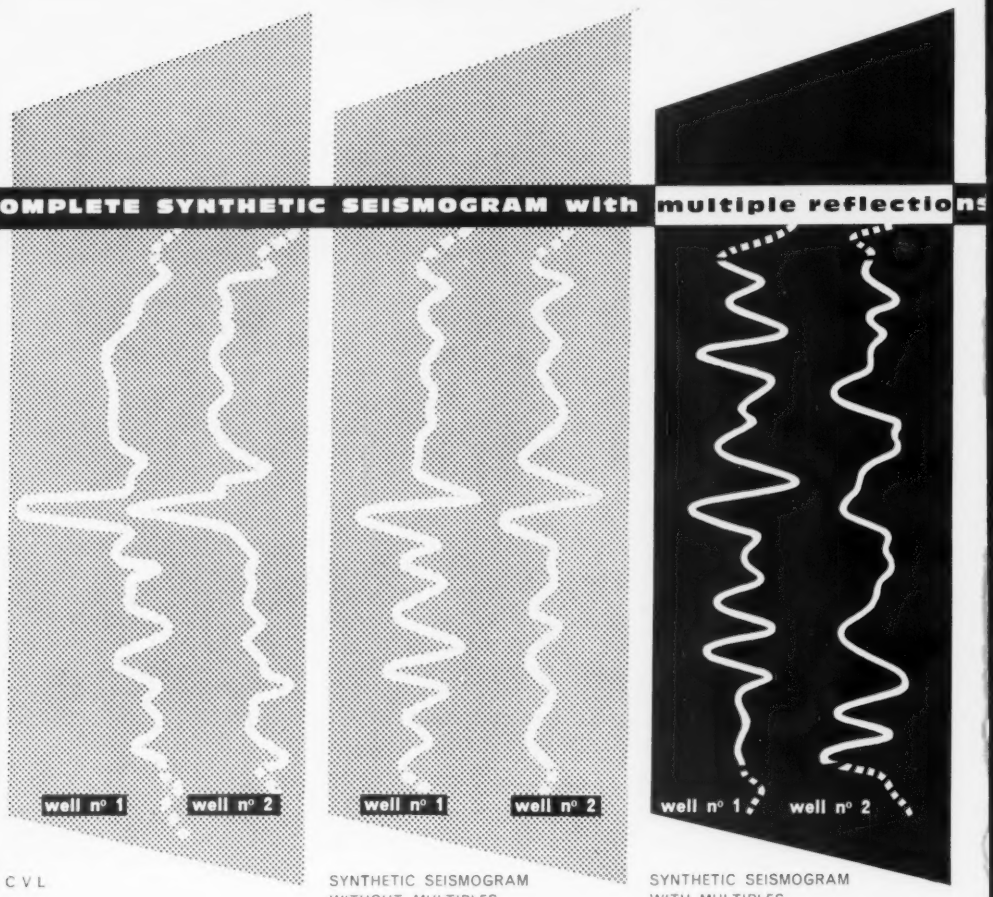

C V L

SYNTHETIC SEISMOGRAM WITHOUT MULTIPLES

SYNTHETIC SEISMOGRAM WITH MULTIPLES

What geological and geophysical information can be obtained after synthetic seismograms are examined and are compared with the actual records ?

The synthetic seismograms make it possible to ascertain the existence and the quality of the horizons which may be used as good markers

The synthetic seismogram leads to improvements of the field techniques : automatic gain control and filtering

The synthetic seismograms are conducive to a more complete and more acurate interpretation

Using the synthetic seismogram your past and present surveys can attain their full value

The cost of a synthetic seismogram with multiple reflections varies with the depth logged : 20 to 25 % of the cost of the logging operations proper

For a borehole of average depth, this cost is no higher than that of one kilometer of seismic profile

YOU TOO WILL BENEFIT FROM THE USE OF THIS NEW GEOPHYSICAL TOOL

GG

COMPAGNIE GÉNÉRALE DE GÉOPHYSIQUE

50, rue Fabert - Paris 7e - Phone : Invalides 46-24

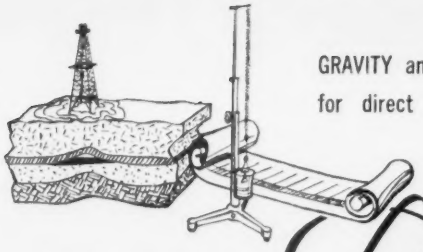

GRAVITY and MAGNETIC SURVEYS and INTERPRETATIONS for direct correlation with subsurface conditions by preparation of **Density Logs** and **Differential Residuals.**

PHONE CApitol 2-6266
1045 ESPERSON BUILDING
HOUSTON 2, TEXAS

Bible **GEOPHYSICAL CO., INC.**
JOHN L. BIBLE, President

ANNOTATED BIBLIOGRAPHY OF ECONOMIC GEOLOGY

25 Volume Index 1928 to 1954
now ready for orders and distribution;
2 parts, A-L, M to Z; total pages 1496.

THIS COMBINED 25-VOLUME INDEX COVERS THE ABSTRACTS AND BIBLIOGRAPHY OF ECONOMIC GEOLOGY AND RELATED MATERIAL THROUGHOUT THE ENTIRE WORLD OVER A PERIOD OF A QUARTER-CENTURY.

Indispensable to all subscribers and users of the Annotated Bibliography of Economic Geology, libraries, investigators, research workers, mining and petroleum companies—a general reference. It incorporates the previous index into a single reference index.

Price during 1961—$20.00; after 1961—$22.50

Published by Economic Geology Publishing Co., publishers of Economic Geology, a semi-quarterly independent journal, and also the organ of the Society of Economic Geologists; Annotated Bibliography of Economic Geology, a semi-annual publication; and Fiftieth Anniversary Volume.

Place orders with

M. M. Leighton, Business Manager
Economic Geology Publishing Co.
105 Natural Resources Bldg.
Urbana, Illinois

Visit COMPAGNIE GENERALE DE GEOPHYSIQUE

BOOTH 35

DENVER November 5th to 9th

31st Annual International Meeting S.E.G.

This film represents the newer way in geophysics

Kodak Linagraph Recording Film, Estar Base has only been around for a little more than a year—but that has been long enough noticeably to affect geophysical working practice.

It has about the same kind and degree of light sensitivity as the long-accepted Kodak Linagraph 480, 483, and 809 papers. This removes the question marks about exposure when you switch over. Its tear strength is, of course, phenomenal. Its dimensional stability is so high that you never have to give it a thought, however large the films you use. As for size, you could order Kodak Linagraph Recording Film in rolls all the way up to 52 inches wide if you needed them for, say, new equipment that computes and displays large-scale seismic sections from taped data.

We give the emulsion the proper characteristics so that it can be used for 1) variable-density and variable-area seismic sections, 2) "wiggle"-trace and modulated blue glow-lamp recording from magnetic tape, 3) seismograms directly in the field, 4) electrical well-logging, 5) conventional oscillography, 6) cathode-ray tube photography from P-11 phosphors. Furthermore the emulsion is hardened so that it can be processed hot without spoiling anything.

If there is anything more you would like to know about it, ask your Kodak Technical Representative or write

Photorecording Methods Division

EASTMAN KODAK COMPANY, Rochester 4, N. Y.

CENTURY serves the world

Century Geophysical Corporation, with its 44 geophysical units presently spread across the globe, is backed and strengthened by the research and development laboratories and the manufacturing facilities of Century Electronics & Instruments, Inc. These two affiliates are working partners in providing many industries with technical services and electronic instrumentation and equipment.

Seismic and gravity meter crew operations, review geophysical interpretations, velocity surveys, data center processing, uranium exploration logging and radiometric analysis are some of the general areas where Century has gained a large backlog of experience and wide acceptance.

Century's facilities are available to assist you in gathering, processing and evaluating scientific data anywhere in the world.

Century Geophysical Corporation *Century Electronics & Instruments, Inc.*

TWX TU-1407 — TULSA, OKLAHOMA

Geophysicist

Schlumberger Well Surveying Corporation maintains a program of long-range industrial research projects at its Research Laboratory in Ridgefield, Connecticut.

The program includes such scientific fields as physical chemistry, nuclear magnetic resonance, nuclear physics electronic systems, sonics, wave propagation, data processing and fluid flow in porous media.

In order to implement our diversified program we have an opening for a Geophysicist with an advanced degree and a strong interest in applied research. The applicant should have a strong foundation in physics and mathematics and a knowledge of geology, geochemistry, and petrophysics.

The position requires a scientist with an analytical mind and good experimental ability. Knowledge of and experience in behavior of fluids in porous media and an interest in oil exploration and reservoir engineering would be valuable.

Our Laboratory is located in a small Connecticut town about 50 miles northeast of New York City. The facilities at the Laboratory are extensive and modern. Working conditions and fringe benefits are consistent with the highest industrial standards.

Please send resume to:
Mr. J. J. McNamara

SCHLUMBERGER WELL
SURVEYING CORPORATION
P.O. Box 307, Ridgefield, Connecticut

ECONOMICS OF MORE EFFICIENT SHOT HOLE DRILLING — NO. 1

COST REDUCTION CREATES NEW BUSINESS
NEW BUSINESS CREATES NEW WEALTH

Basic economics proves that business volume increases as unit costs decrease. This increased production potential applies to seismic exploration. Faster, more efficient drilling with Hawthorne "Blue Demon" Bits, in many cases, provides the equivalent in shot hole production of an extra drill . . . reducing hole cost per foot up to 50% . . . reducing profile costs proportionately.

Using Hawthorne "Blue Demon" Bits, major companies around the world have been able, with the same personnel and equipment, to increase party output more than 100% per month. This increased efficiency has tremendously reduced cost per profile, and has helped to finance new prospects in other areas.

"BLUE DEMON" SAVINGS WILL SUPPORT FUTURE DRILLING PROSPECTS

Drilling conditions will vary, but you can count on decreased costs per profile . . . increased party potential . . . in increasing crew efficiency with "Blue Demon" Bits.

WRITE FOR ILLUSTRATED CATALOG

HERB J. HAWTHORNE INC.

Cable Address: HAWBIT • P. O. Box 7365 • Houston 8, Texas

U.S. Patent Nos.
2,615,684
2,666,622
2,695,158
2,783,973
2,831,657
2,859,942
2,890,020
2,894,726

308

HI-FIX

in action

The HI-FIX trailer becomes a caravan simply by raising the lid

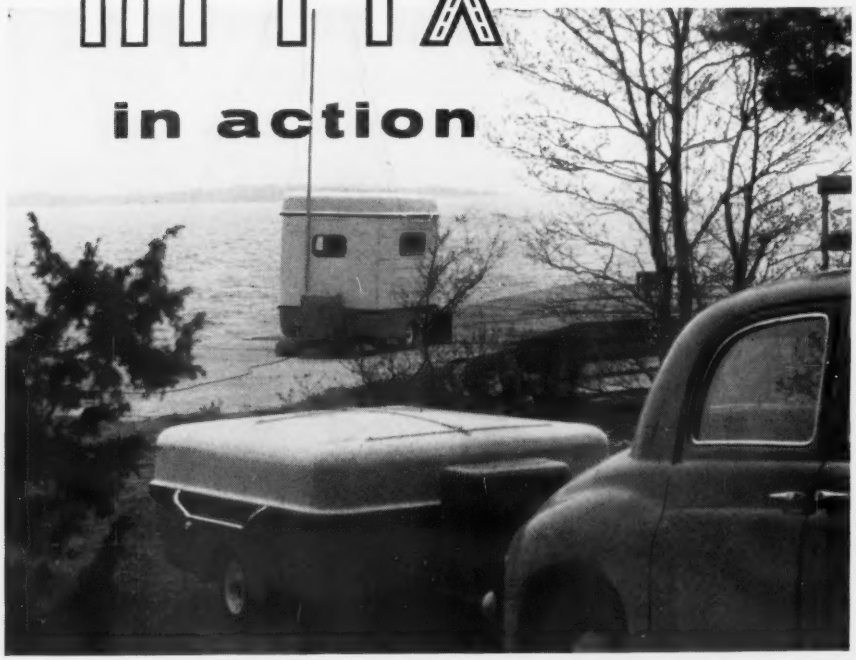

mobile . . . lightweight . . . high accuracy

HI-FIX has made spectacular progress in field operations, providing high accuracy for detailed engineering survey and achieving ranges several times those predicted.

The equipment, which is lightweight and highly mobile, has operated successfully in such searching conditions as the tropical heat of Nigeria and sub-zero temperatures of North America. Its versatility, accuracy and simplicity of operation has made HI-FIX widely accepted for a variety of civil engineering, hydrographic and military purposes.

Operating HI-FIX equipment in the caravan

HI-FIX shows these advantages over other methods:

Only two small units required in each station

Can be operated from caravan, launch or tent

Small transmitter of lower power output, low battery consumption

Narrow bandwidth eliminates effects of noise and interference

Position fixing with an accuracy of a few feet

Optional lane identification

THE DECCA NAVIGATOR COMPANY LIMITED LONDON

Only Vector Cables are completely manufactured in one plant.

Almost all cable is composed of the same basic raw materials but only with Vector Cables do you get complete quality control throughout. Only Vector's modern up-to-date plant is capable of converting the raw materials into the precision cable systems including the various take-outs that are demanded for today's sensitive explorational equipment. Regardless of what your seismic cable needs may be, you can be sure of getting the finest when you specify Vector Cables. Write for our FREE catalog today.

We invite your inquiries for specially designed cables.

Vector Manufacturing Company

5616 Lawndale Houston, Texas

NEW FROM VECTOR!

MODEL RVMP-18

THE WATER PROOF "JR." FIELD REPAIRABLE PLUG

1 *take apart*

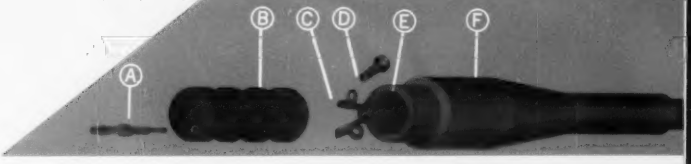

- Ⓐ Famous Vector Replaceable Banana Pin
- Ⓑ Contact Block (fits inside Nipple)
- Ⓒ Crimp Lug
- Ⓓ Screws. (Only two to attach Lugs to Contact Block)
- Ⓔ Cable Jacket
- Ⓕ Rubber Nipple

2 *re-assemble*

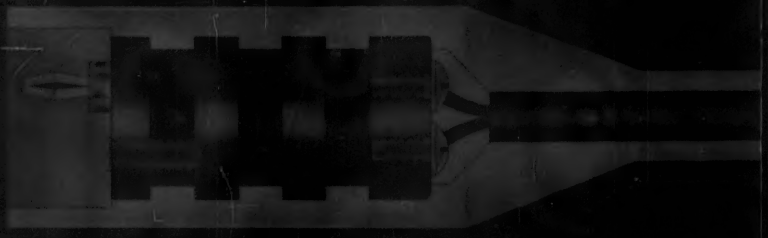

IN LESS THAN 4 MINUTES • A NEW PLUG • REPAIRED ON THE JOB

3 *in perfect operation*

In only 4 minutes you can re-assemble and replace the entire WATER PROOF "JR." PLUG. However, most replacement problems solely involve the Banana Pin, the spring portion of the Plug. Vector's exclusive Banana Pin can be replaced in 42 SECONDS! Once replaced, your Plug has a **Brand New** contact mechanism.

ONLY VECTOR CABLES ARE COMPLETELY MANUFACTURED IN ONE PLANT.

Full information available on request.

Vector Manufacturing Company

5616 Lawndale, Houston, Texas

Seismic Cable Systems

Manufactured to YOUR Specifications

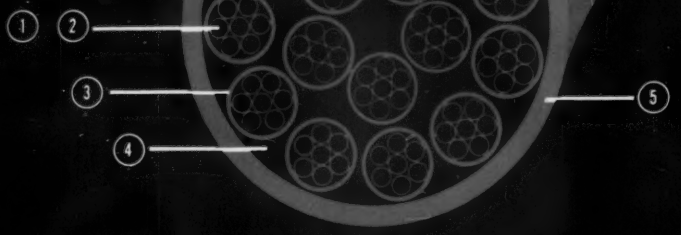

VECTOR'S 6 STEPS TO QUALITY CONTROLLED CABLE.

1 All wire manufactured to our specifications and pre-tested before insulating.
2 Wire is converted into flexible conductors by our specially designed high-speed stranders.
3 Through our unique extrusion processing, primary insulation coatings are applied and tested in our laboratory.
4 Fillers and tape applied on special machines by trained technicians.
5 All rubber and neoprene materials are compounded in our modern up-to-date laboratory.
6 Vector manufactures a complete line of take-outs, geophone fittings and water-proof plugs. We repair and re-assemble all systems including the testing of geophones.

FOR WORLDWIDE GRAVITY AND MAGNETIC SERVICES

rely on Robert H. Ray Companies. Each contract is backed by experience gained from more than twenty years of foreign and domestic operations—research and development in instrumentation and interpretation. Lower cost per station and fast, accurate service from skilled crews are standard benefits you get from the Robert H. Ray Companies. Seismic Services, including Geograph, are also available anywhere in the world. Let us explain how each of these techniques will fit into your Geophysical program.

For Geograph in Europe and the French Zone contact GEOGRAFRANCE, 48 Blvd. de Latour-Maubourg, Paris 7e.

ROBERT H. RAY GEOPHYSICAL COMPANIES
2500 Bolsover, Houston 5, Texas

SUPERIOR SEISMIC PRODUCTS ...BY DU PONT

THERE'S A DU PONT SEISMIC PAPER AND FILM FOR EVERY JOB:

1. SEISMO-WRIT PHOTORECORDING PAPER. Fast, high-density traces, easy to handle – available in standard sizes and in either Type B (standard weight) or Type W (all-rag, extra-thin). Seismo-Writ comes in strong, durable metal containers. All rolls are wrapped in waterproof foil bags for safe storage before you use it ... and for protecting your traces after the shot is made. We even supply you with an address label for easy mailing from the field.

2. CRONAR* RECORDING FILM. Relative speed (tungsten): 30.

3. LINO-FLEX 1. Relative speed (tungsten): 10.

Both of these films are on Du Pont's tried and proven CRONAR polyester photographic film base, which offers unexcelled strength, exceptional dimensional stability and flexibility, rapid drying.

For more information on our seismic papers, films and chemicals, write: E. I. du Pont de Nemours & Co. (Inc.), Photo Products Department, Wilmington 98, Delaware. In Canada: Du Pont of Canada, Ltd., Toronto.

* Du Pont's trademark for its polyester photographic films.

DU PONT

BETTER THINGS FOR BETTER LIVING ... *THROUGH CHEMISTRY*

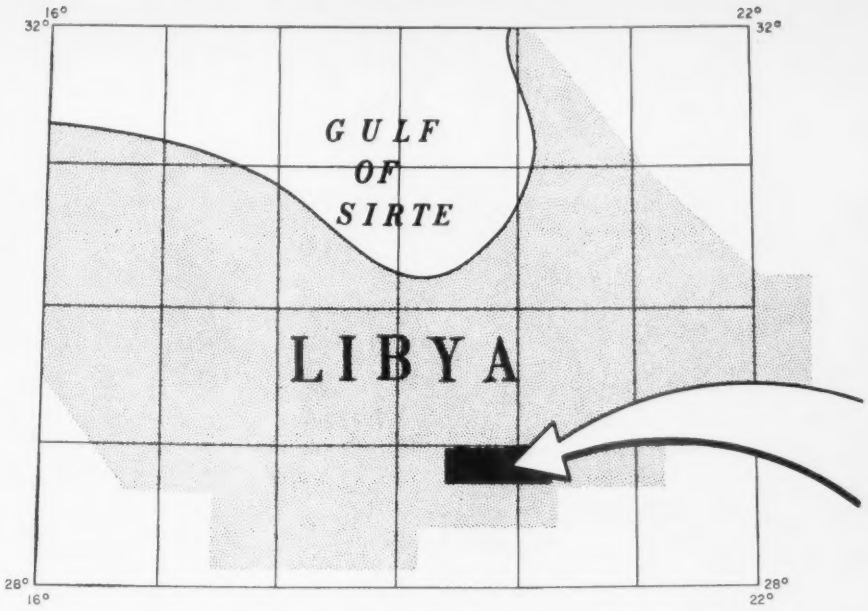

Aeromagnetic data and interpretation offered for extensive Sirte Embayment Survey

Aero Service offers aeromagnetic data and interpretation for 160,000 square kilometers in the Sirte Basin, Libya. Flown late in 1960,* it comprises 25,000 linear kilometers of airborne magnetometer profiles and control flights. Flight direction is east-west. Profiles were flown in bands of 5, with a separation of 5 km. between individual profiles and 20 km. separation between bands. North-south control flights are spaced at 40 km. intervals.

Participants receive one full scale reproduction of each airborne magnetometer profile—one set of isomagnetic contour maps at a scale of 1:100,000 with regional gradient removed, plus composites at a scale of 1:500,000.

An interpretation report by Gravity Meter Exploration Company is also delivered. It includes overlay maps showing basement depth estimates, contours of the regional basement surface, and areas of possible local basement structure.

Participation is invited at a cost of $50,000 for the total area. Costs for smaller areas will be quoted on request.

This broad survey is one of several participation surveys now offered by Aero Service Corporation. Aeromagnetic coverage of the Appalachian Basin area, as well as data for selected areas in North Dakota, Montana, Wyoming, Colorado, Utah, Arizona, New Mexico, Texas, Oklahoma and Florida are offered.

*by Aero Service Corporation and Fairchild Aerial Surveys as a joint venture.

For complete information, please write:

EXPLORATION DIVISION

AERO SERVICE CORPORATION

210 E. Courtland St., Philadelphia 20, Pa., U.S.A.

World's Oldest Flying Corporation

Take a NEW READING ON GRAVITY as an Effective, Economical Exploration Method

If you have not used Gravity, or if your use has been limited in recent years, it will pay you to reappraise the benefits of this fast, low cost exploration method. Instrumentation, operational techniques, and interpretation have been greatly improved enabling many operators to provide *specific and detailed* geologic information. Originally, the Gravity Method was thought of primarily as a means of determining *salt dome configurations*. Now, stratigraphic and structural information can be obtained such as: the areal extent and configuration of sedimentary basins; the maximum thickness and variation in thickness of basin sediments; regional structures within the basins; local and regional fault systems, including horsts and grabens, within the section; and local and regional thrust faults.

To obtain the best results, use the world's most proved gravity instrumentation . . .

There's a *WORDEN* Meter for Every Land Application

The MASTER and PROSPECTOR model *WORDEN* Gravity Meters provide the most demanding operating specifications ever achieved in portable meters. They retain the true portability and flexibility of the quartz element design plus the exclusive "Universal Compensation" feature which extends the temperature compensated range up to 6600 mgls. (world coverage). The MASTER is distinguished from the PROSPECTOR by a low power Temperature Stabilizer, which maintains a nearly constant internal temperature in spite of extreme outside thermal shocks. Both meters are available in Standard and Geodetic models.

The PIONEER is ideally suited for gravity programs in areas of limited latitude and temperature variations and where the need for less frequent base ties exists. Also available in Geodetic model.

The EDUCATOR gravity meter is intended to meet the needs of educational or training programs where the required tolerances are much wider than for commercial programs.

Specifications for the respective *WORDEN* Gravity Meters are shown at right . . . contact TI's Gravity Department for additional information.

Select Your *Worden* Gravity Meter from the widest combination of models and ranges in the industry!

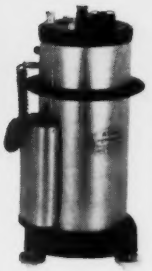

When requesting a quotation, copy the specification categories in this column and specify the values desired from those found under the respective meters.	the *Master*	the *Prospector*	the *Pioneer*	the *Educator*
Minimum Recommended Operating Range—Specify to nearest 100 mgls.* plus latitude and elevation indication	3000 mgls.	3000 mgls.	2400 mgls.	Limited . . . Will be at least 1600 mgls.
Minimum Total Operating Range (Reset) —Specify to nearest 100 mgls.*	5200 mgls.	5200 mgls.	4000 mgls.	Limited . . . Will be at least 2000 mgls.
Small Dial Range	800 Dial Divisions x Small Dial Constant (2200 on Special Order)	800 Dial Divisions x Small Dial Constant (2200 on Special Order)	800 Dial Divisions x Small Dial Constant	800 Dial Divisions x Small Dial Constant
Small Dial Constant—Specify constant desired*	Standard .08 to .11 mgl./Dial Division (From 0.05-1.00 also available)	Standard .08 to .11 mgl./Dial Division (From 0.05-1.00 also available)	Standard .08 to .11 mgl./Dial Division (From 0.05-1.00 also available)	0.10-1.00 mgl./ Dial Division
Small Dial Calibration Linearity over full range	1 part in 1000	1 part in 1000	1 part in 1000	1 part in 1000
Small Dial Reading Accuracy	0.1 of Small Dial Division	0.1 of Small Dial Division	0.1 of Small Dial Division	0.1 of Small Dial Division
External Temperature Control	Temp. Stabilizer requires 1.00 watts power for a 100° F. differential. Four Rechargeable "D" Size Batteries maintain 90° F. differential for 10 hours and are mounted in removable pack on side of meter. Any 4.5 to 12 volt DC source may be substituted.	None	None	None
Small Dial Mechanism	Self counting, read from top and directly coupled (no gears for backlash) with screw which contacts quartz measuring spring.		Side and top reading, directly coupled (no gears for backlash) with screw which contacts quartz measuring spring.	
Large Dial Range — Specify range desired*	800 Dial Divisions x Large Dial Constant			Geodetics not available
Large Dial Constant	Standard 6.5 to 12.0 mgls./D.D.			Geodetics not available
Large Dial Calibration over full range (8 turns)	Curve furnished with values accurate to one part in 1000—measured over full range (8 turns).			Geodetics not available
Size, Inches: Diameter Height	7" 14"	7" 14"	5½" 10½"	5½" 10½"
Weight, Pounds: Net Including carrying case	9¾ lbs. 18 lbs.	7½ lbs. 15¾ lbs.	5⅛ lbs. 12 lbs.	5⅛ lbs. 12 lbs.
*Price of meter is determined mostly by the Ranges and Dial Constant Specified.				

Write for Bulletin No. GM-206

WORDEN Gravity Meters Are Made Exclusively By

TEXAS INSTRUMENTS
INCORPORATED
GEOSCIENCES & INSTRUMENTATION DIVISION
3609 BUFFALO SPEEDWAY • HOUSTON 6, TEXAS • CABLE: TEXINS

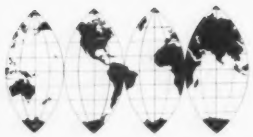

The sun never sets on Petty crews. Below is an advertisement which is appearing currently in an Australian publication in conjunction with full scale surveys being carried out by Petty crews in Queensland and New South Wales. Petty crews work around the clock, around the world

Petty
GEOPHYSICAL
ENGINEERING CO.
30 TANK STREET, P. O. BOX 195
NORTH QUAY, BRISBANE, QUEENSLAND

Capability and efficiency, supported by continual experience since 1925, are now being applied by Petty crews to full scale surveys in Queensland and New South Wales. Petty applies traditional seismic, gravity, and magnetic methods as well as such advanced techniques as the patented Petty principle of horizontal stacking. Adequate supervision is granted from strategically located offices in Quilpie and Brisbane, Queensland and Wallacia, New South Wales, Australia; Bogota, Columbia; Denver, Colorado; Lafayette, Louisiana; Irwin, Pennsylvania; and the home office in San Antonio, Texas.

. . . The gravimetric method is certainly the most powerful branch of geodesy because it can relate the different continents to the same world geodetic system; it is the only method capable of giving the detailed shape of the geoid not only on the continents but also over the oceanic areas. It . . . *

* W. A. Heiskanen in "Latest Achievement of Physical Geodesy" (J. of Geophys. Research 65, p. 2827-2936, Sept. 1960)

ASKANIA

GRAVIMETER SURVEYS OVER LARGE DISTANCES

with the ASKANIA GRAVIMETER Gs-12

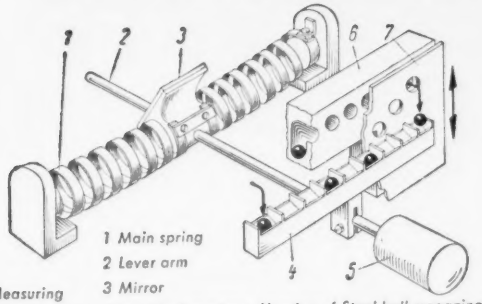

Measuring system: 1 Main spring, 2 Lever arm, 3 Mirror, 4 Steel ball receiver, 5 Mass

Housing: 6 Steel ball magazine, 7 Selector slide

the entire gravitation force acting on the measuring system (M.g.) is nearly *constant*. Any variations in gravity are compensated through a change in mass of the measuring system by adding or removing small balls of an accurately preestablished mass so that the system is largely unaffected by the measuring spring characteristics

- direct measuring range about 2,000 mgal
- measuring accuracy 0.02 mgal

. . . and for gravimetric surveys of the oceans rely on the ASKANIA Seagravimeter Gss-2 after Graf.

ALSO AVAILABLE: Earth Tide Recording Equipment; Magnetic instruments, etc.

Write for detailed information!

ASKANIA-WERKE

Division of Continental Elektroindustrie AG
U. S. Branch
4913 Cordell Avenue, BETHESDA 14, MARYLAND

Take advantage of VELA UNIFORM equipment in your refraction or deep-reflection surveys

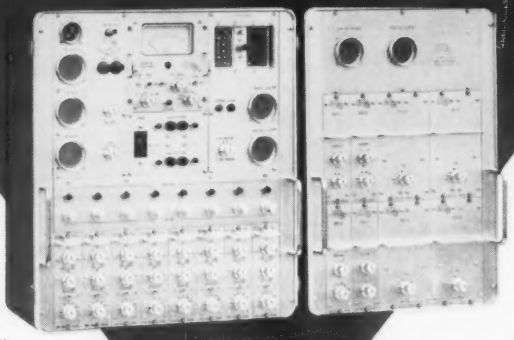

The GTR-200 system was originally developed and is now proven by use for the VELA UNIFORM crustal studies program being conducted by the U.S. Geological Survey. Transistorized, rugged, very-low-frequency refraction amplifiers included in the system provide a new dimension for seismic recording. Dual outputs are provided for both galvos and tape recorders to allow extended effective dynamic range recording. Provisions are made for using special geophones. System noise less than 0.2 microvolts combined with a 60 db. dynamic range make the GTR-200 system ideal for all types of advanced refraction recording studies.

TRANSISTORIZED VERY-LOW FREQUENCY REFRACTION AND DEEP-REFLECTION AMPLIFIER SYSTEM

GTR-200

CONDENSED SPECIFICATIONS

Input:	Transformer input, approximately 1200 ohms resistive above 2 cps.
Frequency Response:	Broad band: Within 3 db—1 to 300 cps.
Filters:	Lo-Cut: 18 db/oct—Out, 3½, 7, 14 cps.
	Hi-Cut: 18 and 36 db/oct—Out, 9, 13, 18, 26, 37, 100 cps.
Distortion:	Less than .5%. Dynamic range 60 db.
Noise:	Approximately .12 microvolts peak-to-peak 1 to 26 cps.
Outputs:	Galvo: Dual output, 0 and -15 db.
	Hi-Z Tape: Dual output, 0 and -30 db.
Power Requirements:	Total 8-channel system approximately .7 amp @ 24 VDC.

SIE DIVISION

DRESSER ELECTRONICS

10201 Westheimer, Zone 42 / P. O. Box 22187, Zone 27 / Houston, Texas

PHONE: SUnset 2-2000 CABLE: SIECO HOUSTON TWX: HO-1185

rld-wide service. Offices in Canada, Europe and Mexico----agents throughout the free world

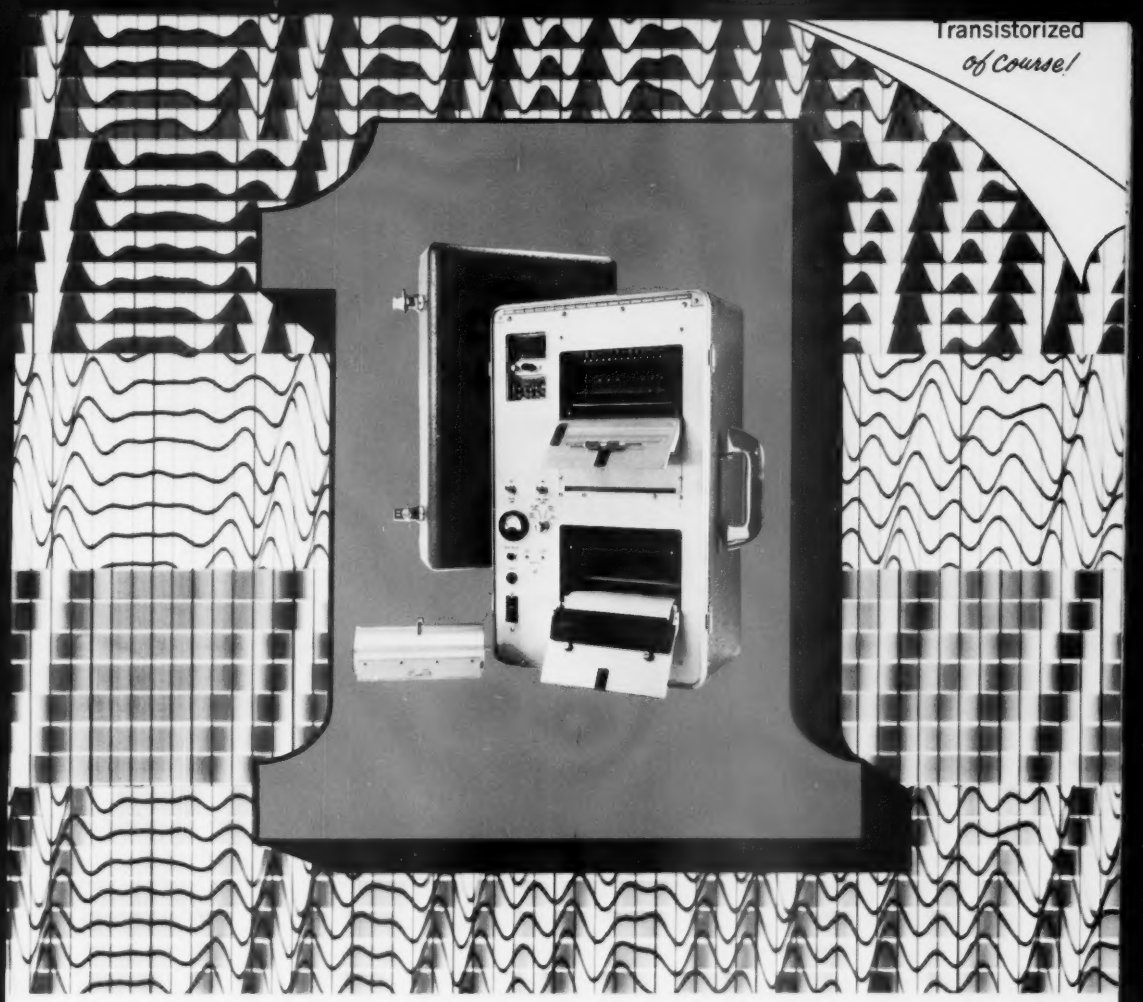

One camera...five displays!

From SIE comes the first means of obtaining five displays from only one oscillograph . . . and with but one galvo block! ■ Choose variable-density, variable-area, conventional wiggle, **variable-density-and-wiggle** or **variable-area-and-wiggle superimposed.** Simple lens-box change converts from variable-density to variable-area. ■ Timing lines may be generated internally from either flasher tubes or standard timing motor. Consistency of paper drive is assured by a synchronous motor with built-in 400 cps power supply.

Answer all your oscillograph recording needs with one instrument

the **TRO-6** *Phone or write for the COMPLETE brochure.*

DAY NIGHT SERVICE
Call: SUnset 2-2083
Houston, Texas

SIE DIVISION DRESSER ELECTRONICS

10201 Westheimer, Zone 42 / P. O. Box 22187, Zone 27 / Houston, Texas

PHONE: SUnset 2-2000 CABLE: SIECO HOUSTON TWX: HO-1185

Equipment backed by 16 years of world leadership and world-wide service. Offices in Canada, Europe and Mexico----agents throughout the free world

Transistorized
of course!

SIE'S PMR-20

Portable FM Magnetic Recording System

- Wide Frequency Response (1 to 500 cps)
- Negligible Phase Shift
- No Modulation Noise
- True High Fidelity
- Low Distortion

Over **eighty** systems
presently in use
supplying full spectrum
High Fidelity FM Magnetic Recordings
for today **AND TOMORROW!**

There is no reason why you should not now record the FULL spectrum of energy in each shot for processing by today's techniques or by whatever better method may be evolved in the future. The SIE PMR-20 "RecorData" FM system gives you such data for refraction, conventional and high-frequency operation . . . and does it all with low-power drain and miniaturized construction. The complete 24-channel transistorized system is housed in two compact, lightweight units. It provides high-fidelity frequency-modulated recordings on standard SIE tapes from the output of standard geophysical amplifiers. System performance is not dependent on tape quality. Look at the brief technical description on the right . . . then write or call for complete information.

CONDENSED SPECIFICATIONS

Channels: 24 geophysical
4 auxiliary (Time break, up-hole, 100 cps and noise cancelling)

Frequency response: 1 cps to 300 cps within 1 db; 3 db down at 500 cps

Signal-to-noise ratio: 60 db (rms), 1 to 500 cps with noise cancelling.
54 db (rms) 20 to 200 cps without noise cancelling.
(Peak-to-peak noise averages 6-10 db higher than rms noise)

Harmonic distortion: Less than 1%

Crossfeed: Below noise level of recording system

Relative timing accuracy: ± 0.25ms.

Power requirement:

	Standby	Operating
Record	2 amp.	7 amp.
Playback	1.5 amp.	6.5 amp.

12 volts D.C.

Dimensions: MR-20 Recorder—8¼"W x 24½"H x 15"D
MU-20 Master Unit—8¼"W x 24½"H x 10½"D

Weight: MR-20 Recorder—60 lbs.
MU-20 Master Unit—45 lbs.

SIE'S DISTORTION-FREE

Transistorized *of course!*

PT-100 Transistorized Seismic Amplifier

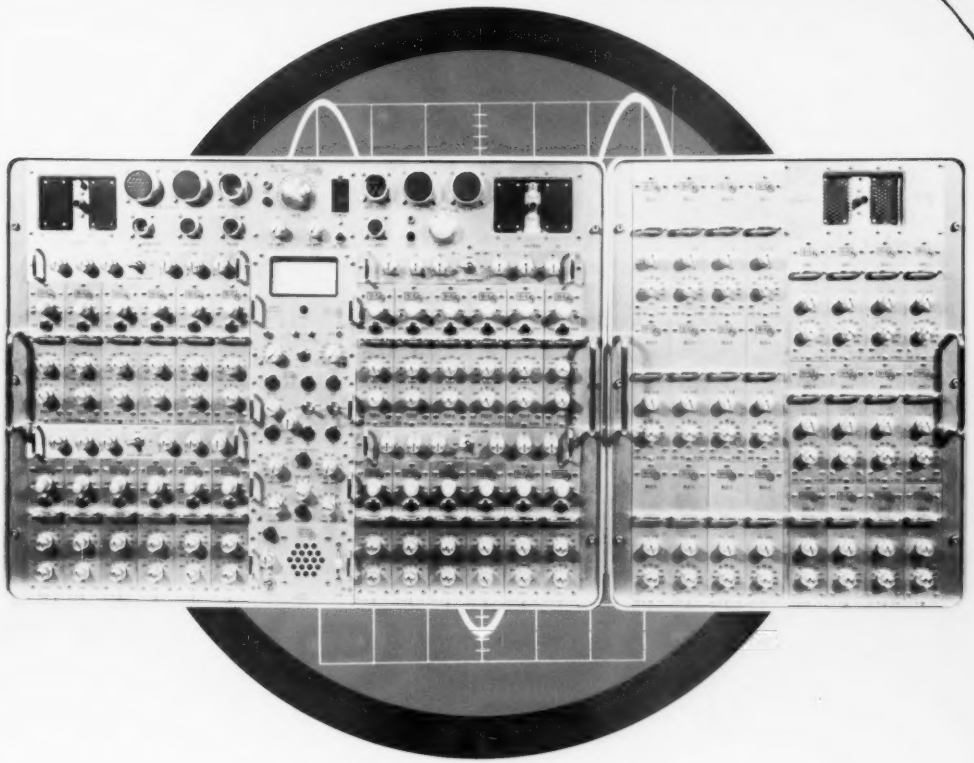

SIGNAL CONTROL

With unique light-sensitive photocells as losser elements, the PT-100 eliminates the usual amplifier AGC problems. The critical "diode-balancing" common to other types of AGC circuits is never required. There is no direct electrical coupling between AGC and signal paths to cause distortion and oscillation. Signal voltages do not cause distortion when applied across losser elements as with diode bridge circuits. Drift and temperature instabilities are eliminated. There is a useful operating range of from one microvolt to one volt input — 1,000,000 to 1! Total harmonic distortion under all normal field operating conditions does not exceed 0.5% including heavy reflection standout. External 4 kc signals may be used for programmed-gain operation during amplitude studies. AGC performance down to 5 cps allows use of the PT-100 in refraction work **with AGC control.**

FREQUENCY RESPONSE

The broad band response extends from 3 to 500 cps. Ten logarithmically-spaced cut-off frequencies are provided — from 16 to 135 cps for the low-cut and 23 to 235 cps for the high-cut filter positions. One or two sections (18 or 36 db/octave) may be used.

NOISE

Noise is less than 0.3 microvolt for "filter-out" bandpass and drops to 0.1 microvolt for normal filter settings — as good or better than most vacuum tube amplifiers.

OPERATION

Operator-oriented master controls provide separate record and playback adjustments for both "early" and "final" gain. Complete built-in amplifier test units make testing and control adjustments rapid and easy.

The PT-100 will provide you a new dimension in recording from refraction through normal reflection up to high frequency use. Phone or write for the COMPLETE brochure.

Every Shot Costs!

Why try to save pennies on doubtful recording supplies.

With the cost of each shot climbing every year, you can't afford to take chances—especially when the most you have to gain is pennies! SIE guarantees quality . . . quality controlled by a team that has been building its reputation with you for over 15 years.

Magnetic tape with higher output, better signal-to-noise ratio, and **guaranteed not to strip oxide in normal use**

Photographic supplies fresh-from-the-factory, laboratory tested, and on hand ready to go the same day your order is received

Recording charts precisely printed and stable under all moisture conditions encountered in field and office operation.

Call SIE . . . and MAKE EVERY SHOT COUNT

SIE DIVISION

DRESSER ELECTRONICS

10201 Westheimer, Zone 42 / P. O. Box 22187, Zone 27 / Houston, Texas

PHONE: SUnset 2-2000 CABLE: SIECO HOUSTON TWX: HO-1185

Equipment backed by 16 years of world leadership and world-wide service. Offices in Canada, Europe and Mexico----agents throughout the free world

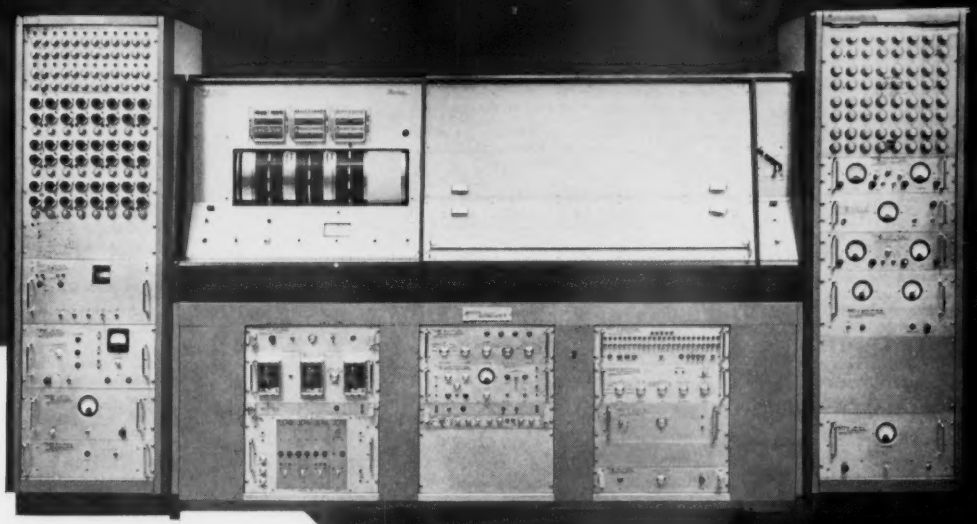

GeoData . . .
since 1957
without a major change!

In 1957 SIE's first GeoData system was put to use. Geophysicists then had the first simplified instrument for analyzing, processing and displaying magnetic recordings of geophysical data. Since that time over fifty playback systems built around the same principles have been supplied by SIE to users around the world — **and no changes have ever been required in the basic portions of the original design!**

GeoData
GEOPHYSICAL DATA PROCESSING SYSTEMS

- *Versatile combinations of photographic display.*
- *Multiple drums for high-production, complex compositing.*
- *Compositing and corrections without intermediate tape.*
- *Flexible electronic time correction system — NMO up to 800 milliseconds.*

Today SIE can fabricate for you from time-proven "building-blocks" virtually any kind of geophysical data processing system. You know beforehand that the equipment will be reliable and accurate. You can assure yourself that SIE geophysical instruments are truly the standard of the industry by asking any of the over 200 using companies. Call SIE to get YOUR system in process.

SIE DIVISION

DRESSER ELECTRONICS

10201 Westheimer, Zone 42 / P. O. Box 22187, Zone 27 / Houston, Texas

PHONE: SUnset 2-2000 CABLE: SIECO HOUSTON TWX: HO-1185

ld-wide service. Offices in Canada, Europe and Mexico----agents throughout the free world

FAIRCHILD AERIAL SURVEYS

all types of
AERIAL SURVEYS,
PHOTOGRAMMETRIC ENGINEERING
AND AIRBORNE GEOPHYSICAL
EXPLORATION

HOME OFFICE:
224 E. Eleventh Street, Los Angeles 15, California
Phone: RIchmond 9-3007 Cable: FAIRMAP

DISTRICT OFFICES:
10 Rockefeller Plaza, New York 20, New York
Phone: PLaza 7-2775
1625 Eye Street, N.W., Washington, D.C.
Phone: NAtional 8-7770
255 Atlantic Ave., Boston 10, Massachusetts
Phone: LIberty 2-2940
5043 Stillbrook Drive, Houston 35, Texas
Phone: PArkview 9-9135

Also representatives in: Buenos Aires, Argentina; Beirut, Lebanon; Bruxelles, Belgium; La Paz, Bolivia; Rio de Janeiro, Brazil; Santiago, Chile; Bogota, Columbia; Maidenhead, England; Paris, France; Guatemala City, Guatemala; Baghdad, Iraq; Lima, Peru; Istanbul, Turkey; Caracas, Venezuela.

A WORLD OF EXPERIENCE

Please mention GEOPHYSICS when answering advertisers

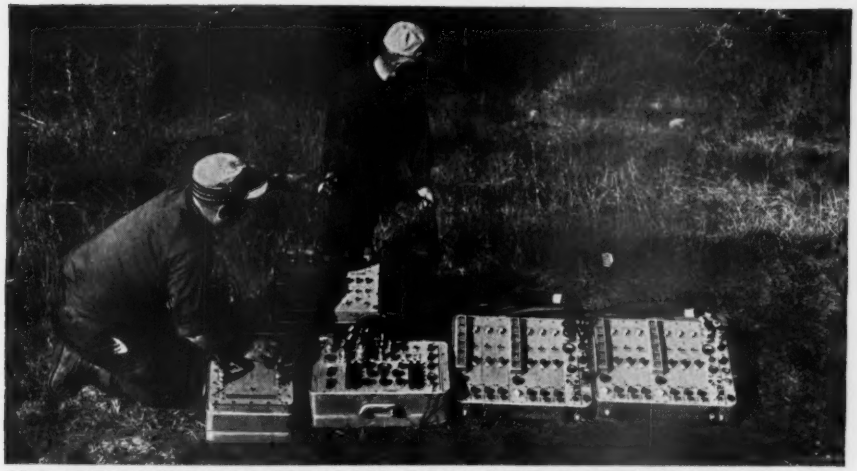

NO RECORDING TRUCK CAN GET BETTER RESULTS THAN WESTERN'S COMPLETELY TRANSISTORIZED PORTABLE TFA SYSTEM

Through Western Geophysical Company's dramatically successful TFA transistorized field amplifiers, Western crews on portable seismic surveys are obtaining results equivalent in all respects to those possible through the best standard, truck-mounted, vacuum tube amplifiers.

The reason: – Every function on the truck-mounted amplifiers is also standard – without compromise – on the TFA. To this flexibility, TFA adds a signal-to-noise ratio equal to that of Western's notably quiet FA35 truck-mounted amplifiers. Also, TFA is temperature-stable from –40°F. to +140°F.

Western's portable seismic system saves you money: Less manpower needed because there is less to carry. The amplifiers are housed in 12-channel suitcases. Each case weighs 42 pounds, complete with satellite-type batteries. The magnetic tape recorder, camera, and control panel also are completely transistorized. Mounted in suitcases, they weigh 55 pounds, 44 pounds and 26 pounds, respectively. The only external power source needed for the entire system is a small 12-volt battery for the motors of the magnetic tape transport and camera.

Western logistics saves you money, too. Western crews have surveyed successfully in the coldest, hottest, wettest, driest, and roughest of oil prospect areas. They are skilled in mastering the toughest supply problems with minimum waste motion.

When you need contract geophysical services for any type of prospect, remember: YOU ARE *SURE* OF MAXIMUM USABLE DATA WITH A WESTERN CREW ON THE JOB!

To discuss, in confidence and without obligation, how Western would work for you, write or call:

Instruments pictured above are (from left) camera, control panel, two TFA cases. Behind camera is the Western magnetic tape transport.

Western
GEOPHYSICAL COMPANY
A DIVISION OF LITTON INDUSTRIES

933 NORTH LA BREA AVENUE, LOS ANGELES 38, CALIFORNIA • OLDFIELD 4-1100
AFFILIATE AND REGIONAL OFFICES THROUGHOUT THE WORLD

Seismos G.m.b.H.,
Wilhelm-Busch-Straße 4,
Hannover, Germany.
Phon 7 08 31
Telex 09 22419

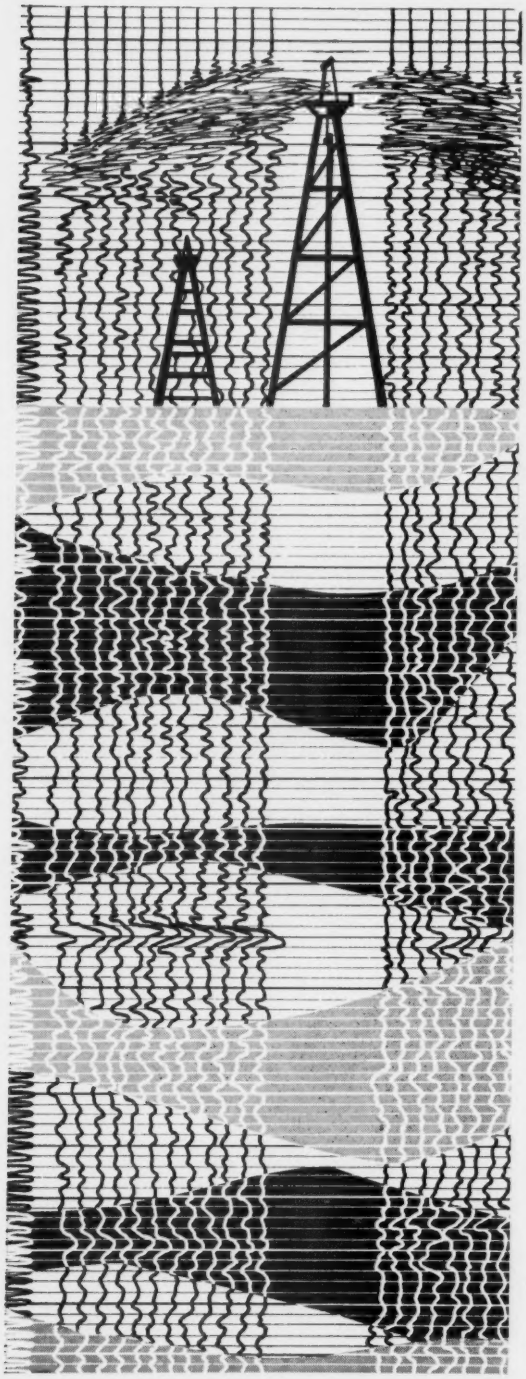

For top response
ask your supplier for

SCOTCH® BRAND

BELTS OR TAPES

Whether you use belt or tape . . . record AM or FM . . . for the best record of your shots it pays to specify "SCOTCH" BRAND Magnetic Products. It's your assurance of top output at low frequencies, plus uniformity of product.

As pioneers in producing magnetic tapes for every type of instrumentation, "SCOTCH" BRAND experts continue to lead in making magnetic coatings and backings of ever-increasing uniformity. Most leading seismographic suppliers rely on "SCOTCH" BRAND basic magnetic products for their own line . . . so for accurate results ask your supplier for "SCOTCH" BRAND.

"SCOTCH" BRAND MAGNETIC PRODUCTS
for geophysical recording

© 1961 3M Co.

MINNESOTA MINING AND MANUFACTURING COMPANY
. . . WHERE RESEARCH IS THE KEY TO TOMORROW
3M

"SCOTCH" is a Reg. TM of 3M Co., St. Paul 6, Minn. Export: 99 Park Avenue, New York. Canada: London, Ontario.

SEISMOGRAPH SURVEYS*

**long and short term contracts*

A. E. "SANDY" McKAY

Central Office
Continental Life Bldg.
Fort Worth, Texas

Division Offices

WEST TEXAS
Midland, Texas
C. N. Page

MID-CONTINENT
Oklahoma City
L. E. Tabor

ROCKY MTS.
Denver, Colorado
C. J. Lomax

Foreign Affiliate: namco INTERNATIONAL

now your tape playback equipment can process data from paper records and well logs

you can often get a more accurate subsurface picture, and thus reduce the likelihood of expensive errors, by transcribing these data onto magnetic tape for processing on a data-reduction system

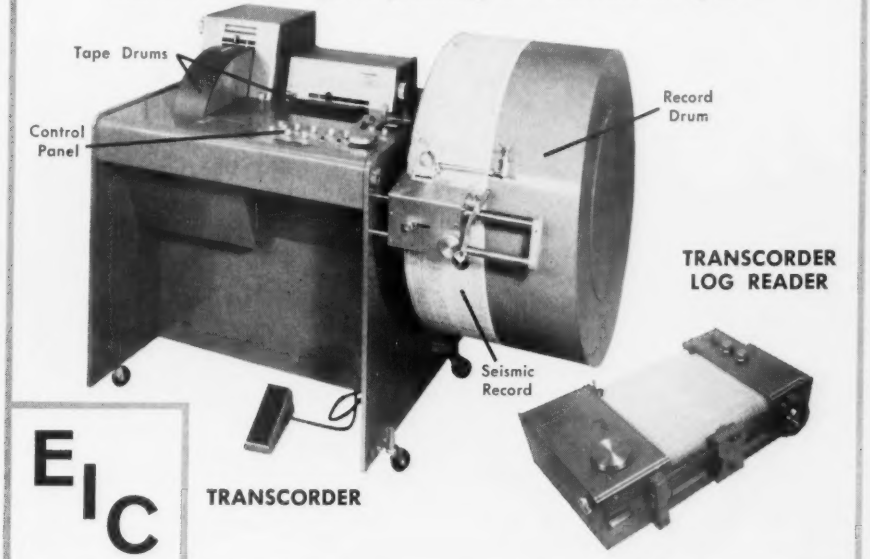

EIC

The Transcorder, EIC's new data-transcribing device, transcribes seismic data onto any standard geophysical tape from paper records, from other sizes of magnetic tape, or, using the Transcorder Log Reader, from well logs. A reproduction of a seismic trace being transcribed can be produced simultaneously for checking purposes.

Magnetic tapes produced by the Transcorder can be processed by playback systems that permit mixing, selective filtering, correcting for moveout, weathering, and elevation, and plotting cross sections by the conventional trace, variable-area, or variable-density methods.

The paper record being transcribed onto tape is mounted on a large revolving drum. The magnetic tape is mounted on another drum that is servo-driven at an infinitely variable rate. The Transcorder will accurately transcribe paper records recorded at speeds ranging from 7.5 to 15 ips. The magnetic recordings produced are accurate within $\pm 1\frac{1}{2}$ ms of the original record at all times.

The Transcorder operator guides the tracking head as the record-carrying drum revolves. (Unskilled office personnel can operate the Transcorder.) The traces are individually transcribed to magnetic tape.

The Transcorder Log Reader, an accessory, permits transcribing well logging data onto magnetic tape in the same manner as conventional seismograms. The resulting tapes can be then converted to cross sections by seismic data reduction systems.

Write or wire EIC for detailed specifications

ELECTRODYNAMIC INSTRUMENT CORPORATION

Subsidiary of Reed Roller Bit Company

1841 Old Spanish Trail • Houston 25, Texas

GRIFFIN TANK

ON THE GO. . . WORLD-WIDE

Wherever the oil industry goes, so goes Griffin — with the most complete line of mobile equipment and supplies.

GRIFFIN TANK AND WELDING SERVICE

3031 ELM STREET • PHONE Riverside 1-6811 • DALLAS 1, TEXAS

reduce field recording costs with this 157-lb portable seismic system

this complete 24-channel seismic system produces high-quality tape-recorded data, keeps your operating costs and field-equipment investment low

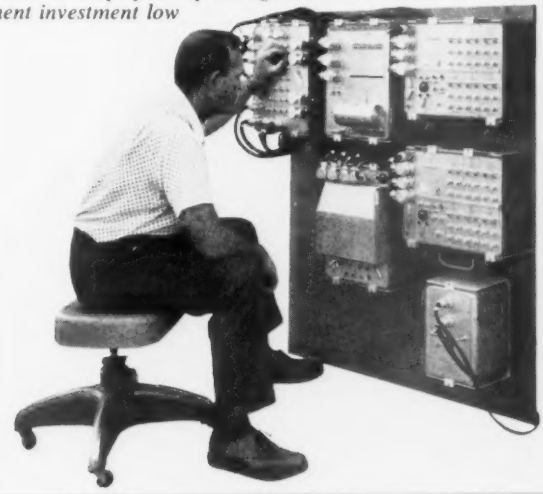

EIC

Although it weighs only 157 lb, the PSS-50 is a complete seismic system, consisting of two 12-channel seismic amplifiers, a tape-transport unit, a translator unit, and a master control unit.

The system's low cost and weight were gained by designing it to utilize fully the capabilities of magnetic tape and by including only needed filtering and display capabilities. The result is a truly portable system that performs superbly.

The seismic amplifiers have a flat frequency response from 8 to 250 cps. Filtering is provided by a separate plug-in unit. Filtering available includes 12 to 24 db per octave slopes, with 20, 30, and 40 cps cutoff points. Cutoff frequencies can easily be changed by plug-in capacitance boards.

A master control unit provides uphole level control, leakage and continuity testing, trip indicator and manual control, trip sensitivity control, master suppression control, avc on-off control, and a test oscillator. Timing accuracy is ± 1 ms.

The tape transport unit has a full 28-channel magnetic recorder, featuring standard EIC door-mounted recording heads. Heads can be interchanged without disassembling the tape transport. Recording heads have excellent low-frequency and transient response. The accurate, reliable drive system uses a hysteresis synchronous motor and a spur-gear transmission.

The translator unit has a playback amplifier with additional avc and filtering control. Traces are displayed on electrosensitive paper by a rectilinear pen writer. Each data channel is played out sequentially and automatically. Timing is provided by preprinted timing lines, with the 100 cps timing trace from the tape played out as a check. Two paper speeds are available, one for a full-length record, the other for expanding the first third of the record (covering the first-break region) over the full paper length. Accuracy from trace to trace is ± 1 ms.

Power required for the PSS-50 is 12 v at 8 a during standby and 18 a while recording.

Write or wire EIC for detailed specifications

ELECTRODYNAMIC INSTRUMENT CORPORATION

Subsidiary of Reed Roller Bit Company

1841 Old Spanish Trail • Houston 25, Texas

Please mention GEOPHYSICS when answering advertisers

Seismic Engineering COMPANY

ENGINEERED SEISMIC SURVEYS

6111 MAPLE AVENUE • DALLAS • TEXAS

R. D. Arnett C. G. McBurney J. H. Pernell

this versatile playback system simplifies your toughest data analysis problems

using EIC's central office seismic data reduction system, you can easily apply precise corrections to field-recorded tapes, use mixing, compositing, or stacking, select the most effective presentation modes

Field Tape Playback Unit

Plotting and Re-record Assembly

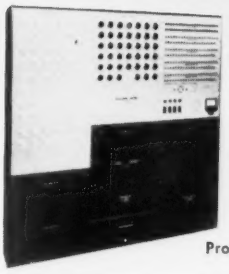

Programming Assembly

C-850

EIC

When you own the C-850, you have the most flexible single system available for sequential playback of magnetic tapes. It lets you make maximum static corrections of ±100 ms and dynamic corrections up to 400 ms (at a maximum rate of 500 ms per sec). Timing accuracy is ±1 ms. Any geophone spread length or arrangement can be handled.

During playback, time-corrected seismic data are plotted simultaneously to photographic cross sections. You can choose conventional - trace, variable - area, or variable - density cross sections, or any two of these three. Seismic data can be referenced to any desired datum plane on the cross-section plots. As many as 864 traces can be recorded on a single cross section, which may be as large as 72 x 72 in.

Corrected data are re-recorded during playback for future evaluation. As many as 12 channels of re-recorded tape can be played back for mixing, compositing, or stacking to cross-section plots.

The C-850 can be supplied with any standard-size tape transport. It handles up to 50 seismic and information channels at tape speeds of 7.5, 3.75, or 3.6 ips. It can reproduce direct, FM, or PWM recordings. Re-recording is by FM. Cross-section plotting speed is from 7.5 to 10 ips.

Distortion on FM is less than 1%, on direct magnetic recording, less than 2.5%. Frequency response is from 5 to 500 cps. Signal-to-noise ratio is 52 db (rms-rms) on direct recording, 46 db (rms-rms) on FM.

Such standard EIC design features as door-mounted recording heads and 400-cps hysteresis synchronous motors make the C-850 reliable, easy to maintain, and relatively inexpensive.

Write or wire EIC for detailed specifications

ELECTRODYNAMIC INSTRUMENT CORPORATION

Subsidiary of Reed Roller Bit Company

1841 Old Spanish Trail • Houston 25, Texas

Please mention GEOPHYSICS when answering advertisers

MARINE GEOPHYSICAL SERVICES CORP.
MARINE GEOPHYSICAL INTERNATIONAL, INC.

2418 TANGLEY
HOUSTON 5, TEXAS
Telephone: JA 6-4428 – JA 2-7711
Cable: MARGEO

MARINE PETROLEUM EXPLORATION SURVEYS
MARINE ENGINEERING AND CONSTRUCTION SURVEYS
MARINE RADAR POSITIONING SERVICE
WATER BOTTOM MAPPING
AUXILIARY MARINE SERVICES

here's a low-cost, rugged field office playback system that really takes abuse

you get simple, precision operation with minimum maintenance costs when you buy EIC's durable, highly accurate field office seismic data reduction system. and it's priced lowest in its field!

PB 50/60

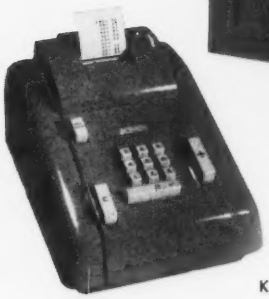

Keyboard Input Unit

EIC

The PB-50/60 sequential playback system was engineered and built to give reliable service under adverse field conditions. Its single-console construction makes it easy to move from one location to another, and its rugged, simple construction makes it easy to maintain. Despite its low cost, the PB-50/60 gives you great flexibility of operation and ±1 ms accuracy.

Normal moveout corrections up to 240 ms are available at a maximum rate of 500 ms per sec. Maximum weathering and elevations corrections of ±100 ms can be applied. All corrections are inserted easily and rapidly by a keyboard input unit.

Timing lines on cross sections are recorded directly from field timing signals, giving you accurate trace plots that are in true relation to each other and to record time. Seismic information can be accurately referenced to any desired datum plane. Either conventional-trace or variable - density cross sections are plotted photographically on 24 x 72-in. tape or film. This system can be supplied with any standard-size tape transport.

Modifications of the basic PB-50/60 can be supplied to meet specific requirements.

Write or wire EIC for detailed specifications

ELECTRODYNAMIC INSTRUMENT CORPORATION

Subsidiary of Reed Roller Bit Company

1841 Old Spanish Trail • Houston 25, Texas

Please mention GEOPHYSICS when answering advertisers

fidelity, timing accuracy mark this direct recording magnetic tape system

this direct recording magnetic tape system updates seismic systems to provide high-quality tape-recorded data for analysis in seismic data reduction systems

DR-50

The DR-50 magnetic recording systems produced by EIC record up to 50 seismic and information channels. Record - reproduce heads have excellent low-frequency and transient response. They are mounted on the access door so that they can be inspected, adjusted, or replaced without disturbing the tape transport.

The neatly packaged plug-in amplifiers used as dual-purpose record and reproduce units provide proper playback compensation down to 5 cps.

The DR-50 features timing accuracy of ±1 ms, with trace - to - trace accuracy of ±0.5 ms. Frequency response is from 10 to 500 cps. Signal-to-noise ratio is 52 db (rms). Total harmonic distortion is 2.5%. The DR-50 is driven by EIC's reliable 400-cycle synchronous motor.

The DR-50 is available either with or without a buffer unit. The buffer is used when the seismic amplifier cannot drive the recording heads directly or when a superior signal-to-noise ratio is needed for field playback. EIC engineers are experienced at integrating systems with existing amplifiers and can provide turnkey installation of DR-50 systems.

you get dependable field performance from this rugged recording oscillograph

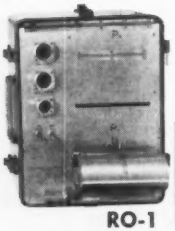

RO-1

The RO-1 recording oscillograph photographically records up to 28 seismic data traces on 6-in. paper or film. A 400 cps hysteresis synchronous motor provides uniform paper speeds from 3 to 45 ips. Speeds are selected by interchanging easily replaceable drive gears. Precise time correlation is insured by sharply defined timing lines. The RO-1 has 28 pencil-type galvanometers that are available in natural frequencies from 125 to 500 cps. Both galvanometers and front-surfaced mirrors can be adjusted readily in the field. Because the RO-1 produces very little noise in the battery circuit, a single battery can power both the camera and the seismic amplifier. This simplifies battery-charging problems and makes the RO-1 especially suitable for truck mounting.

EIC

ELECTRODYNAMIC INSTRUMENT CORPORATION

Subsidiary of Reed Roller Bit Company

cut uphole shooting time and costs with this precision interval timer

you can obtain weathering and subweathering velocities accurately and efficiently with this interval timer, without using costly seismic recording systems

GT-1

EIC

EIC's GT-1 geophysical interval timer is a precision digital readout instrument that simplifies uphole shooting operations. It provides an immediate visual display of the time interval from shot detonation to the initial seismic wave received by an uphole geophone. Accuracy is ±0.5 ms. A maximum time interval of 255.75 ms can be recorded.

The GT-1 is completely transistorized. It is powered by self-contained dry-cell batteries. The unit's total weight, including batteries, is only 17 lb. Its aluminum carrying case is 16 x 9 x 7¾ in.

now you see results of filtering, stacking, mixing without waiting for cross sections

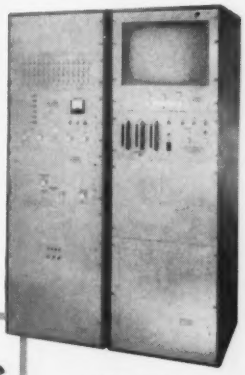

MSS-100

The MSS-100, a remarkable new multitrace electrostatic storage system developed by EIC, lets you store up to 28 seismic data traces for visual readout on a 17-inch, TV-type, video monitor. This advance in the art of handling seismic data can help you cut the cost of analyzing geophysical data.

The MSS-100 stores data from tape-recorded seismic traces in a special storage tube and displays them continuously on the monitoring tube. Traces can be displayed for as long as 20 minutes without appreciable deterioration. They can be erased instantly to permit storing new data.

Vertical timing lines can be displayed on the video monitor at 1/100-second intervals, with 1/10-second lines accentuated. Either the 1/100- or 1/10-second lines can be omitted if desired.

EIC

1841 OLD SPANISH TRAIL • HOUSTON 25, TEXAS

PC-3 Case
Shown actual size

You get all these outstanding features *only in HS-J* —the industry's *true sub-miniature geophone*— more than 70,000 units in field service

The HS-J basic unit is now available in the new PC series cases, made of virtually indestructible Kraylastic and engineered to provide these advantages:

1 Knot anchoring — makes takeout as strong as the cable itself.

2 Dependable watertight seal by injection of epoxy into closed case.

3 Plastic case is designed to provide complete insulation from ground.

4 Radius at cable entries gives longer flexing arc — adds to cable life.

5 Easy field cabling, with knot anchoring of takeouts and replaceable plastic sealing compound.

PC-5 Case
Shown actual size
(Marsh model also available in brass case.)

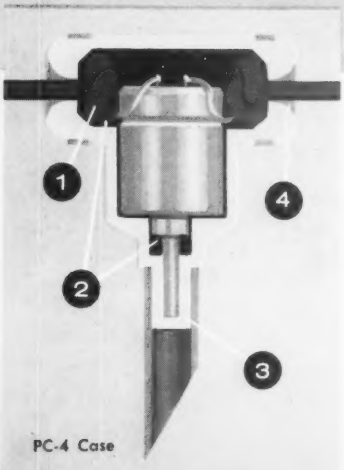

PC-4 Case

We cordially invite you to visit us at Booths 32-33, SEG Convention, Denver, November 5-9.

HALL-SEARS, INC.

WORLD WISE in Seismic Instrumentation

2424 Branard **Houston 6, Texas**

LONDON
PARIS
THE HAGUE
CALGARY

WE COVER THE WORLD TO HELP YOU FIND OIL

Exploration in 55 foreign countries and in the United States for 30 years has given SSC crews experience in almost every conceivable type of environment. From small, one-crew jobs to large surveys using many crews, SSC has continually provided effective results at reasonable costs.

At your disposal, SSC has a wide range of specialized equipment designed to produce results anywhere in the world.

Call on SSC's experience for your geophysical surveys, anywhere in the free world.

Seismograph Service Corporation

P. O. Box 1590 • TULSA, OKLAHOMA • National 7-3330

WORLD WIDE SUBSIDIARIES: SSC of Argentina • SSC of Bolivia • SSC of Canada • SSC of Colombia • SSC International • SSC of Libya • SSC of Mexico • Seismograph Service Limited • England • Seismograph Service de Espana • Compagnie Française de Prospection Sismique

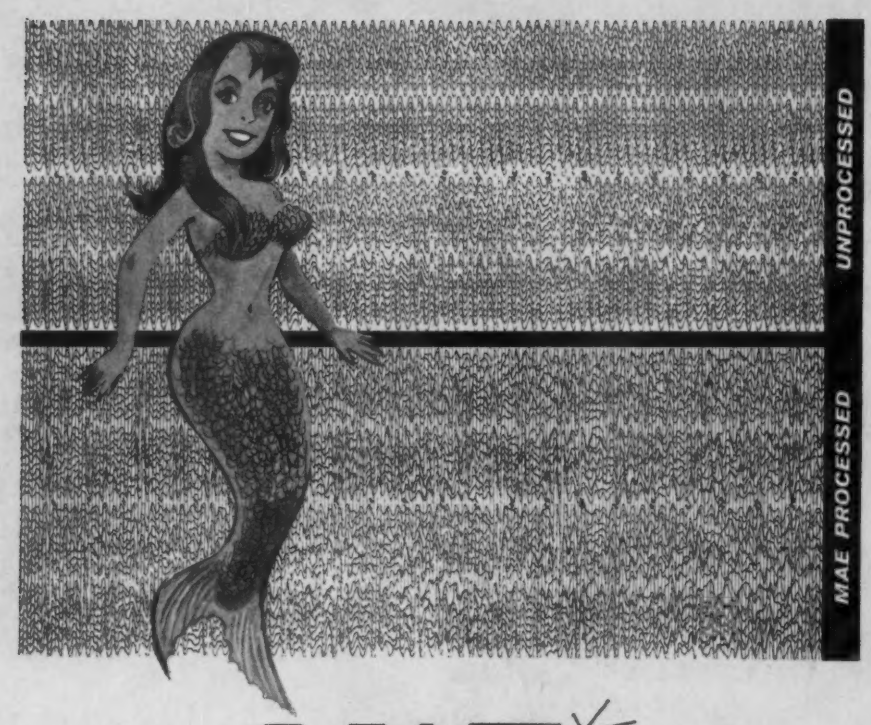

what can MAE* mean to you

Who said mermaids were mythical? MAE is a mermaid, but marine seismic explorationists know she's anything but a legend!

In areas where water reverberations mask reflections from depth, MAE (GSI's Multiple Analyzer Eliminator) is not only a fact, but a definite factor in providing workable seismic data. GSI... *and only GSI* offers the advantages of MAE, and MAE-processing can only be accomplished if the special recording techniques used on GSI vessels in both hemispheres are used in the original data gathering.

Make a date to meet MAE... she'll make your marine operations run smoother.

*MAE IS A GSI SERVICE MARK

GEOPHYSICAL SERVICE INC.

900 EXCHANGE BANK BLDG. • DALLAS 35, TEXAS

A TEXAS INSTRUMENTS COMPANY